

# **SIMULATION STUDIES ON DIFFERENT DESIGN PARAMETERS OF SPURS (GROYNES)**

By  
**ROY MATHEW**

## **THESIS**

Submitted in partial fulfilment of the  
requirement for the degree

*Master of Technology in Agricultural Engineering*  
Faculty of Agricultural Engineering & Technology  
Kerala Agricultural University

Department of  
*Land and Water Resources & Conservation Engineering*  
Kelappaji College of Agricultural Engineering and Technology  
**TAVANUR 679 573**  
**MALAPPURAM**

**1995**

170621

631.3  
ROY/SI



## DECLARATION

I hereby declare that this thesis entitled "Simulation Studies on Different Design Parameters of Spurs (Groynes)" is a bonafide record of research work done by me during the course of research and that the thesis has not previously formed the basis for the award to me of any degree, diploma, associateship, fellowship, or other similar title of any other University or Society.

Tavanur,

21 Feb., 1995.



ROY MATHEW

**CERTIFICATE**

Certified that this thesis entitled "Simulation Studies on Different Design Parameters of Spurs (Groynes)" is a record of research work done independently by Mr Roy Mathew, under my guidance and supervision and that it has not previously formed the basis for the award of any degree, fellowship or associateship to him.

Tavanur,

21 Feb., 1995.


*Xavier*  
Shri. Xavier K. Jacob  
(Chairman, Advisory Board)  
Assistant Professor  
Department of Land and Water  
Resources & Conservation Engineering  
K.C.A.E.T., Tavanur


**CERTIFICATE**

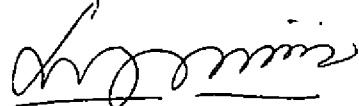
We, the undersigned, members of the Advisory Committee of Mr Roy Mathew, a candidate for the degree of Master of Technology in Agricultural Engineering majoring in Soil and Water Engineering agree that the thesis entitled "Simulation Studies on Different Design Parameters of Spurs (Groynes)" may be submitted by Mr Roy Mathew in partial fulfilment of the requirement for the degree.

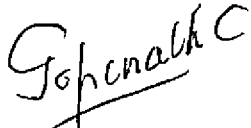
*Xavier:*  
*15-6-95*

**Shri. Xavier K. Jacob**  
Chairman  
Assistant Professor  
Department of Land and Water Resources &  
Conservation Engineering  
KCAET, Tavanur.

  
**Dr. K. John Thomas**  
Dean in-charge  
KCAET, Tavanur  
MEMBER

  
**Shri. Alexander Seth**  
Assistant Professor  
Department of Irrigation &  
Drainage Engineering  
KCAET, Tavanur  
MEMBER

  
**Shri. M. R. Sankaranarayanan**  
Assistant Professor  
(Agrl. Engg.)  
College of Horticulture  
Vellanikkara  
MEMBER

  
**External Examiner**

**ACKNOWLEDGEMENTS**

I, with immense pleasure express my deep sense of gratitude to Sri. Xavier K. Jacob , Assistant Professor, Department of Land and Water Resources & Conservation Engineering , KCAET, Tavanur, Chairman of the Advisory Committee for his inspiring advices ,encouragement and constructive criticisms during the course of this work.

I am greatly indebted to Sri.K.Sasidharan, Chief Engineer, Irrigation and Administration,Kerala to permit me to do the model study at KERI, Peechi.

I owe to Sri. C.K.Prabhakaran, Director,KERI, Peechi on behalf of this work and the success with in the period.

It is my privilege to acknowledge the sincere help and proper suggestions from Smt. Elizabeth Thomas, Joint Director, KERI, Peechi.

I am expressing my heart felt reverence and obedience to Sri.M.P. Sankaranarayanan,Deputy Director,Hydraulic Division No.II,KERI,Peechi, for his constructive suggestions and constant backing.

It is my greatest privilege to acknowledge the sincere advice and valuable help rendered to me by Prof.Dr.K.John Thomas, Dean i/c, KCAET, Tavanur as a member of my Advisory Committee.

My heartfelt thanks are due to Sri.M.R. Sankaranarayanan, Asst. Professor (Agrl.Engg.), College of Horticulture, Vellanikkara and Sri. Alexander Seth, Asst. Professor, Department of Irrigation and Drainage, KCAET,Tavanur and members of the Advisory Committee for their catalytic comments and creative suggestions.

I am thanking from my depths Sri. K.D.Namboothiripad, Head , Extension and Education Division, CWRDM , Calicut for his advice and help rendered during the study.

I do acknowledge the timely help rendered by Dr. K.I.Koshy, Head, Department of Supportive and Allied courses, KCAET, Tavanur during the analysis of the experimental data.

I wish to place on record my sincere thanks to Sri. A. P. Ananthanarayanan, Deputy Director, Hydraulic Division No. I, KERI, Peechi for his enthusiasm to this work.

I am extending my gratitude to all the staff of the Hydraulic Divisions of KERI, Peechi who assisted for the progress of my work

I acknowledge with infinite gratefulness, sincere advices of all the staff members of KCAET, Tavanur.

My sincere thanks are extended to my friends at KCAET, Tavanur for their remarkable cooperation and encouragement to me during the tenure.

I am thankful to the Kerala Agricultural University for granting me finance to pursue this work.

My profound appreciation to Blaise Computer Consultancy, Mannuthy, for the care and interest taken in typing the manuscript neatly.

The task would not have been completed successfully but for the patience and love of my parents, my gratitude to them for bearing with all the inconveniences.

**ROY MATHEW**

- *Dedicated to My Parents and Teachers*



## CONTENTS

Chapter	Title	Page No.
	LIST OF TABLES	viii
	LIST OF FIGURES	ix
	LIST OF PLATES	xvi
	SYMBOLS AND ABBREVIATIONS	xviii
I	INTRODUCTION	1
II	REVIEW OF LITERATURE	6
III	MATERIALS AND METHODS	19
IV	RESULTS AND DISCUSSION	46
V	SUMMARY	168
	REFERENCES	i - iv
	APPENDICES	
	ABSTRACT	

## LIST OF TABLES

Table No.	Title	Page No.
1	Details of experiments-Rigid bed and Single spur	38
2	Details of experiments-Rigid bed and Multiple spurs	39
3	Details of experiments-Mobile bed and Single spur	44
4	Details of experiments-Mobile bed and Multiple spurs	45
5	Grain size determination by sieve analysis	126
6	Specific gravity determination by pycnometer method	126

## LIST OF FIGURES

Figure No.	Title	Page No.
1.	Typical design of spur	11
2.	Variation of $(D + ds)/D$ with $F$ and $\alpha$	16
3.	Variation of $(D + ds)/D$ with $F^2/\alpha^3$	16
4.	Details of the model (Not to scale)	20
5.	Details of spur models tested (a) Dimensions tested (b) Spur angles tested (c) Spur spacings tested	24
6.	Head Versus discharge curve of cipolletti weir used	26
7.	Cipolletti weir for discharge measurement	27
8.	Stage discharge curve at c/s 7 in the model	30
9.	Locations of measuring stations for velocity measurement for (a) Single spur (b) Multiple spur scheme	33
10.	Flow pattern without spur for discharge rates (a) 14.14 lps (b) 28.28 lps (c) 42.42 lps	48
11.	Flow pattern for single spur ( $L=25$ cm, $\theta=90^\circ$ ) for discharge rates (a) 14.14 lps (b) 28.28 lps (c) 42.42 lps	49
12.	Flow pattern for single spur ( $L=35$ cm, $\theta=90^\circ$ ) for discharge rates (a) 14.14 lps (b) 28.28 lps (c) 42.42 lps	50
13.	Flow pattern for single spur ( $L=45$ cm, $\theta=90^\circ$ ) for discharge rates (a) 14.14 lps (b) 28.28 lps (c) 42.42 lps	51
14.	Flow pattern for single spur ( $L=55$ cm, $\theta=90^\circ$ ) for discharge rates (a) 14.14 lps (b) 28.28 lps (c) 42.42 lps	52
15.	Flow pattern for single spur ( $L=25$ cm, $\theta=100^\circ$ ) for discharge rates (a) 14.14 lps (b) 28.28 lps (c) 42.42 lps	53
16.	Flow pattern for single spur ( $L=35$ cm, $\theta=100^\circ$ ) for discharge rates (a) 14.14 lps (b) 28.28 lps (c) 42.42 lps	54
17.	Flow pattern for single spur ( $L=45$ cm, $\theta=100^\circ$ ) for discharge rates (a) 14.14 lps (b) 28.28 lps (c) 42.42 lps	55
18.	Flow pattern for single spur ( $L=55$ cm, $\theta=100^\circ$ ) for discharge rates (a) 14.14 lps (b) 28.28 lps (c) 42.42 lps	56

19.	Flow pattern for single spur (L=25 cm, $\theta = 110^\circ$ ) for discharge rates (a)14.14 lps (b)28.28 lps (c)42.42 lps	57
20.	Flow pattern for single spur (L=35 cm, $\theta = 110^\circ$ ) for discharge rates (a)14.14 lps (b)28.28 lps (c)42.42 lps	58
21.	Flow pattern for single spur (L=45 cm, $\theta = 110^\circ$ ) for discharge rates (a)14.14 lps (b)28.28 lps (c)42.42 lps	59
22.	Flow pattern for single spur (L=55 cm, $\theta = 110^\circ$ ) for discharge rates (a)14.14 lps (b)28.28 lps (c)42.42 lps	60
23.	Flow pattern for single spur (L=25 cm, $\theta = 120^\circ$ ) for discharge rates (a)14.14 lps (b)28.28 lps (c)42.42 lps	61
24.	Flow pattern for single spur (L=35 cm, $\theta = 120^\circ$ ) for discharge rates (a)14.14 lps (b)28.28 lps (c)42.42 lps	62
25.	Flow pattern for single spur (L=45 cm, $\theta = 120^\circ$ ) for discharge rates (a)14.14 lps (b)28.28 lps (c)42.42 lps	63
26.	Flow pattern for single spur (L=55 cm, $\theta = 120^\circ$ ) for discharge rates (a)14.14 lps (b)28.28 lps (c)42.42 lps	64
27.	Effect of spur angle on velocity at opposite bank for a discharge of 14.14 lps.	68
28.	Effect of spur angle on velocity at opposite bank for a discharge of 28.28 lps.	69
29.	Effect of spur angle on velocity at opposite bank for a discharge of 42.42 lps.	70
30.	Effect of spur length on velocity at opposite bank (spur angle = $90^\circ$ )	71
31.	Velocity grid without spur for discharge rates (a) 14.14 lps (b) 28.28 lps (c) 42.42 lps.	72
32.	Velocity grid along single spur (L=25 cm, $\theta = 90^\circ$ )for discharge rates (a)14.14 lps (b)28.28 lps (c)42.42 lps	73
33.	Velocity grid along single spur (L=35 cm, $\theta = 90^\circ$ )for discharge rates (a)14.14 lps (b)28.28 lps (c)42.42 lps	74
34.	Velocity grid along single spur (L=45 cm, $\theta = 90^\circ$ )for discharge rates (a)14.14 lps (b)28.28 lps (c)42.42 lps	75
35.	Velocity grid along single spur (L=55 cm, $\theta = 90^\circ$ )for discharge rates (a)14.14 lps (b)28.28 lps (c)42.42 lps	76
36.	Velocity grid along single spur (L=25 cm, $\theta = 100^\circ$ )for discharge rates (a)14.14 lps (b)28.28 lps (c)42.42 lps	77
37.	Velocity grid along single spur (L=35 cm, $\theta = 100^\circ$ )for discharge rates (a)14.14 lps (b)28.28 lps (c)42.42 lps	78

38.	Velocity grid along single spur (L=45 cm, $\theta = 100^\circ$ ) for discharge rates (a)14.14 lps (b)28.28 lps (c)42.42 lps	79
39.	Velocity grid along single spur (L=55 cm, $\theta = 100^\circ$ ) for discharge rates (a)14.14 lps (b)28.28 lps (c)42.42 lps	80
40.	Velocity grid along single spur (L=25 cm, $\theta = 110^\circ$ ) for discharge rates (a)14.14 lps (b)28.28 lps (c)42.42 lps	81
41.	Velocity grid along single spur (L=35 cm, $\theta = 110^\circ$ ) for discharge rates (a)14.14 lps (b)28.28 lps (c)42.42 lps	82
42.	Velocity grid along single spur (L=45 cm, $\theta = 110^\circ$ ) for discharge rates (a)14.14 lps (b)28.28 lps (c)42.42 lps	83
43.	Velocity grid along single spur (L=55 cm, $\theta = 110^\circ$ ) for discharge rates (a)14.14 lps (b)28.28 lps (c)42.42 lps	84
44.	Velocity grid along single spur (L=25 cm, $\theta = 120^\circ$ ) for discharge rates (a)14.14 lps (b)28.28 lps (c)42.42 lps	85
45.	Velocity grid along single spur (L=35 cm, $\theta = 120^\circ$ ) for discharge rates (a)14.14 lps (b)28.28 lps (c)42.42 lps	86
46.	Velocity grid along single spur (L=45 cm, $\theta = 120^\circ$ ) for discharge rates (a)14.14 lps (b)28.28 lps (c)42.42 lps	87
47.	Velocity grid along single spur (L=55 cm, $\theta = 120^\circ$ ) for discharge rates (a)14.14 lps (b)28.28 lps (c)42.42 lps	88
48.	Flow pattern for multiple spur scheme (L=25 cm, spacing=2L) for discharge rates (a)14.14 lps (b)28.28 lps (c)42.42 lps	91
49.	Flow pattern for multiple spur scheme (L=25 cm, spacing=3L) for discharge rates (a)14.14 lps (b)28.28 lps (c)42.42 lps	92
50.	Flow pattern for multiple spur scheme (L=25 cm, spacing=4L) for discharge rates (a)14.14 lps (b)28.28 lps (c)42.42 lps	93
51.	Flow pattern for multiple spur scheme (L=25 cm, spacing=5L) for discharge rates (a)14.14 lps (b)28.28 lps (c)42.42 lps	94
52.	Flow pattern for multiple spur scheme (L=35 cm, spacing=2L) for discharge rates (a)14.14 lps (b)28.28 lps (c)42.42 lps	95
53.	Flow pattern for multiple spur scheme (L=35 cm, spacing=3L) for discharge rates (a)14.14 lps (b)28.28 lps (c)42.42 lps	96
54.	Flow pattern for multiple spur scheme (L=35 cm, spacing=4L) for discharge rates (a)14.14 lps (b)28.28 lps (c)42.42 lps	97
55.	Flow pattern for multiple spur scheme (L=35 cm, spacing=5L) for discharge rates (a)14.14 lps (b)28.28 lps (c)42.42 lps	98

56.	Flow pattern for multiple spur scheme (L=45 cm, spacing=2L) for discharge rates (a)14.14 lps (b)28.28 lps (c)42.42 lps	99
57.	Flow pattern for multiple spur scheme (L=45 cm, spacing =3L) for discharge rates (a)14.14 lps (b)28.28 lps (c)42.42 lps	100
58.	Flow pattern for multiple spur scheme (L=45 cm, spacing =4L) for discharge rates (a)14.14 lps (b)28.28 lps (c)42.42 lps	101
59.	Flow pattern for multiple spur scheme (L=45 cm, spacing =5L) for discharge rates (a)14.14 lps (b)28.28 lps (c)42.42 lps	102
60.	Flow pattern for multiple spur scheme (L=55 cm, spacing =2L) for discharge rates (a)14.14 lps (b)28.28 lps (c)42.42 lps	103
61.	Flow pattern for multiple spur scheme (L=55 cm, spacing =3L) for discharge rates (a)14.14 lps (b)28.28 lps (c)42.42 lps	104
62.	Flow pattern for multiple spur scheme (L=55 cm, spacing =4L) for discharge rates (a)14.14 lps (b)28.28 lps (c)42.42 lps	105
63.	Flow pattern for multiple spur scheme (L=55 cm, spacing =5L) for discharge rates (a)14.14 lps (b)28.28 lps (c)42.42 lps	106
64.	Velocity grid along multiple spur scheme (L=25cm, spacing=2L) for discharge rates (a)14.14 lps (b)28.28 lps (c)42.42 lps	107
65.	Velocity grid along multiple spur scheme (L=25cm, spacing=3L) for discharge rates (a)14.14 lps (b)28.28 lps (c)42.42 lps	108
66.	Velocity grid along multiple spur scheme (L=25cm, spacing=4L) for discharge rates (a)14.14 lps (b)28.28 lps (c)42.42 lps	109
67.	Velocity grid along multiple spur scheme (L=25cm, spacing=5L) for discharge rates (a)14.14 lps (b)28.28 lps (c)42.42 lps	110
68.	Velocity grid along multiple spur scheme (L=35cm, spacing=2L) for discharge rates (a)14.14 lps (b)28.28 lps (c)42.42 lps	111
69.	Velocity grid along multiple spur scheme (L=35 cm, spacing=3L) for discharge rates (a)14.14 lps (b)28.28 lps (c)42.42 lps	112
70.	Velocity grid along multiple spur scheme (L=35 cm, spacing=4L) for discharge rates (a)14.14 lps (b)28.28 lps (c)42.42 lps	113
71.	Velocity grid along multiple spur scheme (L=35 cm, spacing=5L) for discharge rates (a)14.14 lps (b)28.28 lps (c)42.42 lps	114
72.	Velocity grid along multiple spur scheme (L=45cm, spacing=2L) for discharge rates (a)14.14 lps (b)28.28 lps (c)42.42 lps	115
73.	Velocity grid along multiple spur scheme (L=45cm, spacing=3L) for discharge rates (a)14.14 lps (b)28.28 lps (c)42.42 lps	116

74.	Velocity grid along multiple spur scheme (L=45cm,spacing=4L) for discharge rates (a)14.14 lps (b)28.28 lps (c)42.42 lps	117
75.	Velocity grid along multiple spur scheme (L=45cm,spacing=5L) for discharge rates (a)14.14 lps (b)28.28 lps (c)42.42 lps	118
76.	Velocity grid along multiple spur scheme (L=55 cm,spacing=2L) for discharge rates (a)14.14 lps (b)28.28 lps (c)42.42 lps	119
77.	Velocity grid along multiple spur scheme (L=55 cm,spacing=3L) for discharge rates (a)14.14 lps (b)28.28 lps (c)42.42 lps	120
78.	Velocity grid along multiple spur scheme (L=55 cm,spacing=4L) for discharge rates (a)14.14 lps (b) 28.28 lps (c) 42.42 lps	121
79.	Velocity grid along multiple spur scheme (L=55cm,spacing=5L) for discharge rates (a)14.14 lps (b)28.28 lps (c)42.42 lps	122
80.	Grain size distribution curve of the sand used	125
81.	Scour pattern without spur for discharge rates (a) 28.28 lps (b) 42.42 lps	127
82.	Scour pattern for single spur (L=25 cm, $\theta = 90^\circ$ ) for discharge rates (a) 28.28 lps (b) 42.42 lps	128
83.	Scour pattern for single spur (L=35 cm, $\theta = 90^\circ$ ) for discharge rates (a) 28.28 lps (b) 42.42 lps	129
84.	Scour pattern for single spur (L=45 cm, $\theta = 90^\circ$ ) for discharge rates (a) 28.28 lps (b) 42.42 lps	130
85.	Scour pattern for single spur (L=55 cm, $\theta = 90^\circ$ ) for discharge rates (a) 28.28 lps (b) 42.42 lps	131
86.	Scour pattern for single spur (L=25 cm, $\theta =100^\circ$ ) for discharge rates (a) 28.28 lps (b) 42.42 lps	132
87.	Scour pattern for single spur (L=35 cm, $\theta =100^\circ$ ) for discharge rates (a) 28.28 lps (b) 42.42 lps	133
88.	Scour pattern for single spur (L=45 cm, $\theta =100^\circ$ ) for discharge rates (a) 28.28 lps (b) 42.42 lps	134
89.	Scour pattern for single spur (L=55 cm, $\theta =100^\circ$ ) for discharge rates (a) 28.28 lps (b) 42.42 lps	135
90.	Scour pattern for single spur (L=25 cm, $\theta =110^\circ$ ) for discharge rates (a) 28.28 lps (b) 42.42 lps	136
91.	Scour pattern for single spur (L=35 cm, $\theta =110^\circ$ ) for discharge rates (a) 28.28 lps (b) 42.42 lps	137
92.	Scour pattern for single spur (L=45 cm, $\theta =110^\circ$ ) for discharge rates (a) 28.28 lps (b) 42.42 lps	138

93.	Scour pattern for single spur (L=55 cm, $\theta = 110^\circ$ ) for discharge rates (a) 28.28 lps (b) 42.42 lps	139
94.	Scour pattern for single spur (L=25 cm, $\theta = 120^\circ$ ) for discharge rates (a) 28.28 lps (b) 42.42 lps	140
95.	Scour pattern for single spur (L=35 cm, $\theta = 120^\circ$ ) for discharge rates (a) 28.28 lps (b) 42.42 lps	141
96.	Scour pattern for single spur (L=45 cm, $\theta = 120^\circ$ ) for discharge rates (a) 28.28 lps (b) 42.42 lps	142
97.	Scour pattern for single spur (L=55 cm, $\theta = 120^\circ$ ) for discharge rates (a) 28.28 lps (b) 42.42 lps	143
98.	Trend lines for scour versus spur angles for the constrictions tested (Discharge = 14.14 lps)	146
99.	Trend lines for scour versus spur angles for the constrictions tested (Discharge = 28.28 lps)	147
100.	Trend lines for scour versus spur angles for the constrictions tested (Discharge = 42.42 lps)	148
101.	Maximum depth of scour versus length of (spur angle = $90^\circ$ )	149
102.	Variation of $(D + ds)/D$ with F and $\alpha$ for single spur	150
103.	Variation of $(D + ds)/D$ with $F^2/\alpha^3$ for single spur	151
104.	Trend lines for LBP/L versus spur angles for the constrictions tested (Discharge = 42.42 lps)	152
105.	Trend lines for LBP/L versus spur angles for the constrictions tested (Discharge = 42.42 lps)	153
106.	Scour pattern for multiple spur scheme (L=25 cm, spacing = 3L) for discharge rates (a) 28.28 lps (b) 42.42 lps	155
107.	Scour pattern for multiple spur scheme (L=25 cm, spacing = 4L) for discharge rates (a) 28.28 lps (b) 42.42 lps	156
108.	Scour pattern for multiple spur scheme (L=25 cm, spacing = 5L) for discharge rates (a) 28.28 lps (b) 42.42 lps	157
109.	Scour pattern for multiple spur scheme (L=35 cm, spacing = 3L) for discharge rates (a) 28.28 lps (b) 42.42 lps	158
110.	Scour pattern for multiple spur scheme (L=35 cm, spacing = 4L) for discharge rates (a) 28.28 lps (b) 42.42 lps	159
111.	Scour pattern for multiple spur scheme (L=35 cm, spacing = 5L) for discharge rates (a) 28.28 lps (b) 42.42 lps	160



112.	Scour pattern for multiple spur scheme (L=45 cm, spacing = 3L) for discharge rates (a) 28.28 lps (b) 42.42 lps	161
113.	Scour pattern for multiple spur scheme (L=45 cm, spacing = 4L) for discharge rates (a) 28.28 lps (b) 42.42 lps	162
114.	Scour pattern for multiple spur scheme (L=45 cm, spacing = 5L) for discharge rates (a) 28.28 lps (b) 42.42 lps	163
115.	Variation of $(D + ds)/D$ with $F$ and $c$ for multiple spur scheme	165
116.	Variation of $(D + ds)/D$ with $F^2/c^3$ for multiple spur scheme	166
117.	Variation of $(D + ds)/D$ with discharge intensity ( $q$ )	167

## LIST OF PLATES

Plate No.	Title	Page No.
1	Overall view of the model	22
2	Measurement of flow using Cipolletti weir	28
3	Experiment setup for flow pattern observation	32
4	View of the current meter	35
5	Measurement of velocity using current meter	35
6	View of the model at rigid bed condition	40
7	View of the model at mobile bed condition	40
8	Scour pattern around single spur	43
9	Scour pattern around multiple spurs	43

## SYMBOLS AND ABBREVIATIONS

ASCE	- American Society of Civil Engineers
B,b	- channel width at constricted section
CBIP	- Central Board of Irrigation and Power
cm	- centimetre(s)
cm <sup>3</sup> /sec	- cubic centimetres per second
c/s	- cross section(s)
CWPRS	- Central Water and Power Research Station
d	- depth of flow for non scouring bed
db	- scour dpth measured from bed level
ds	- maximum depth of scour at spur nose
D	- average flow depth
D <sub>1</sub>	- depth of maximum scour below maximum water level
D <sub>L</sub>	- Lacey's scour depth
D <sub>50</sub>	- effective size of the bed material
<u>et al.</u>	- and others
F	- Froude number
Fig.	- Figure
ft	- feet
gm	- gram
IAHR	- International Association of Hydraulic Research
IS	- Indian Standard (s)
KCAET	- Kelappaji College of Agricultural Engineering and Technology
KERI	- Kerala Engineering Research Institute
L,l	- spur projected length

LBP	- length of bank protected
lps	- litres per second
m	- metre(s)
mm	- millimetre(S)
m <sup>3</sup>	- cubic metre(s)
min	- minute(s)
N	- Number of revolutions per second
No.	- Number
pp	- pages
q	- discharge intensity
Q	- discharge
sec	- second(s)
T,t	- time
V	- velocity
y	- depth of flow
'	- minute(s)
:	- is to
/	- per
%	- percent
°	- degree
θ	- spur angle
∞	- opening ratio

# Introduction

---

## INTRODUCTION

Rivers constitute the most valuable natural wealth of a country. They occupy an important place in every stage of human development. They are responsible for the development of industry and agriculture in a country. But these rivers can also do much havoc. If the rivers are allowed to pursue their own course unhampered, they cause floods, erosion of banks and loss of valuable property. It is therefore necessary to control or train the rivers and try to make them behave as we desire.

River training in its broad meaning covers all engineering works constructed on a river to guide and confine the flow to the river channel and to control and regulate the river bed configurations for effective and safe movement of floods and river sediment. It is a very comprehensive subject which includes flood detention reservoirs, flood control works, regional training of rivers usually major ones and local training of rivers such as the protection of a railway bridge or a town. Before we attempt to train a river, it is essential to know its behaviour and have considerable data such as flood hydrographs, gauges, types of bed material etc. No two rivers are alike and as such the problems to be solved will be quite varying in nature.

Most of the river basins in our country are alluvial in nature and therefore notoriously unstable. The constant and unpredictable shifting of these river courses brings every year untold devastation and misery to millions in the country. The rivers swollen with heavy floods, inundate vast areas of fertile and cultivable land damaging standing crops. Huge quantities of sand deposited on the inundated lands, render them unproductive over long periods. Cities, towns and villages are eroded and washed away. Lines of communication are threatened and weirs, barrages and irrigation works are in constant danger of getting out flanked. Bank erosion is one of the major problems caused by floods in the river basins of Kerala, especially for the rivers Bharathapuzha, Periyar and Pamba. To make rivers behave as desired and to prevent their ravages, training works for flood control and bank protection on a large scale are therefore imperative here which in turn focus on the importance of spurs.

Spurs are structures constructed transverse to the river flow and extend from the bank into the river. They are known by several names, the most popular being spurs, spur dikes and transverse dikes and constitute probably the most widely used training measure. Spurs are more successful than other training measures where problem involved is of protecting a valuable land, towns, villages or highways etc. against erosion or for flow diversion or

maintenance of a particular channel. This is because of the fact that they throw water away from the affected bank causing deposition along the bank, thus may protect the stream bank more effectively and at less cost than other training measures.

Spurs have served as one of the important river training measures since historic times. Historical records reveals that in the East, the first attempt at river training consisted of embankments constructed across spill channels. The river was confined to flow in a single deep channel by groynes projecting from river banks, designed to prevent erosion. Spurs as river training measures have been designed and constructed since long in India, especially at barrages and bridges even before 1900 as mentioned in Springs book on guide bank design.

Spurs serve one or more of the following functions:

- (1) Training a river along a desired course by attracting, deflecting or repelling the flow in a channel.
- (2) Creating a slack flow with the object of silting up the area in the vicinity.
- (3) Protecting the river bank by keeping the flow away from it.
- (4) Contracting a wide river channel usually for the improvement of depth for navigation.



However no well defined design procedures for the spurs have been formulated yet. The spurs are in many cases built based upon the experience and engineering judgements of site engineers, who are familiar with the behaviour of rivers. It is also seen that there are no specific formulae for the design parameters of spurs, other than certain guidelines based upon width, depth of flow, discharge intensity of river etc.

Due to uncertain behaviour of rivers and lack of any rigid mathematical formulae for designing training works, it is always useful to test such measures in hydraulic models and visualise their behaviours. Today hydraulic models are very useful aid in engineering practice provided the results are properly interpreted. Models can predict with fair degree of certitude the outcome of a training or of a control measure. Physical model studies related to solution of specific river training problems by use of spurs have been conducted by many investigators which throw light on various parameters like scour downstream of spurs, constriction, angle of approach, flow characteristics, bed material properties etc.

However no serious attempt have so far been made to bring together the experiences to evolve standard designs for spurs indicating the conditions under which they could

be used and extent of protection that could be expected there of. In this study an attempt is made to analyse various design parameters of spurs such as length, spacing, angle etc by simulation techniques.

The main objective of the research work is to conduct simulation studies on spurs (groynes) with rigid bed as well as mobile bed condition under varying design parameters such as length, spacing etc.

The specific objectives of the study are as follows:

1. To select and modify an existing river model or flume at KERI, Peechi to suit the objectives of the study.
2. To study the velocity distribution along the spur as well as on various cross sections of the model or the flume for different design parameters of spurs.
3. To study the flow pattern along the model or the flume for different design parameters of spurs.
4. To study the scour pattern and maximum scour depth for different design parameters of spurs.

# Review of Literature

---

## REVIEW OF LITERATURE

The importance of rivers has been recognised from very early times. World history shows that progress of civilisation followed river valleys and basins. They have occupied a very prominent place in every stage of human development. But these rivers can cause floods, erosion of banks and loss of valuable property etc., if they are not trained or controlled as we desire. Spurs are very successful training measure for flood control and bank protection in a river and probably the most widely used training work. Spurs are structures constructed perpendicular to the river flow and extend from the bank into the river. They train the river by attracting, deflecting or repelling the flow in the river and protect the river bank by keeping the flow away from it. Different types of spurs such as submerged, non-submerged, permeable, impermeable, attracting, deflecting, repelling, Hockey type, T-headed type etc. are used based on their performance in the river training problem.

### 2.1 Spurs As River Training Measure

River training by embankment for flood protection has a long history and must be the one of the earliest engineering achievements of man. In the East, the first attempt at river training consisted of embankments constructed across spill channels. In Europe, structures

like spurs were used for improvement of the navigability of rivers by maintaining a narrow and deep channel needed for expeditious navigation. Even before 1900, spurs were used at barrages and bridges in India. A summary of the relevant conclusions of the various investigators connected to the subject is given below, under different sub headings.

## **2.2 Design Aspects of Spur Like Structures**

The design of a spur under various conditions depend on the following important parameters namely, (a) discharge in the river (b) angle of attack (c) sediment load in the river (d) meander length (e) curvature of the river etc. Secondly depending on the purpose, groynes can be used singly or in series. The various design parameters of spurs such as length, spacing, angle etc. should be designed accurately because of the large investment of capital and labour involved in the construction of these structures.

### **2.2.1 Length and Orientation of Spur**

No general rules have been formulated for fixing the length of groynes as it depends entirely on the exigency arising in a specific case. The length should not be shorter or longer as it adversely affects the adjacent or opposite bank. The groyne should make an angle upstream with the bank in the range of  $60^\circ$  to  $85^\circ$ ;  $70^\circ$  to  $85^\circ$  is considered a more desirable range.

Moni (1961) conducted experiments to study the effect of groyne on movable beds and banks and showed that the groyne should be less than 1/3 the width of the river to have no effect on opposite bank and the repelling groyne is always preferable to an attracting groyne for bank protection.

Gupta et al (1969) carried out dimensional analysis, for the flow in a curved alluvial river with spurs and indicated that the ratio  $l/b$  depends on  $A$  (Arc/chord ratio) and froude number  $F$ . They concluded that the minimum spur length required to control a riverloop can be determined from the model scour pattern at nose etc. They gave an empirical relation  $l/b = 0.11 (A/\sqrt{F})^{3/2}$  for the determination of spur length.

Garde et al (1969) analysed the model data to determine the criteria for the determination of length of bank protected by a spur on the basis of dimensional analysis. They have shown that the protected length ( $N$ ) is a function of the length ( $l$ ) and inclination ( $\theta$ ) of the spur, radius of curvature of stream ( $R$ ), channel width ( $B$ ) and opening ratio ( $\alpha$ ). They have collected data recommended by various research stations and on the analysis of the same, they also gave a graphical relation between  $N/b$  and  $R/b$  for design purpose. They recommended that  $\alpha$  should always be

greater than 0.7 so that the spur will interfere with the river regime the least. They also recommended that the spur should make an angle of  $95^{\circ}$  to  $110^{\circ}$  with the bank.

Varshney and Mathur, (1972) have attempted to formulate empirical rules for specific case of repelling spur based on some field data and dimensional analysis. They gave some guidelines for spur location, spur length and orientation based on froude number, discharge intensity etc.

Miller et al (1983) conducted model studies on a spur placed in a flume to investigate parameters utilized in spur design. They establish a data base of the pertinent spur design parameters from laboratory studies in order to provide guidelines for the use of spurs for bank protection and flow control alignment for highway embankments and stream crossings. They investigated the relationship between spur design parameters of orientation to flow, projected length, crest elevation and scour. They found impermeable groynes produce the greatest change in scour elevation with spur projected length and relative velocity at spur tip increase with spur projected length. They also found that length of bank protected, scour elevation are always increased with spur angle and relative velocity at spur tip reduces with increasing spur angle.

CWPRS (1987) undertook the research project "Design of Spurs" and conducted laboratory experiments where in the

performances of spurs under straight reach was studied. The results obtained from single spur study indicated that the constriction of channel by spur should be restricted to 0.2 of the flow width and single spur provides protection to river for 3-5 times its length.

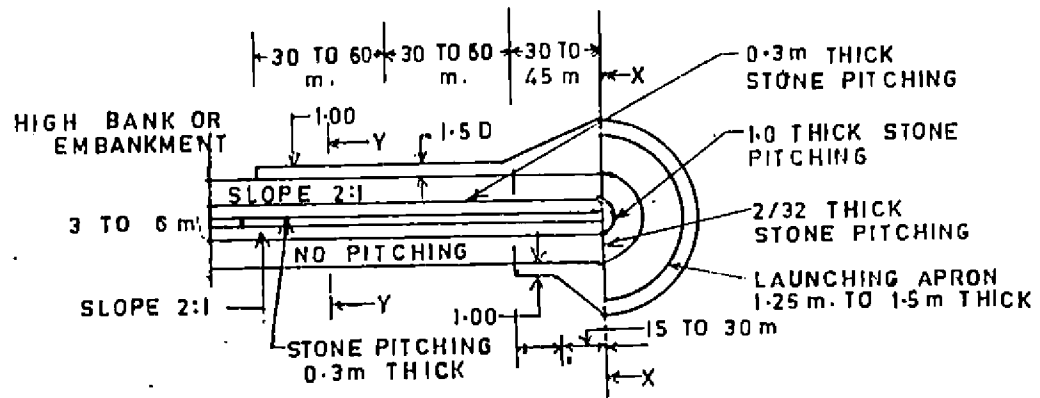
### 2.2.2 Height of Spurs

Spurs are normally designed for full height upto the bank level. If height is kept smaller, they are likely to function similar to weirs, causing excessive velocities to develop on the face and also on the river bank. Miller et al (1983) conducted experiments on submerged and non-submerged spurs and found that the elevated crest conditions gave greater local scour at the spur tip than did the submerged crest condition. They also found that non submerged spur gave more relative velocity at spur tip.

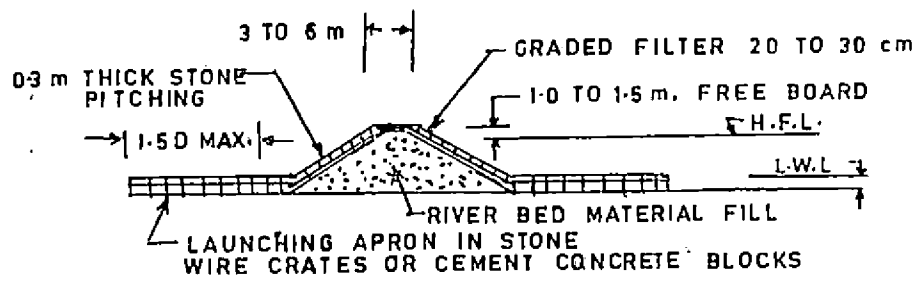
### 2.2.3 Top Width

The top width of spur should be 3 m to 6 m at formation level and a free board of 1 m to 1.5 m should be provided above the highest flood level (HFL). Slopes on upstream shank and nose should be 2 H : 1 V and the slope of downstream face may be 1.5 H : 1 V to 2 H:1V (Fig. 1) as per standards.

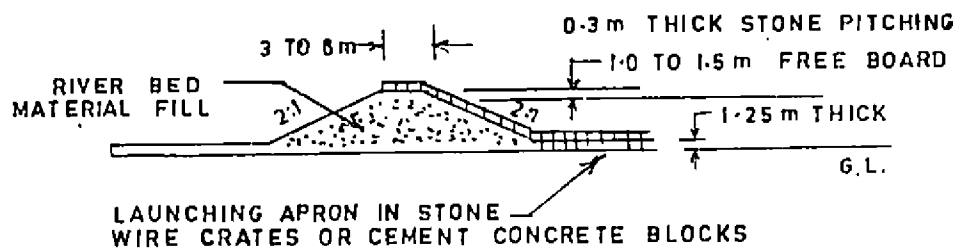




PLAN



SECTION — X X



SECTION — Y Y

FIG. 1. TYPICAL DESIGN OF SPUR

(Source - Manual on river behaviour control and training. CBIP)

#### 2.2.4 Spacing Between Spurs

Depending on the purpose, groynes can be used singly or in series. The choice of using them in a series arises, if the reach to be protected is long. In a straight reach of the river, usually a series of spurs are required to provide bank protection while in a curved reach the river can be trained by a limited number of spurs.

The general practice is to adopt a spacing equal to a certain proportion of the length of the groyne (usually 2 to 2.5 times) varying with the width of the river. Mustaq Ahmed (1951) carried out experiments in order to find out optimum spacing and length of spur dikes for effective protection of the bank. T-headed spur dikes were used for this study instead of simple straight ones. It was observed that a single T-headed spur dike could protect the bank to a length of 3-5 times the projection of spur dikes. Further he has shown that if two spur dikes are used, the optimum spacing should be approximately five times the projection of spur dikes. It was also suggested that if the bank to be protected is considerably long, more spur dikes with the above mentioned spacing could be used.

CWPRS (1987) shows that spur scheme with  $L/B = 0.2$  and spacing between spurs as  $5L$  is more economical for bank protection in a straight reach.

Kong et al (1990) pointed that the economical arrangement of groynes may be calculated by which the hydraulic contraction ratio of every groyne is equal.

#### 2.2.5 Scour Depth

During heavy floods the bed of the channel around spur like structures gets scoured to greater depth, sometimes even to the extent of exposing their foundation. One of the consideration in the design of foundation of these structures is the probable maximum depth of scour. Also the launching apron laid around spur dikes as a protection against scour, are designed after an estimation of maximum scour depth likely to occur around them.

Lacey (1930) was the first to give certain empirical formulae for determining the depth of scour at different modifications of an alluvial channel. Lacey's scour depth given by  $D_L = 0.47 (Q/f)^{1/3}$  where  $Q$  is the discharge and  $f$  is the silt factor. Analysis of available data of scour depth at the nose of the spurs is generally of the order between  $2.25 D_L - 3.5 D_L$  in case of 1:3 slope.

Many of the investigators namely Khosla et al (1936), Inglis (1939), Blench (1957) etc. made some modifications to Lacey's equation by applying correction factors to it. Inglis suggested a scour depth for straight spur dike facing upstream ranging from  $2.25 D_L$  to  $3.8 D_L$ . Blench proposed a coefficient ranging from 2 - 2.75 to Lacey's equation for the determination of scour depths at spur dike nose.

Laursen (1953) studied scour around obstruction in a channel and proposed a design curve of  $ds/b$  against  $D/b$  based on the experimental data where  $ds$  is the maximum scour depth and  $b$  is the width of the channel. Andru (1956) collected all available data on scour depths obtained from various sources and proposed an equation for scour depth prediction  $D_s (F_b)^{1/3} = 2.05 q_1^{2/3}$  where  $F_b$  is the bed factor,  $q_1$  is the discharge per foot width of the contracted section.

Mustaq Ahmed (1951), Garde et al (1961) and Quader (1982) have conducted model experiments for studying the effect of discharge intensity, flow concentration and angle of attack on the scour depth at a spur nose. Following formula for estimating maximum scour has been proposed  $D_s = k q_1^{2/3}$  where  $D_s$  = depth of maximum scour below maximum water level,  $q_1$  = discharge intensity at the spur construction,  $k$  = a constant depending up on the flow concentration, inclination of spur and angle of attack.

Garde et al (1961) conducted model studies on a spur placed at right angle to the flow in a flume dressed with sand of 0.29 mm size. The constriction ratio was kept 0.33 in all experiments while the discharge intensity and depth of flow were varied. Considering that the scour around the spur is essentially a bed load problem, dimensional analysis was done and from the experimental data, he derived the following relationship for a single spur placed

at right angles to flow as  $D_s/D = 0.03 \{ \tau^* (V/V^*)^5 \}^{1/2}$   
 where  $D_s$  = depth of flow at maximum scour bed,  $D$  = average  
 flow depth,  $V^*$  = shear velocity  $V$  = average flow velocity,  
 $\tau^*$  = shear stress.

While studying the effect of constriction ratio on the scour in the model by varying it from 10 % to 47 %, Garde et al (1961) further found that for a spur inclined at 90 to the flow and placed in sand of 0.25 mm size, two parameters viz froude number  $F$  and ratio  $b/B$  are adequate for defining the flow and geometry of the spur. Based on dimensional analysis and experiments results, they derived the relationship:  $D_s / D = K (b/B)^{1/3} F^{2/3}$ , where  $K$  = a constant whose value depends on average drag coefficient  $C$  of the sediment. Graphical representation of this relations is shown in Fig. 2 & 3.

Govinda Rao and Sharma, (1965) have given the equation  $db/y = MF/C - P$  for scour around deflecting spur dikes. Where  $db$  = scour depth measured from bed level,  $y$  = depth of flow,  $F$  = froud number,  $c$  = ratio of actual waterway at the top of spur to the approach water way,  $P$  = a constant which depends on sediments size.

Rajaratnam et al (1983) studied the development of clear water scour near simple groyne like structure. They conclude that the growth of maximum depth of scour with time

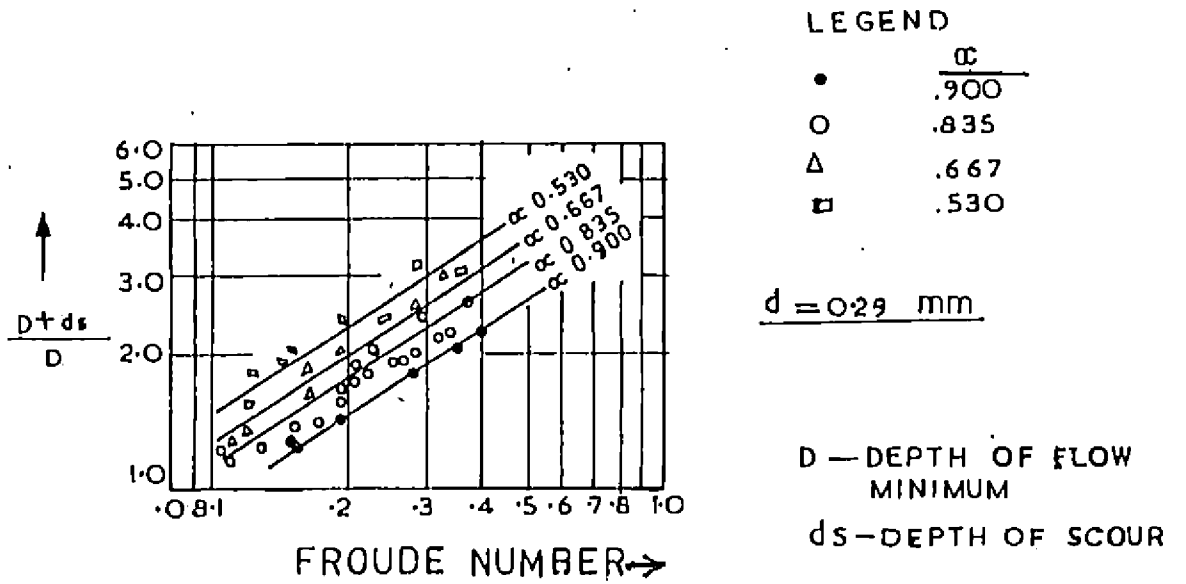


FIG. 2. VARIATION OF  $(D + ds)/D$  WITH  $F$  AND  $\alpha$

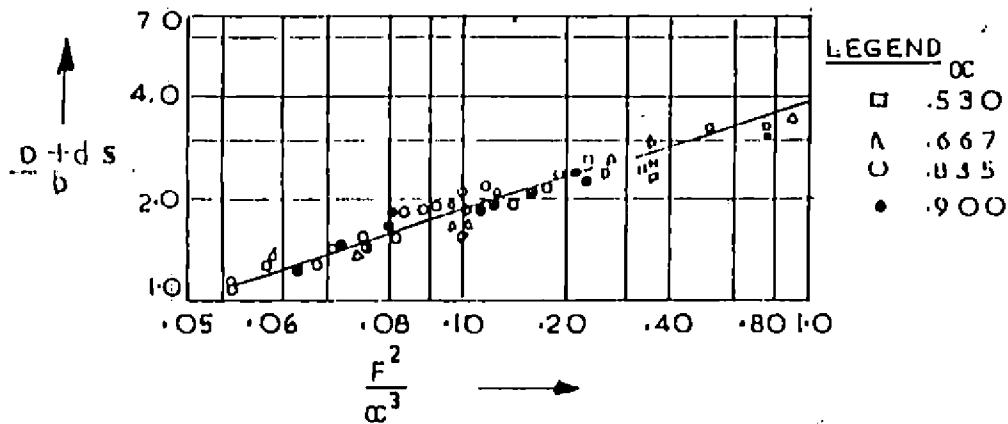


FIG. 3. VARIATION OF  $(D + ds)/D$  WITH  $F^2/\alpha^3$

(SOURCE - Design of spurs (groynes), CWPRS)

has been found to be similar. Further the characteristics of the scour hole in the end state have also been found to be similar. They developed simple correlation for predicting the maximum depth of clear water scour in the end state.

CWPRS (1987) conducted experiments on spurs and found maximum scour depth rapidly increases after  $L/B = 0.16$  in case of perpendicularly placed single spur to a straight reach.

### **2.3 Flow Near Spur and Velocity Distribution around Spur.**

If a spur is constructed in the channel, the velocity field and pressure field are changed. As the water level increases the flow upstream of the spur is restricted, and then part of the stream expands suddenly downstream the spur. The flow is blocked by the spur and a part flows around the spur head, another submerges along the upstream surface of the spur changing direction and then flowing by the spur head.

France (1968), Dou (1978), Wan (1987) studied the flow near groyne like structure and indicated that the length of recirculating region increases with the length of groyne.

From the experimental results of France (1968) and Wan (1987) the length of recirculating region is found to be

almost independent in the range of  $60^\circ - 150^\circ$ . For less than  $60^\circ$  the flow near the bed follows the downstream face of the groyne and reducing the mean length of recirculating region.

Rajaratnam et al (1983) presented the structure of turbulent flow near groyne like structures. The disturbed flow was analysed by splitting it into a deflected flow region and shear layer. The deflected flow condition due to spurs have been analysed. He found shear stress amplification  $\tau_{om}/\tau_{oo}$  varies with  $b/B$ .

Rajaratnam et al (1983) and Lu Yougjun (1988) shows that velocity and stress field are scarcely affected by the rate of beam width restriction ( $L/B$ ).

Lu Yougjun (1988), Lu Yougjun and Zhon Yaoting (1989) studied the flow near unsubmerged groyne like structure. They found there exists a mainflow region and a complete recirculating region, and studied about the recirculating flow region near spurs. Experiments gave a result that recirculating flows near spur were of weak intensities and were within the relatively dead water.

In addition, they have also studied velocity field near the hook groyne and training structure and velocity field near redeveloping region behind the groyne by using similarity.



# Materials and Methods

---

## MATERIALS AND METHODS

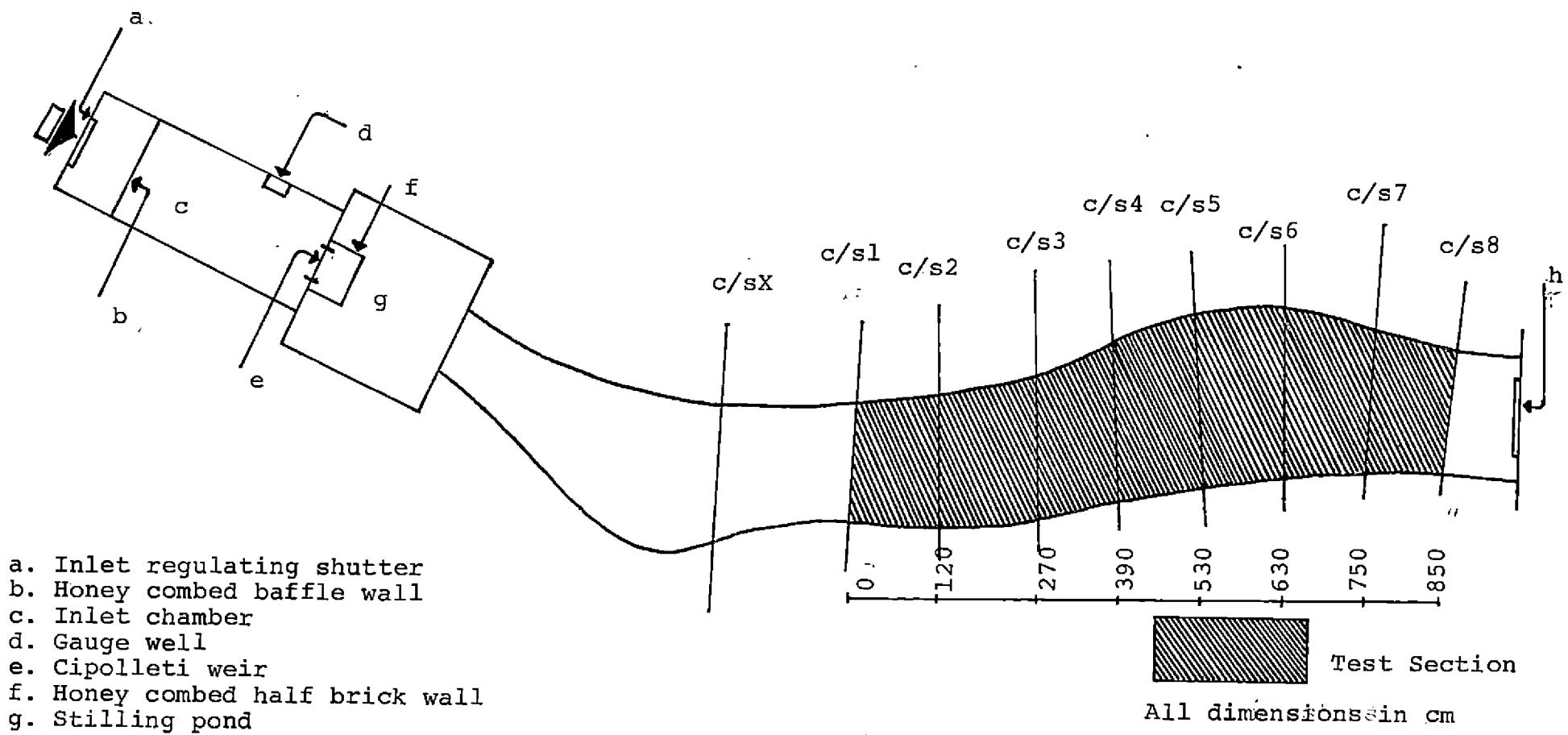
This chapter describes the materials used and the methods employed for achieving the objectives. A model study to analyse various design parameters of spurs (groynes) was conducted at KERI, Peechi during the months of March to September 1994.

### 3.1 Location

The model study was conducted in the outdoor model area of hydraulic division No.II of KERI, Peechi in Trichur district of Kerala. The place is situated at  $10^{\circ} 26'$  North latitude and  $76^{\circ} 24'$  East longitude.


### 3.2 Model

A distorted type 3D river model of Aranmula water stadium in Pamba river was selected for the study. It was constructed in the outdoor model area of KERI, Peechi for erosion studies in Pamba river. The sides of the model were made with clay and the river bed was formed rigid as well as mobile condition according to the objectives of the study. Inlet and outlet regulating shutters were provided for controlling discharge and depth of flow respectively. The details of the model set up are shown in Fig.4. The shaded portion in the Fig.4 was selected as the test section for the present study. It measures a length of 8.50 m, depth 0.4 m and width varying from 1.60 to 2.60 m. The study was



- a. Inlet regulating shutter
- b. Honey combed baffle wall
- c. Inlet chamber
- d. Gauge well
- e. Cipolletti weir
- f. Honey combed half brick wall
- g. Stilling pond
- h. Tail water regulating shutter

FIG. 5. DETAILS OF THE MODEL (NOT TO SCALE)

 Test Section  
 All dimensions in cm

aimed at comparing different design parameters of spurs such as length, angle, spacing, etc. for different discharges and to obtain suitable values for design parameters at the test section. Three discharge rates were chosen as 14.14 lps, 28.28 lps and 42.42 lps from the flood details of the river and the availability of water at the experiment site. From theoretically prepared rating curve at c/s 7 downstream of the test section, depths of flow corresponding to discharges chosen were computed as 4.00 cm, 6.10 cm and 7.80 cm respectively at that cross section. The over all picture of the model under study is given in Plate 1.

### 3.3 Model scale

The experimenter connected with model study is usually confronted with four availables: (a) time, (b) space, (c) money and (d) water supply while selecting scale ratios for models. In nature when the size of the stream is small, depths increase relatively in proportion to widths, which is nature's way of maintaining turbulence. To conform with this, river models are made with vertical scales larger than horizontal scales. It is useful in getting accuracy in vertical measurement, shortening of model test times, high flow velocities in a model, etc. In practice, models of rivers are being designed to scale ratios of horizontal dimensions not much larger than 1:100 and not much smaller than 1:200. The ratios of vertical dimensions are not much larger than 1:50 and not much smaller than 1:150.



Plate 1 Overall view of the model

The model selected in the present study was constructed with a horizontal scale 1 in 100 and vertical scale 1 in 50 with giving considerations to above facts.

i.e. Horizontal scale ratio  $L_r = (L_{\text{proto}})/(L_{\text{model}}) = 100$

Vertical scale ratio  $D_r = (D_{\text{proto}})/(D_{\text{model}}) = 50$

As the model satisfies Froude's law, velocity ratio  $V_r = \sqrt{g_r D_r} = \sqrt{D_r}$ . Since the value of "g" is same for both prototype and model. Therefore  $V_r = \sqrt{50} = 7.071$ .

Discharge ratio  $Q_r = (Q_{\text{proto}})/(Q_{\text{model}}) = (A_p \times V_p)/(A_m \times V_m)$   
 $= (L_p \times D_p^{1.5})/(L_m \times D_m^{1.5}) = 35355.33$

Time ratio  $T_r = T_p/T_m = L_r/V_r = L_r/\sqrt{D_r} = 14.142$

### 3.4 Spur model

The spurs used in the model were of 'Anjhily' wood planks of thickness 3mm and projected lengths of 25cm, 35cm, 45cm and 55cm. Different lengths of spurs were computed from the relation  $(B-L)/B \leq 0.7$  with a view that it will not affect much in the opposite bank.

The spur nose was rounded and the height selected was 25cm sufficient to project well above the water surface. The spur orientation selected were  $90^\circ$ ,  $100^\circ$ ,  $110^\circ$  and  $120^\circ$  downstream with the bank. The details of the spur models tested are shown in Fig. 5. The spur model was fixed at c/s 2 on the right bank of the model with a view that the

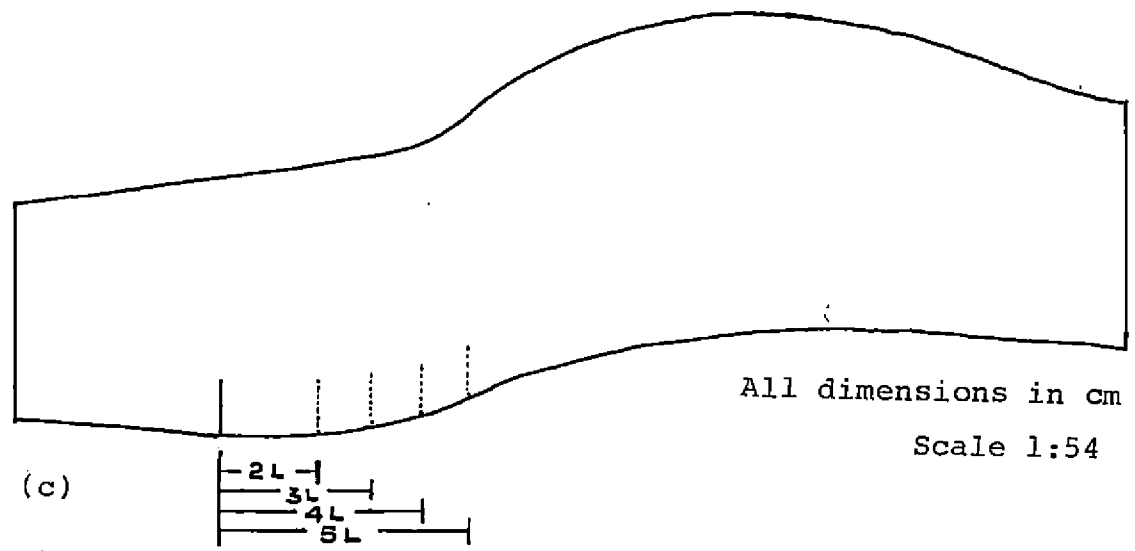
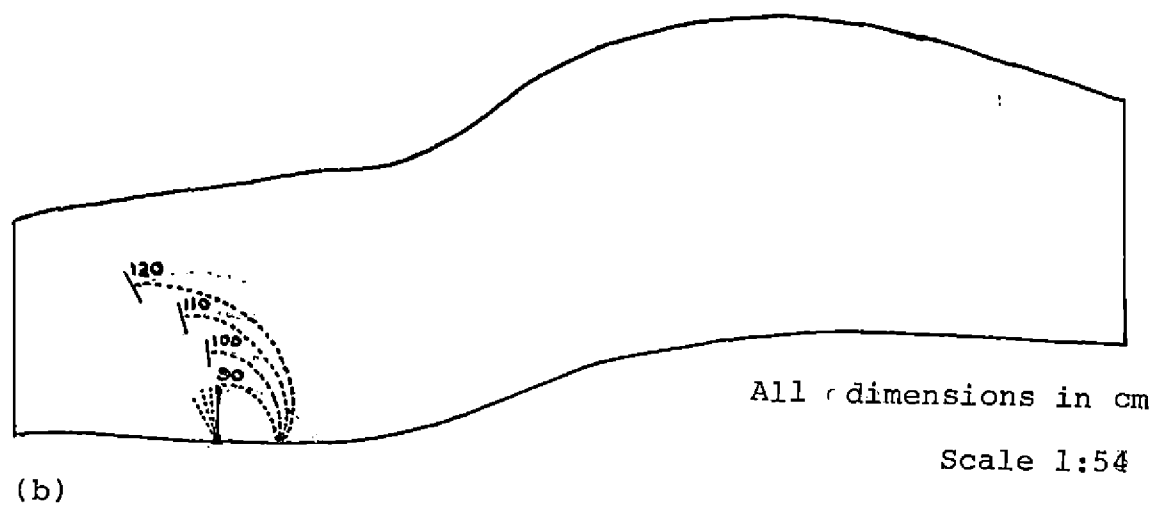
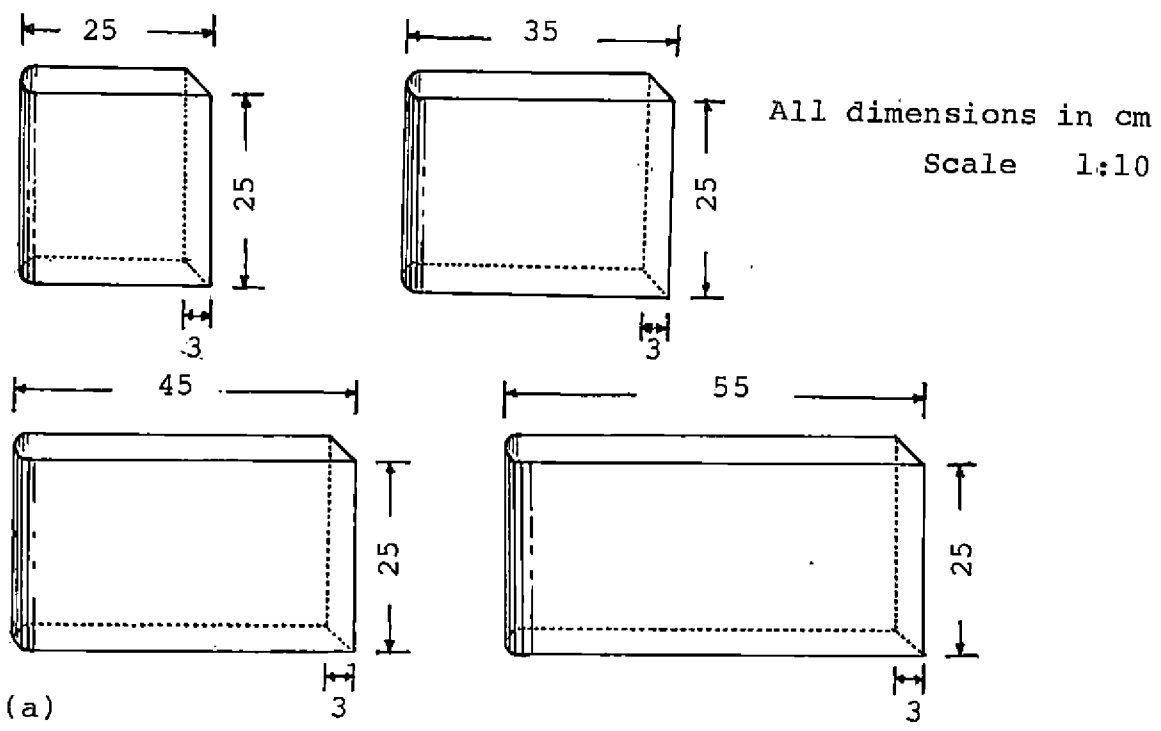


FIG. 58 DETAILS OF SPUR MODELS TESTED (a) DIMENSIONS TESTED

entrance effects didnot extend upto this distance and sufficient length of bed downstream of the spur model was given to contain the scour pattern.

In the multiple spur study perpendicularly placed spurs (two in series) of length 25cm, 35cm, 45cm and 55cm with spacing of 2L,3L,4L and 5L have been investigated.

### 3.5 Discharge Measurement

A Cipoletti weir was used to regulate the model discharge. It was fitted at the end of the inlet chamber so that by measuring the head of water over the weir, the discharge could be calculated. The head of water over the weir was measured by a standard hook gauge fitted in a gauge well which is at a small distance upstream of the weir. Before the start of the experimental study, calibration of weir was made and heads of water over the weir corresponding to various discharges chosen were maintained according to the calibration curve of the weir. The head discharge relationship obtained is given in Fig. 6. A view of the cipolleti weir and the cipolleti weir as used in the model for flow measurement are shown in Fig.7 and Plate 2 respectively.

### 3.6 Supply of Water into The Model

Water is supplied from the dam reservoir near the experiment site through a controlled supply line and a



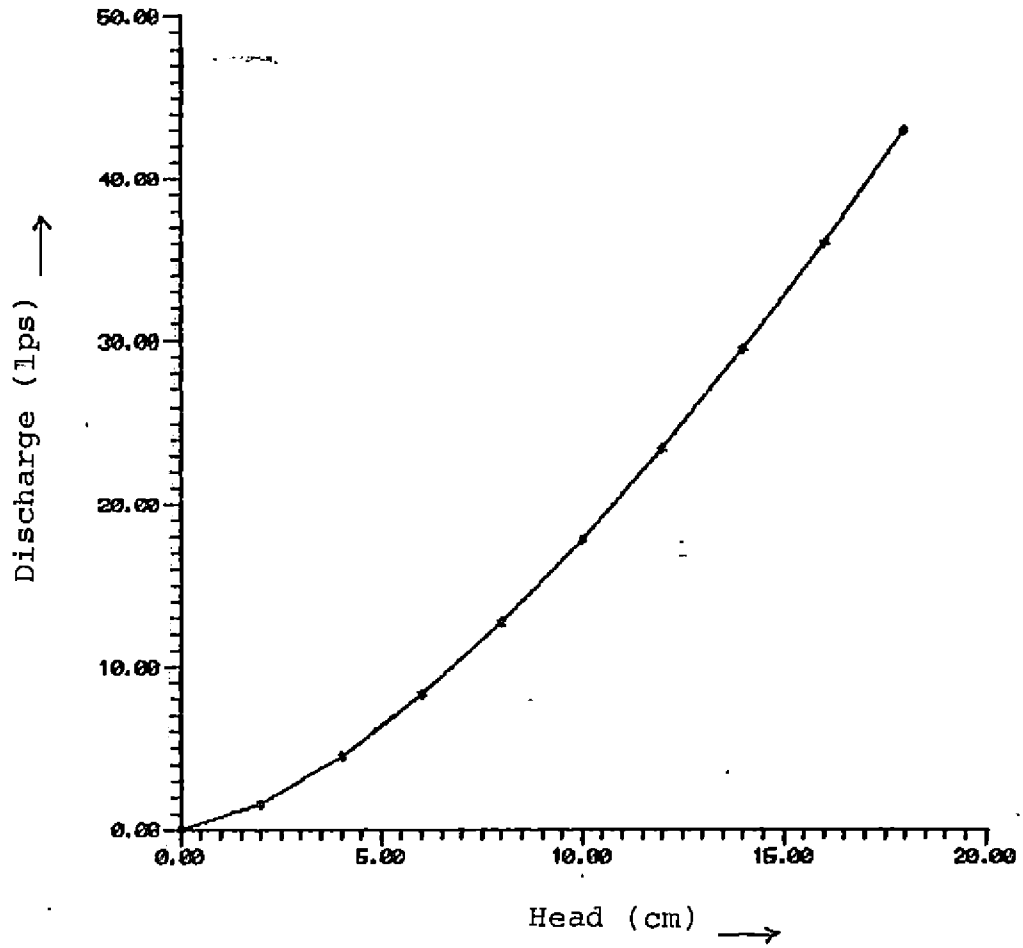
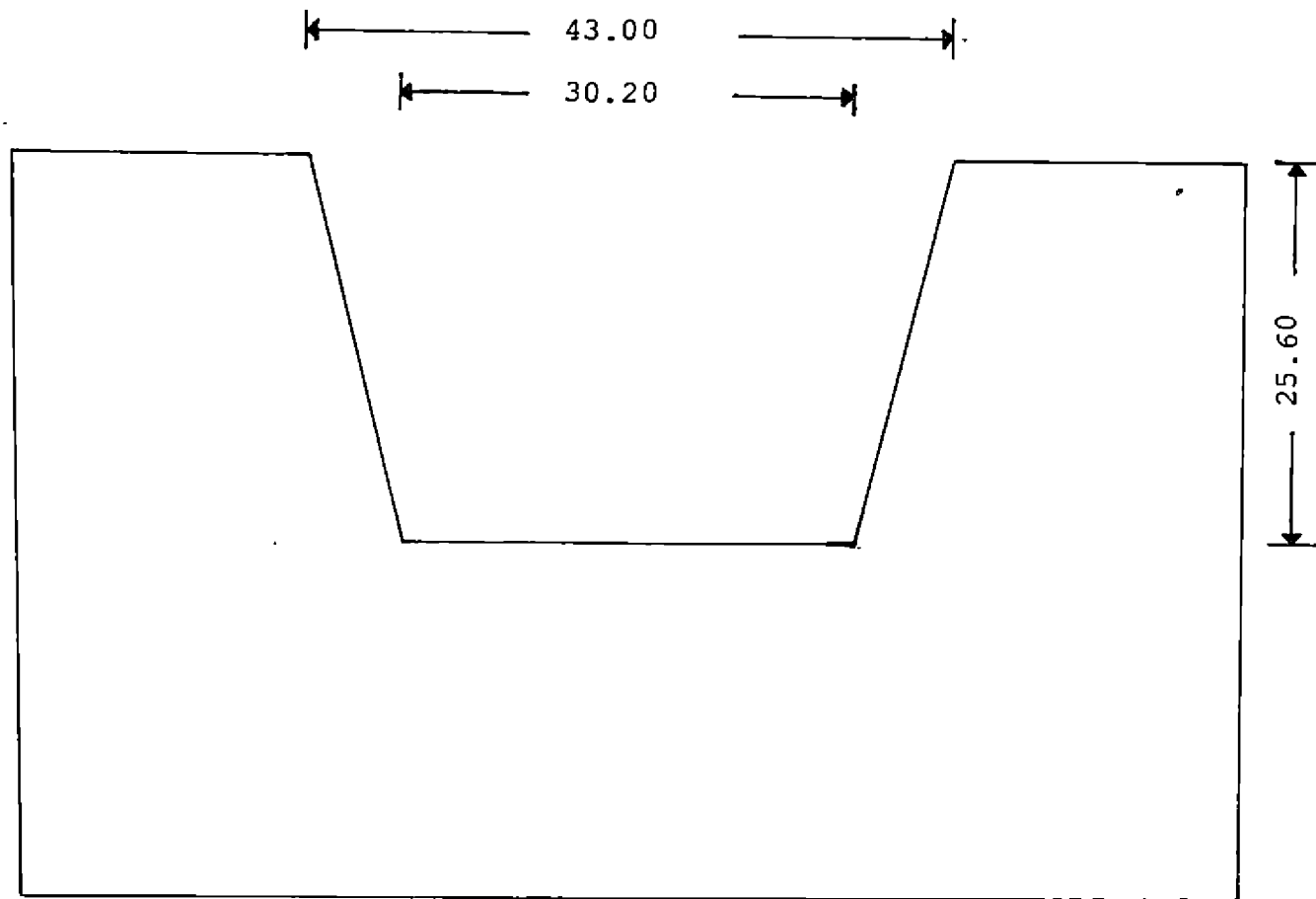


FIG. 6. HEAD VERSUS DISCHARGE CURVE OF CIPOLLETTI WEIR USED



All dimensions in cm  
Scale 1:5

FIG. 7 CIPOLETTI WEIR FOR DISCHARGE MEASUREMENT



Plate 2 Measurement of flow using Cipolletti weir

flume. The quantity of water required to maintain each discharge is admitted into the inlet chamber of the model by adjusting inlet regulating shutter. Honey combed baffle wall at the inlet chamber entry distributed the flow uniformly over the entire width of the chamber and also helped in dissipating the excess energy of the flow. Water then passes over the cipolleti weir and dropped into the stilling pool and then let into the model as could be seen in Fig. 4.

### 3.7 Preparation of Stage Discharge Curve

In case of river models, a stage discharge relationship for the full range from the minimum discharge to the maximum was required for proving the model. So depths of flow corresponds to each discharge used in the study were found at c/s 7 which is near to downstream of the test section. It was computed by preparing stage discharge curve theoretically at that cross section from the model dimensions. The depth of flow according to the stage discharge curve prepared was maintained by lowering or raising the water regulating shutter. The stage discharge curve prepared at c/s 7 is shown in Fig. 8.

### 3.8 Flow Pattern Observation

In the flow pattern observation, pearls were used as floats throughout the experimental study. Flow patterns were observed by putting pearls in a cross section " X "

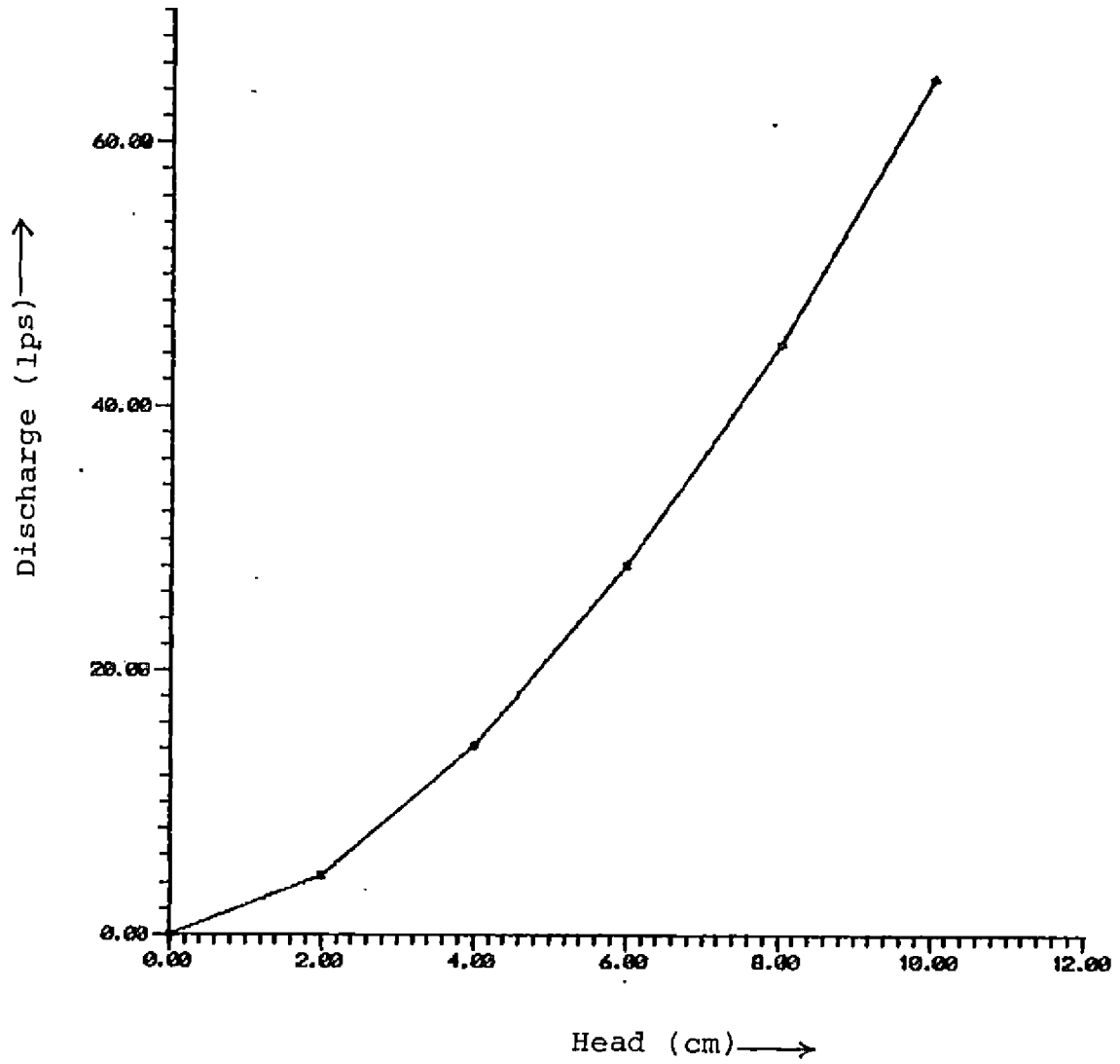


FIG. 8. STAGE DISCHARGE CURVE AT C/s 7 IN THE MODEL

upstream of the test section at equal distances of 25 cm from left bank and noting the distance from the left bank through which the pearls passes in the subsequent cross sections. Mild steel anglers were marked and placed at each cross sections, so that the distance through which the pearls passes in each cross sections could be noted. With these data, flow patterns at each experiment condition could be plotted. The experiment setting for flow pattern observation is shown in Plate 3.

### 3.9 Measurement of Velocity

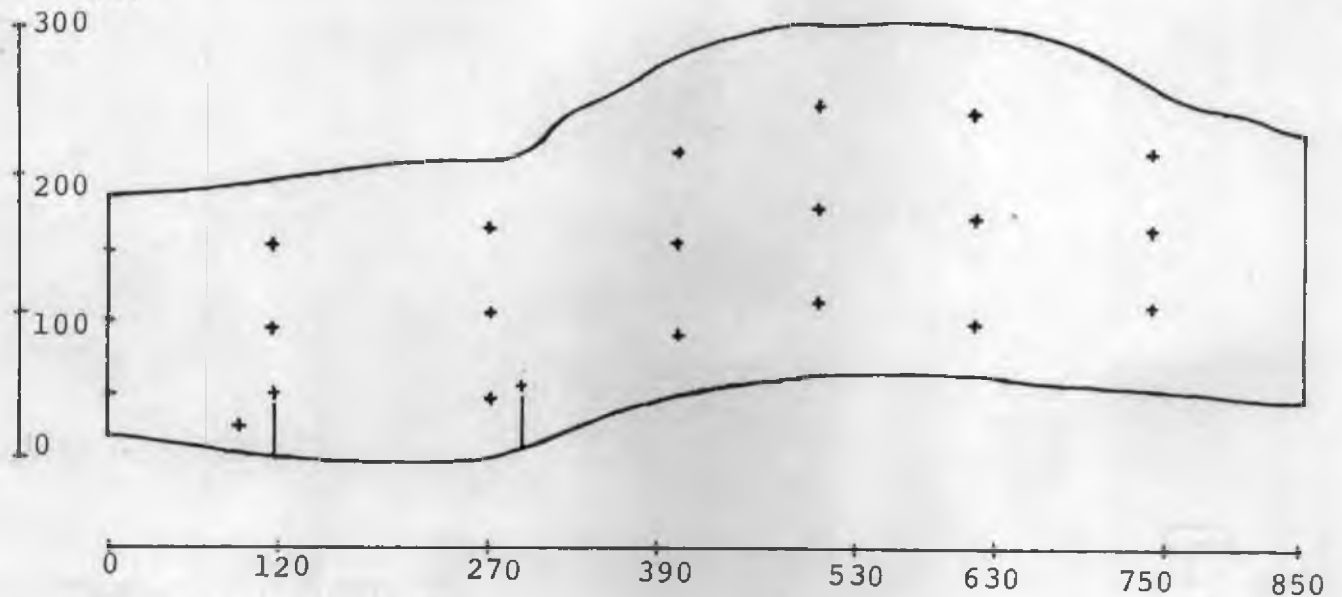
The velocity is measured using a pigmy water current meter fitted with a counter. It is small sized one with a single revolution contact box. It is used specially for measuring flow of water in shallow streams, irrigation channels etc. where the velocity and depth are insufficient for obtaining measurements with large meters. Velocity measurements were taken at  $0.6 D$  depth at various cross sections along and across the model where  $D$  is the depth of the flow at the measuring section. Locations of measuring stations is as shown in Fig 9. Number of revolutions for 30 seconds is noted at each point of measurement and hence the number of revolutions per second could be calculated. Observations should be repeated at least three times at a point to get average velocity. Velocity of flow is computed from the rating equation  $V = 0.3371 N$  where  $N$  is the number of revolutions per second. The details of the



Plate 3 Experiment setup for flow pattern observation



(a)



(b)

All dimensions in cm  
Scale 1:54

**FIG. 9 LOCATION OF MEASURING STATIONS FOR VELOCITY MEASUREMENT FOR (a) SINGLE SPUR (b) MULTIPLE SPUR SCHEME**



current meter is shown in Plate 4. The current meter as used in the model for velocity measurement is shown in Plate 5.

### 3.10 Measurement of Scour and Water Depth

A point gauge mounted on a movable rectangular frame 2.5 m length and 0.3 m wide was used for measuring cross sectional bed profile data as well as water depth at various cross sections. The gauge can be moved along the length of the frame and measurement per 12.5 cm distance interval near the spur model could be made. The frame is placed over the model and depth of bed at measuring points is noted before the introduction of spurs. After allowing water flow for 2-4 hours with spur placed in the model, the depth of bed below the initial level is again measured. So that scour or deposition can be noted. A stationary gauge was placed at c/s 7 and was used to measure water surface elevation when setting and measuring water surface elevation at that section.

### 3.11 Null Point Determination

When water strikes the bank there is the possibility of the bank being eroded. The position of the null point which is defined as the point where the jet of water flowing through the contracted area hit the side wall on the spur side, therefore, is of considerable practical importance in the protection of the bank from erosion. This position

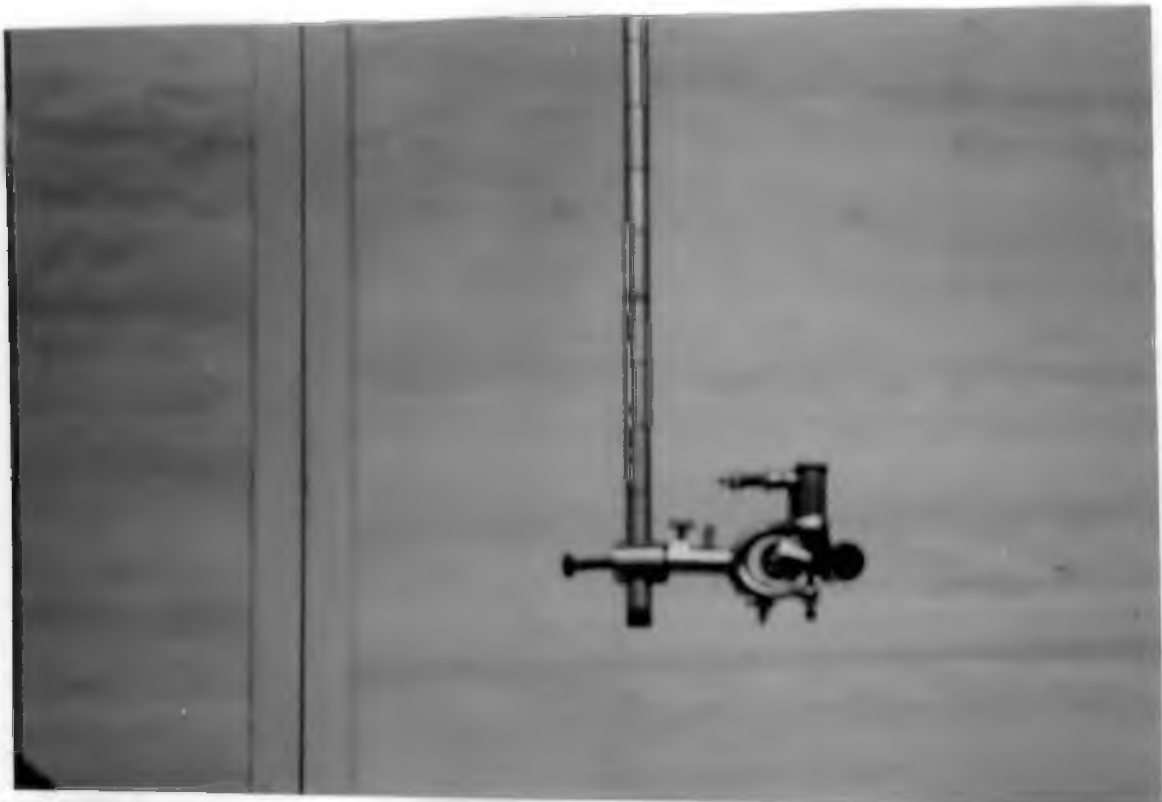


Plate 4 View of the current meter



Plate 5 Measurement of velocity using current meter

will also throw some light on the desirable and safe distance between two spurs. So when scour reached equilibrium condition, the null point was located by dropping potassium permanganate solution at different points along the side wall. At a certain point the coloured solution neither moved upstream nor downstream. However this point was fluctuating and it was very difficult to locate it accurately.

### 3.12 Sediments

A well graded sand of size  $D_{50} = 0.57$  mm and specific gravity 2.48 was used in the mobile bed study. The mean diameter of the sand was determined by sieving through 2.36 mm, 1.18 mm, 0.6 mm, 0.15 mm & 0.075 mm sieves and plotting grain distribution curve. The specific gravity of the sand was determined with the help of a pycnometer.

### 3.13 Rigid Bed Study

River bed of the model was formed as rigid condition by cement plaster. A slope of 1 in 525 was given to the bed profile for maintaining flow of water through the model. The over all view of the model at rigid bed condition is shown in Plate 6.

### 3.13.1 Single Spur.

First of all the water was let into the model without spur for the desired discharge. Tailwater has been adjusted by keeping the required depth of water in c/s 7 as obtained from rating curve prepared for that cross section. After the flow of water was stabilized with rigid bed of the model, flow pattern and velocity distribution have been observed by using pearls as floats and current meter respectively. Water depths were measured by using point gauges. Similar observations were also made for other discharges. Again experiments were conducted with spur models placed in the test section to see the velocity distribution and flow pattern under varying spur lengths and spur angles for three different discharges. The details of the experiments are given in Table 1. In all 51 runs were made. From the data collected, effect of different spur configurations on velocity distribution and flow pattern were obtained.

### 3.13.2 Multiple Spurs

Rigid bed study was also conducted for multiple spurs (two in series) with different spacings. Perpendicularly placed spurs were only used in this study. The details of the experiments are given in Table 2. In all 48 runs were made. The effect of different spur lengths with different spacings on velocity distribution and flow pattern were obtained from these studies.

Table 1. Details of experiments-rigid bed and single spur

Sl. No.	Experiment series	Discharge (lps)	Spur length	Spur angle	Remarks
1	a1	14.14	-	-	Experiments without spur
2	a2	28.28	-	-	
3	a3	42.42	-	-	
4	a4	14.14	25	90	
5	a5	28.28	25	90	
6	a6	42.42	25	90	
7	a7	14.14	25	80	
8	a8	28.28	25	80	
9	a9	42.42	25	80	
10	a10	14.14	25	70	
11	a11	28.28	25	70	
12	a12	42.42	25	70	
13	a13	14.14	25	60	
14	a14	28.28	25	60	
15	a15	42.42	25	60	
16	a16	14.14	35	90	
17	a17	28.28	35	90	
18	a18	42.42	35	90	
19	a19	14.14	35	80	
20	a20	28.28	35	80	
21	a21	42.42	35	80	
22	a22	14.14	35	70	
23	a23	28.28	35	70	
24	a24	42.42	35	70	
25	a25	14.14	35	60	
26	a26	28.28	35	60	
27	a27	42.42	35	60	
28	a28	14.14	45	90	
29	a29	28.28	45	90	
30	a30	42.42	45	90	
31	a31	14.14	45	80	
32	a32	28.28	45	80	
33	a33	42.42	45	80	
34	a34	14.14	45	70	
35	a35	28.28	45	70	
36	a36	42.42	45	70	
37	a37	14.14	45	60	
38	a38	28.28	45	60	
39	a39	42.42	55	60	
40	a40	14.14	55	90	
41	a41	28.28	55	90	
42	a42	42.42	55	90	
43	a43	14.14	55	80	
44	a44	28.28	55	80	
45	a45	42.42	55	80	
46	a46	14.14	55	70	
47	a47	28.28	55	70	
48	a48	42.42	55	70	
49	a49	14.14	55	60	
50	a50	28.28	55	60	
51	a51	42.42	55	60	

Table 2. Details of experiments-rigid bed and multiple spurs

Sl. No.	Experiment series	Discharge (lps)	Spacing bet. spurs (cm)	Remarks
1	S1	14.14	50	
2	S2	28.28	50	
3	S3	42.42	50	Spur length
4	S4	14.14	75	
5	S5	28.28	75	L=25cm
6	S6	42.42	75	
7	S7	14.14	100	
8	S8	28.28	100	
9	S9	42.42	100	
10	S10	14.14	125	
11	S11	28.28	125	
12	S12	42.42	125	
13	S13	14.14	70	
14	S14	28.28	70	
15	S15	42.42	70	Spur length
16	S16	14.14	105	
17	S17	28.28	105	L=35cm
18	S18	42.42	105	
19	S19	14.14	140	
20	S20	28.28	140	
21	S21	42.42	140	
22	S22	14.14	175	
23	S23	28.28	175	
24	S24	42.42	175	
25	S25	14.14	90	
26	S26	28.28	90	
27	S27	42.42	90	Spur length
28	S28	14.14	135	
29	S29	28.28	135	L=45cm
30	S30	42.42	135	
31	S31	14.14	180	
32	S32	28.28	180	
33	S33	42.42	180	
34	S34	14.14	225	
35	S35	28.28	225	
36	S36	42.42	225	
37	S37	14.14	110	
38	S38	28.28	110	
39	S39	42.42	110	Spur length
40	S40	14.14	165	
41	S41	28.28	165	L=55cm
42	S42	42.42	165	
43	S43	14.14	220	
44	S44	28.28	220	
45	S45	42.42	220	
46	S46	14.14	275	
47	S47	28.28	275	
48	S48	42.42	275	



Plate 6 View of the model at rigid bed condition



Plate 7 View of the model at mobile bed condition

### 3.14 Mobile bed study

River bed of the model was formed as mobile condition by a well graded sand of size  $D_{50} = 0.57\text{mm}$  with 15 cm thickness . A slope of 1 in 525 similar to the rigid bed condition was given to the bed profile. An overall view of the model at mobile bed condition is shown in Plate. 7.

#### 3.14.1 Single Spur

Before the beginning of each run the sand bed was levelled by means of a wooden template to give an approximate predetermined slope of 1 in 525. The desired discharge was then allowed to flow through the model by opening the inlet regulating shutter slowly so that the sand bed was not disturbed. The tailwater regulating shutter was carefully adjusted to get the desired depth of flow in the model at c/s 7 corresponding to the discharge used. Then water was allowed to flow for two or three hours during which time the bed of the model adjusted itself to the condition of the flow. When a stable flow condition was attained readings of the water surface and bed surface were taken at various cross sections along the model.

Then the spur model was introduced in the model at c/s 2 which is fixed as spur location. When scour reached equilibrium condition, the null point was located by dropping potassium permanganate solution.

The flow was then slowly stopped and tailwater



regulating shutter was lowered to drain the water in the model without disturbing the scour pattern. Point gauge readings of the bed around the spur dike were taken along and across the model with respect to initial bed level. So that scour or deposition can be noted. Maximum scour depth in front of each spur was also recorded. With the data collected, contour maps of the scoured bed around the spur dike could be plotted. Plate 8 shows scour pattern obtained after experiment run.

Then bed of the model was again levelled to give same slope as mentioned above and similar experiments were conducted with different spur lengths and spur angles, but with same discharge. After the study with this discharge, another two sets of experiments were conducted for other discharges. The details of the experiments with mobile bed condition are given in Table 3. In all 51 runs were made. The effect of different spur lengths and spur angles on scour pattern were obtained from these studies.

#### **3.14.2 Multiple Spur.**

Mobile bed study was also conducted for multiple spurs to find optimum spacing. The same procedure as in the case of single spur study was adopted. The details of the experiments are given in Table 4. In all 27 runs were made. The effect of different spur length with different spacings on scour pattern were obtained from these studies. Plate 9 shows scour pattern obtained with multiple spur scheme after experiment run.



Plate 8 Scour pattern around single spur



Plate 9 Scour pattern around multiple spurs

Table 3. Details of experiments-mobile bed and single spur

Sl. No.	Experiment series	Discharge (lps)	Spur length	Spur angle	Remarks
1	b1	14.14	-	-	Experiments without spur
2	b2	28.28	-	-	
3	b3	42.42	-	-	
4	b4	14.14	25	90	
5	b5	28.28	25	90	
6	b6	42.42	25	90	
7	b7	14.14	25	80	
8	b8	28.28	25	80	
9	b9	42.42	25	80	
10	b10	14.14	25	70	
11	b11	28.28	25	70	
12	b12	42.42	25	70	
13	b13	14.14	25	60	
14	b14	28.28	25	60	
15	b15	42.42	25	60	
16	b16	14.14	35	90	
17	b17	28.28	35	90	
18	b18	42.42	35	90	
19	b19	14.14	35	80	
20	b20	28.28	35	80	
21	b21	42.42	35	80	
22	b22	14.14	35	70	
23	b23	28.28	35	70	
24	b24	42.42	35	70	
25	b25	14.14	35	60	
26	b26	28.28	35	60	
27	b27	42.42	35	60	
28	b28	14.14	45	90	
29	b29	28.28	45	90	
30	b30	42.42	45	90	
31	b31	14.14	45	80	
32	b32	28.28	45	80	
33	b33	42.42	45	80	
34	b34	14.14	45	70	
35	b35	28.28	45	70	
36	b36	42.42	45	70	
37	b37	14.14	45	60	
38	b38	28.28	45	60	
39	b39	42.42	55	60	
40	b40	14.14	55	90	
41	b41	28.28	55	90	
42	b42	42.42	55	90	
43	b43	14.14	55	80	
44	b44	28.28	55	80	
45	b45	42.42	55	80	
46	b46	14.14	55	70	
47	b47	28.28	55	70	
48	b48	42.42	55	70	
49	b49	14.14	55	60	
50	b50	28.28	55	60	
51	b51	42.42	55	60	

Table 4. Details of experiments-Mobile bed and multiple spurs

Sl. No.	Experiment series	Discharge (lps)	Spacing bet. spurs (cm)	Remarks
1	T1	14.14	50	
2	T2	28.28	50	
3	T3	42.42	50	Spur length
4	T4	14.14	75	
5	T5	28.28	75	L=25cm
6	T6	42.42	75	
7	T7	14.14	100	
8	T8	28.28	100	
9	T9	42.42	100	
10	T10	14.14	125	
11	T11	28.28	125	
12	T12	42.42	125	
13	T13	14.14	70	
14	T14	28.28	70	
15	T15	42.42	70	Spur length
16	T16	14.14	105	
17	T17	28.28	105	L=35cm
18	T18	42.42	105	
19	T19	14.14	140	
20	T20	28.28	140	
21	T21	42.42	140	
22	T22	14.14	175	
23	T23	28.28	175	
24	T24	42.42	175	
25	T25	14.14	90	
26	T26	28.28	90	
27	T27	42.42	90	Spur length
28	T28	14.14	135	
29	T29	28.28	135	L=45cm
30	T30	42.42	135	
31	T31	14.14	180	
32	T32	28.28	180	
33	T33	42.42	180	
34	T34	14.14	225	
35	T35	28.28	225	
36	T36	42.42	225	

## Results and Discussion

---

## RESULTS AND DISCUSSIONS

The results of study conducted are discussed in detail in this chapter. The analysis of different design parameters of spurs with rigid bed as well as mobile bed conditions are explained. Selection of suitable spur length, spur angle and spur spacing for the test section are also described.

### 4.1 Rigid bed experiments

#### 4.1.1 Single Spur

Experiments were conducted on a rigid bed in order to see the flow pattern and velocity distribution under varying spur length, spur angle and discharge rate as explained in chapter 3.13.1. Initially data were taken without spur in the test section for discharge rates 14.14 lps, 28.28 lps and 42.42 lps. Following this, analysis of various design parameters like spur length, spur angle were done for the three discharge rates mentioned above. It was done by placing spur models of different projected lengths of 25 cm, 35 cm, 45 cm, and 55 cm with different spur angles of 90°, 100°, 110° and 120° in the test section. Detailed analysis of collected data and the results so obtained are presented below under various sub headings.

##### 4.1.1.1 Flow pattern data

Data on flow pattern in the test section was collected from the model by dropping floats in an upstream cross

section 'X' for the three discharge rates 14.14 lps, 28.28 lps and 42.42 lps. From these data, flow patterns at each experiment condition were plotted and are presented in Fig. 10 to 26.

From the analysis of flow patterns obtained with each spur configuration, it was observed that the flow concentration at the spur tip increased with the increase in spur length and it decreased with the increase in spur angle. However the flow concentration vary significantly with the increase of spur angle in the case of spur model with the length 55 cm. This may be probably due to the fact that there is considerable increase in the angle of attack of the flow with the increase in spur angle.

Another trend observed from the figures is that the flow diversion to the opposite bank increased with increasing spur length. The same trend was observed with the increase in spur angle which may be because, greater the spur angle greater is the extent to which the flow gets diverted after striking the spur. However it was observed that the spur length of 25 cm did not bring about a considerable effect on flow diversion with increase in spur angle. This is evident from the comparison of Fig. 10 and Fig. 11, 15, 19, 23. This may be due to the fact that the constriction is getting reduced as the spur angle increases, it is not sufficient enough to produce noticeable effects on flow diversion.

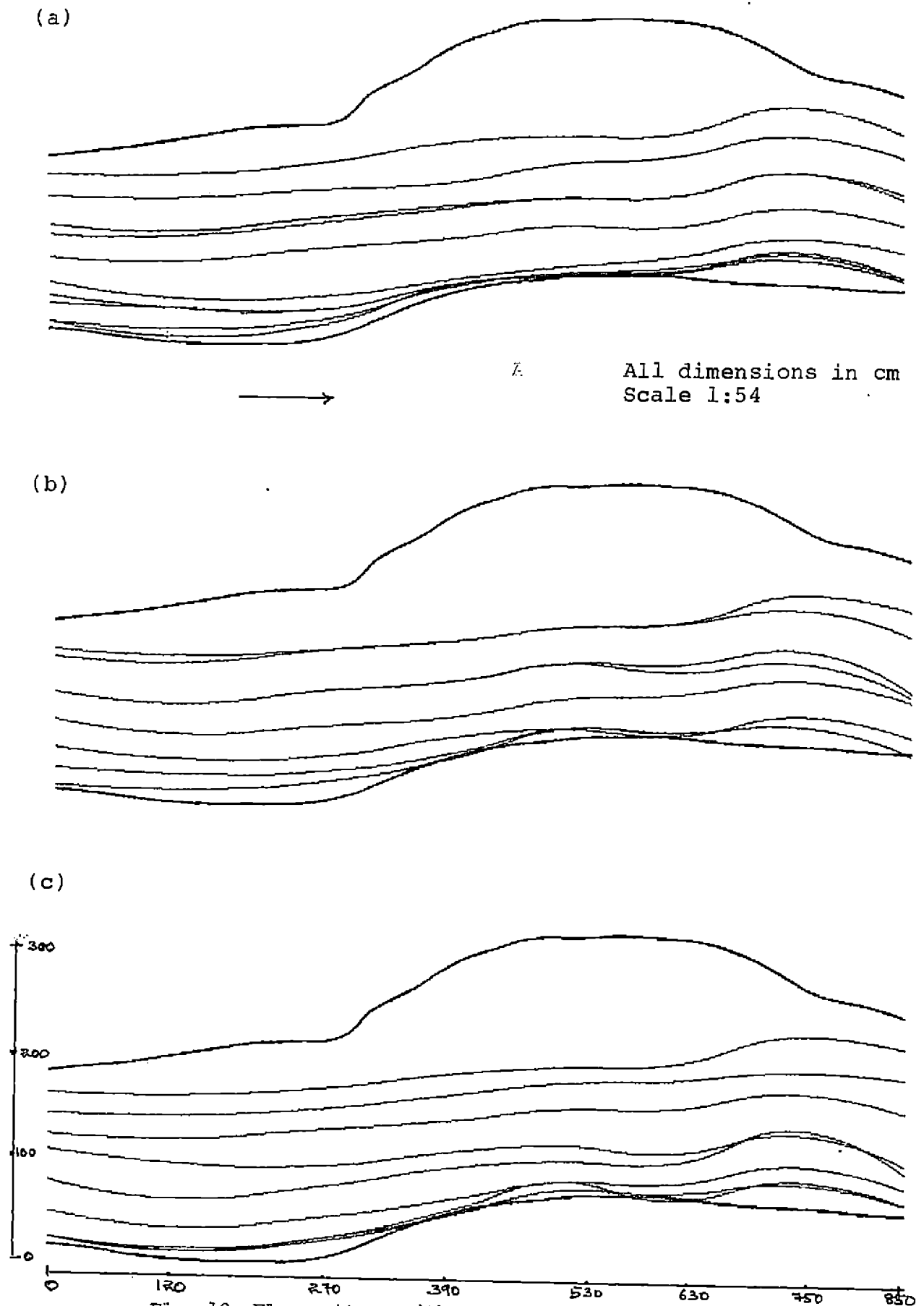
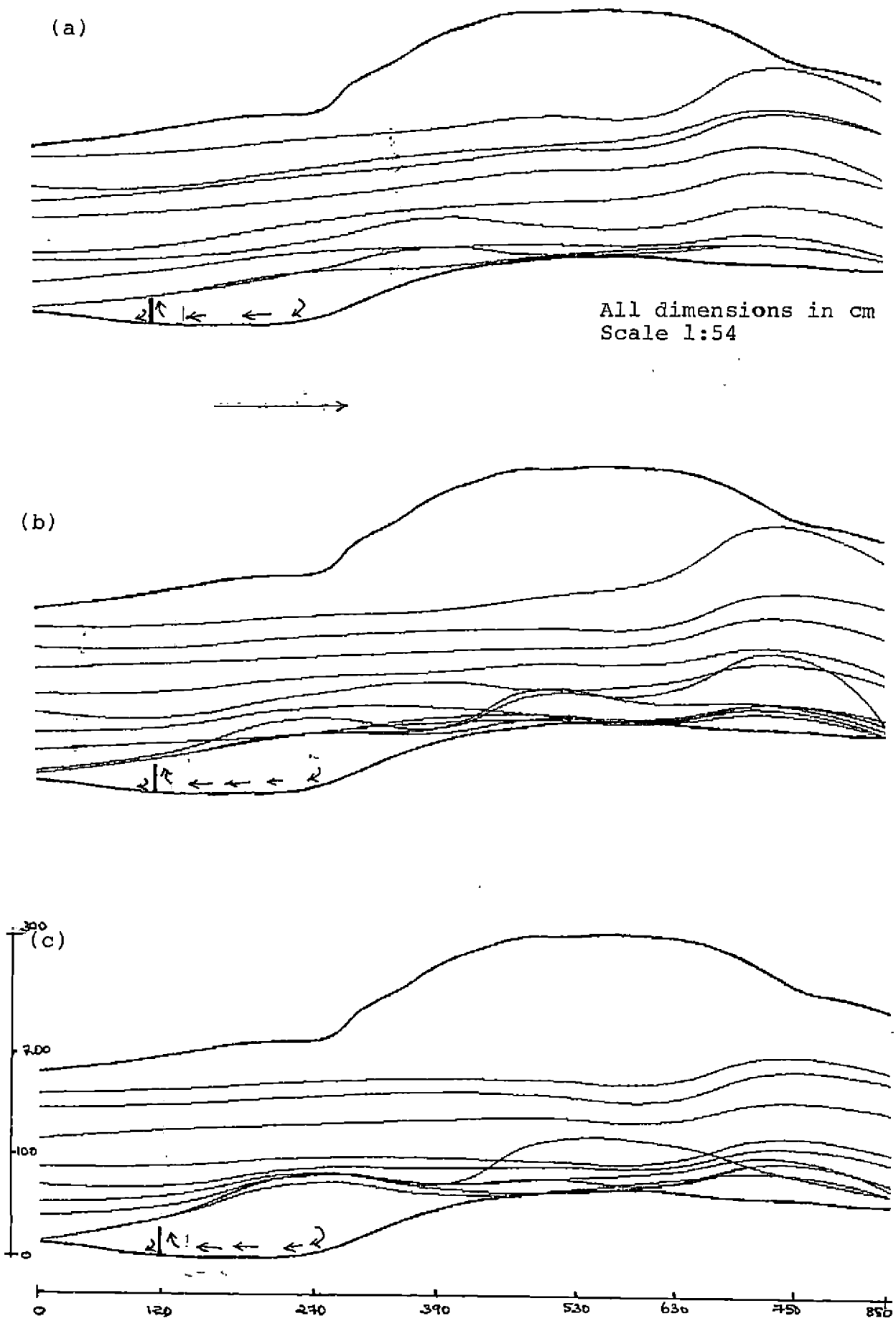


Fig. 10. Flow pattern without spur for discharge rates  
(a) 14.14 lps (b) 28.28 lps (c) 42.42 lps





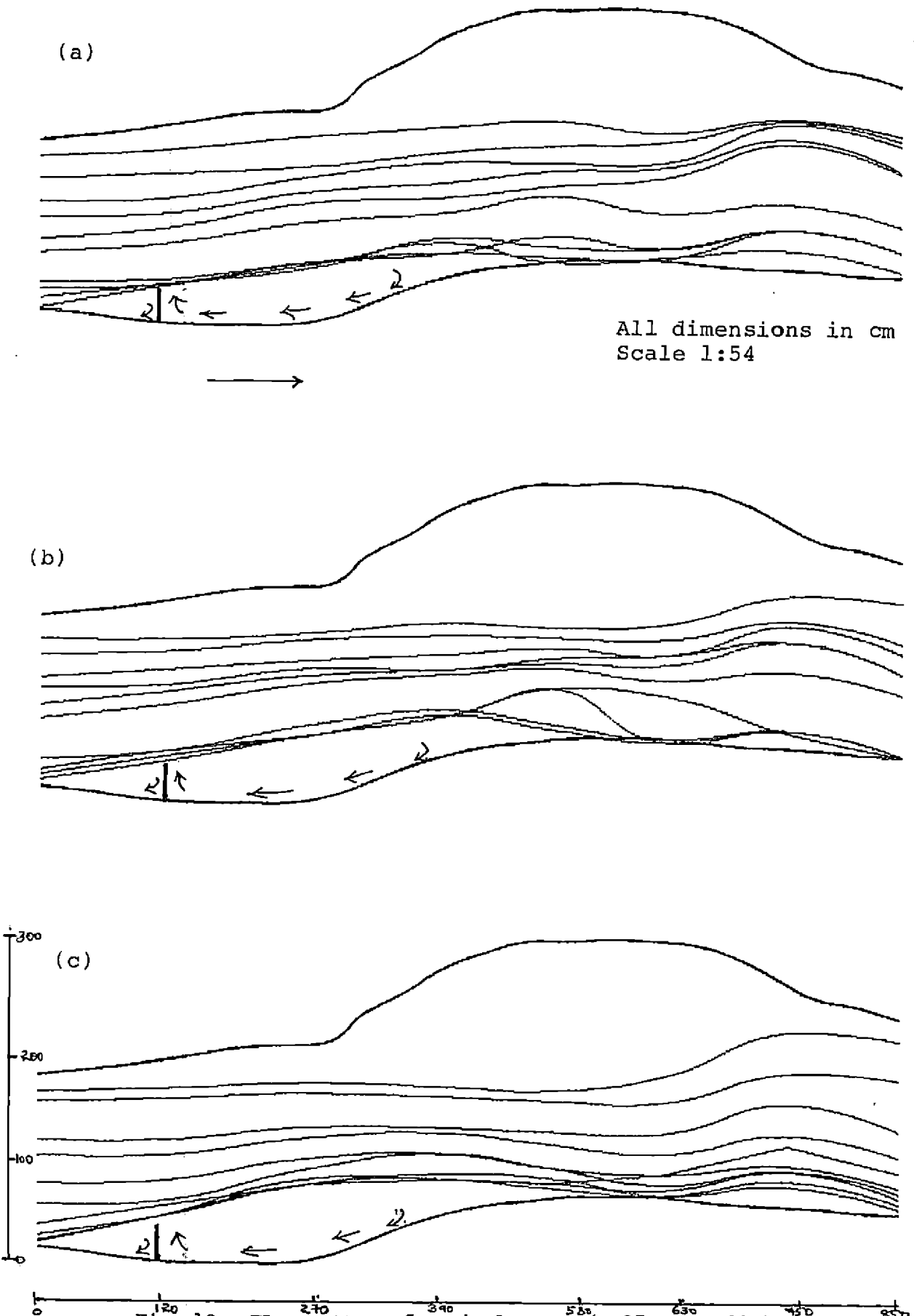


Fig. 12. Flow pattern for single spur ( $L=35$  cm,  $\theta=90^\circ$ ) for discharge rates (a)14.14 lps (b)28.28 lps (c)42.42 lps

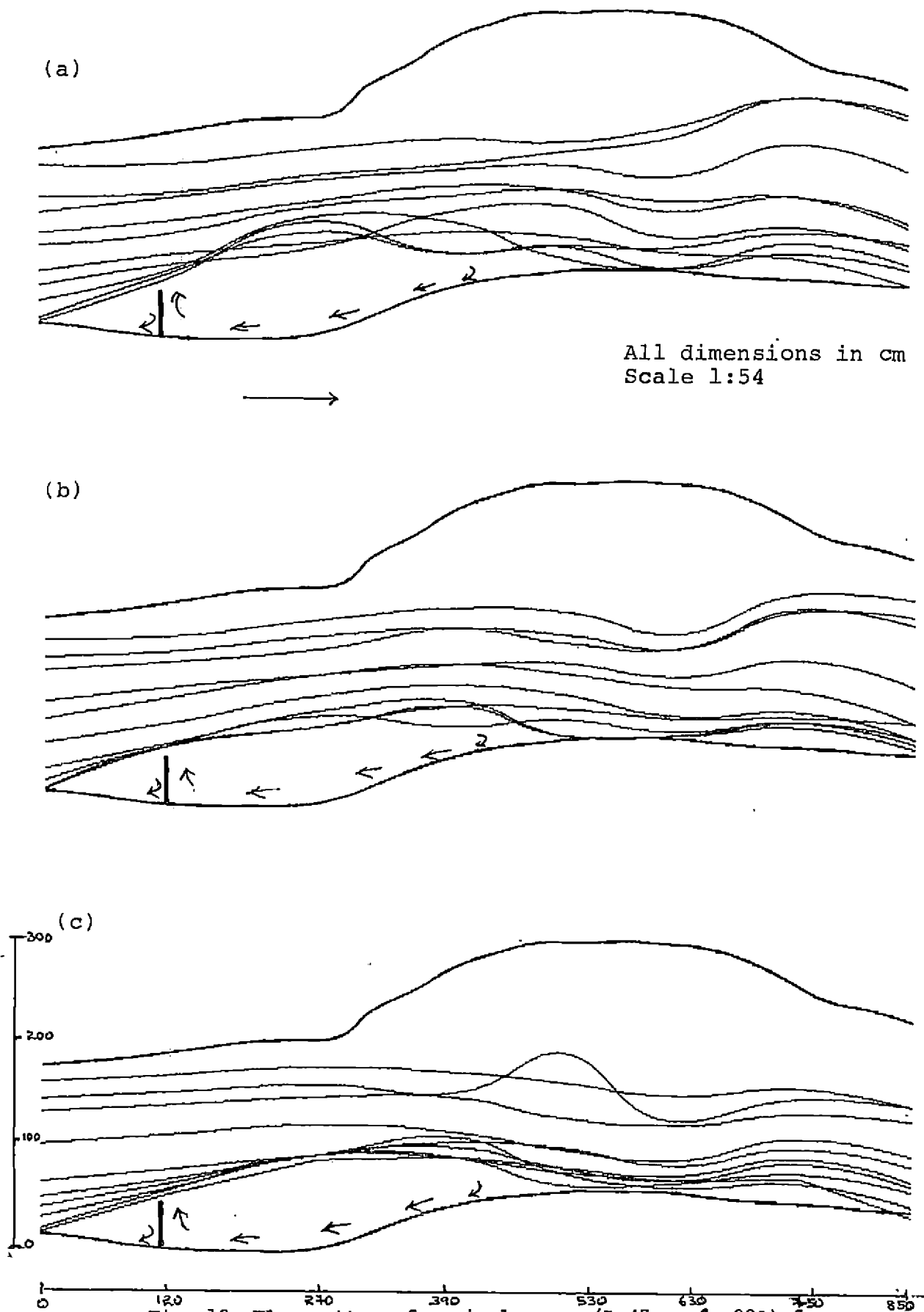


Fig. 13. Flow pattern for single spur ( $L=45$  cm,  $\theta=90^\circ$ ) for discharge rates (a) 14.14 lps (b) 28.28 lps (c) 42.42 lps

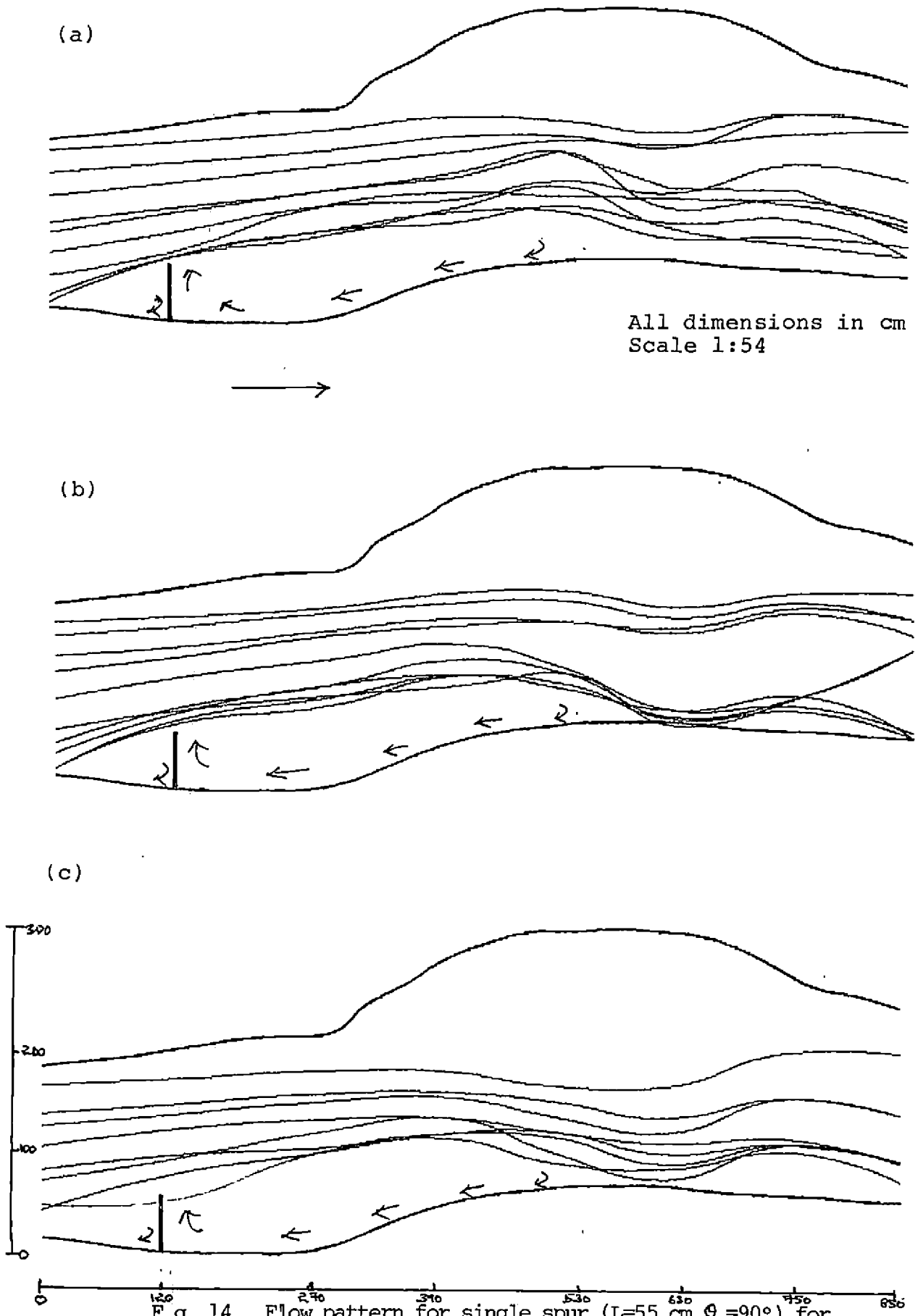


Fig. 14. Flow pattern for single spur ( $L=55$  cm,  $\theta=90^\circ$ ) for discharge rates (a)14.14 lps (b)28.28 lps (c)42.42 lps

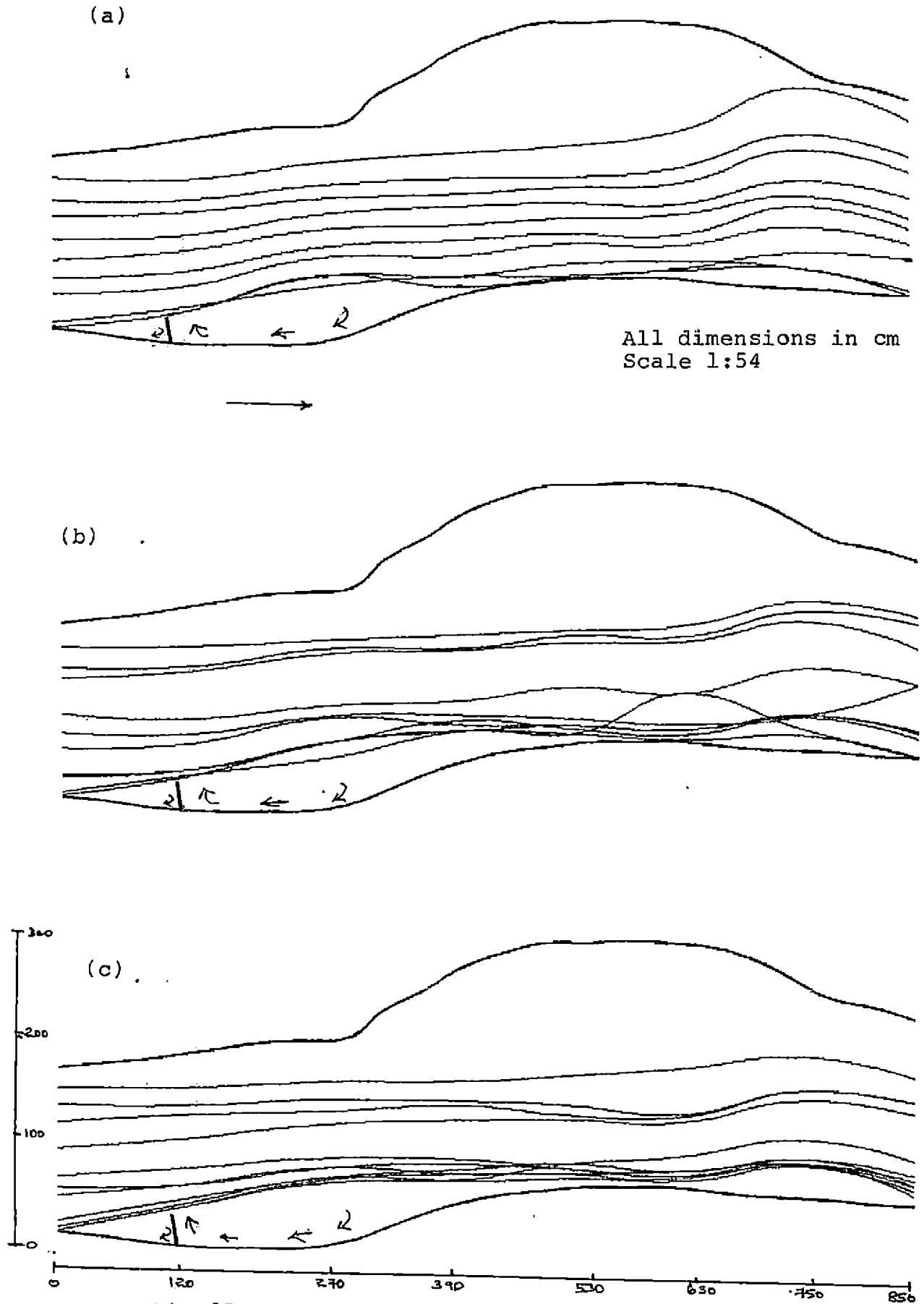


Fig. 15. Flow pattern for single spur ( $L=25$  cm,  $\theta=100^\circ$ ) for discharge rates (a) 14.14 lps (b) 28.28 lps (c) 42.42 lps

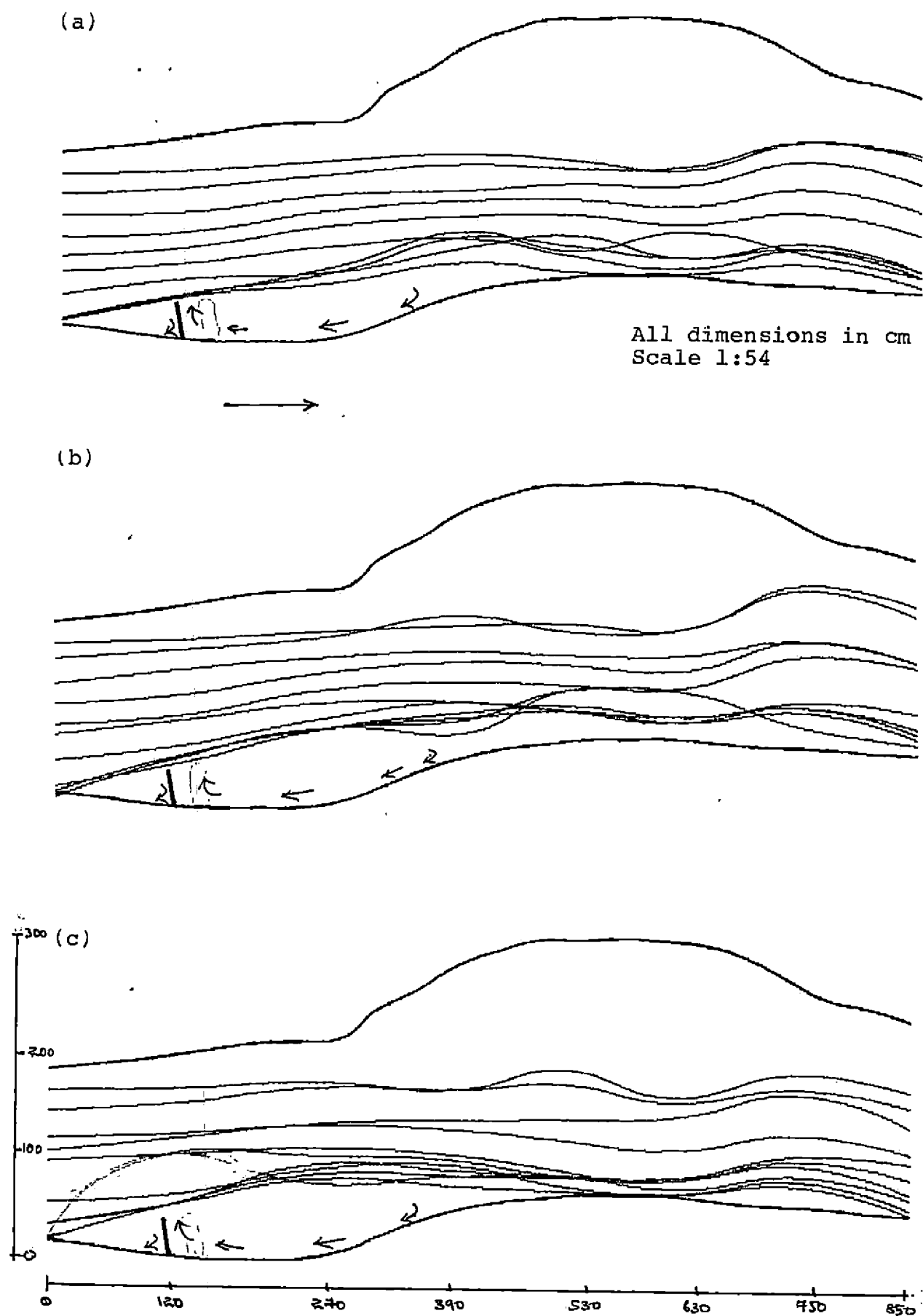


Fig. 16. Flow pattern for single spur. ( $L=35$  cm,  $\phi=100^\circ$ ) for discharge rates (a) 14.14 lps (b) 28.28 lps (c) 42.42 lps

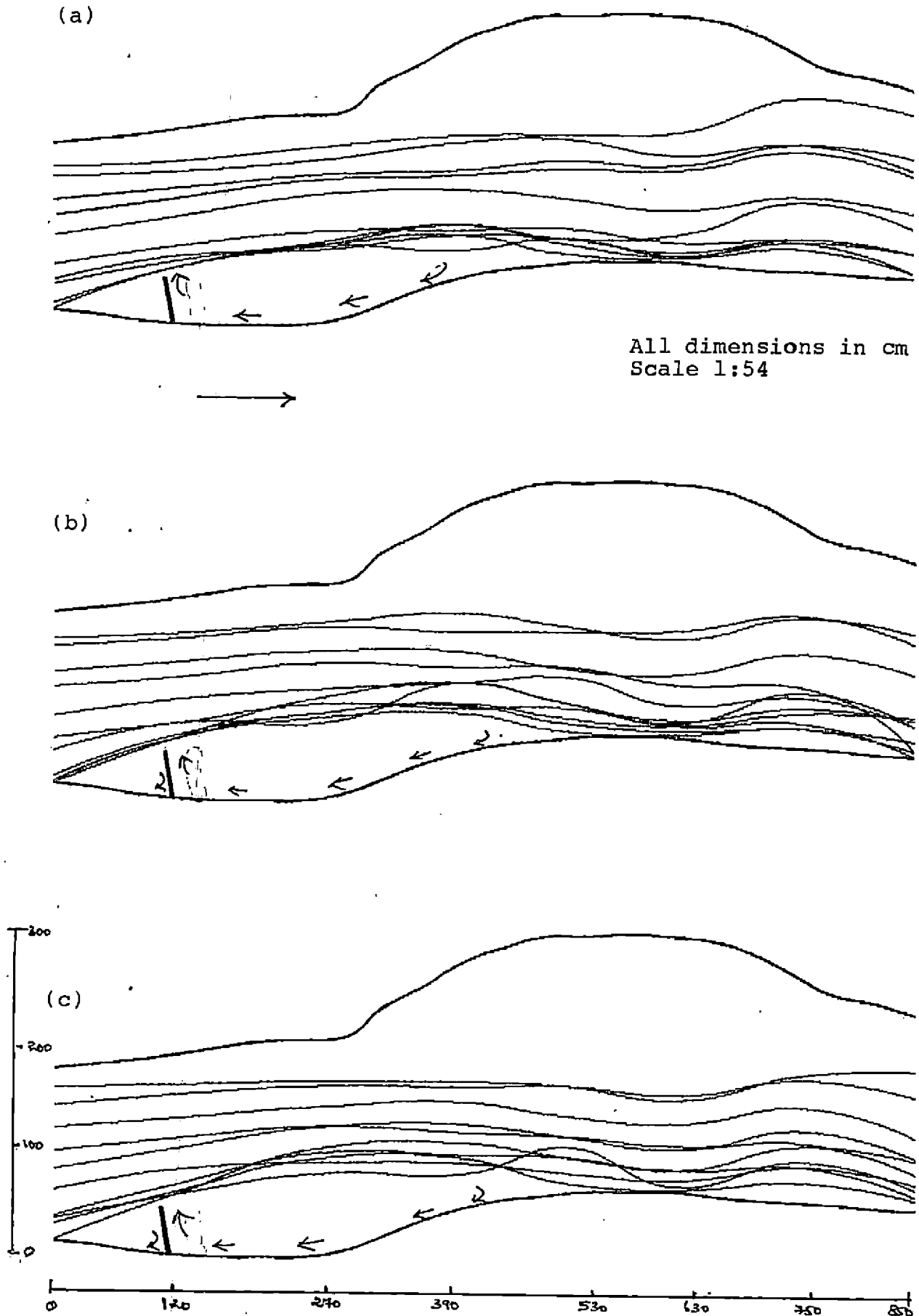


Fig. 17. Flow pattern for single spur ( $L=45$  cm,  $\theta=100^\circ$ ) for discharge rates (a) 14.14 lps (b) 28.28 lps (c) 42.42 lps

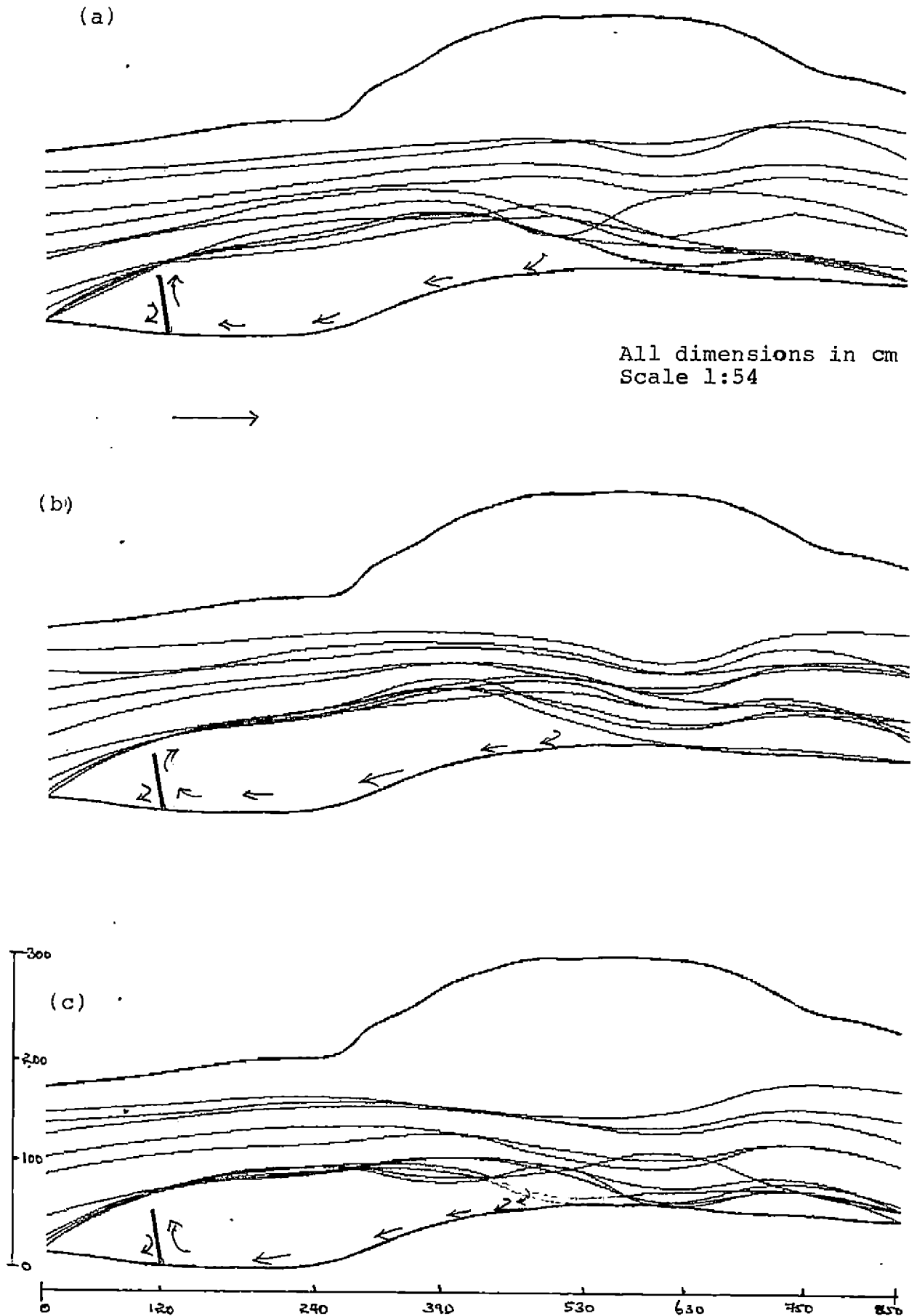


Fig. 18. Flow pattern for single spur ( $L=55$  cm,  $\theta=100^\circ$ ) for discharge rates (a) 14.14 lps (b) 28.28 lps (c) 42.42 lps



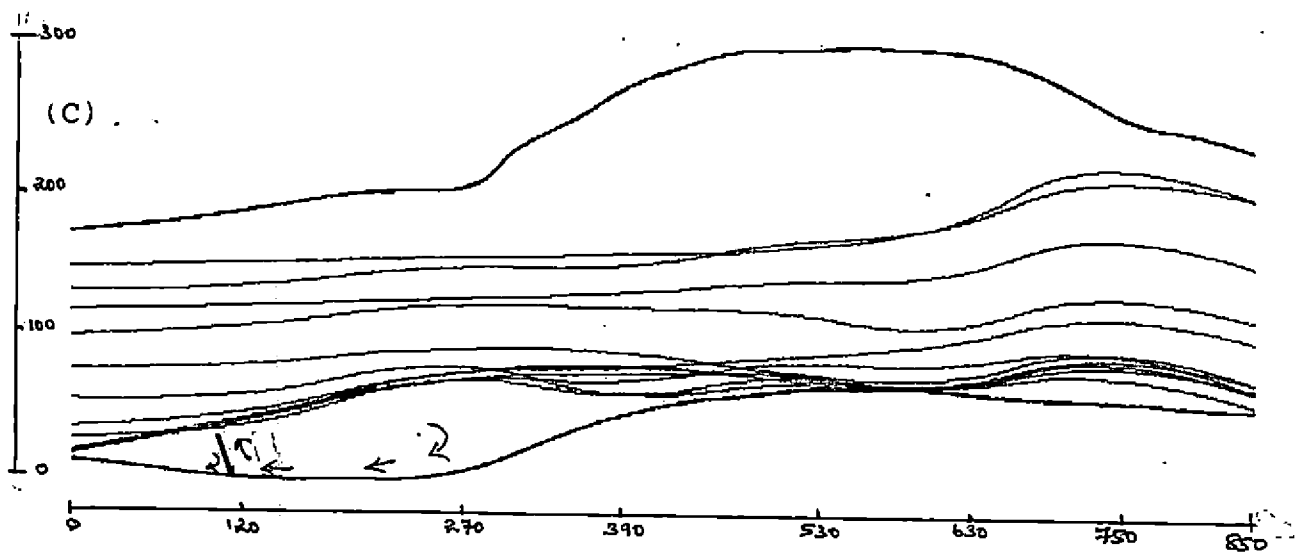
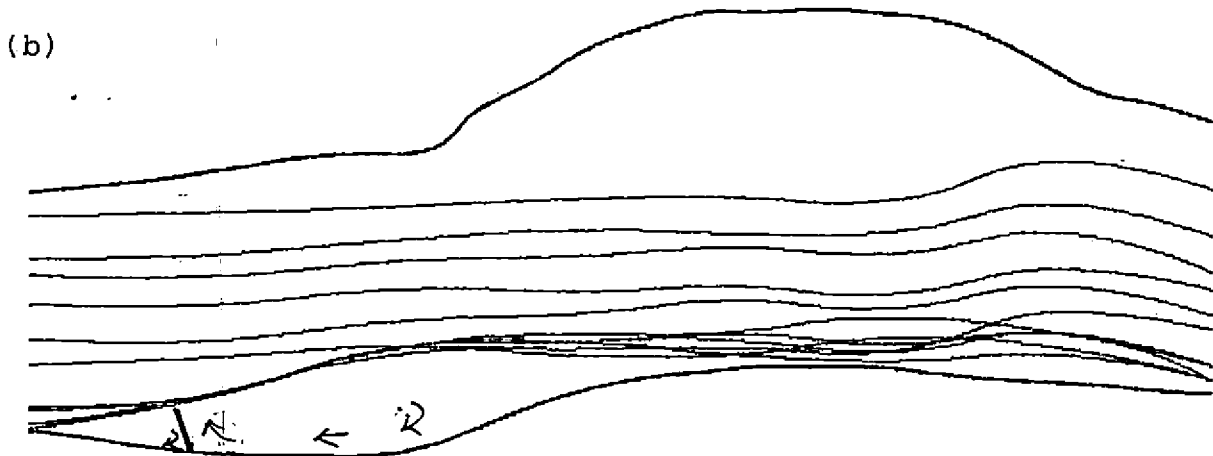
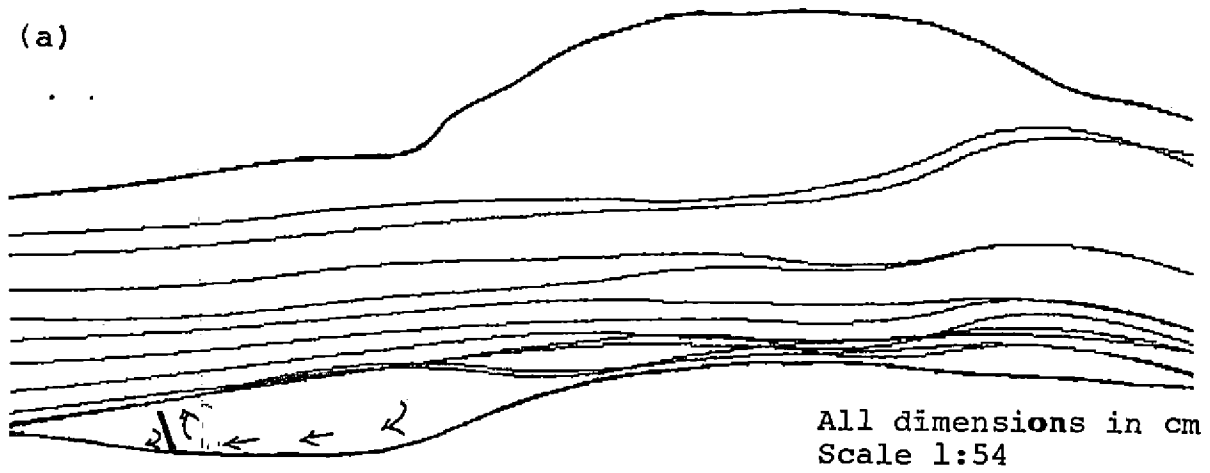


Fig. 19. Flow pattern for single spur ( $L=25$  cm,  $\theta=110^\circ$ ) for discharge rates (a) 14.14 lps (b) 28.28 lps (c) 42.42 lps

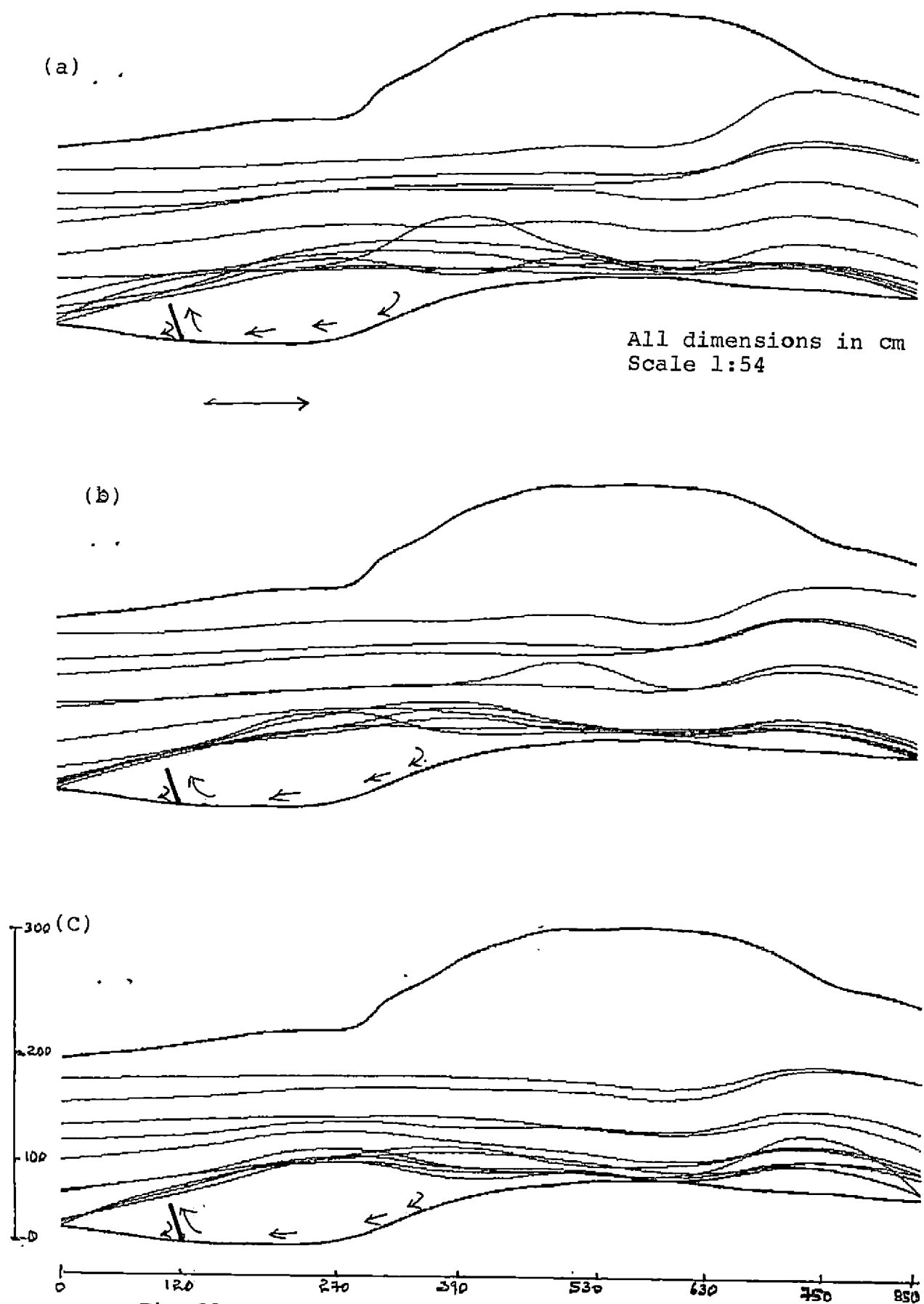


Fig. 20. Flow pattern for single spur ( $L=35$  cm,  $\theta=110^\circ$ ) for discharge rates (a) 14.14 lps (b) 28.28 lps (c) 42.42 lps

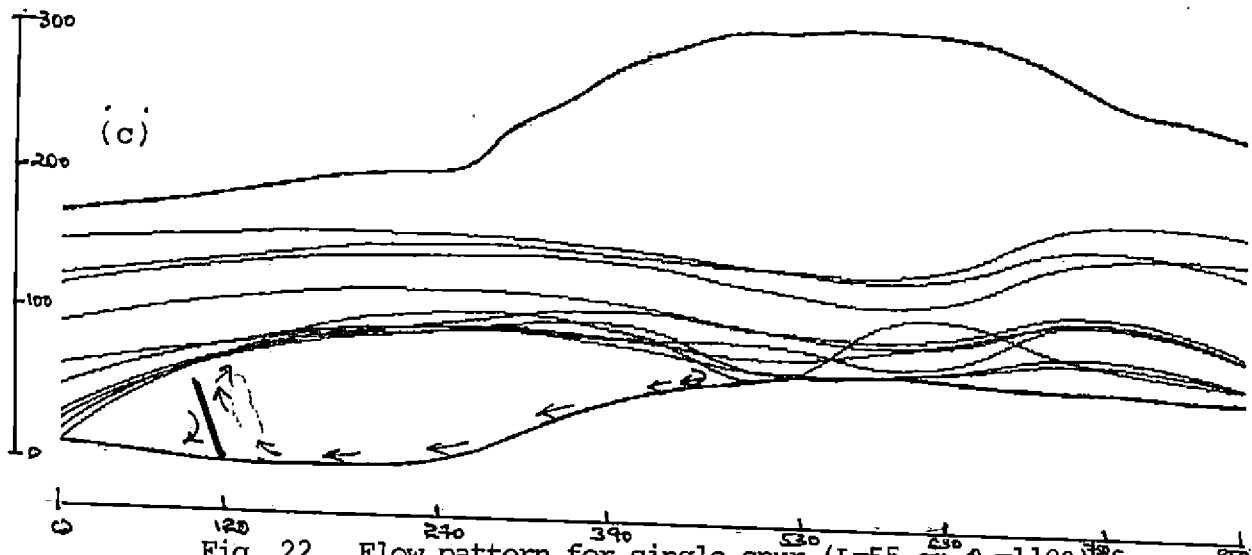
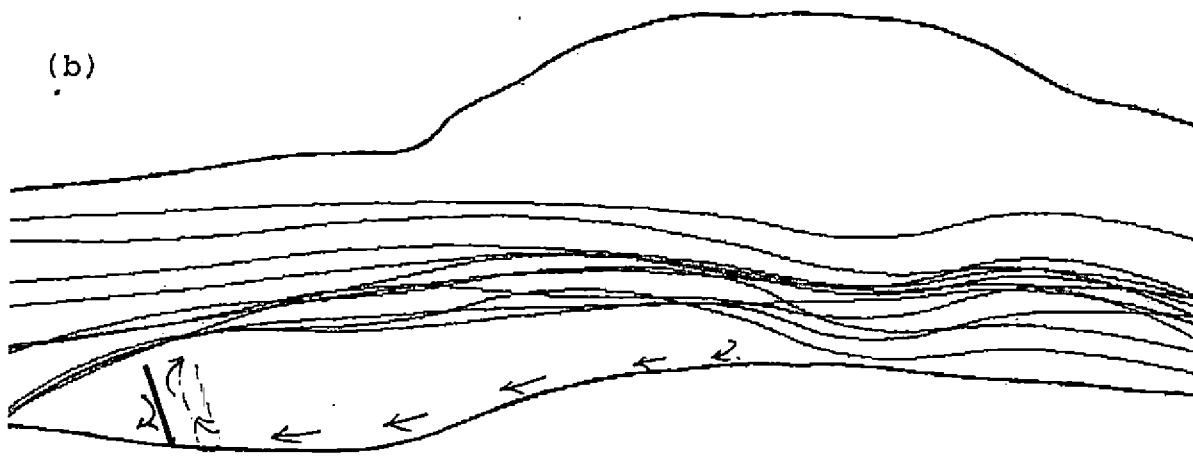
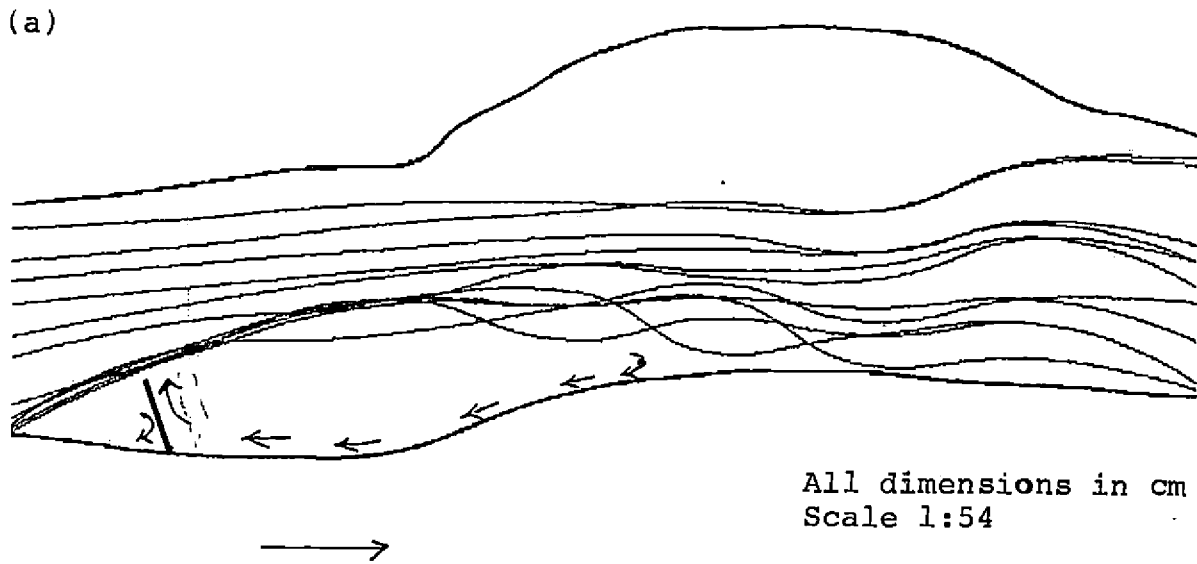


Fig. 22. Flow pattern for single spur ( $L=55$  cm,  $\theta = 110^\circ$ ) for discharge rates (a) 14.14 lps (b) 28.28 lps (c) 42.42 lps

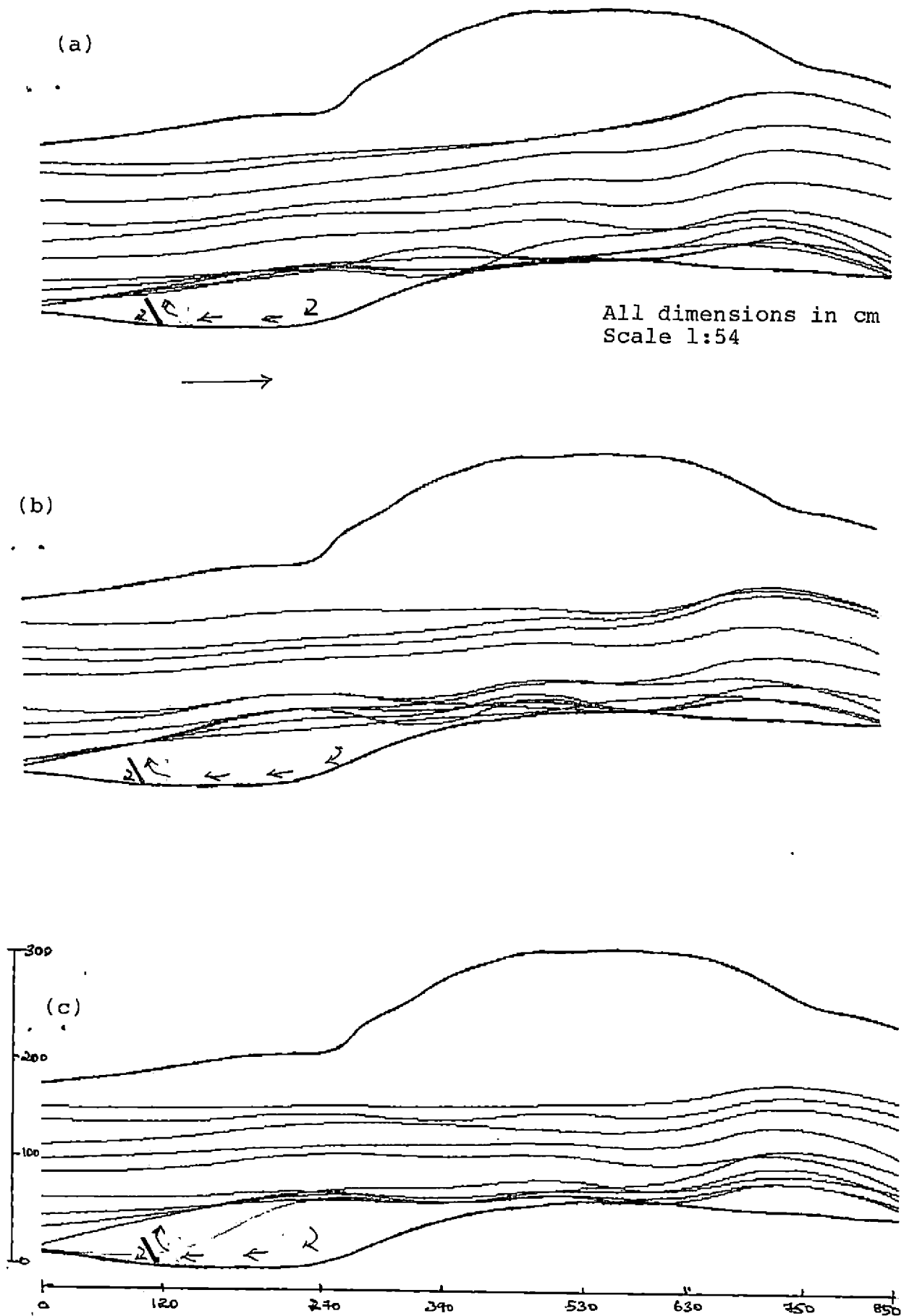
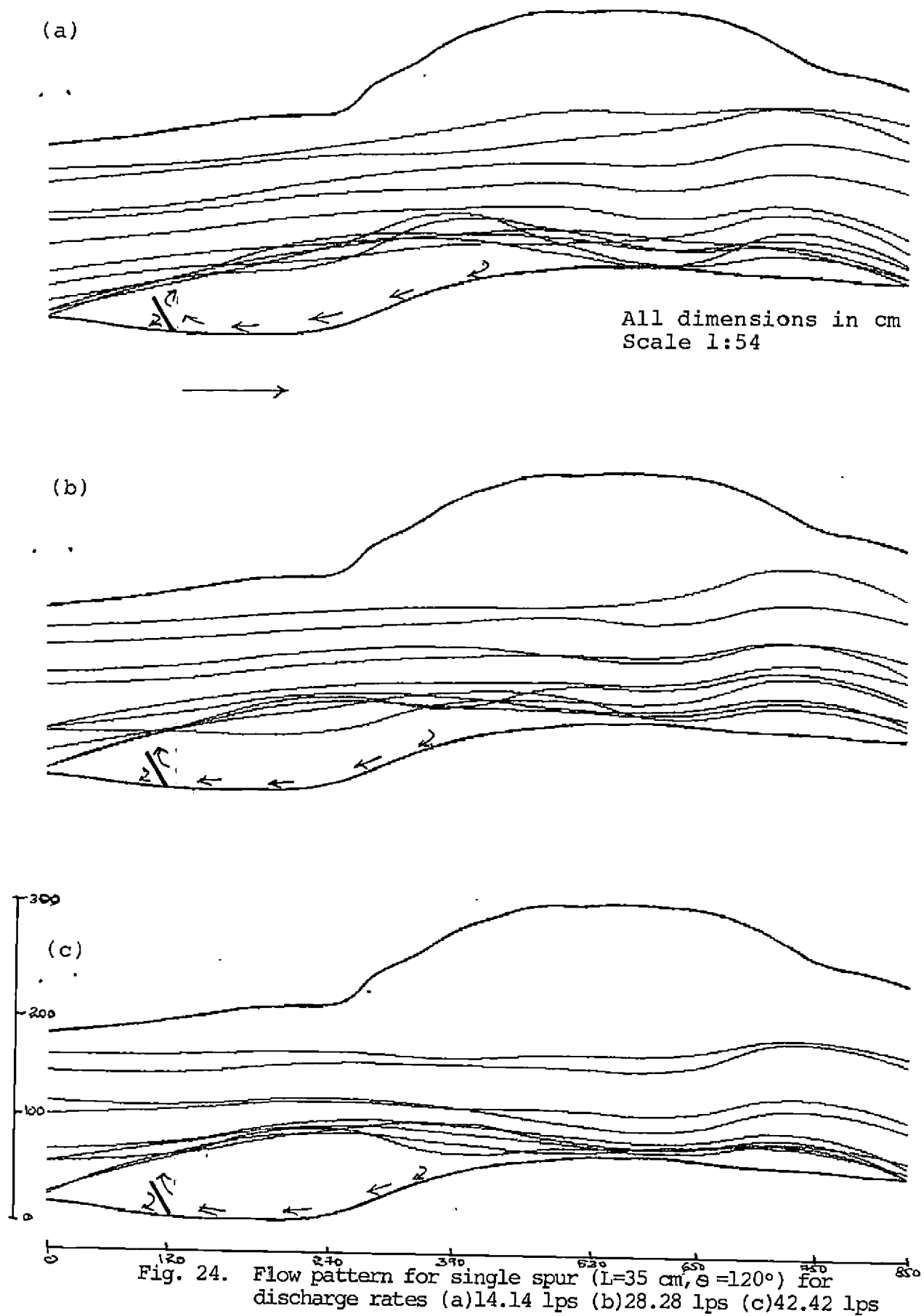


Fig. 23. Flow pattern for single spur ( $L=25$  cm,  $\theta=120^\circ$ ) for discharge rates (a) 14.14 lps (b) 28.28 lps (c) 42.42 lps



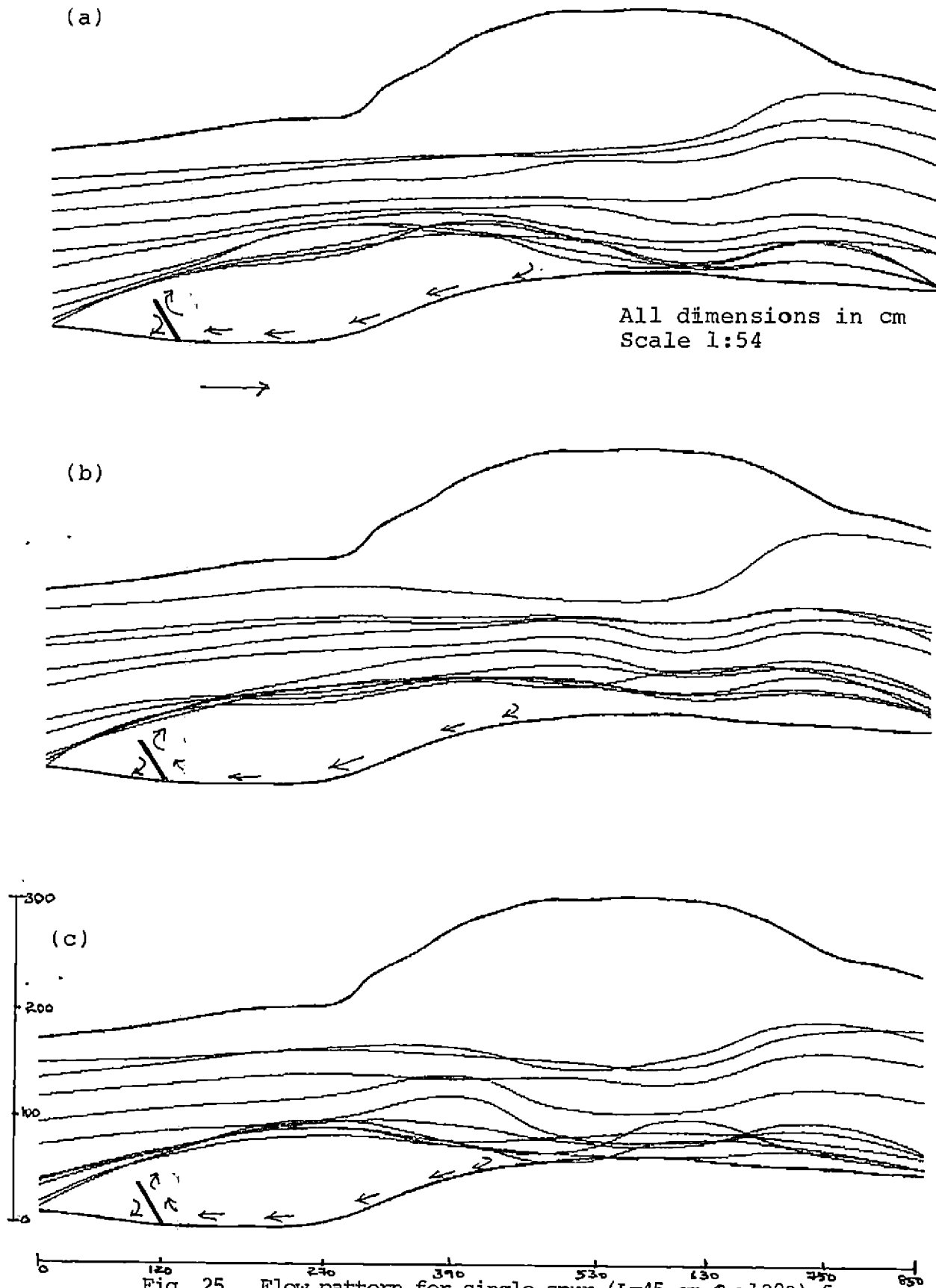


Fig. 25. Flow pattern for single spur ( $L=45$  cm,  $\theta=120^\circ$ ) for discharge rates (a) 14.14 lps (b) 28.28 lps (c) 42.42 lps

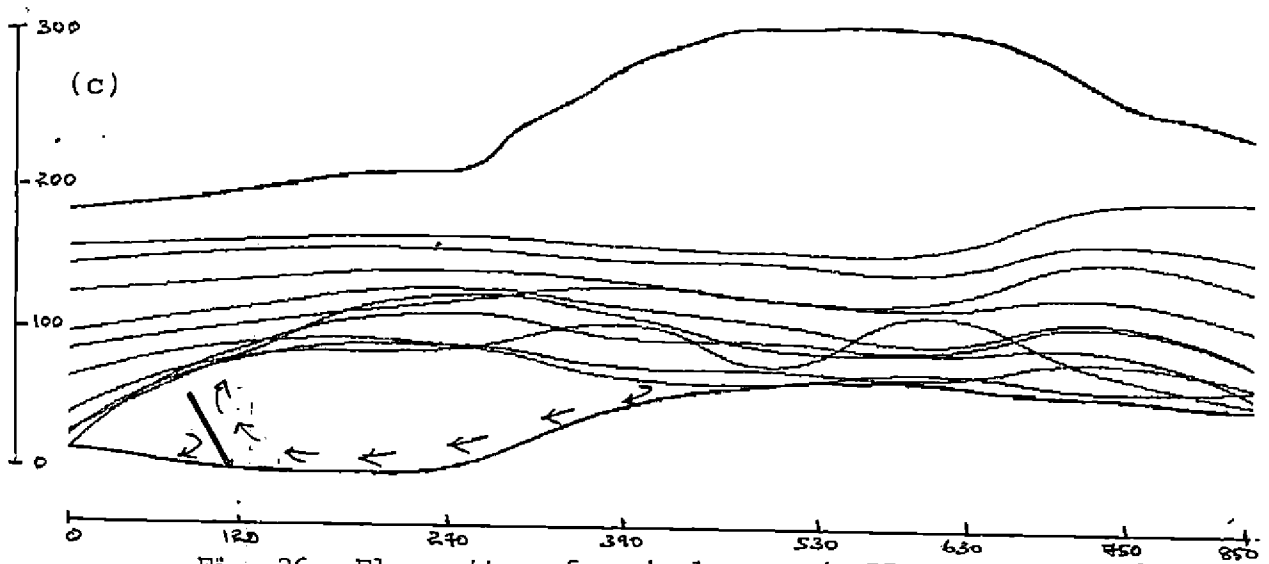
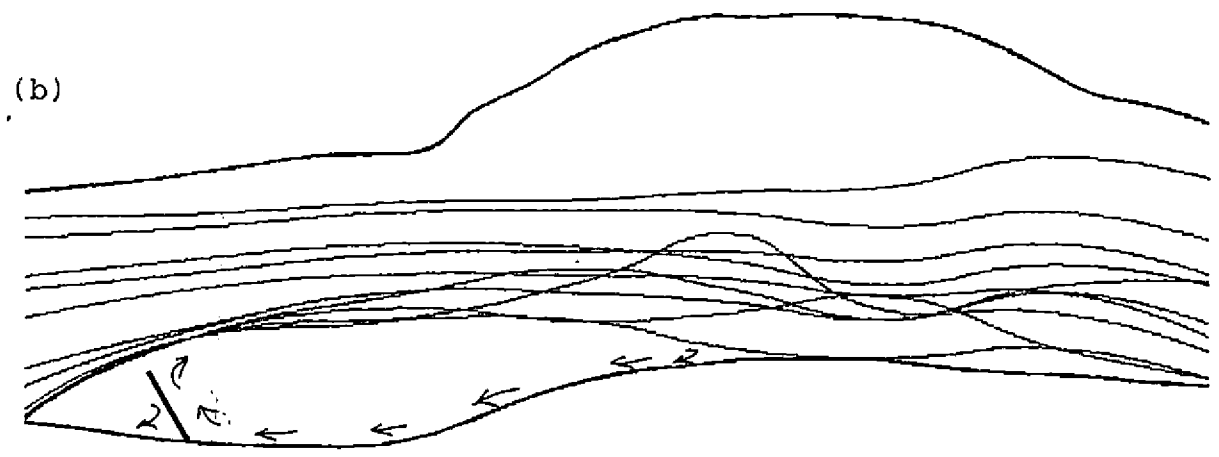
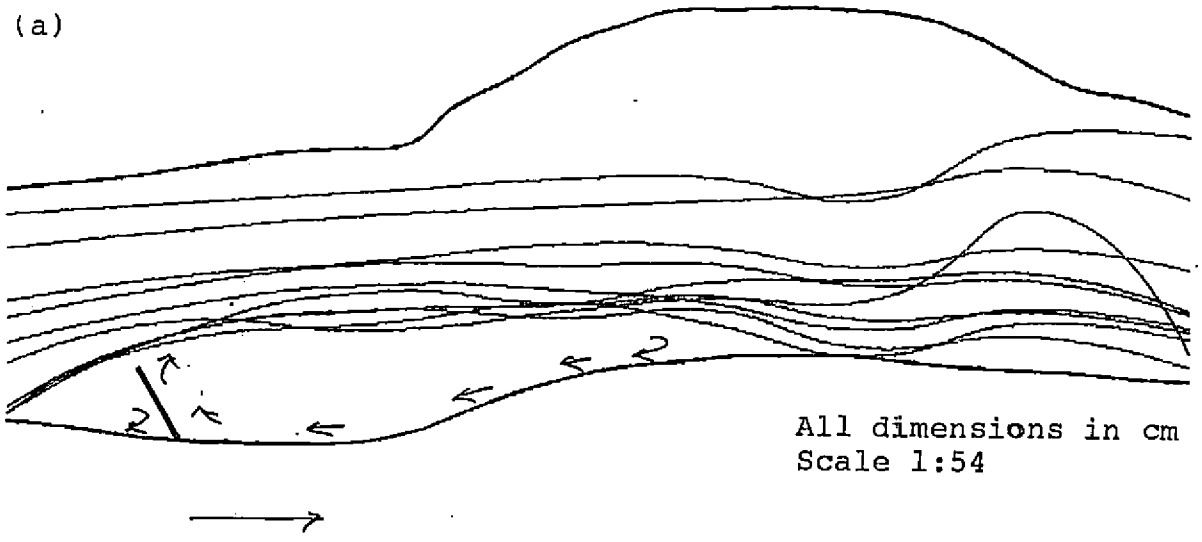


Fig. 26. Flow pattern for single spur ( $L=55$  cm,  $\theta=120^\circ$ ) for discharge rates (a)14.14 lps (b)28.28 lps (c)42.42 lps

Another observation evident from the flow pattern is the effect of spur projected length on the length of bank protected downstream of the spur tip. The observation of flow pattern obtained in all cases indicate that the length of bank protected by the spurs always increases with increasing spur length regardless of spur angle. Thus from the analysis of flow pattern at each experiment condition on the rigid bed, it can be observed that spur design parameters like spur length and spur angle do have significant effect on the length of the bank protected, flow diversion etc. From the observations a spur length ranging between 25 cm and 55 cm and at angle ranging from  $90^\circ$  to  $110^\circ$  downstream with the bank was found to give desirable results, as it maintains considerable length of the bank protected and on the other hand does not give so much of flow diversion as to have damaging effects on the opposite bank. As the results obtained are of highly system dependent and of qualitative nature, case to case analysis is a precondition for applying the above results for other similar situations.

#### 4.1.1.2 Velocity data

Data on velocities at measuring points along and across the test section were collected from the model by using a pigmy water current meter. From the velocity data obtained with different spur configurations, effect of spur angle on velocities at opposite bank was studied by comparing these



velocities with those obtained without spur. Velocity data at a point near left bank in c/s 3 was found to be affected more by the attack of flow, and thus was taken for plotting purposes.

Figures 27, 28 and 29 present graphs showing percentage increase in velocities at the opposite bank versus  $\cos (180 - \theta)$  for the discharge rates 14.14 lps, 28.28 lps and 42.42 lps respectively where  $\theta$  is the angle made by spur downstream with the bank. It can be seen from these figures that percentage increase in velocity at opposite bank shows an increasing trend with spur angle. As indicated earlier in the case of flow patterns, there is greater flow diversions for higher angles, which may be the obvious reason for the indicated higher velocities. However for spur angle as high as  $120^\circ$ , the percentage increase in velocity found to be deviating from the increasing trends. This may be probably due to the fact that for higher angles, the flow near the bed follows the downstream face of the groyne and the flow continues along the bank. The graphs also indicate the fact that the percentage increase in velocities at opposite bank is lesser for  $90^\circ$  spur angle for all spur lengths and discharge rates tested. Hence spur angle of  $90^\circ$  may be considered suitable for the test section. The data on velocity at the opposite bank with various spur angle are presented in Appendix-I.

In order to find suitable ratio of length of spur to width of the channel at spur location ( L/B ratio ) at spur angle  $90^\circ$ , effect of spur length on velocities at the opposite bank were compared with those velocities obtained without spur. Figure 30 shows a graph of percentage increase in velocity at opposite bank versus L/B ratio. It can be seen from the figure that slope of the curve becomes steeper for L/B greater than 0.19. This observation is found similar for all discharge rates tested in this study. This means that L/B greater than 0.19 causes a velocity that has an erosive effect on the opposite bank. This finding is found to be coherent with that made by CWPRS(1987). The data on velocities at opposite bank for different L/B ratios are presented in the Appendix-I.

Thus from the analysis of velocity distribution at each spur configurations, it can be seen that spur model with  $L/B = 0.19$  and angle  $\Theta = 90^\circ$  is found suitable for the test section under present study.

In order to find the extent of protection given to the bank by the provision of a single spur, velocities for measuring grid with each spur configurations were taken and are presented in Fig. 31 to 47. It can be seen from these figures that the length of bank protected increased with the increase in spur length. But length of bank protected remained independent of spur angle. This may be probably due to the fact that the effect of greater flow diversion

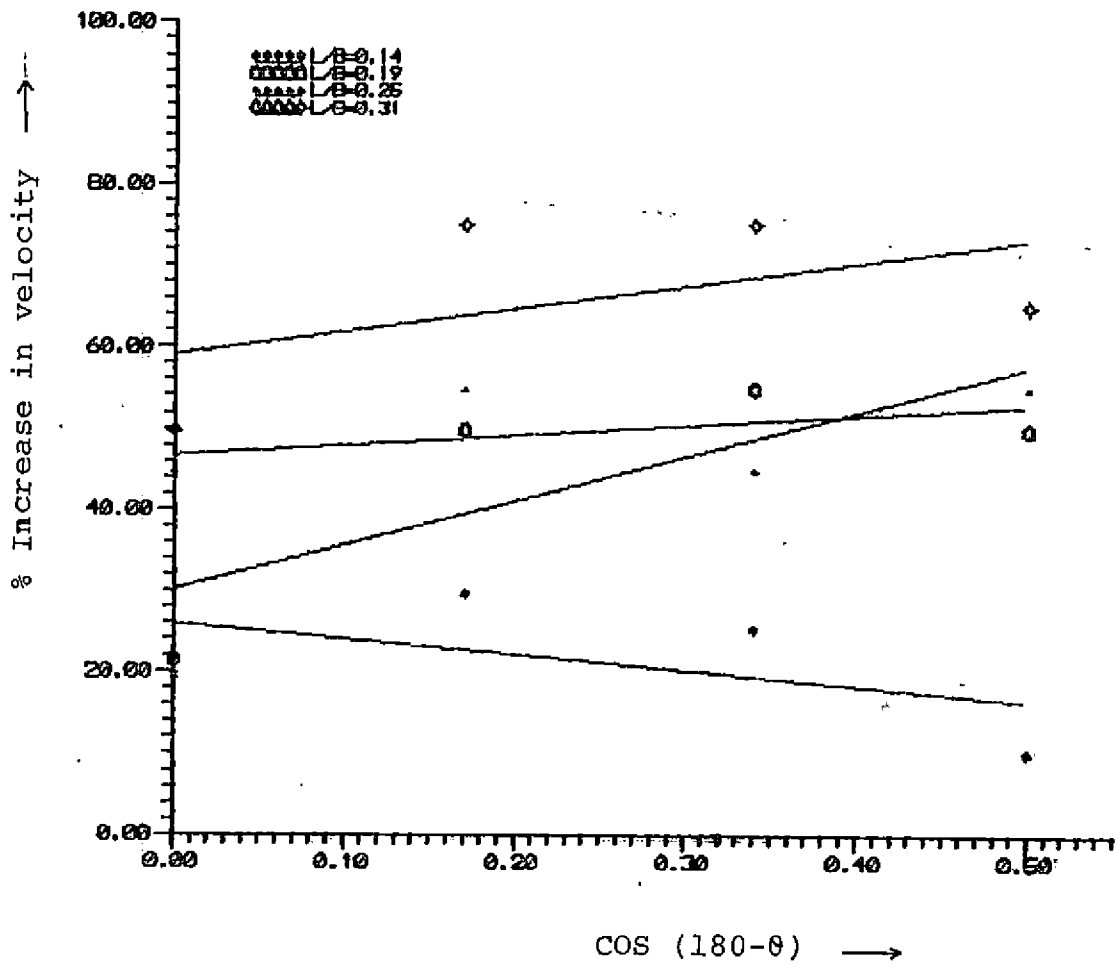


Fig. 27. Effect of spur angle on velocity at opposite bank for a discharge of 14.14 lps.

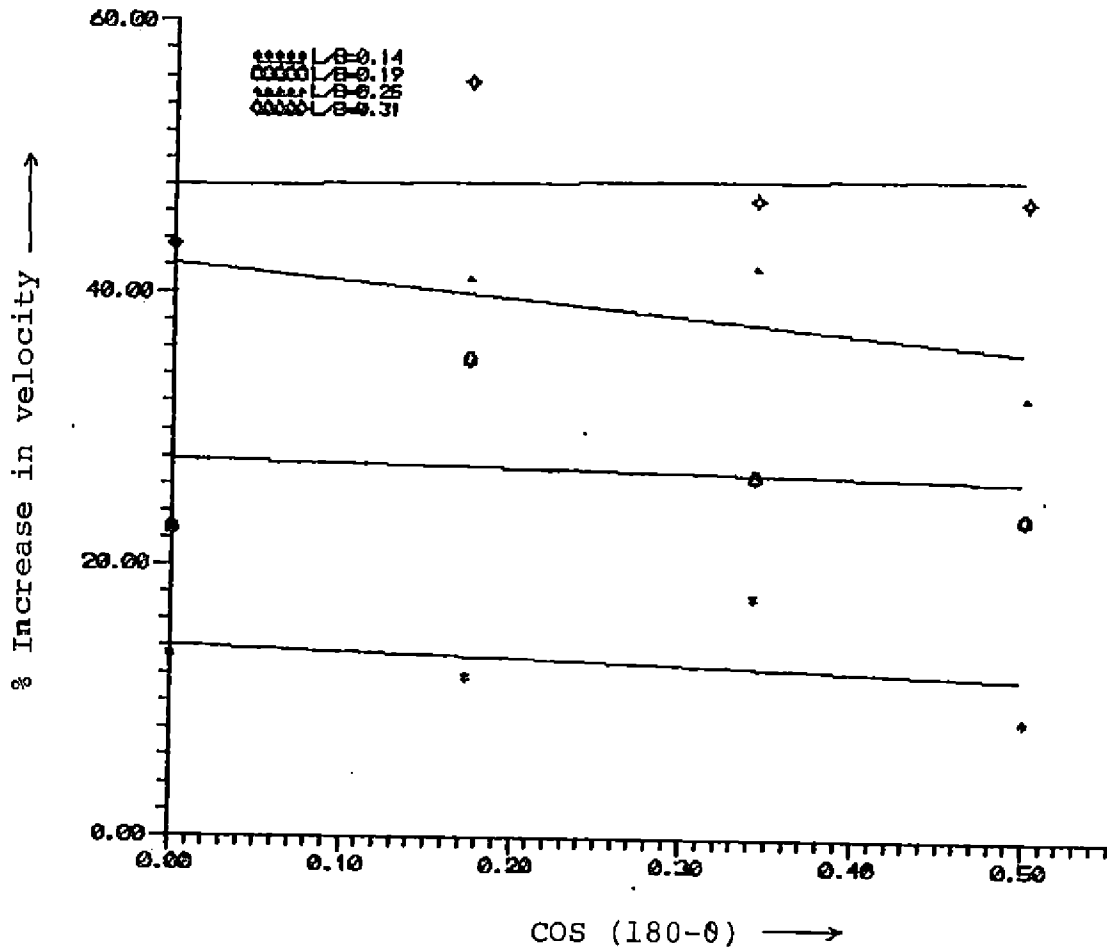


Fig. 28. Effect of spur angle on velocity at opposite bank for a discharge of 28.28 lps.

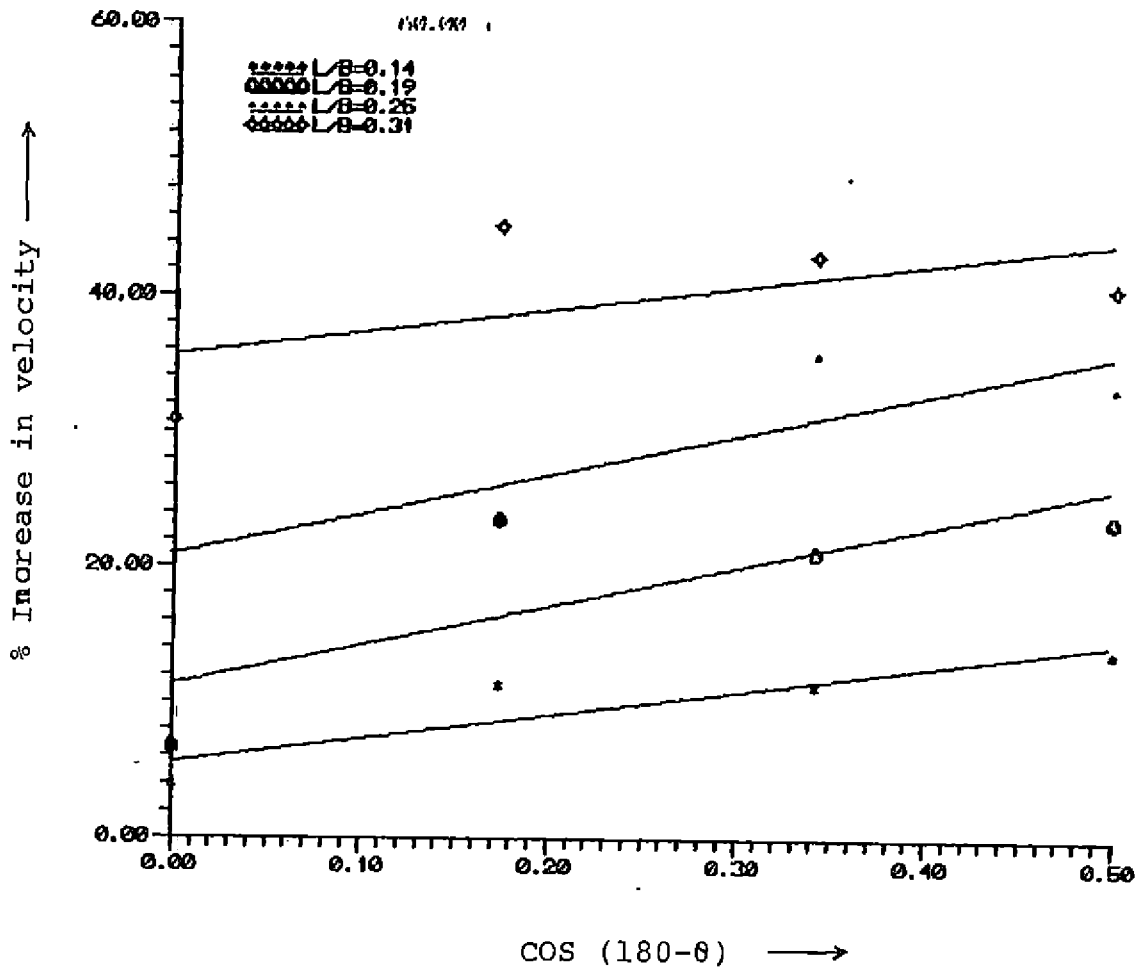


Fig. 29. Effect of spur angle on velocity at opposite bank for a discharge of 42.42 lps.

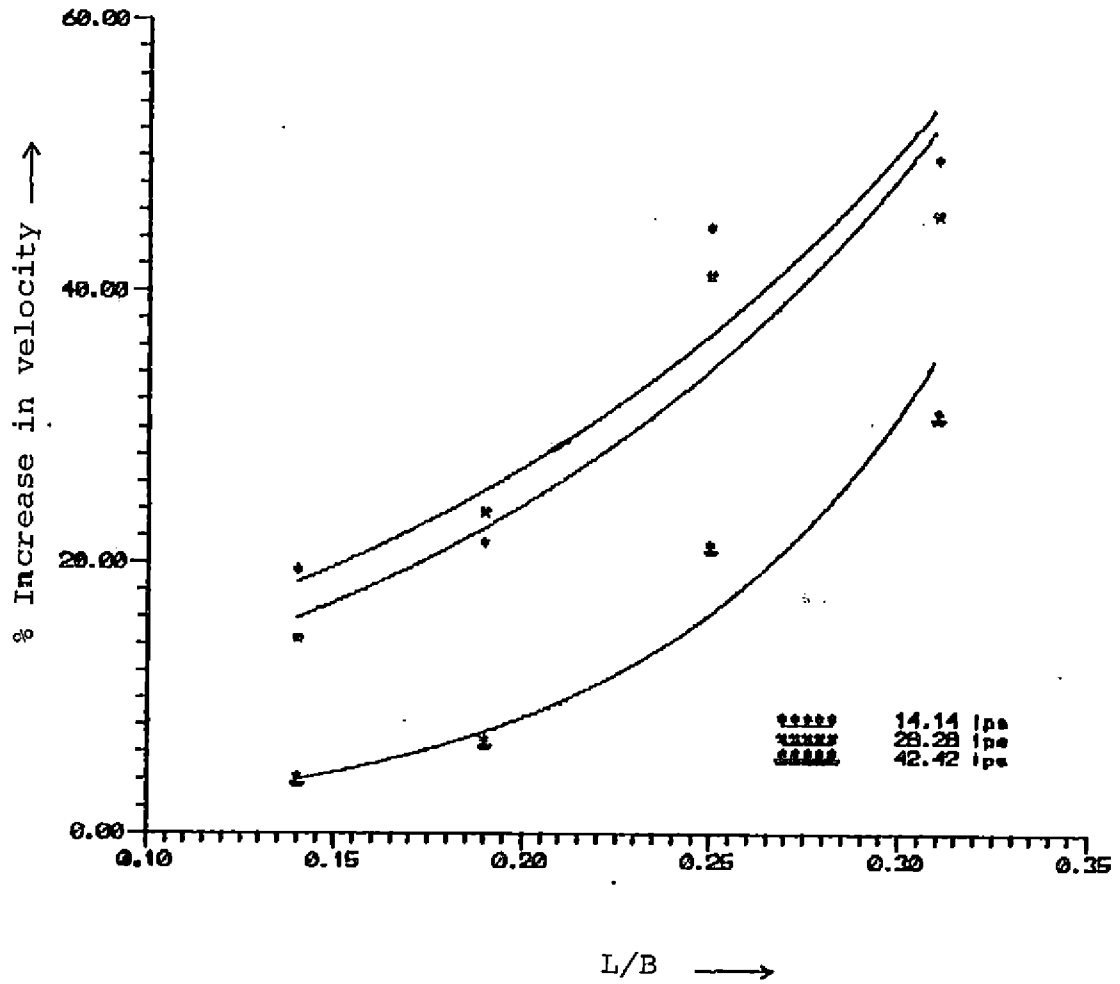
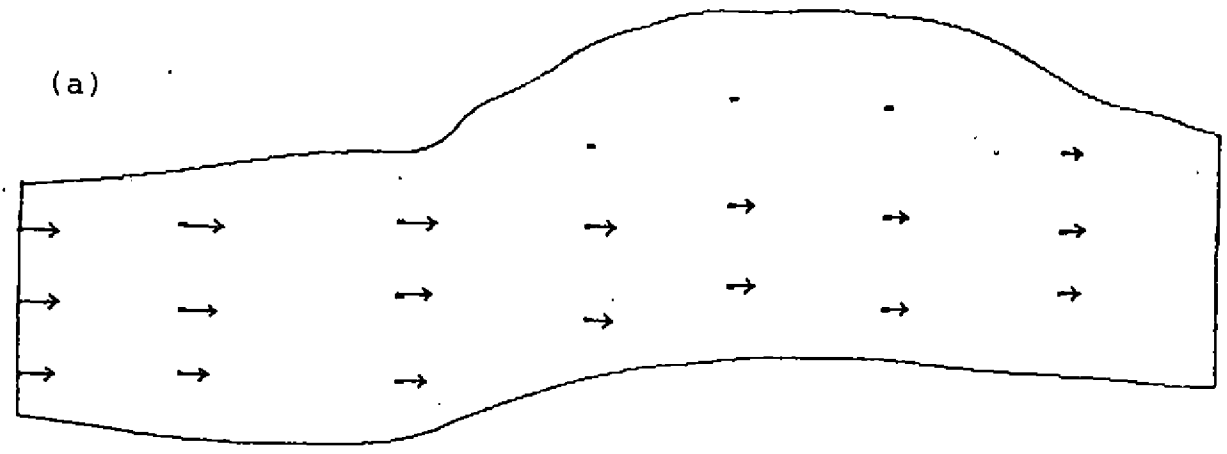


Fig. 30. Effect of spur length on velocity at opposite bank (spur angle = 90°)



Scale  
Velocity 1 cm = 55 cm/sec  
Length 1 cm = 54 cm

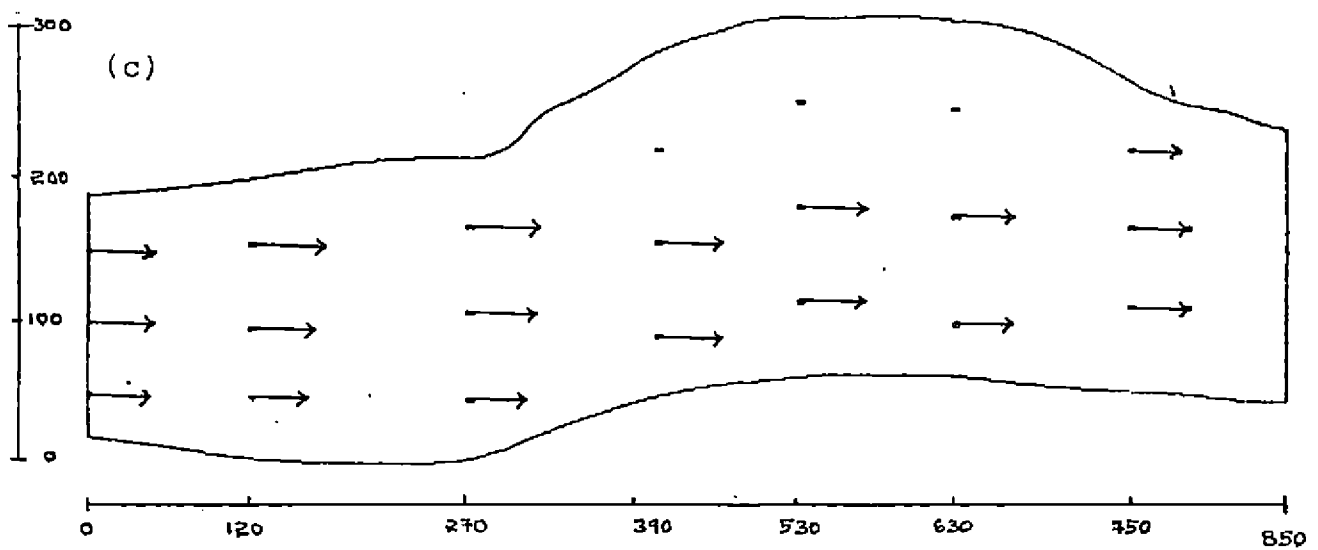
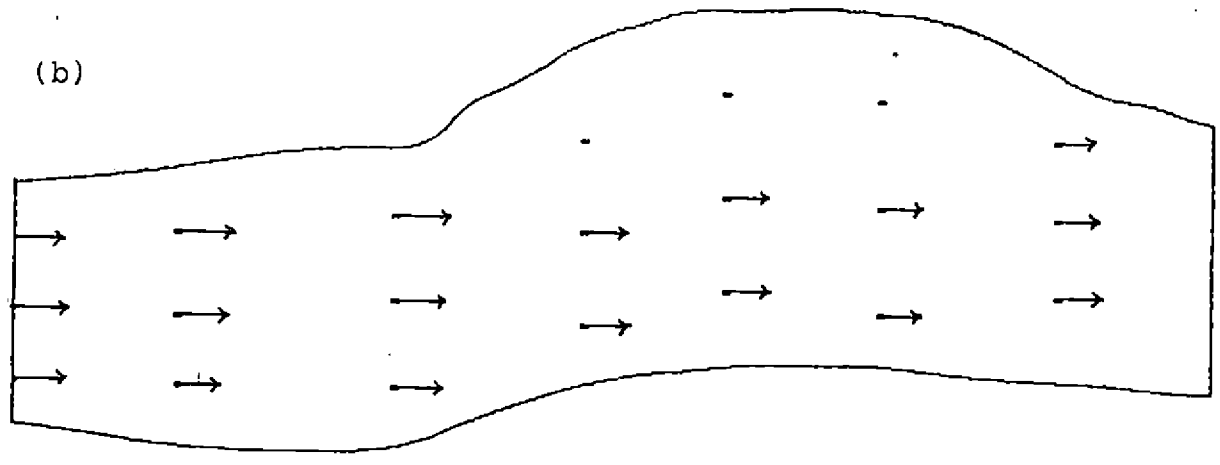


Fig. 31. Velocity grid without spur for discharge rates  
(a) 14.14 lps (b) 28.28 lps (c) 42.42 lps.

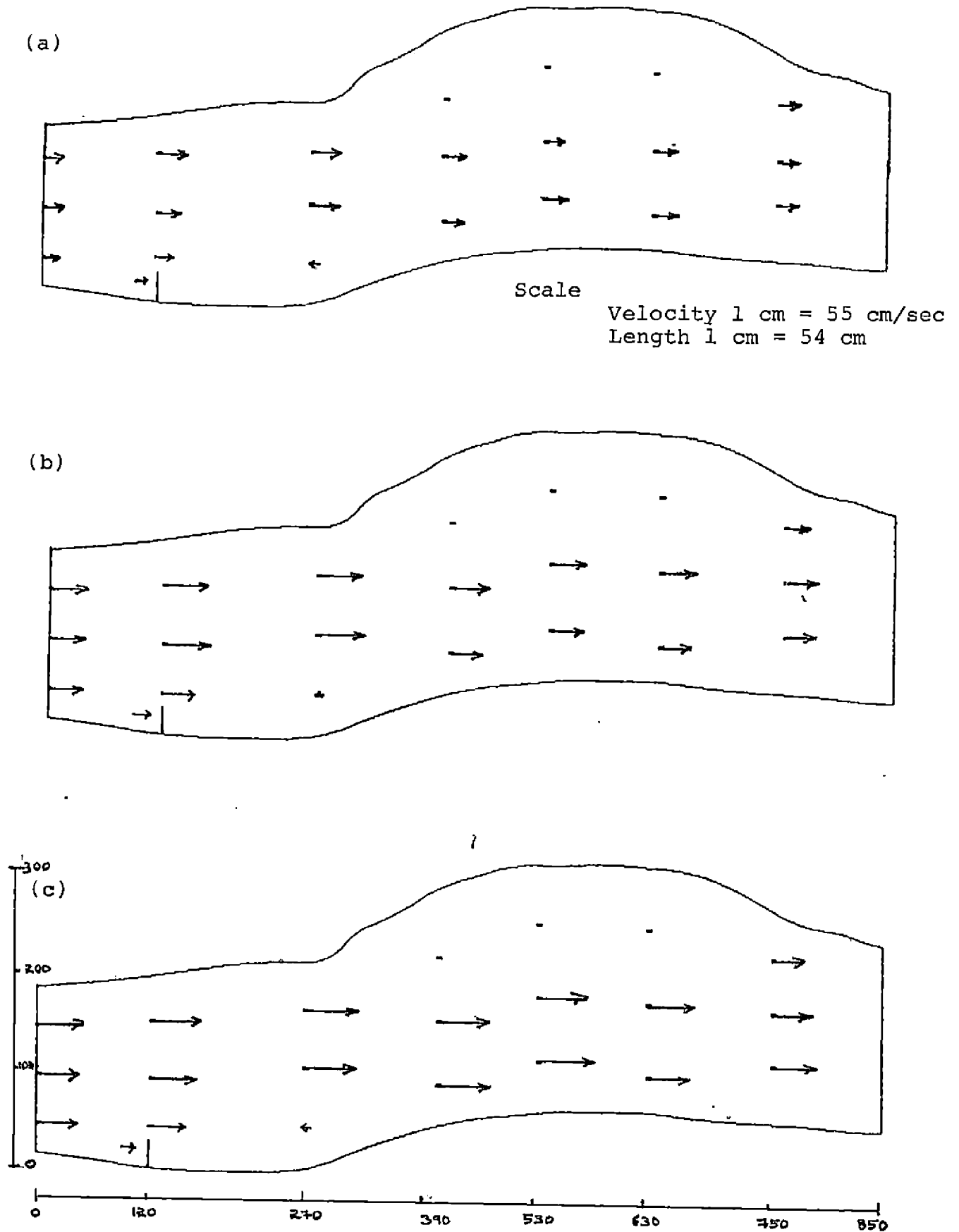


Fig. 32. Velocity grid along single spur ( $L=25$  cm,  $\theta = 90^\circ$ ) for discharge rates (a) 14.14 lps (b) 28.28 lps (c) 42.42 lps



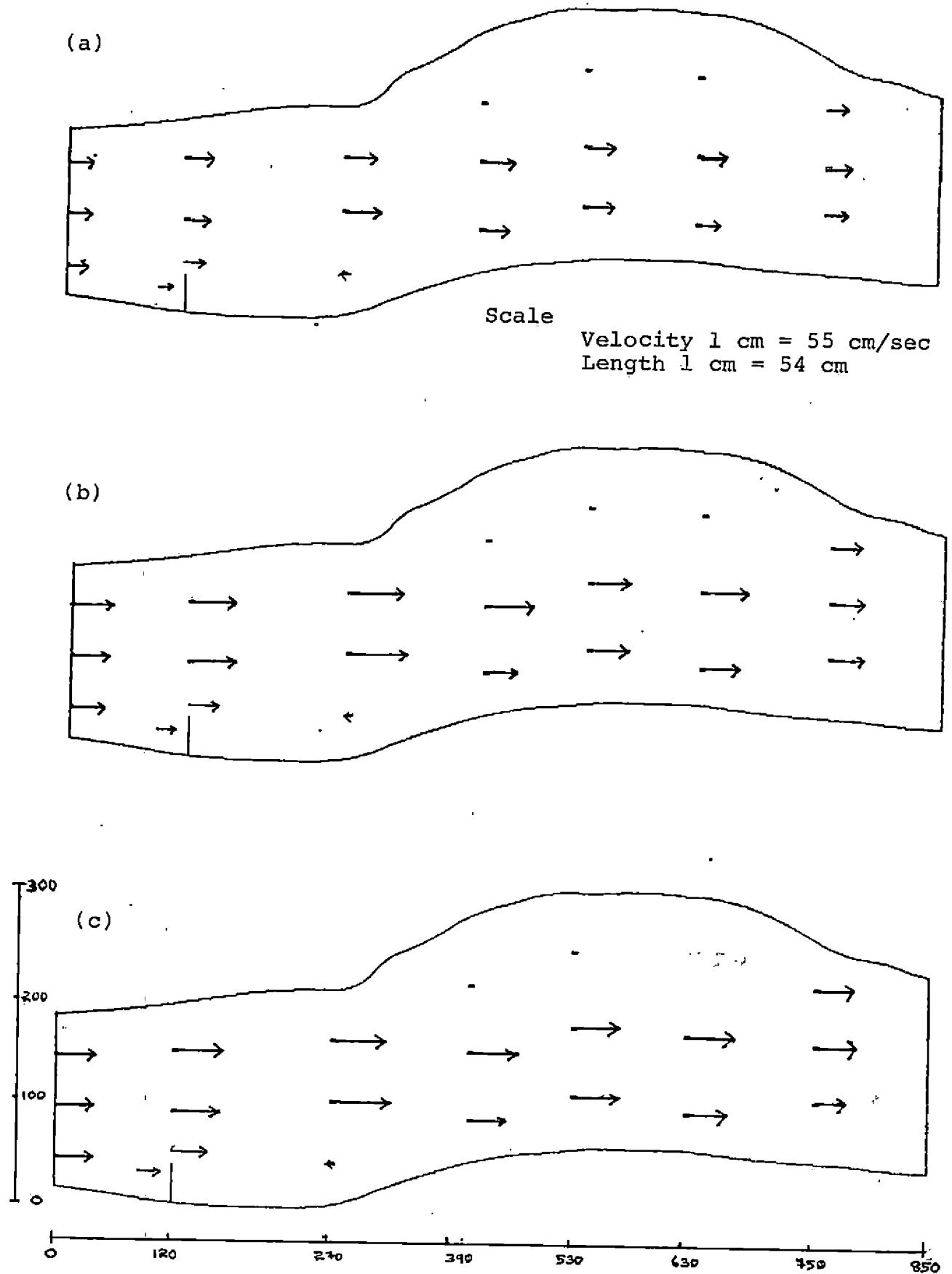


Fig. 33. Velocity grid along single spur ( $L=35$  cm,  $\theta = 90^\circ$ ) for discharge rates (a) 14.14 lps (b) 28.28 lps (c) 42.42 lps

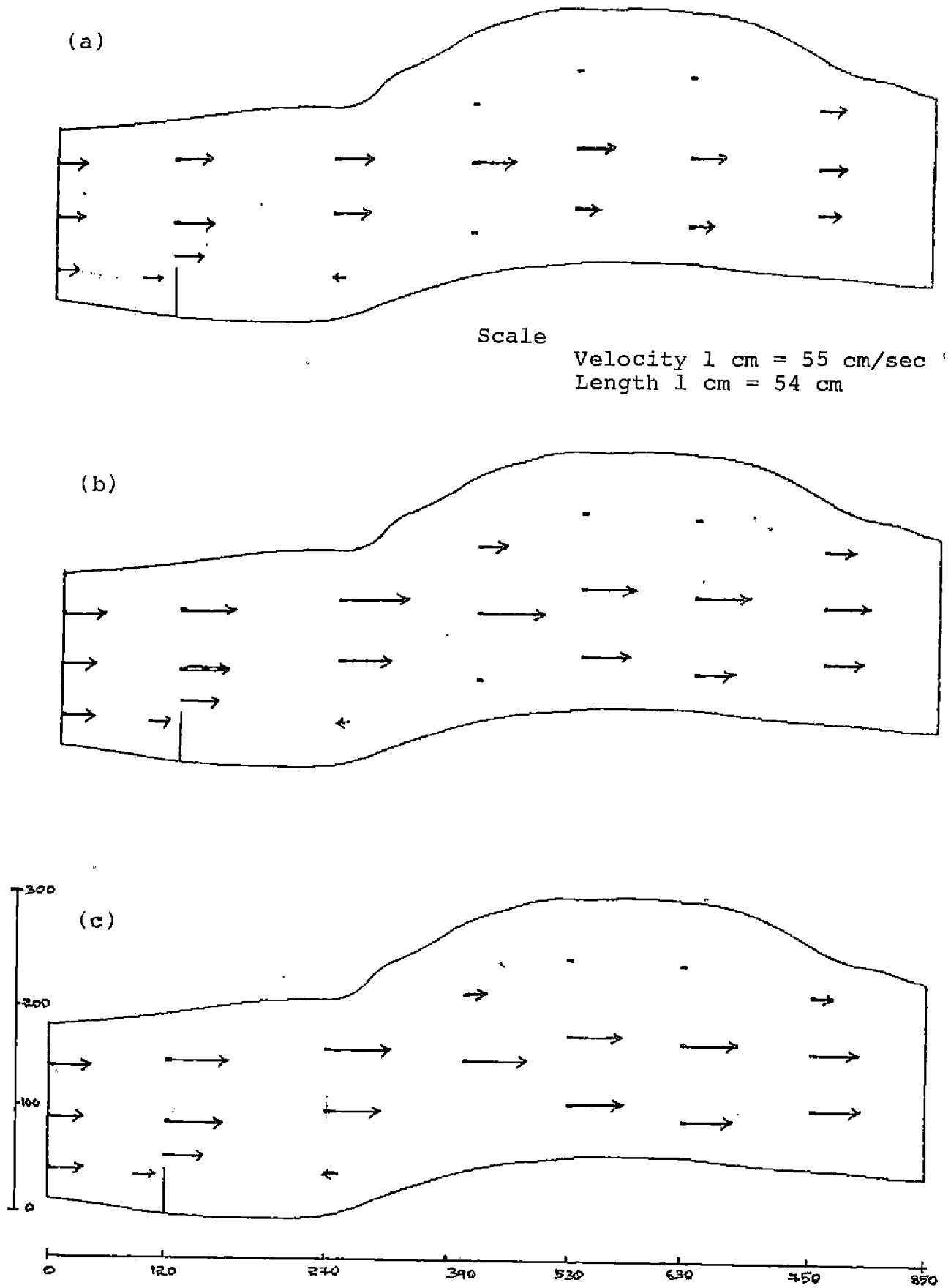


Fig. 34. Velocity grid along single spur ( $L=45$  cm,  $\phi = 90^\circ$ ) for discharge rates (a) 14.14 lps (b) 28.28 lps (c) 42.42 lps

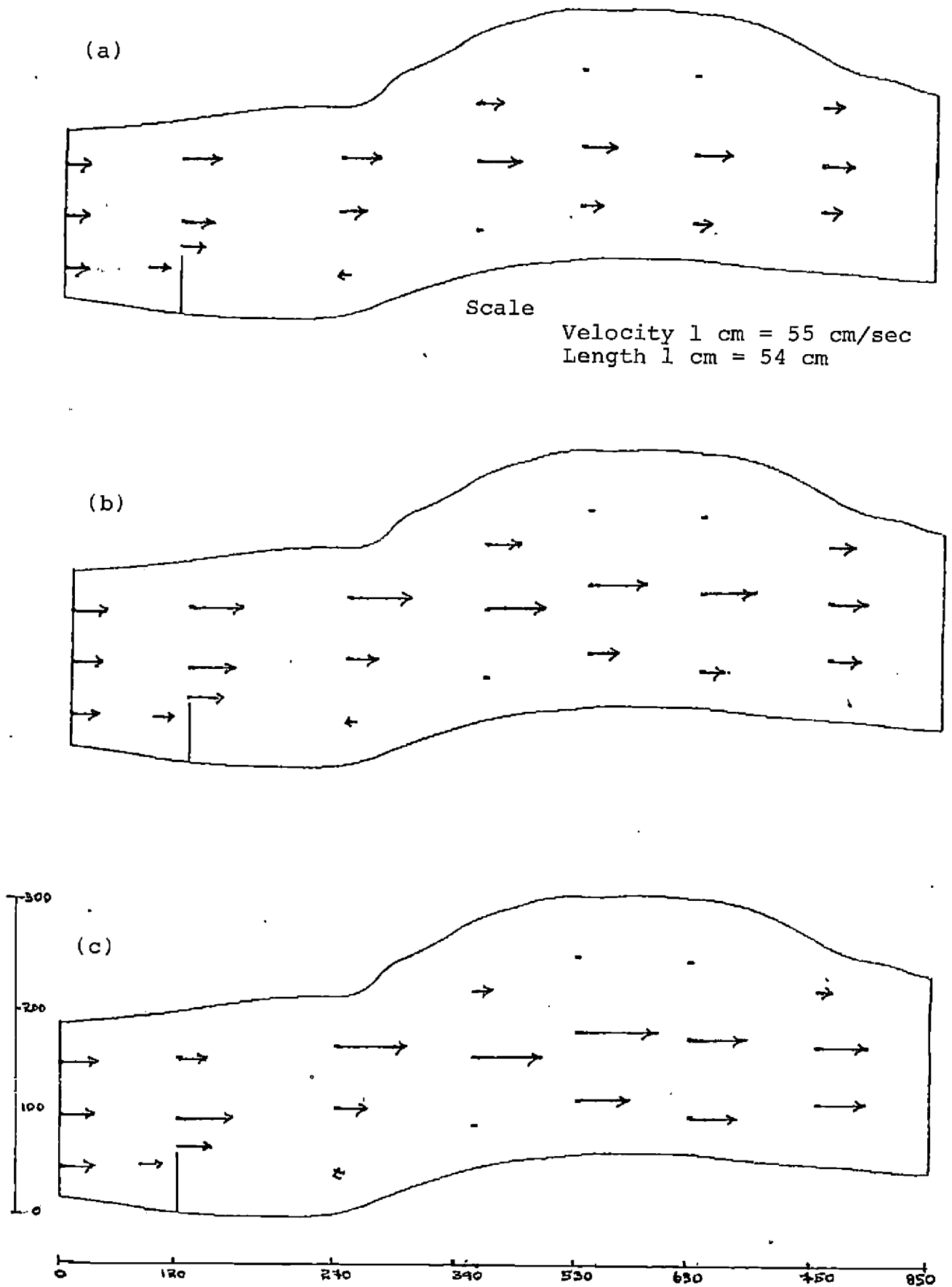


Fig. 35. Velocity grid along single spur ( $L=55$  cm,  $\theta = 90^\circ$ ) for discharge rates (a) 14.14 lps (b) 28.28 lps (c) 42.42 lps

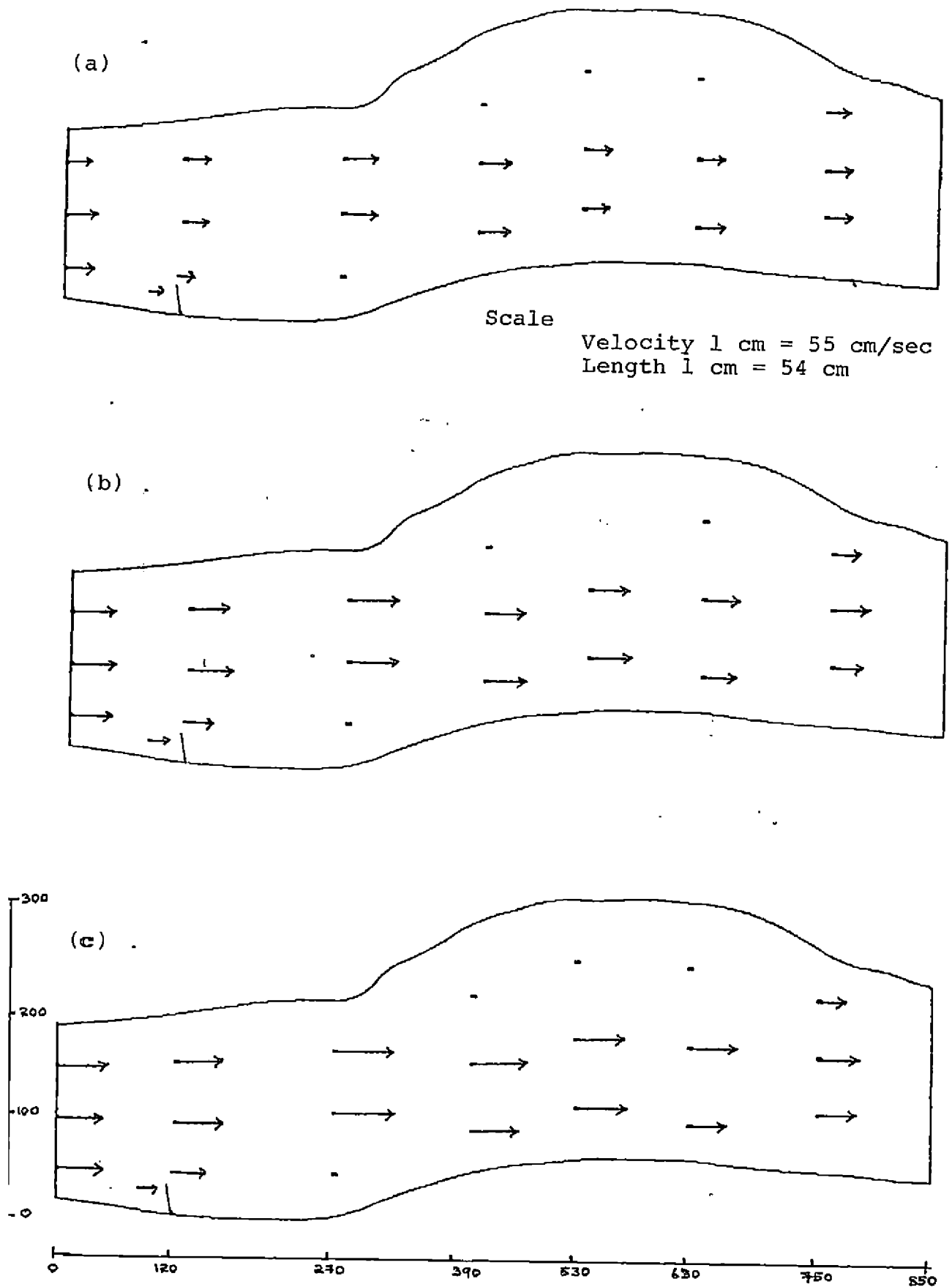


Fig. 36. Velocity grid along single spur ( $L=25$  cm,  $\theta = 100^\circ$ ) for discharge rates (a) 14.14 lps (b) 28.28 lps (c) 42.42 lps

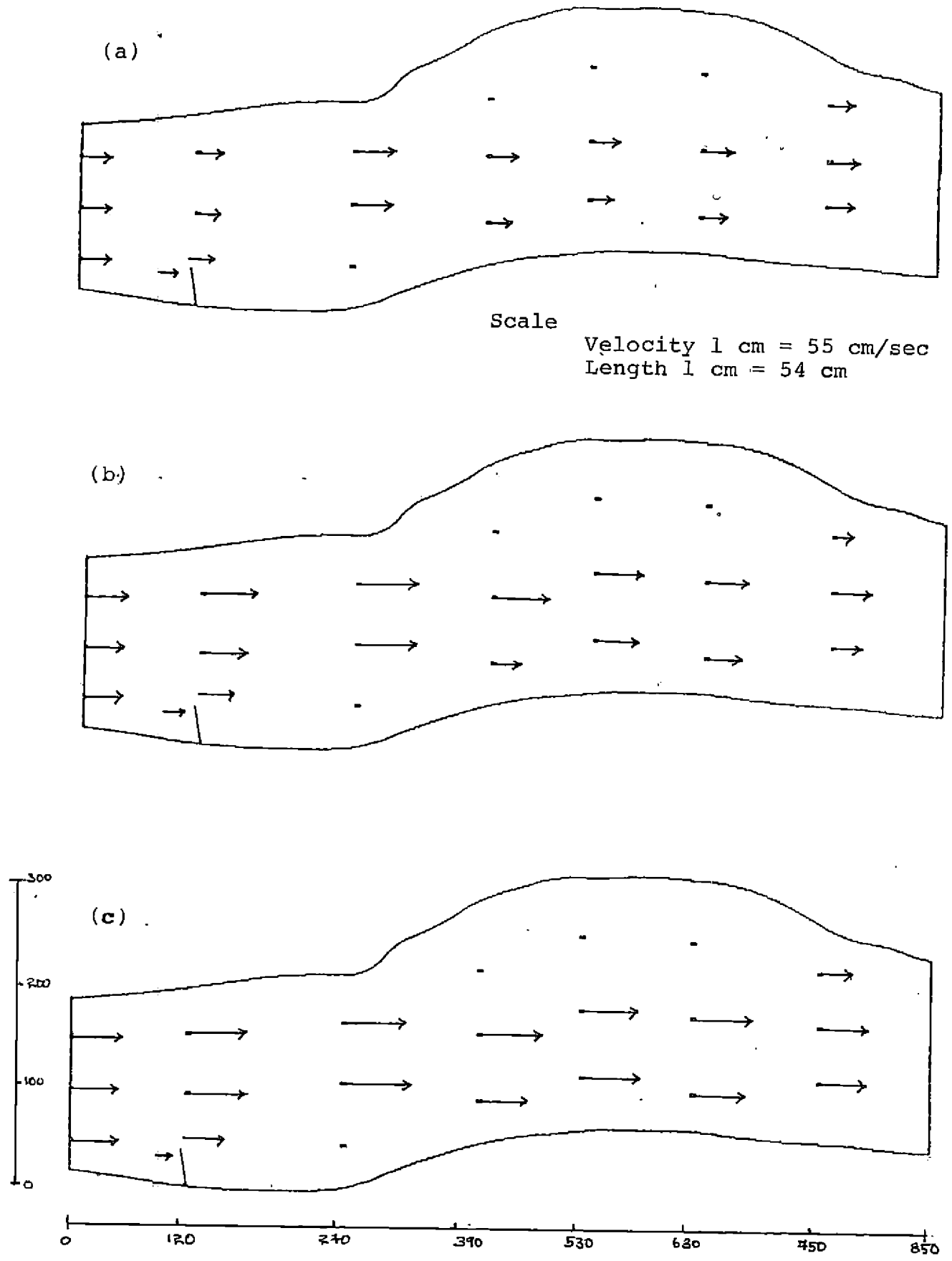


Fig. 37. Velocity grid along single spur ( $L=35$  cm,  $\theta = 100^\circ$ ) for discharge rates (a) 14.14 lps (b) 28.28 lps (c) 42.42 lps

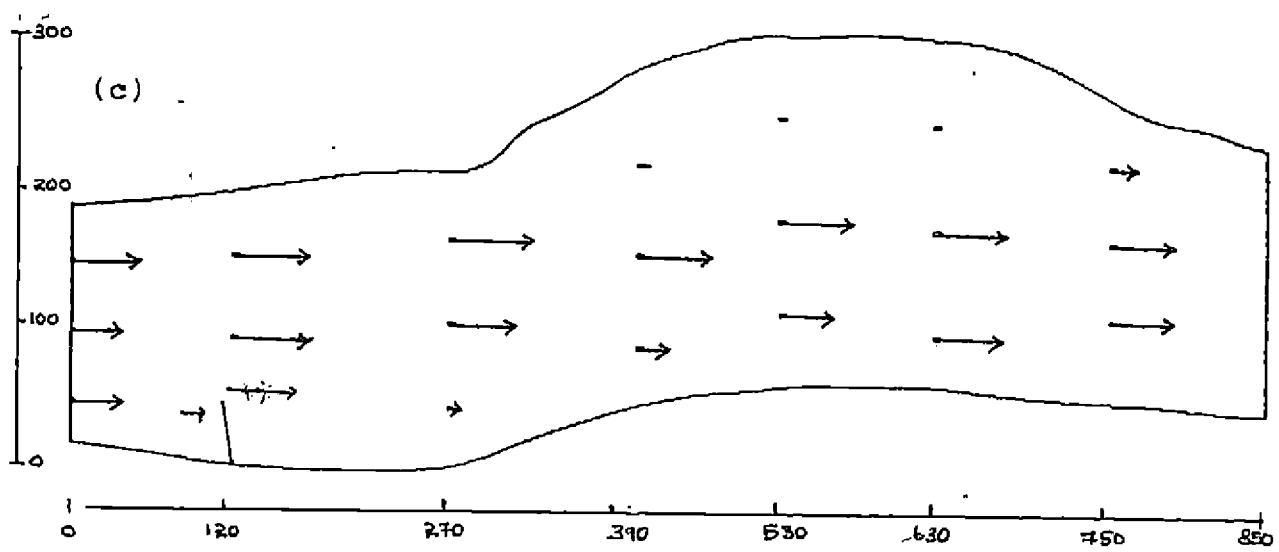
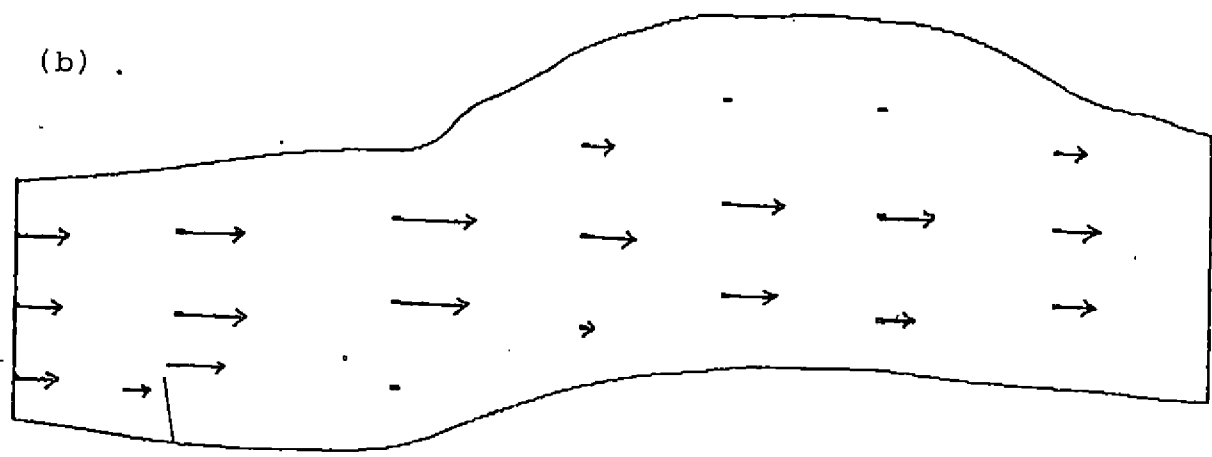
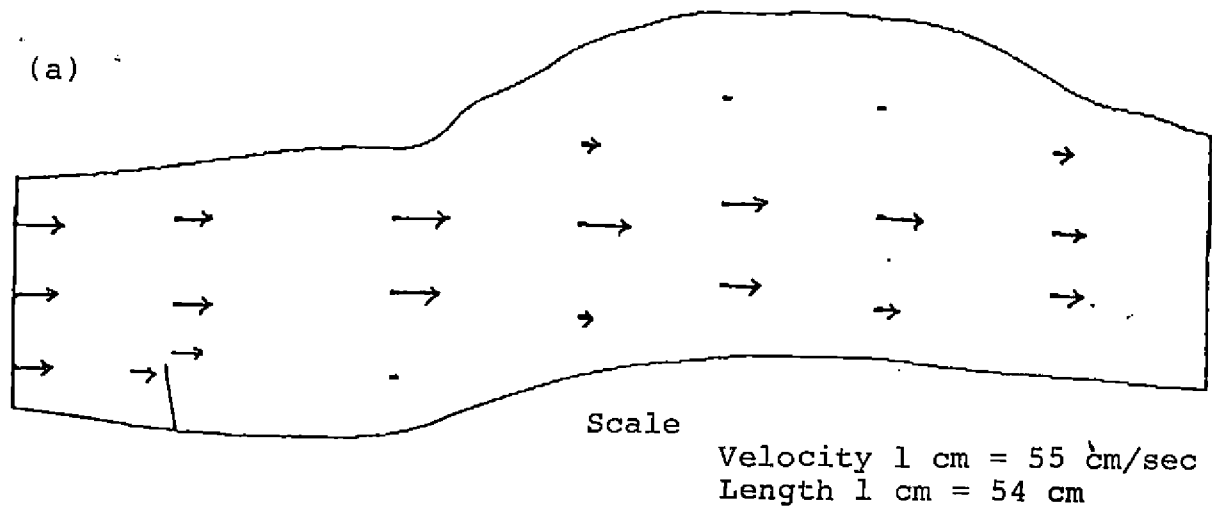


Fig. 38. Velocity grid along single spur ( $L=45$  cm,  $\theta = 100^\circ$ ) for discharge rates (a) 14.14 lps (b) 28.28 lps (c) 42.42 lps

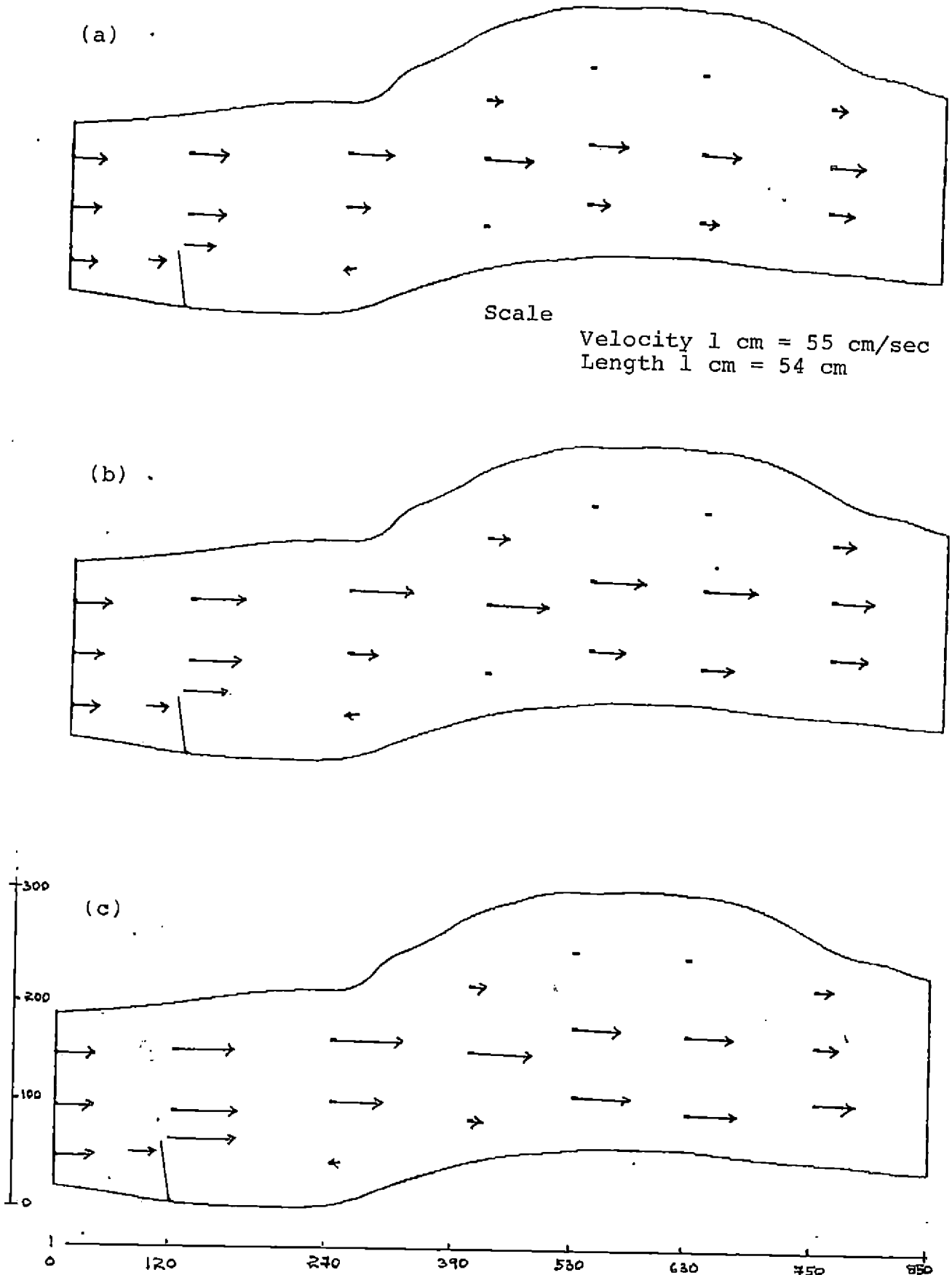


Fig. 39. Velocity grid along single spur ( $L=55$  cm,  $\Theta = 100^\circ$ ) for discharge rates (a) 14.14 lps (b) 28.28 lps (c) 42.42 lps

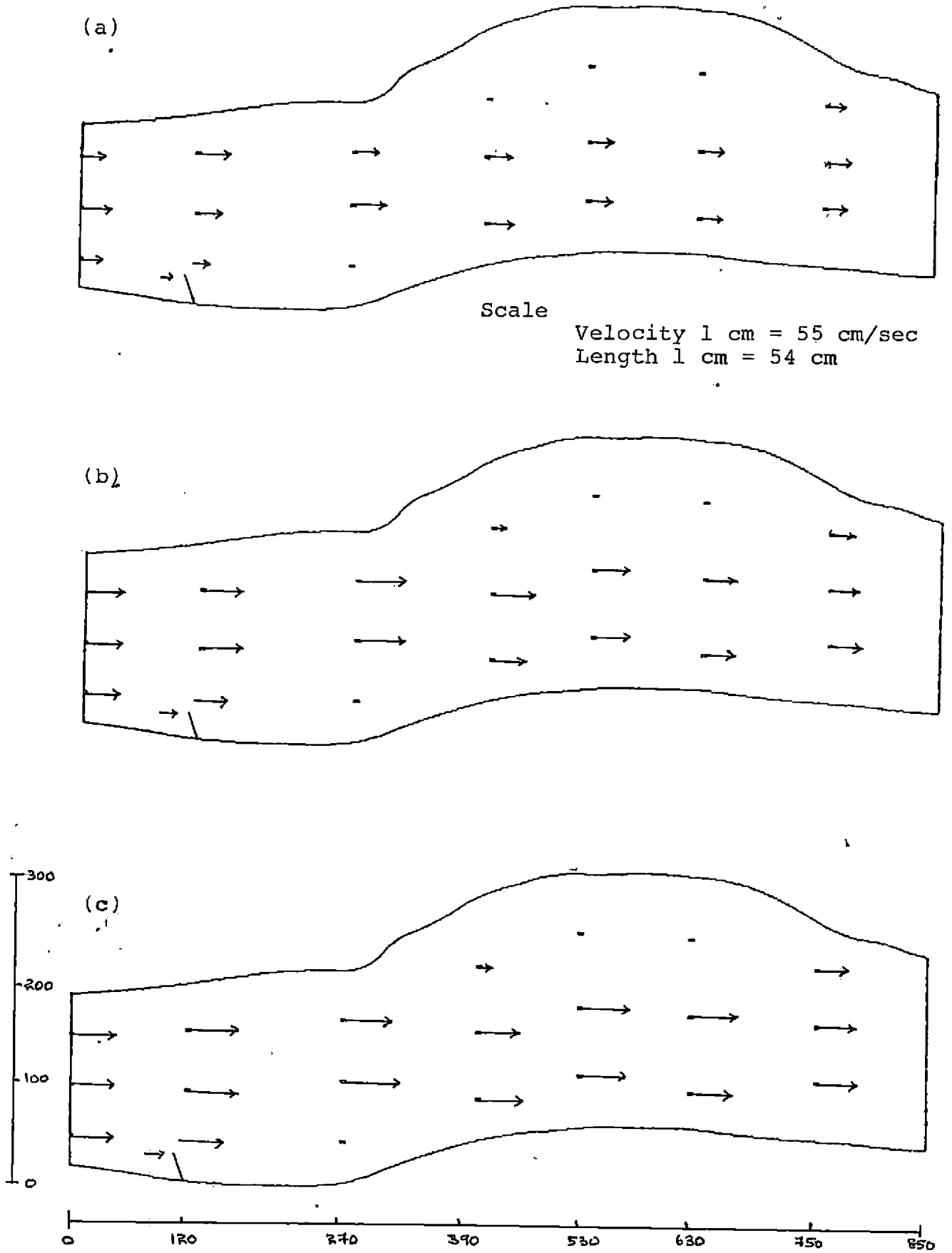


Fig. 40. Velocity grid along single spur ( $L=25$  cm,  $\theta = 110^\circ$ ) for discharge rates (a) 14.14 lps (b) 28.28 lps (c) 42.42 lps



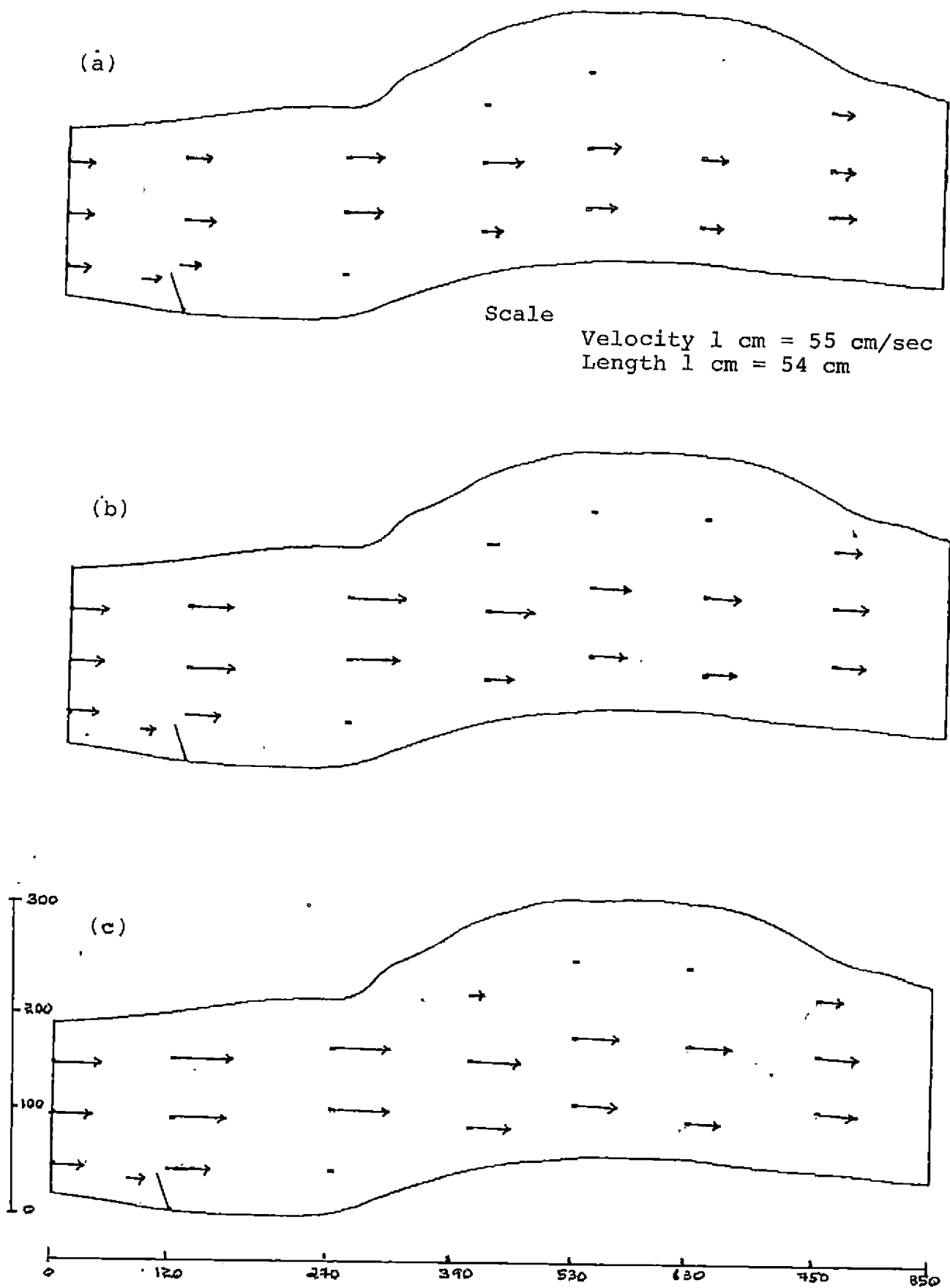


Fig. 41. Velocity grid along single spur ( $L=35$  cm,  $\theta = 110^\circ$ ) for discharge rates (a) 14.14 lps (b) 28.28 lps (c) 42.42 lps

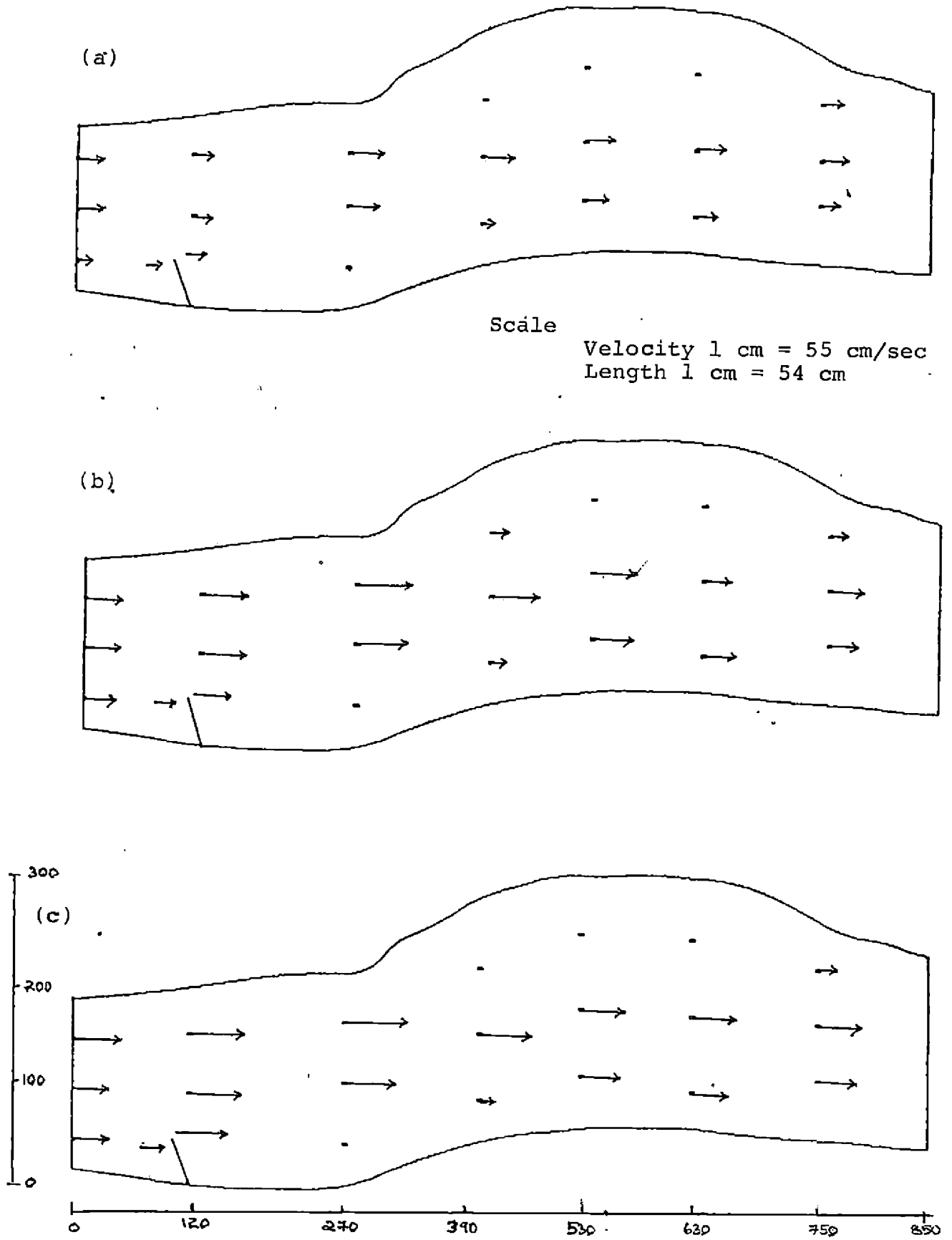


Fig. 42. Velocity grid along single spur ( $L=45$  cm,  $\theta = 110^\circ$ ) for discharge rates (a) 14.14 lps (b) 28.28 lps (c) 42.42 lps

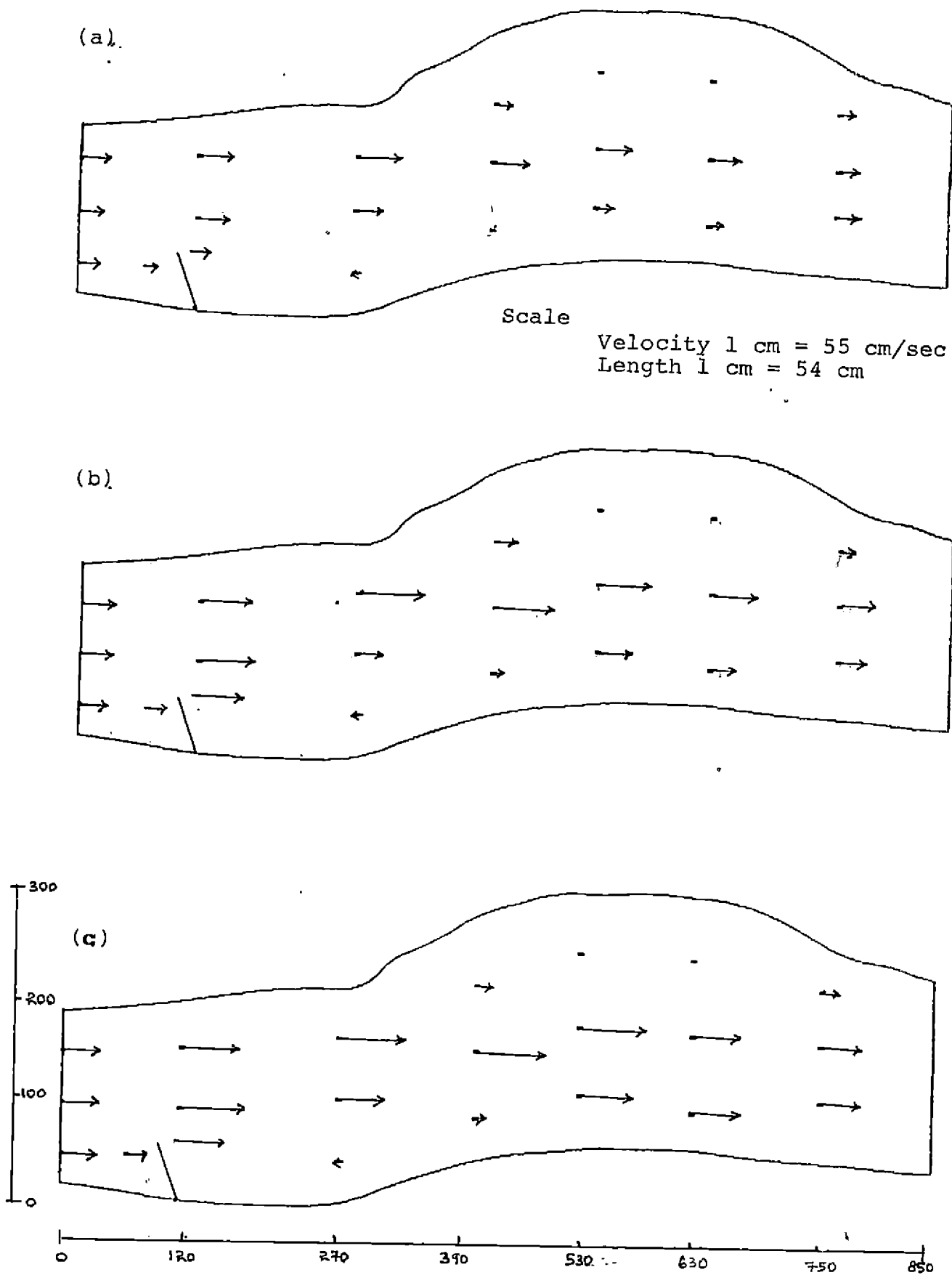


Fig 43. Velocity grid along single spur ( $L=55$  cm,  $\theta = 110^\circ$ ) for discharge rates (a) 14.14 lps (b) 28.28 lps (c) 42.42 lps

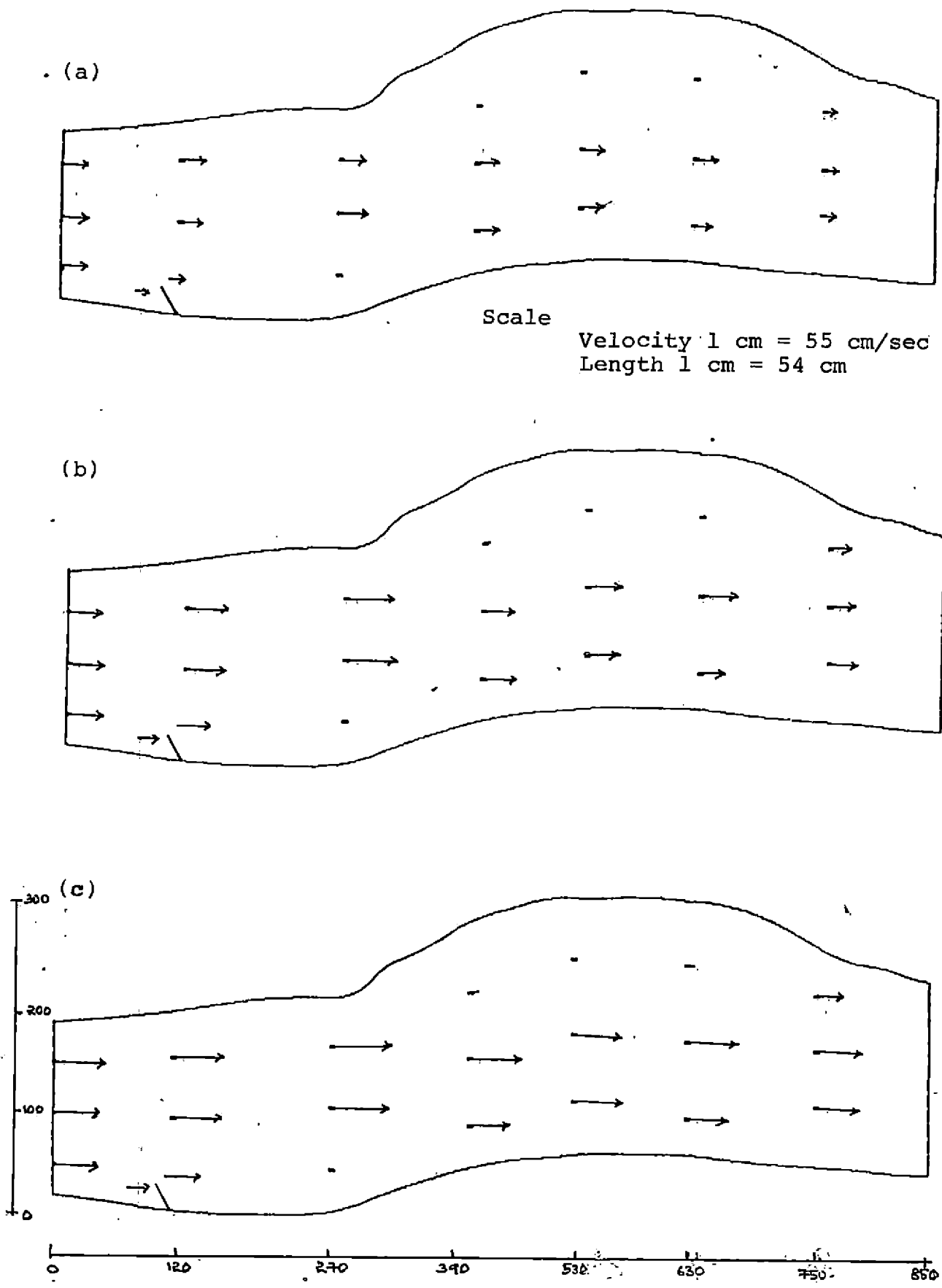


Fig. 44. Velocity grid along single spur ( $L=25$  cm,  $\theta = 120^\circ$ ) for discharge rates (a)14.14 lps (b)28.28 lps (c)42.42 lps

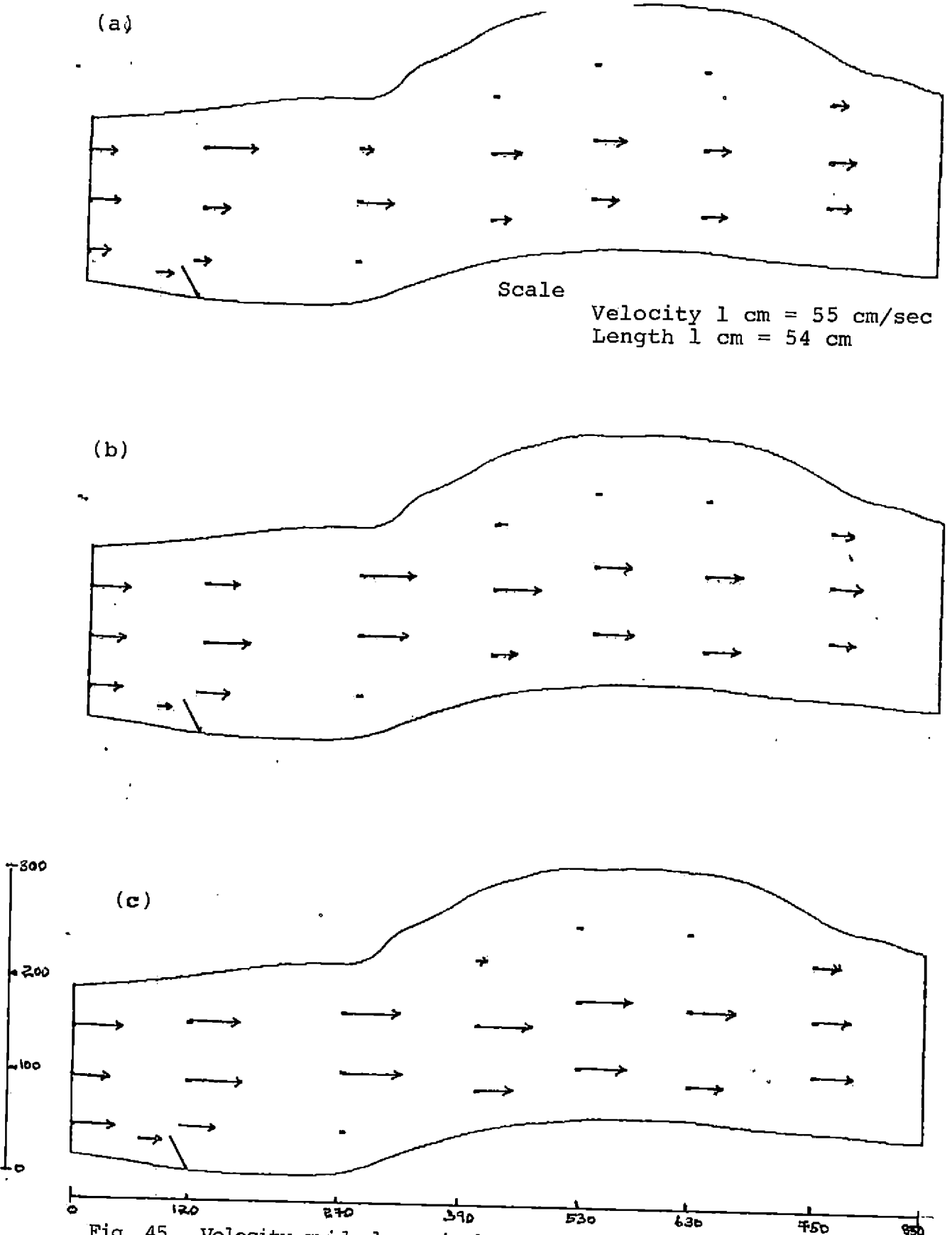
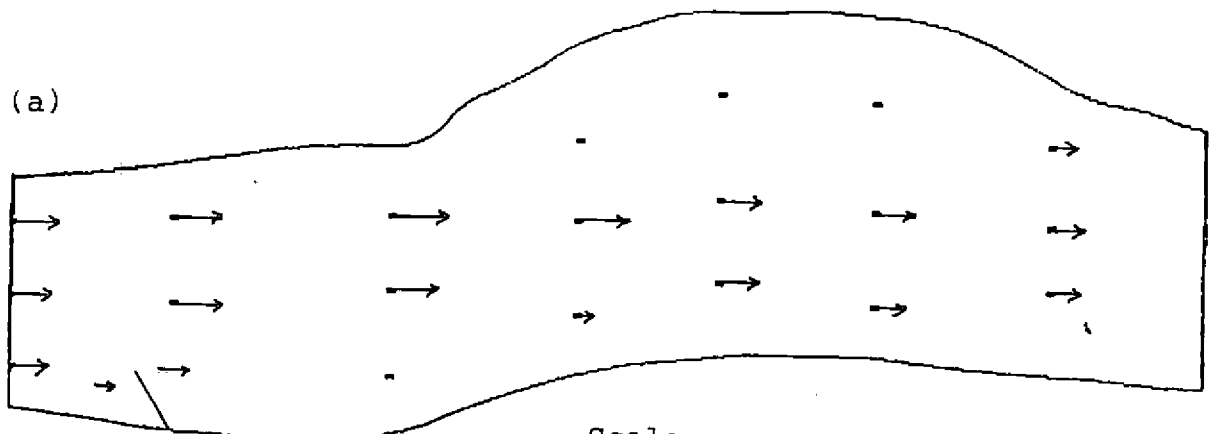


Fig. 45. Velocity grid along single spur ( $L=35$  cm,  $\theta = 120^\circ$ ) for discharge rates (a) 14.14 lps (b) 28.28 lps (c) 42.42 lps



Scale  
 Velocity 1 cm = 55 cm/sec  
 Length 1 cm = 54 cm

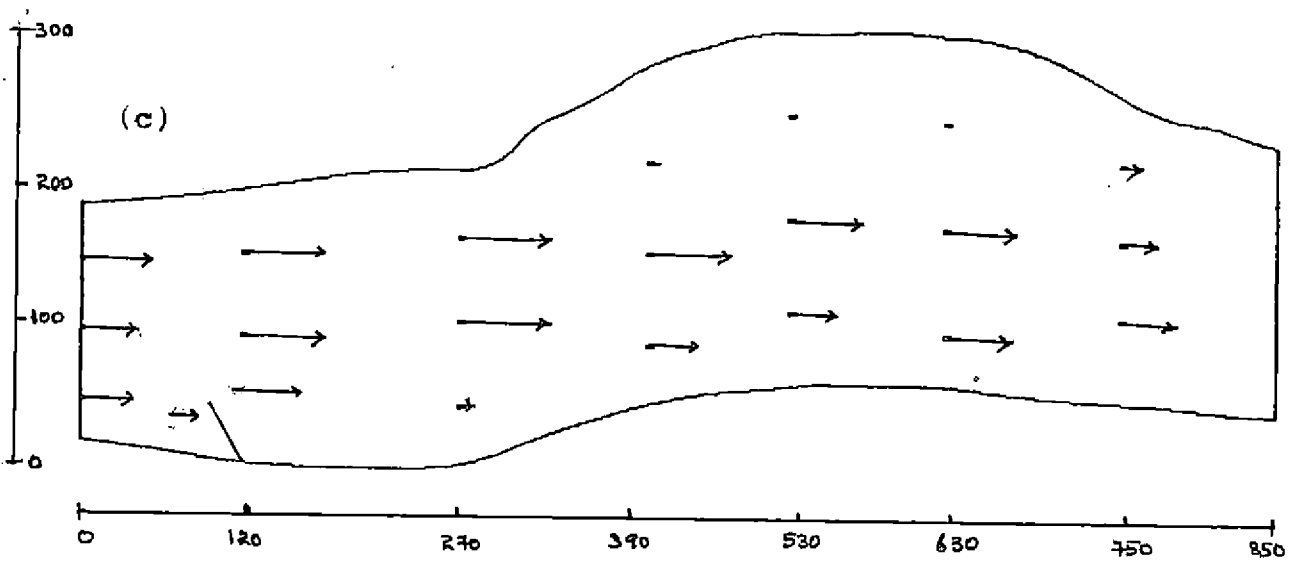
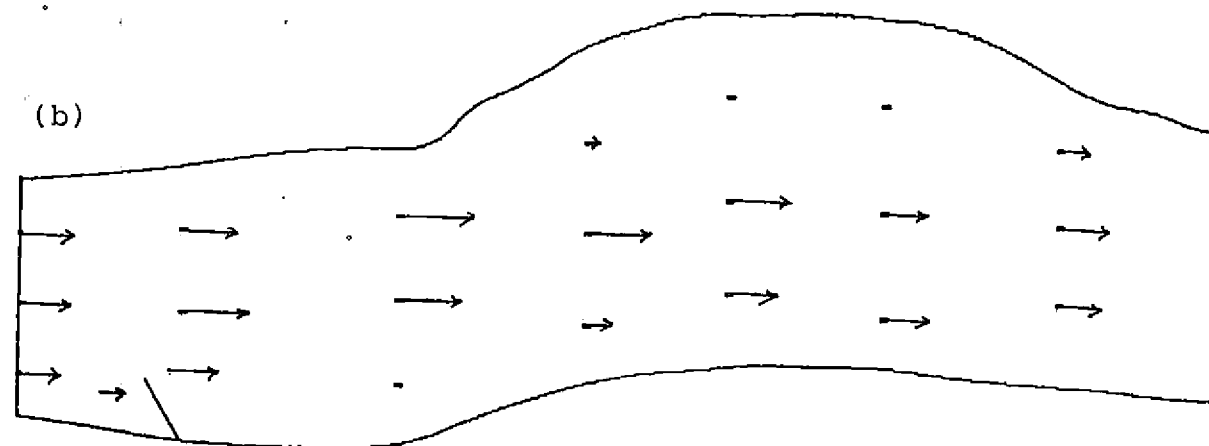


Fig. 46. Velocity grid along single spur ( $L=45$  cm,  $\Theta = 120^\circ$ ) for discharge rates (a) 14.14 lps (b) 28.28 lps (c) 42.42 lps

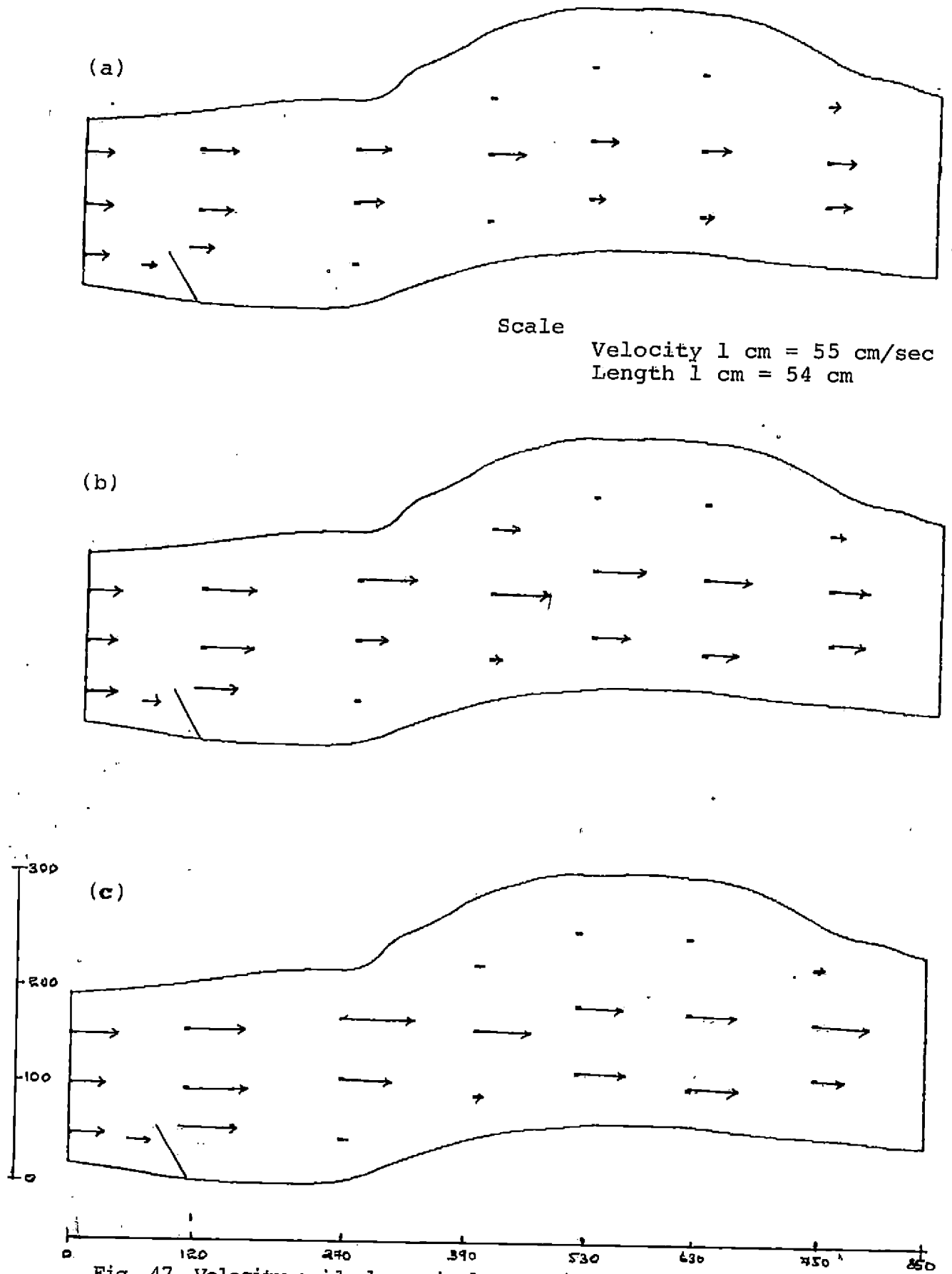


Fig. 47. Velocity grid along single spur ( $L=55$  cm,  $\theta = 120^\circ$ ) for discharge rates (a) 14.14 lps (b) 28.28 lps (c) 42.42 lps

achieved by greater spur angles is compensated by the reduction in constriction of the channel.

#### 4.1.2 Multiple spur experiments

Experiments were conducted on rigid bed to analyse design parameters of spurs such as length, angle and spacing as explained in chapter 3.12.2. It was done by placing spur models of different lengths viz, 25 cm, 35 cm, 45 cm, and 55 cm with different spacings of  $2L$ ,  $3L$ ,  $4L$  and  $5L$  where  $L$  is the length of spur model under study.

Data on flow pattern and velocity distribution in the test section were collected from the model as same as in single spur study. From flow patterns plotted (Fig.48 to 63) with collected data, it was observed that the length of bank protected increased with the increase in spur spacing. It was also observed that spurs with  $2L$  spacing function as a single spur only, since almost all of flow diversion is effected by the first spur itself. It can be seen from comparison of figures 11,15,19,23 with figures 47,51,55,59.

Another trend observed from the figures is that the effect of second spur on flow diversion increased with the increase in spur spacing. It may be due to the fact that as the flow diverted from the first spur, it reaches the vicinity of the second spur with larger spacings.



But contrary to the general trend, it was observed that when the spacing is  $5L$ , the diverted flow from the second spur is getting attracted towards the downstream bank after a short distance. This is entirely due to the typical bend of the model under study.

In order to analyse the extent of bank protection achieved by provision of spurs as well as to study the increase in velocity at opposite bank, velocities for measuring grid along multiple spurs were taken and are presented in Fig.64 to 79. It can be seen from these figures that the reduction in velocities along the affected bank were increased with spur length and spur spacing. It is probably because of greater spur length and spur spacing causes greater constriction of the channel and this effect is multiplied by providing spurs with greater spacing.

By analysis of these figures, it can also be seen that velocity at opposite bank increased with increasing spur length as well as spur spacing. But velocity of flow at a point near the opposite bank against first spur is independent of positioning of the second spur. From the analysis of velocities at downstream points near left bank, it can be seen that velocities increased with increase in spur spacing. This increment is evident in the case of

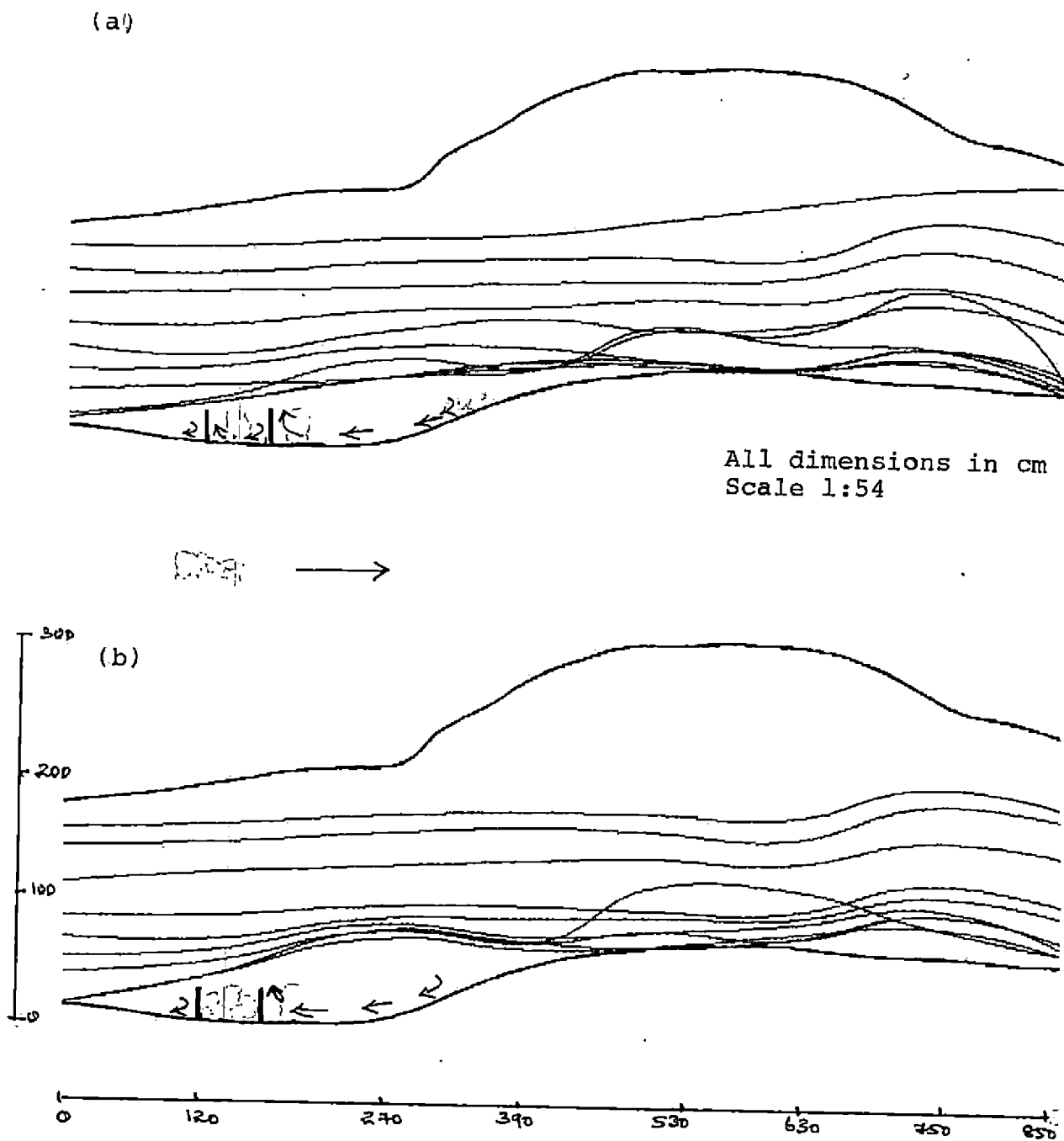


Fig. 48. Flow pattern for multiple spur scheme ( $L=25$  cm, spacing= $2L$  for discharge rates (a) 28.28 lps (b) 42.42 lps

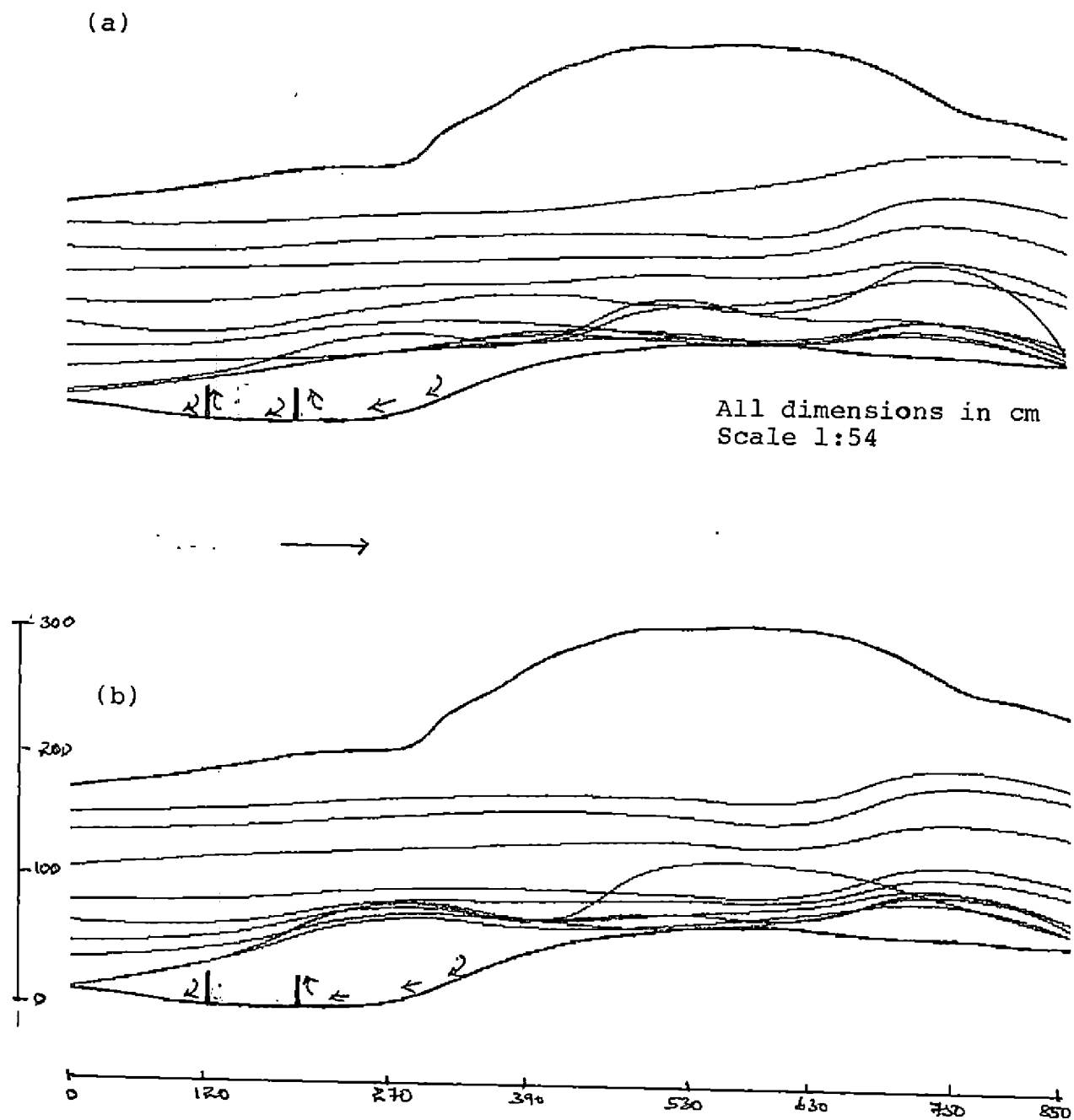


Fig. 49. Flow pattern for multiple spur scheme ( $L=25$  cm, spacing= $3L$ ) for discharge rates (a) 28.28 lps (b) 42.42 lps

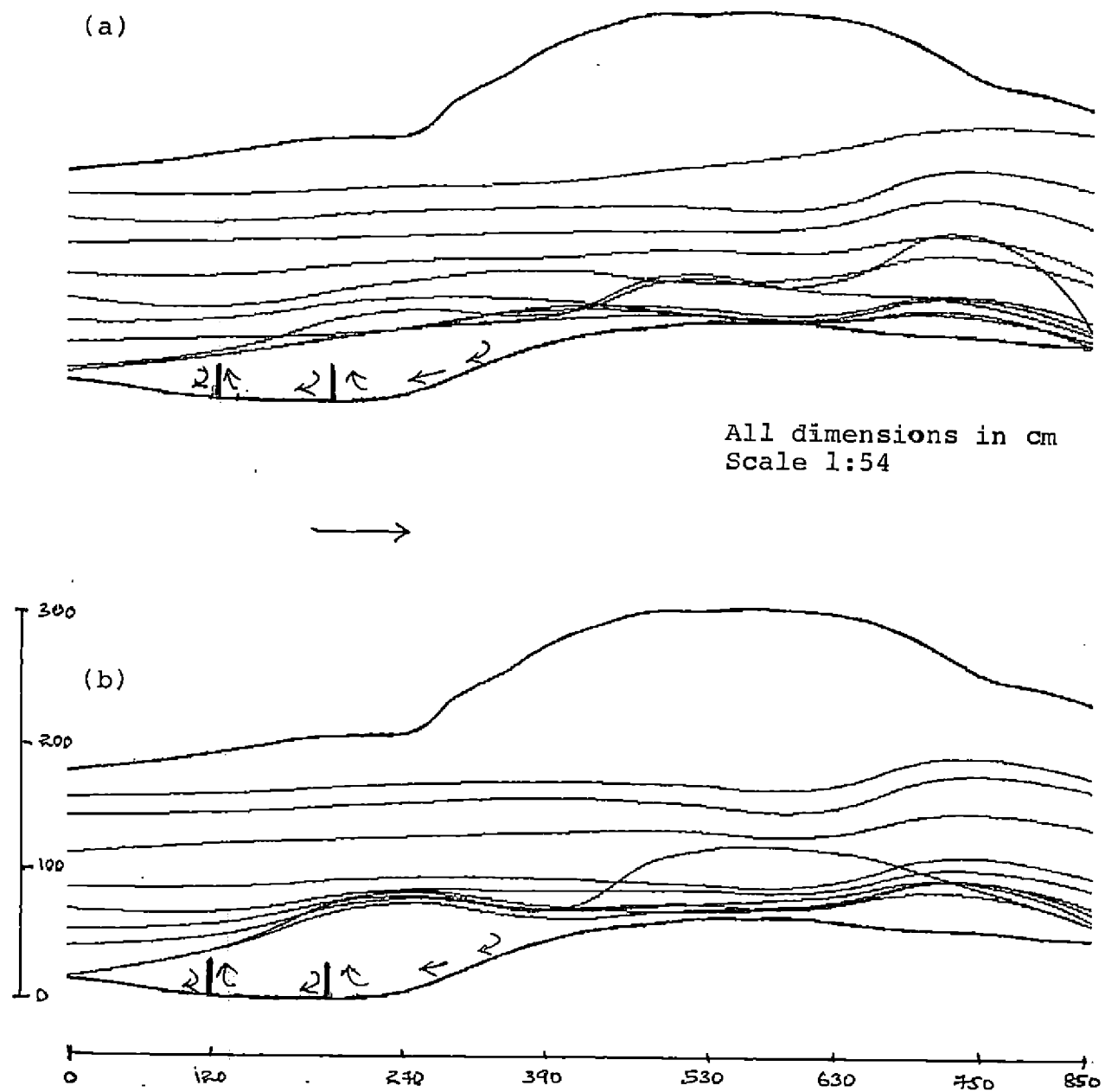
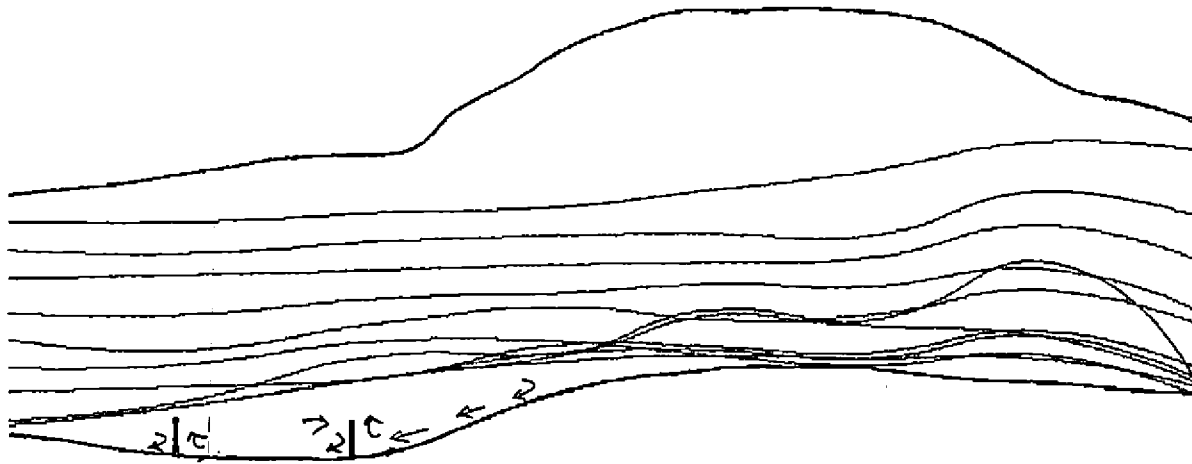


Fig. 50. Flow pattern for multiple spur scheme ( $L=25$  cm, spacing= $4L$ ) for discharge rates (a) 28.28 lps (b) 42.42 lps

(a)



All dimensions in cm  
Scale 1:54

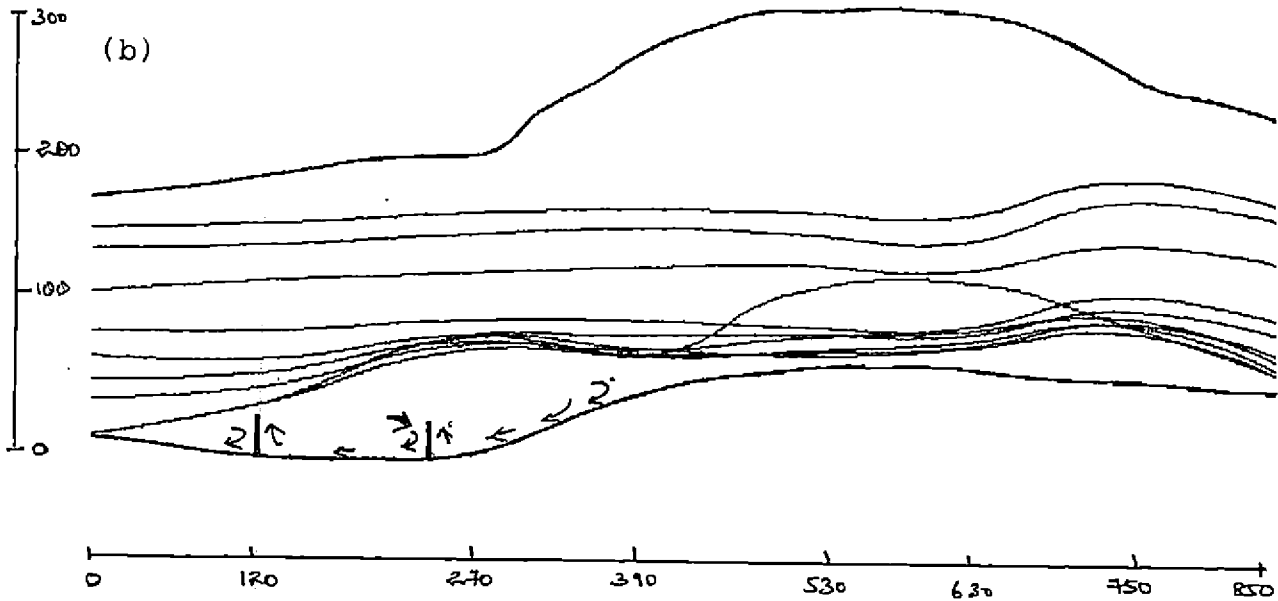
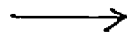


Fig. 51. Flow pattern for multiple spur scheme ( $L=25$  cm, spacing  $=5L$ )  
for discharge rates (a) 28.28 lps (b) 42.42 lps

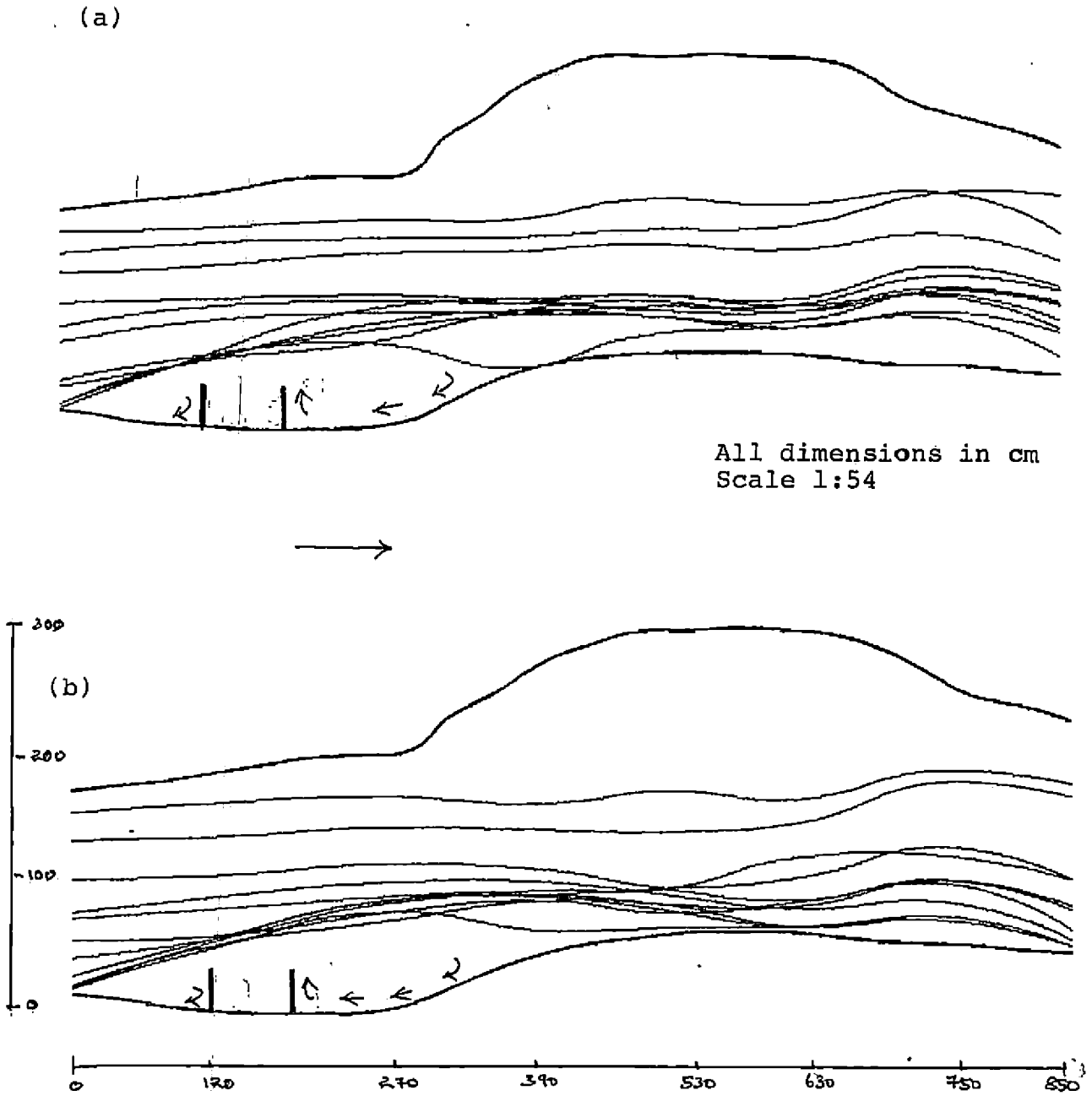


Fig. 52. Flow pattern for multiple spur scheme( $L=35$  cm, spacing  $=2L$ )  
for discharge rates (a)28.28 lps (b)42.42 lps

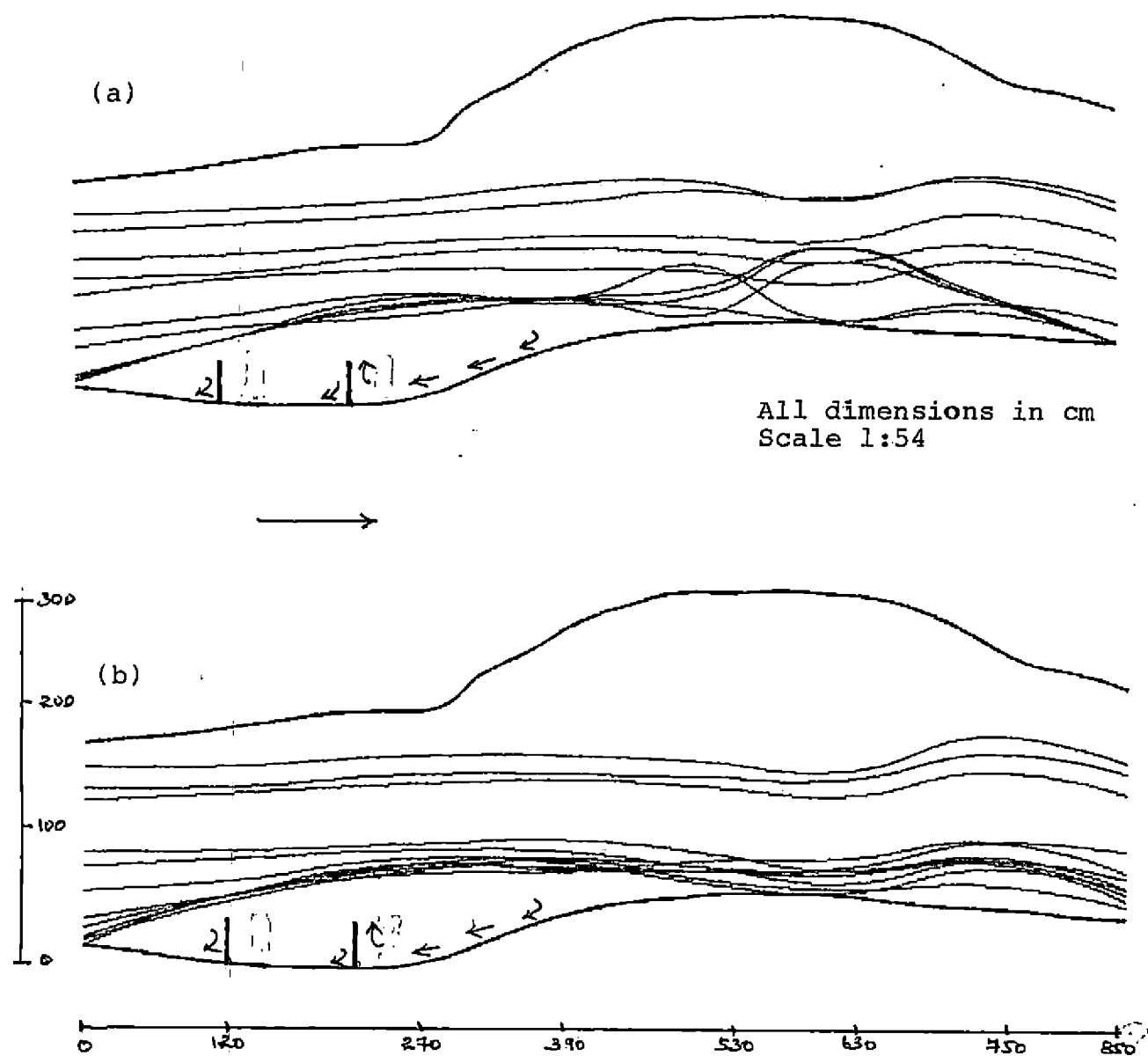


Fig. 53. Flow pattern for multiple spur scheme ( $L=35$  cm, spacing  $=3L$ )  
for discharge rates (a) 28.28 lps (b) 42.42 lps

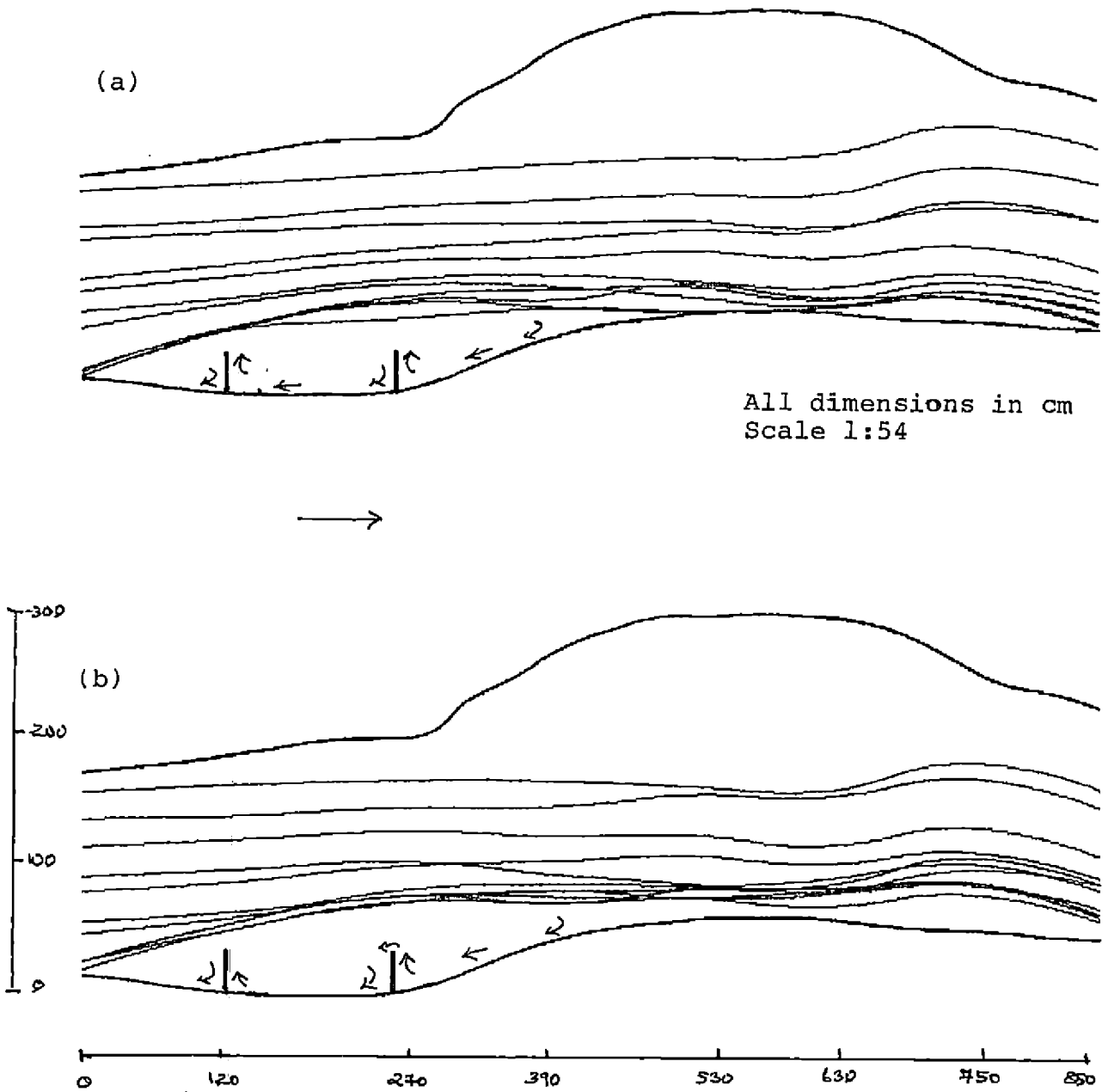


Fig. 54. Flow pattern for multiple spur scheme ( $L=35$  cm, spacing  $=4L$ )  
for discharge rates (a) 28.28 lps (b) 42.42 lps



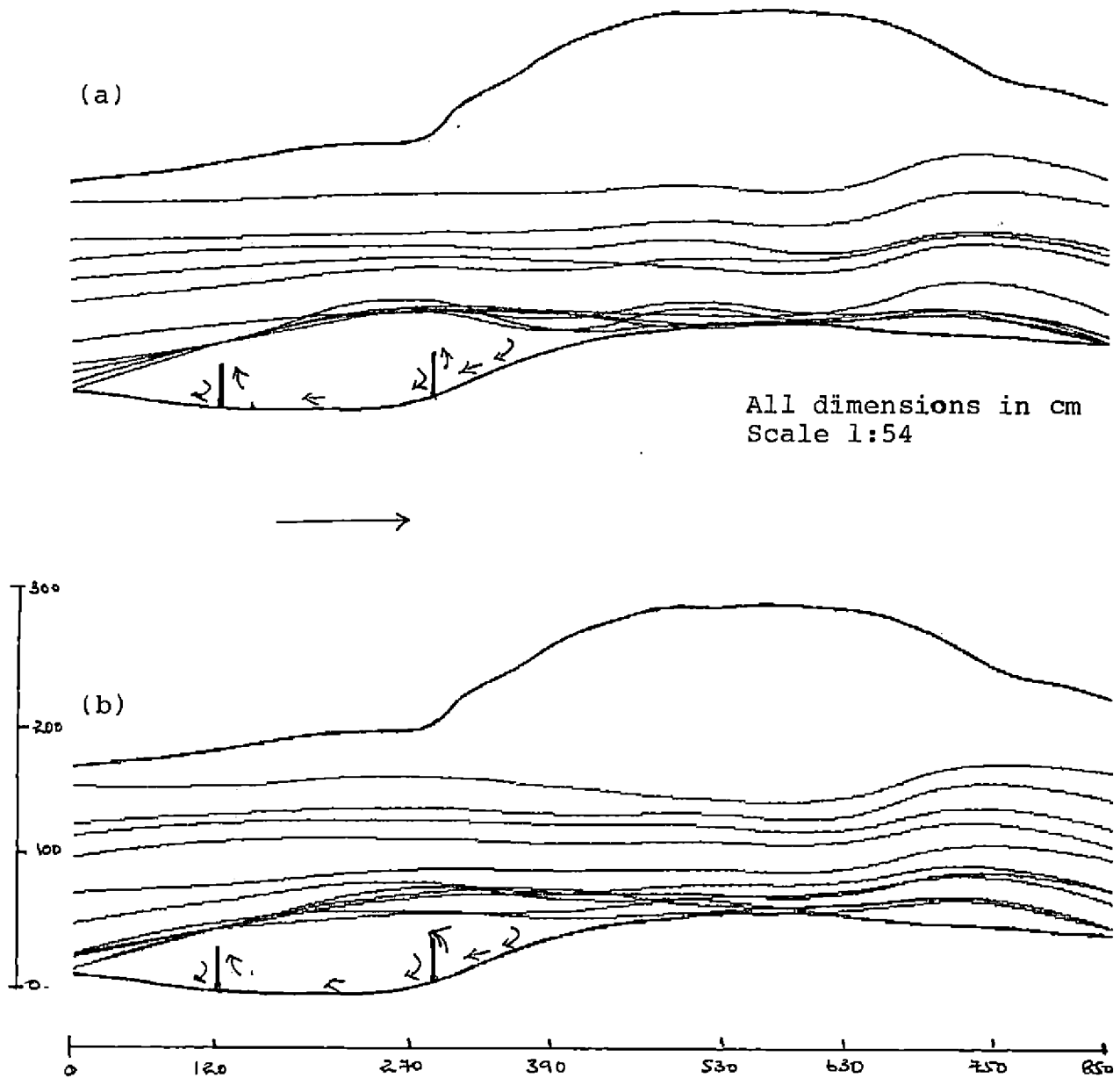


Fig. 55. Flow pattern for multiple spur scheme ( $L=35\text{cm}$ , spacing  $=5L$ ) for discharge rates (a) 28.28 lps (b) 42.42 lps

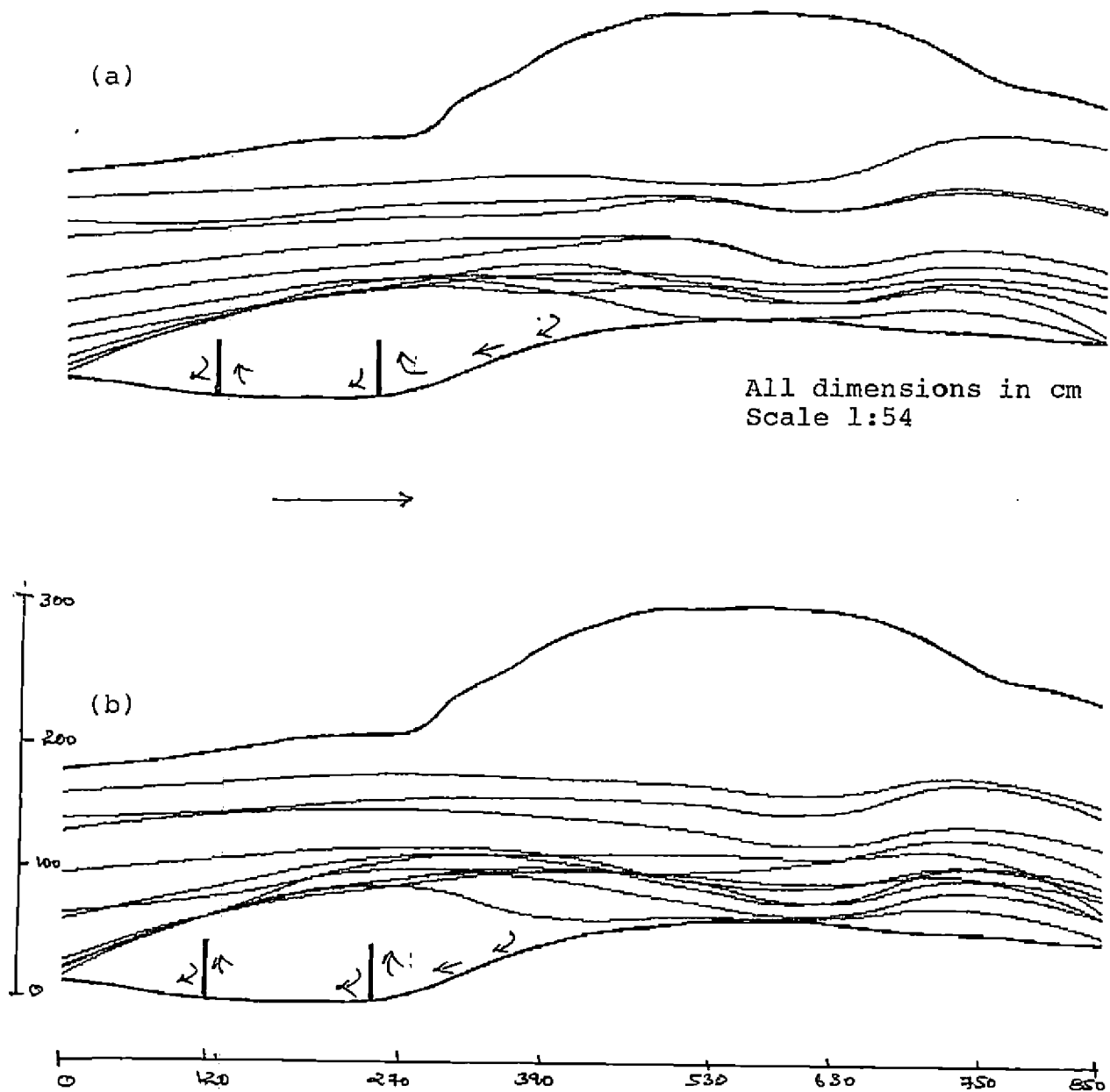


Fig. 57. Flow pattern for multiple spur scheme ( $L=45$  cm, spacing  $=3L$ ) for discharge rates (a) 28.28 lps (b) 42.42 lps

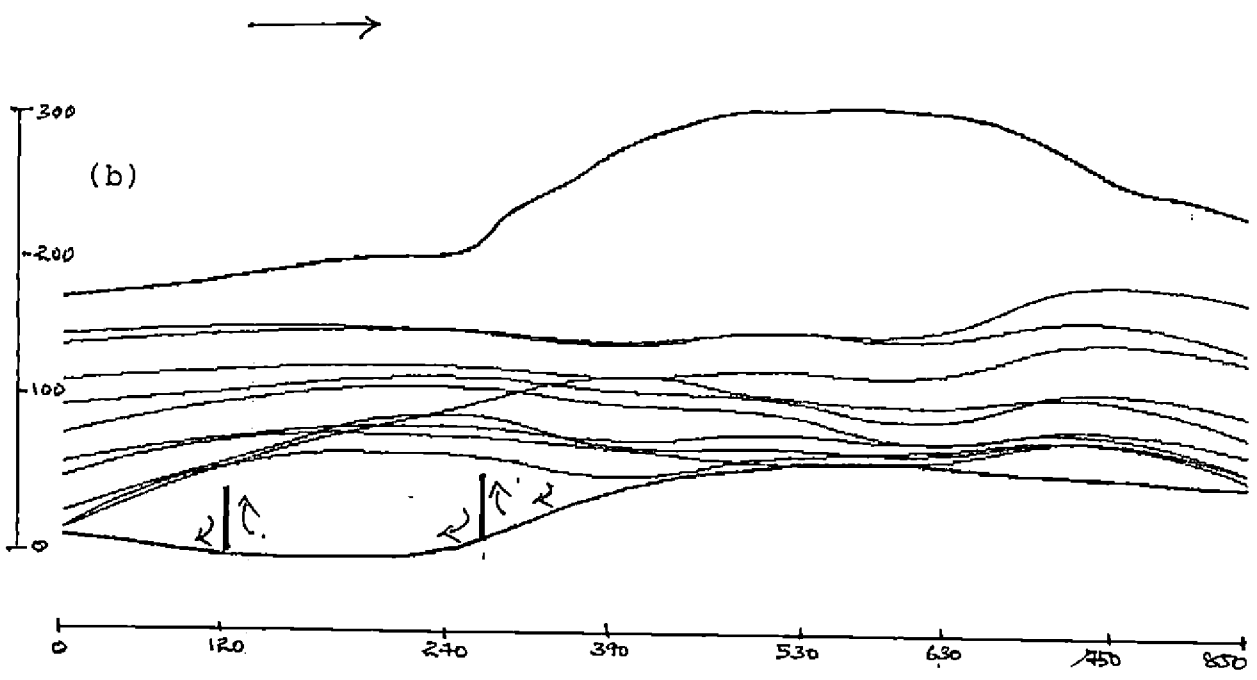
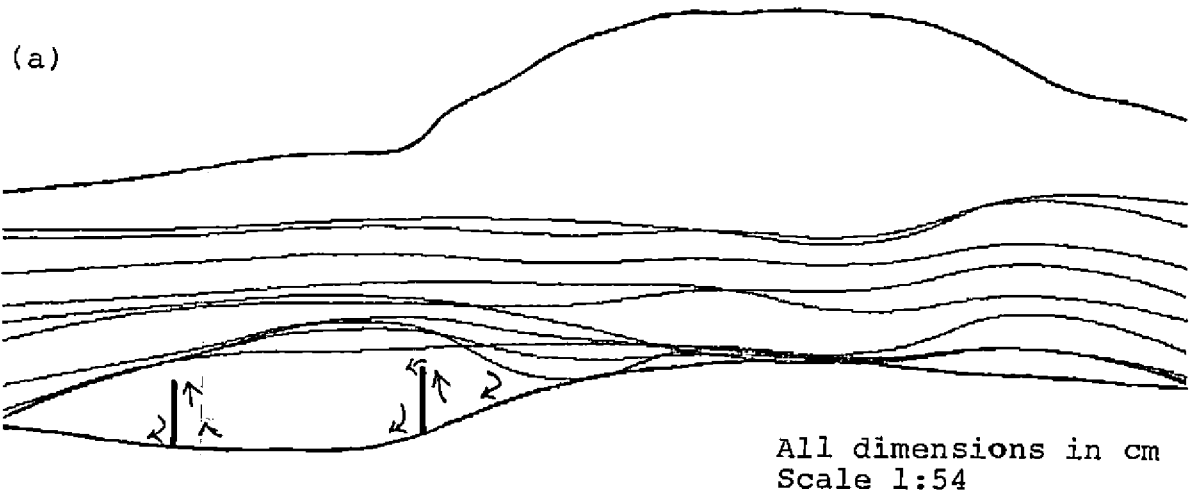


Fig. 58. Flow pattern for multiple spur scheme ( $L=45$  cm, spacing  $=4L$ ) for discharge rates (a) 28.28 lps (b) 42.42 lps

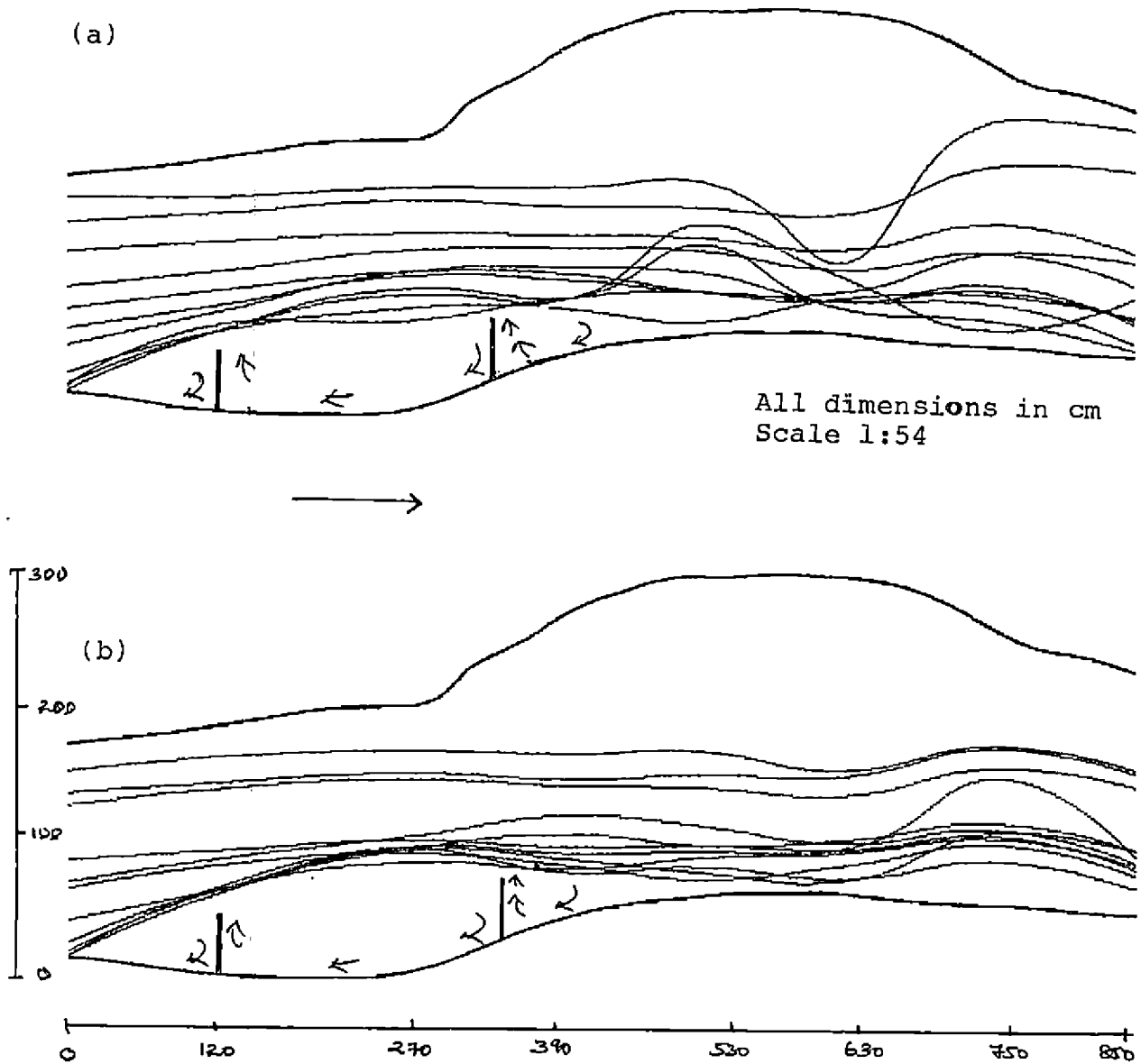


Fig. 59. Flow pattern for multiple spur scheme ( $L=45$  cm, spacing  $=5L$ )  
for discharge rates (a) 28.28 lps (b) 42.42 lps

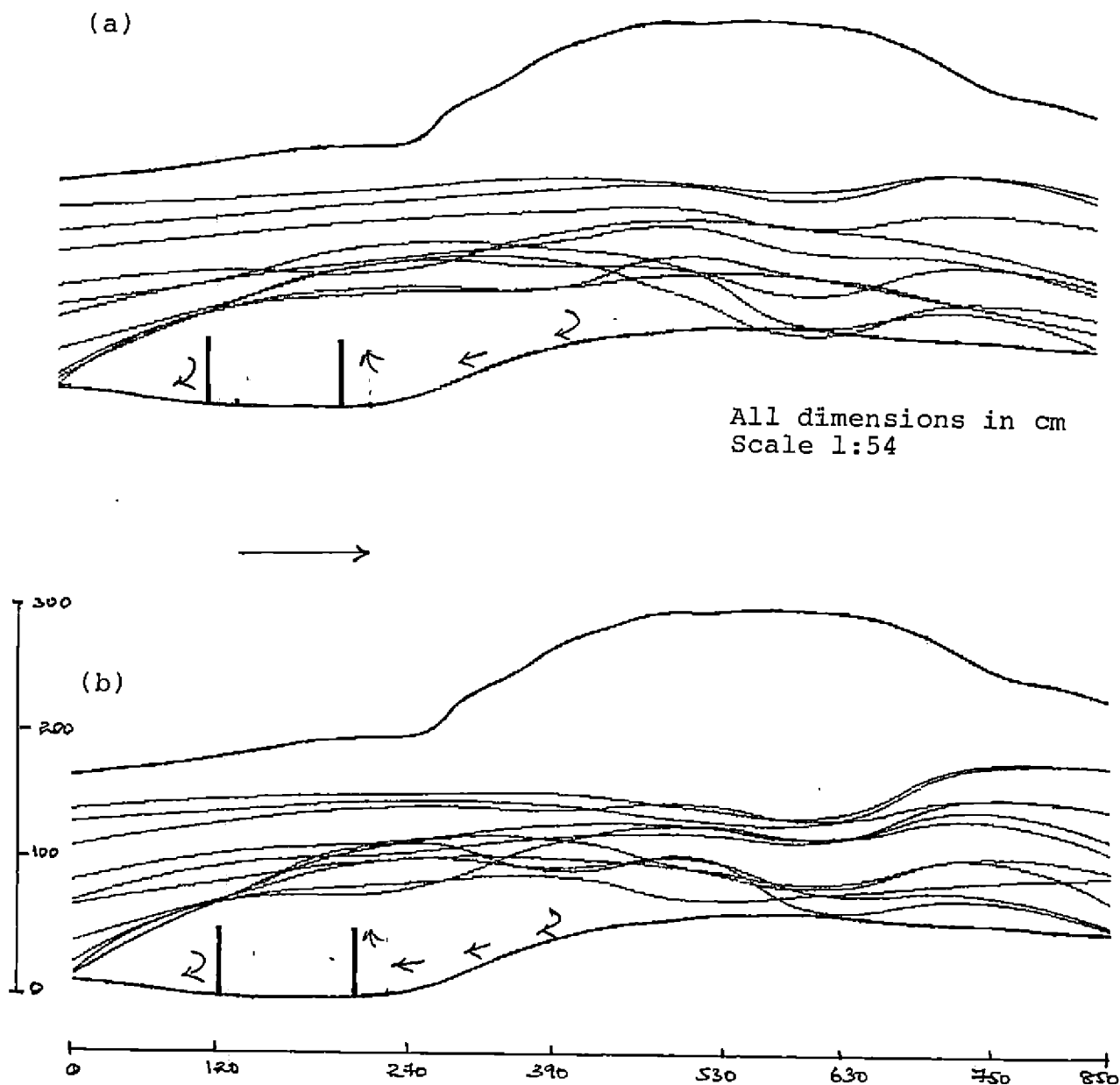


Fig. 60. Flow pattern for multiple spur scheme ( $L=55$  cm, spacing  $=2L$ )  
for discharge rates (a) 28.28 lps (b) 42.42 lps

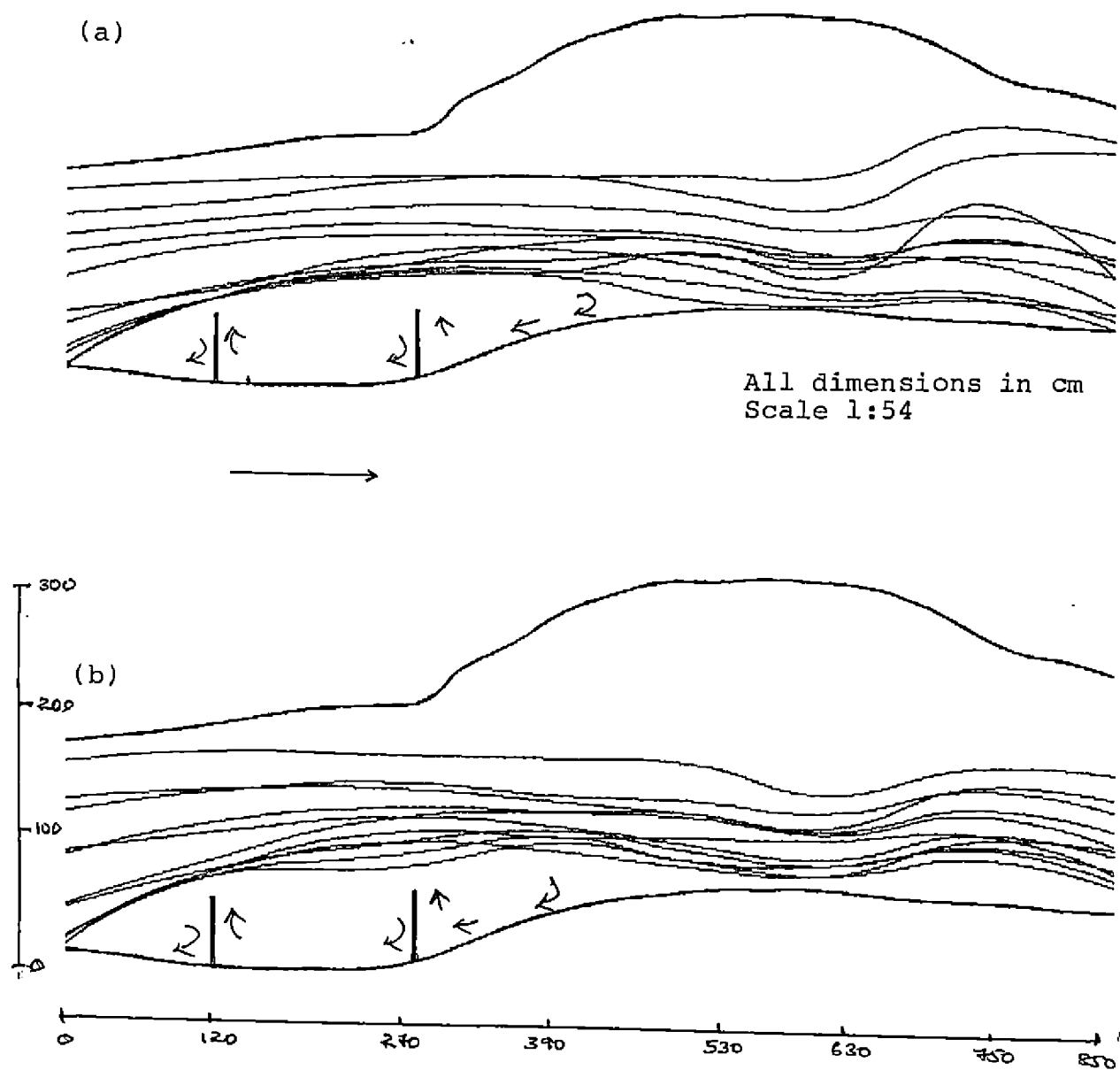


Fig. 61.. Flow pattern for multiple spur scheme ( $L=55$  cm, spacing  $=3L$ )  
for discharge rates (a) 28.28 lps (b) 42.42 lps

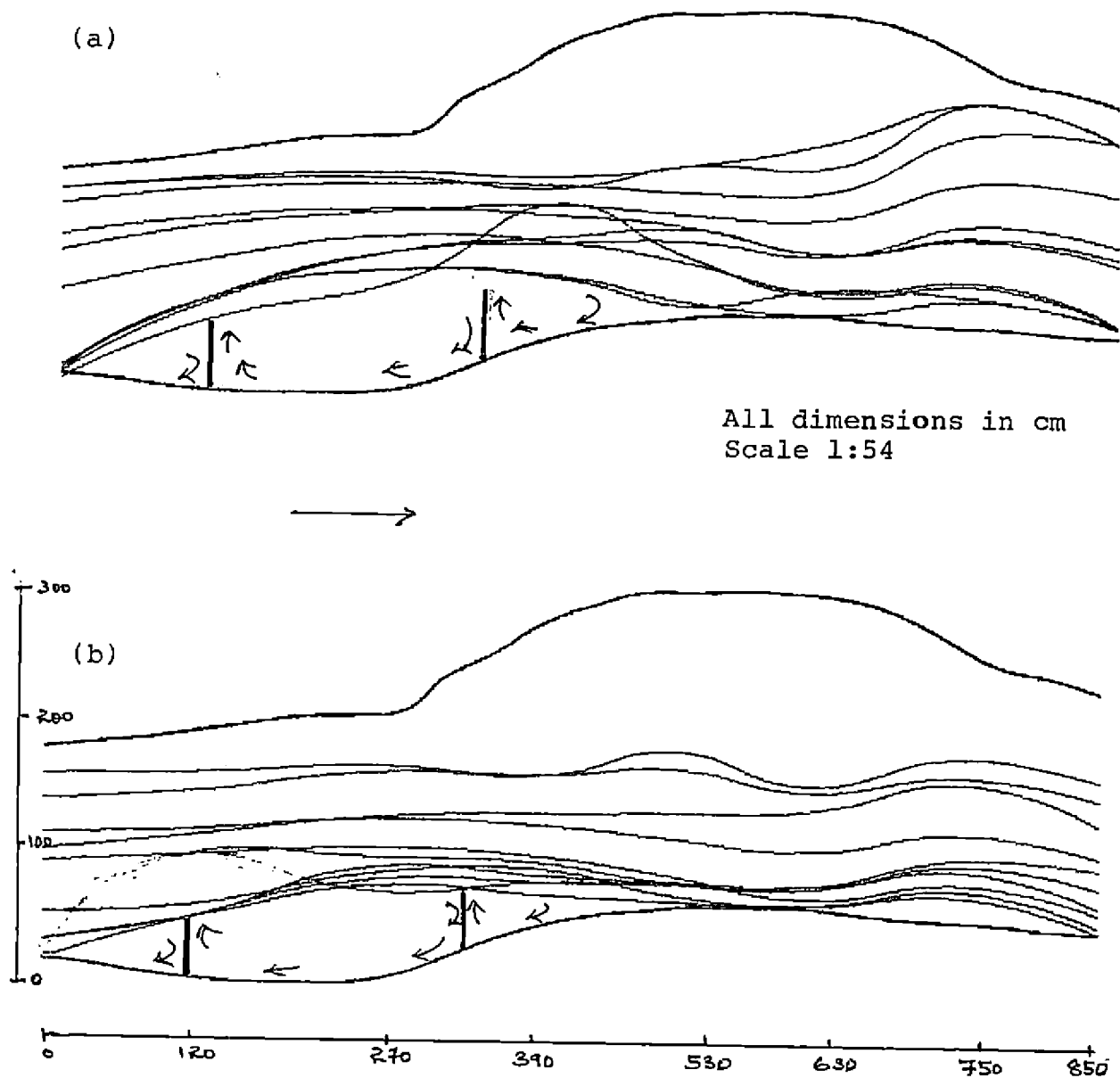


Fig. 62. Flow pattern for multiple spur scheme ( $L=55$  cm, spacing  $=4L$ ) for discharge rates (a) 28.28 lps (b) 42.42 lps

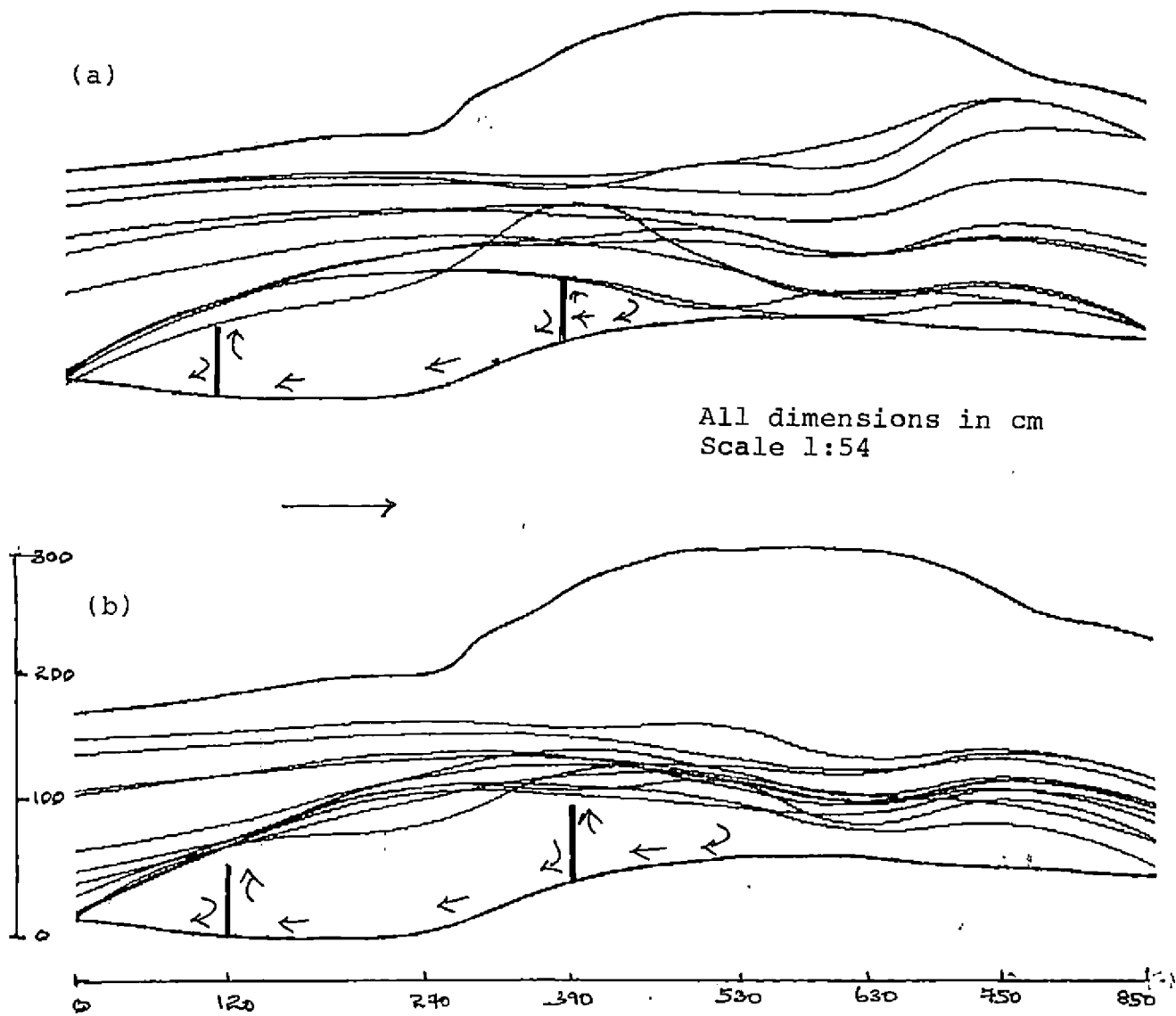


Fig. 63. Flow pattern for multiple spur scheme ( $L=55$  cm, spacing  $=5L$ )  
for discharge rates (a) 28.28 lps (b) 42.42 lps



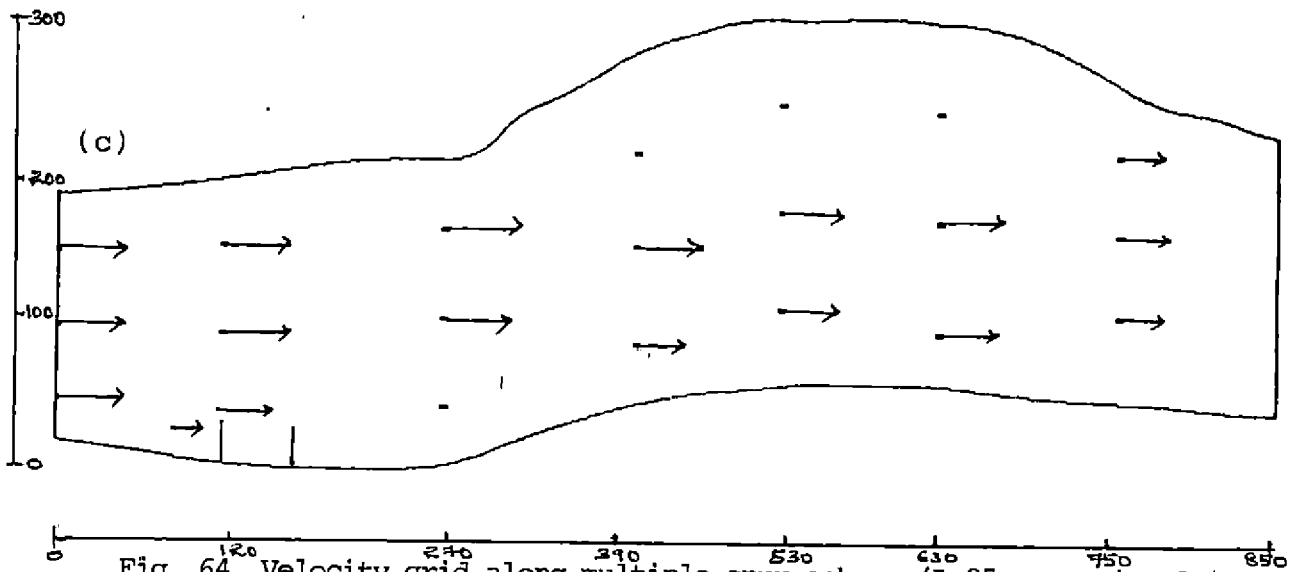
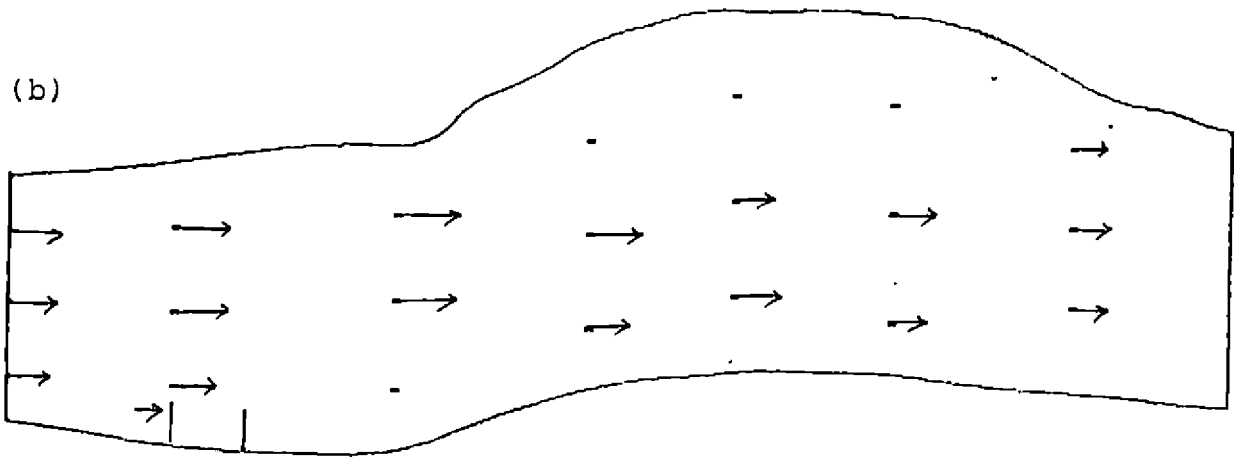
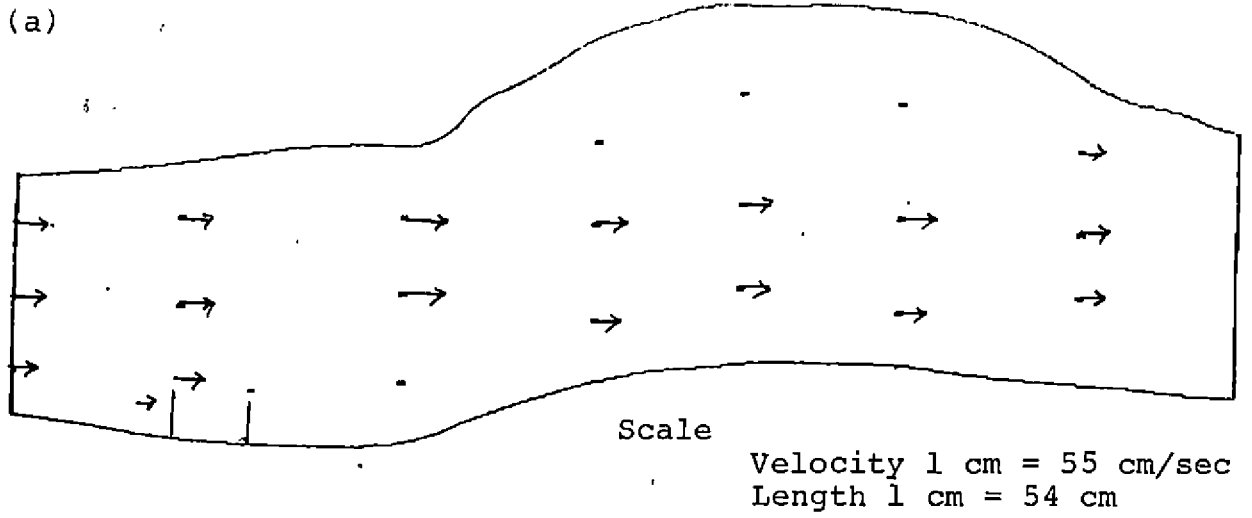


Fig. 64. Velocity grid along multiple spur scheme ( $L=25\text{cm}$ , spacing= $2L$ ) for discharge rates (a)14.14 lps (b)28.28 lps (c)42.42 lps

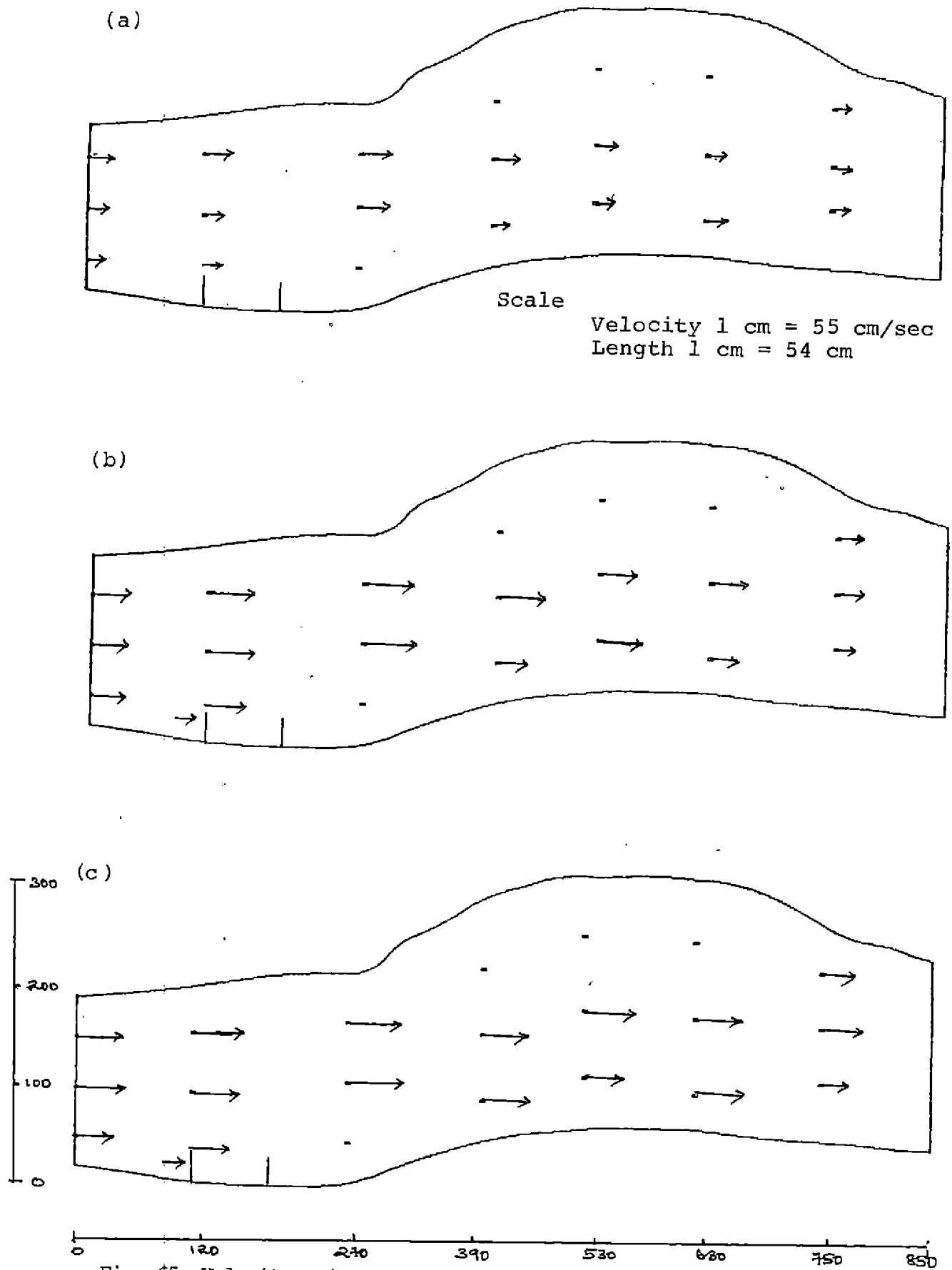


Fig. 65. Velocity grid along multiple spur scheme ( $L=25\text{cm}$ , spacing= $3L$ )  
for discharge rates (a)14.14 lps (b)28.28 lps (c)42.42 lps

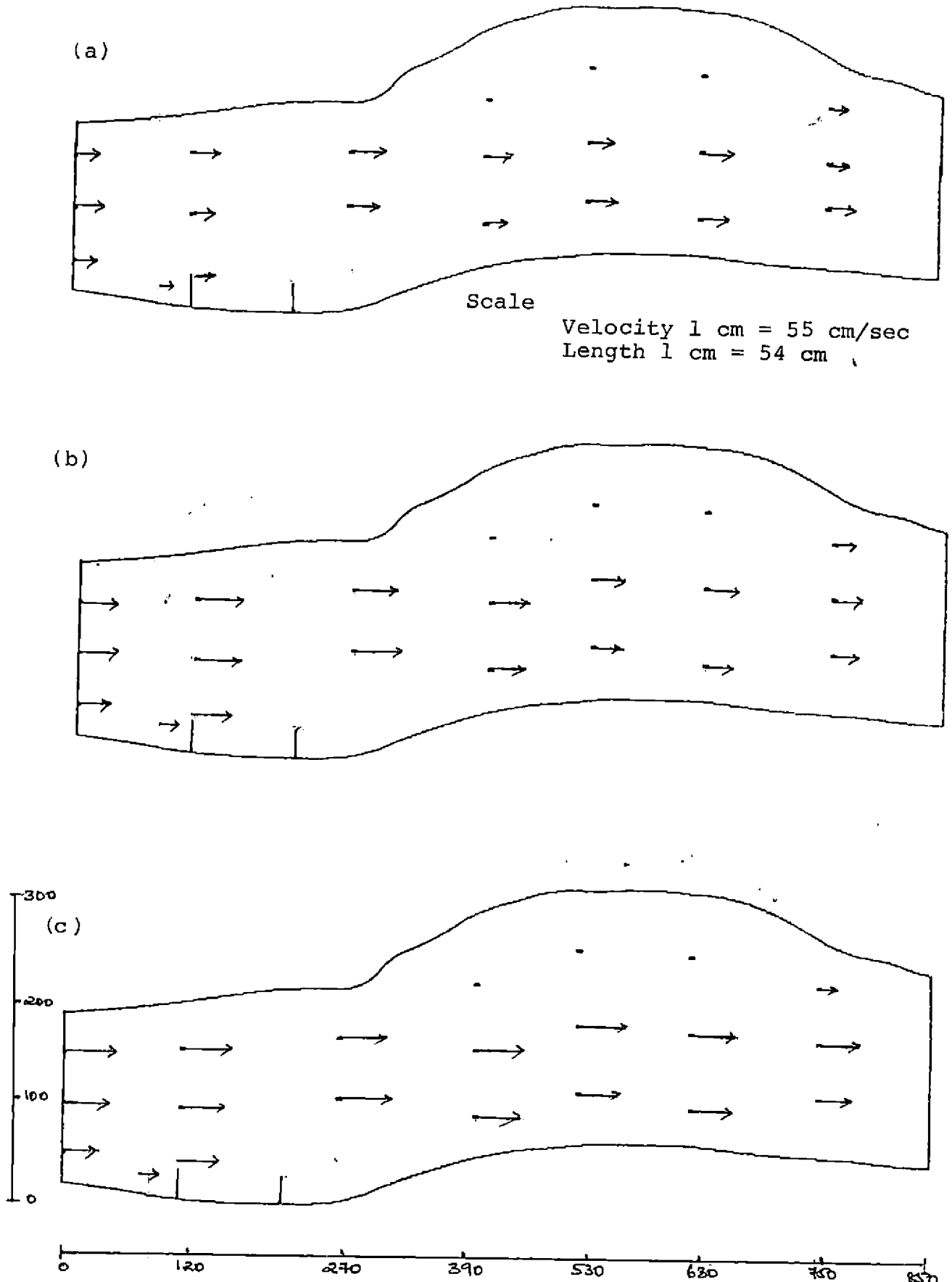


Fig. 66. Velocity grid along multiple spur scheme ( $L=25\text{cm}$ , spacing= $4L$ ) for discharge rates (a)14.14 lps (b)28.28 lps (c)42.42 lps

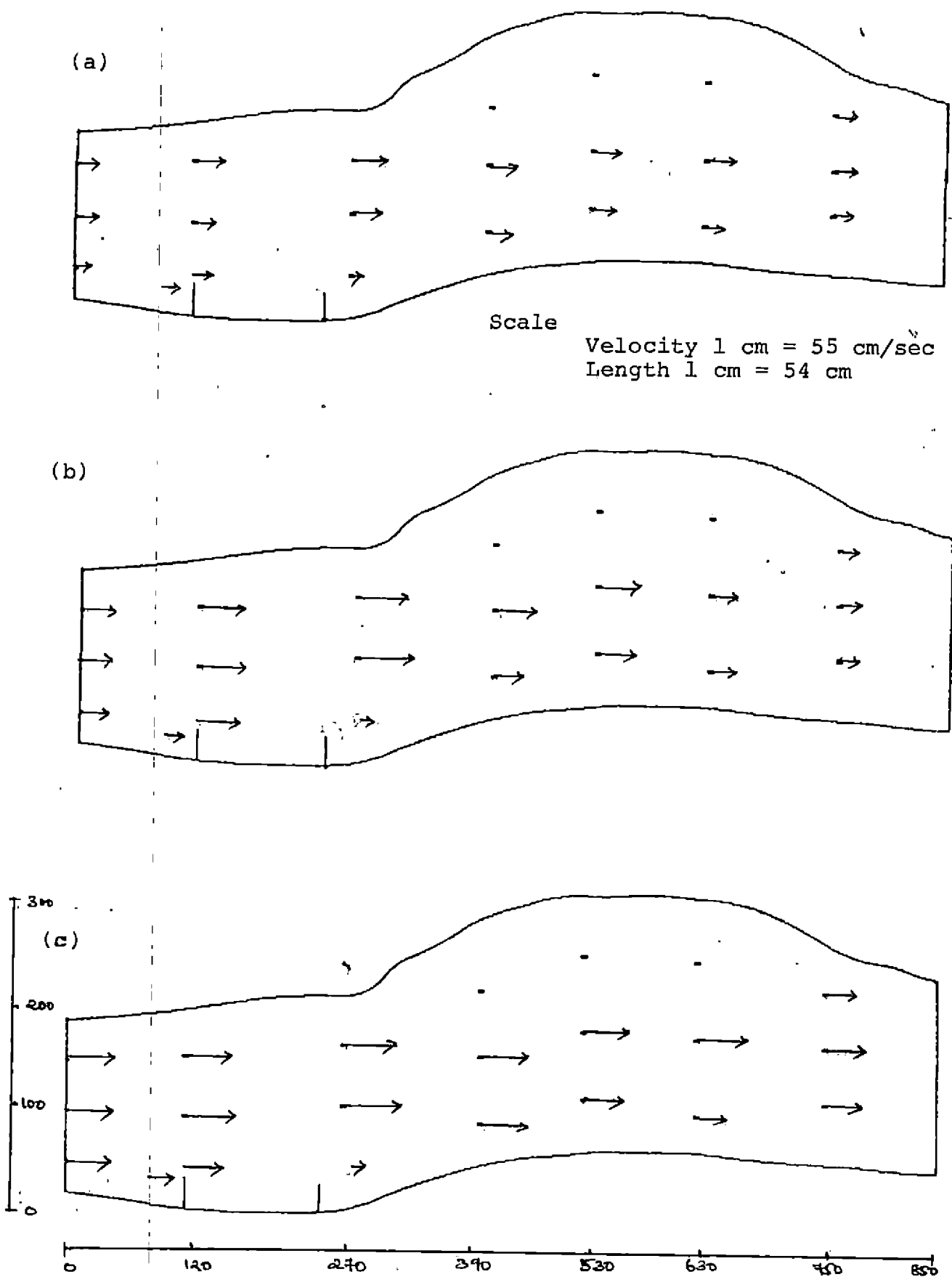


Fig. 67. Velocity grid along multiple spur scheme ( $L=25\text{cm}$ , spacing= $5L$ )  
for discharge rates (a)14.14 lps (b)28.28 lps (c)42.42 lps

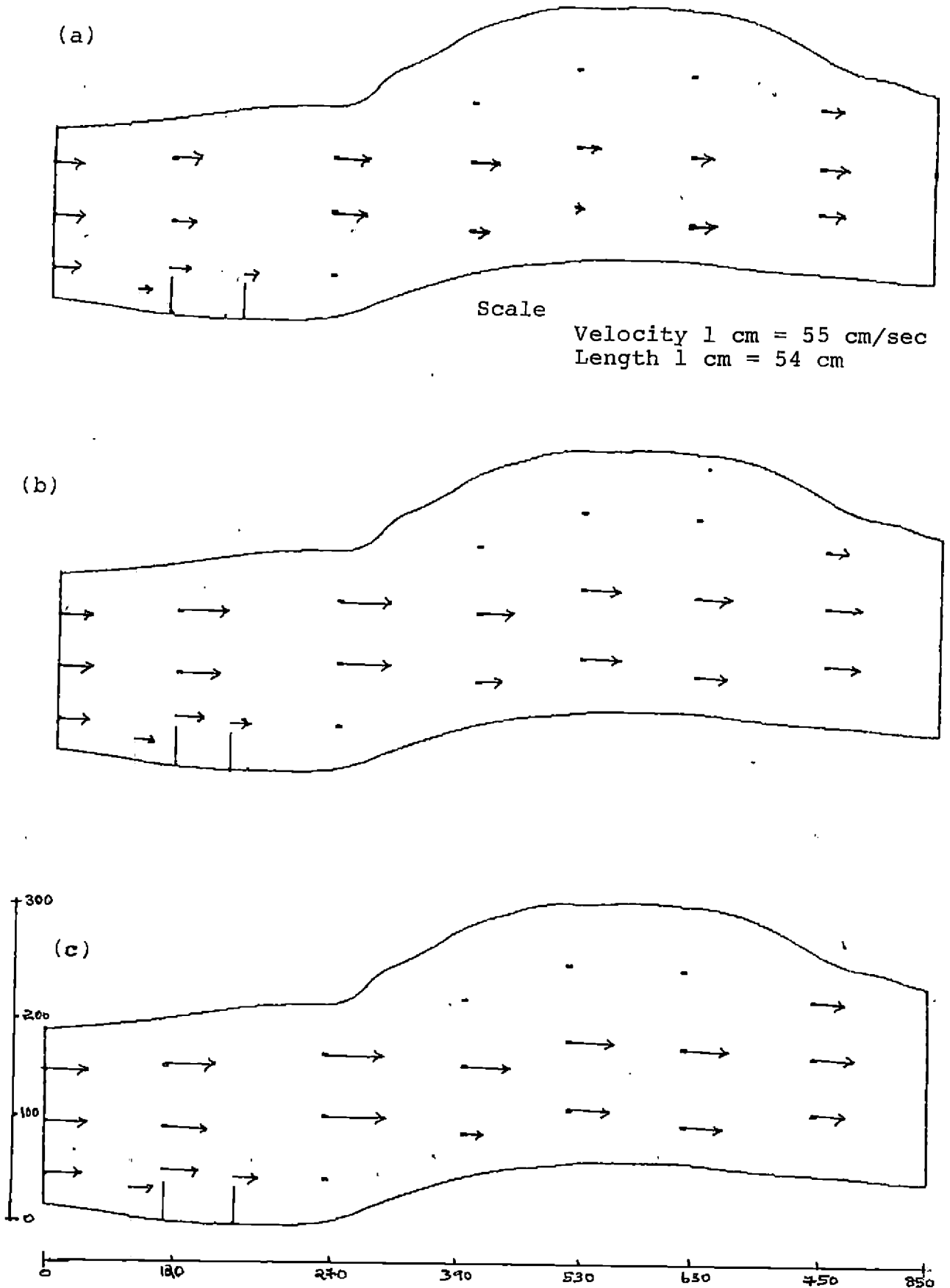


Fig. 68. Velocity grid along multiple spur scheme ( $L=35\text{cm}$ , spacing= $2L$ ) for discharge rates (a)14.14 lps (b)28.28 lps (c)42.42 lps

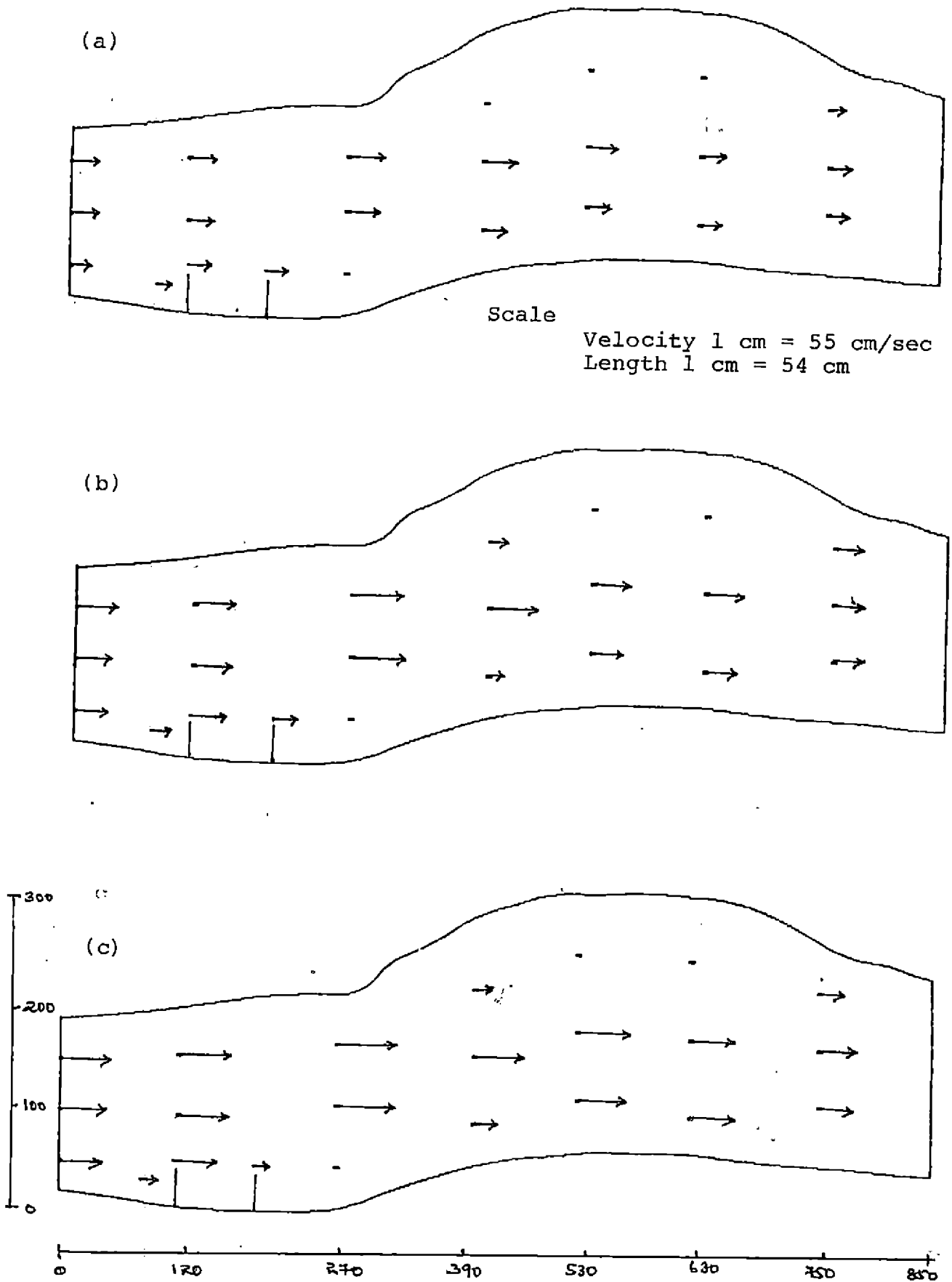
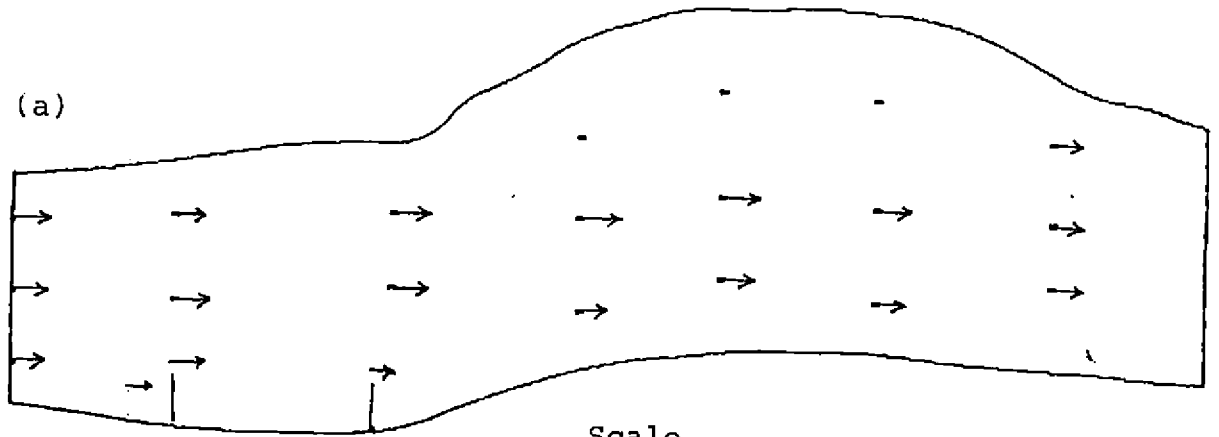


Fig. 69. Velocity grid along multiple spur scheme ( $L=35$  cm, spacing= $3L$ ) for discharge rates (a) 14.14 lps (b) 28.28 lps (c) 42.42 lps



Scale  
 Velocity 1 cm = 55 cm/sec  
 Length 1 cm = 54 cm

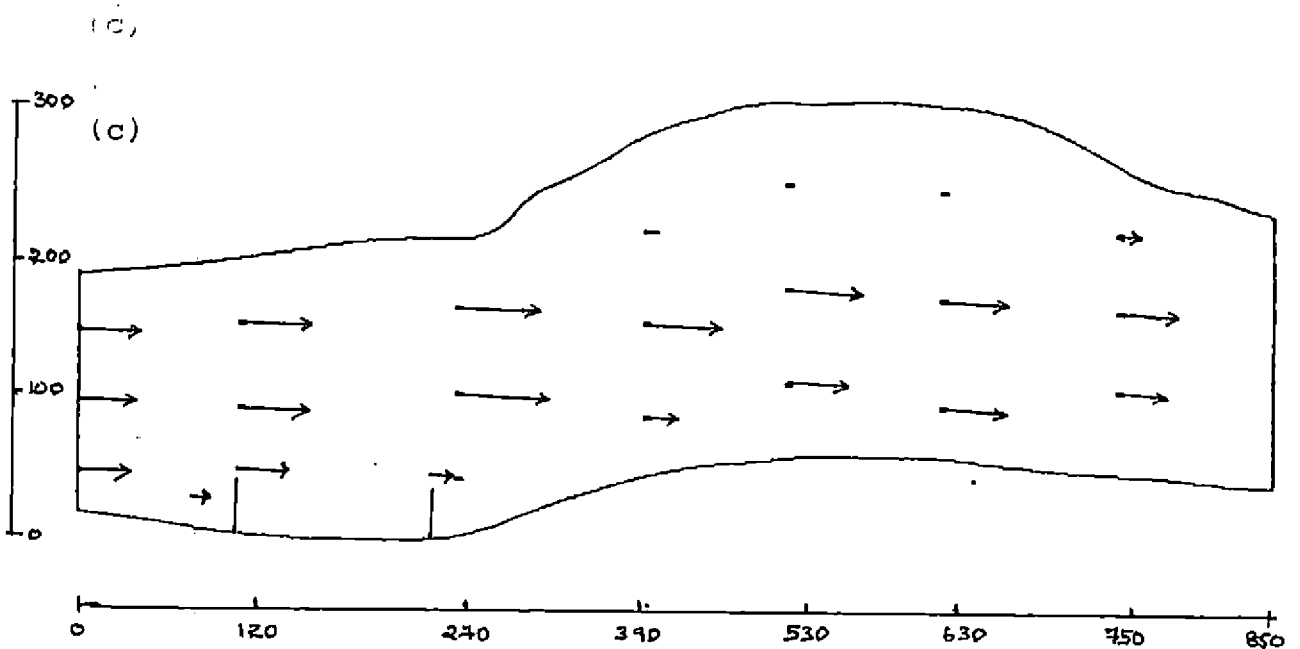
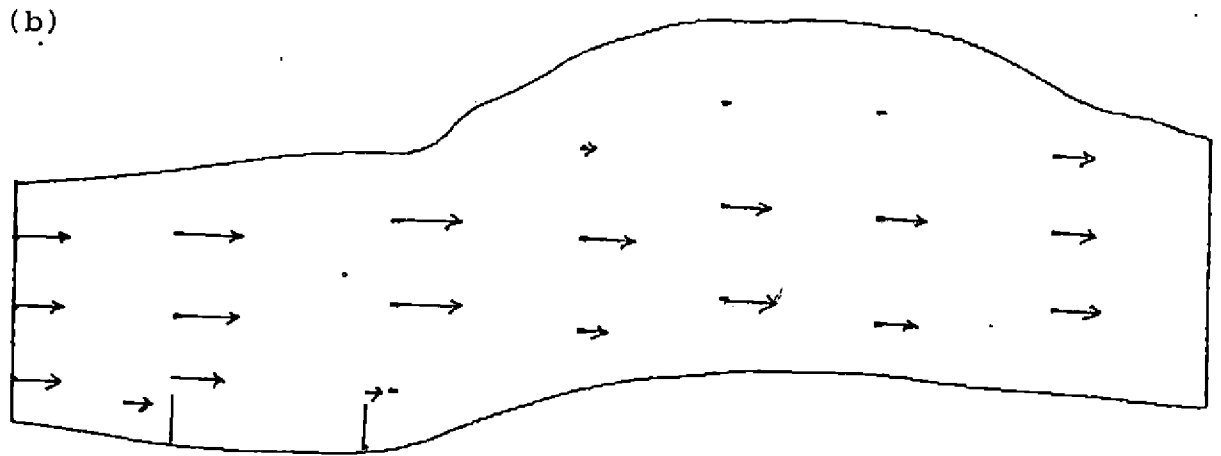


Fig. 70. Velocity grid along multiple spur scheme ( $L=35$  cm, spacing= $4L$ ) for discharge rates (a)14.14 lps (b)28.28 lps (c)42.42 lps

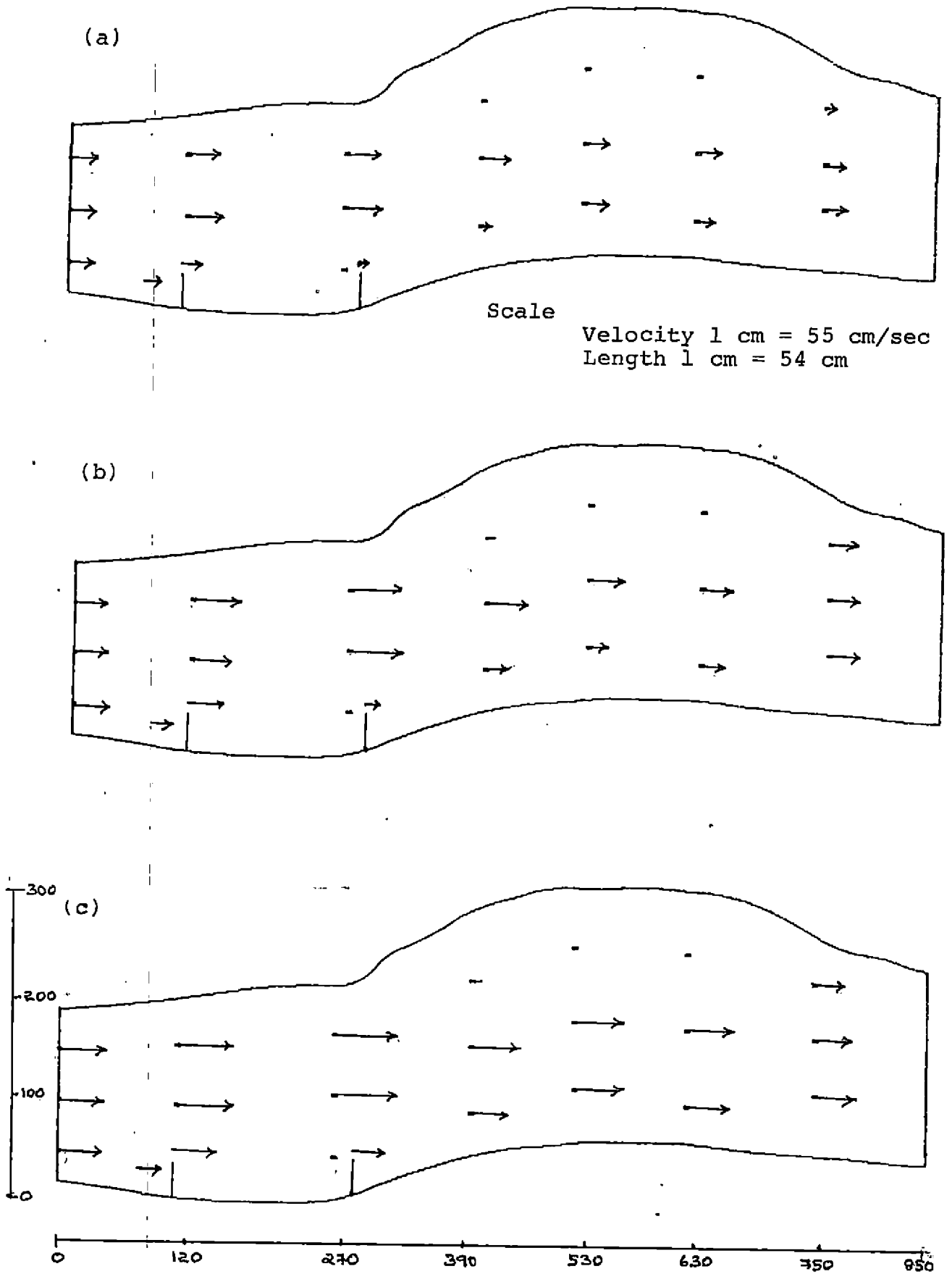


Fig. 71. Velocity grid along multiple spur scheme ( $L=35$  cm, spacing= $5L$ ) for discharge rates (a) 14.14 lps (b) 28.28 lps (c) 42.42 lps



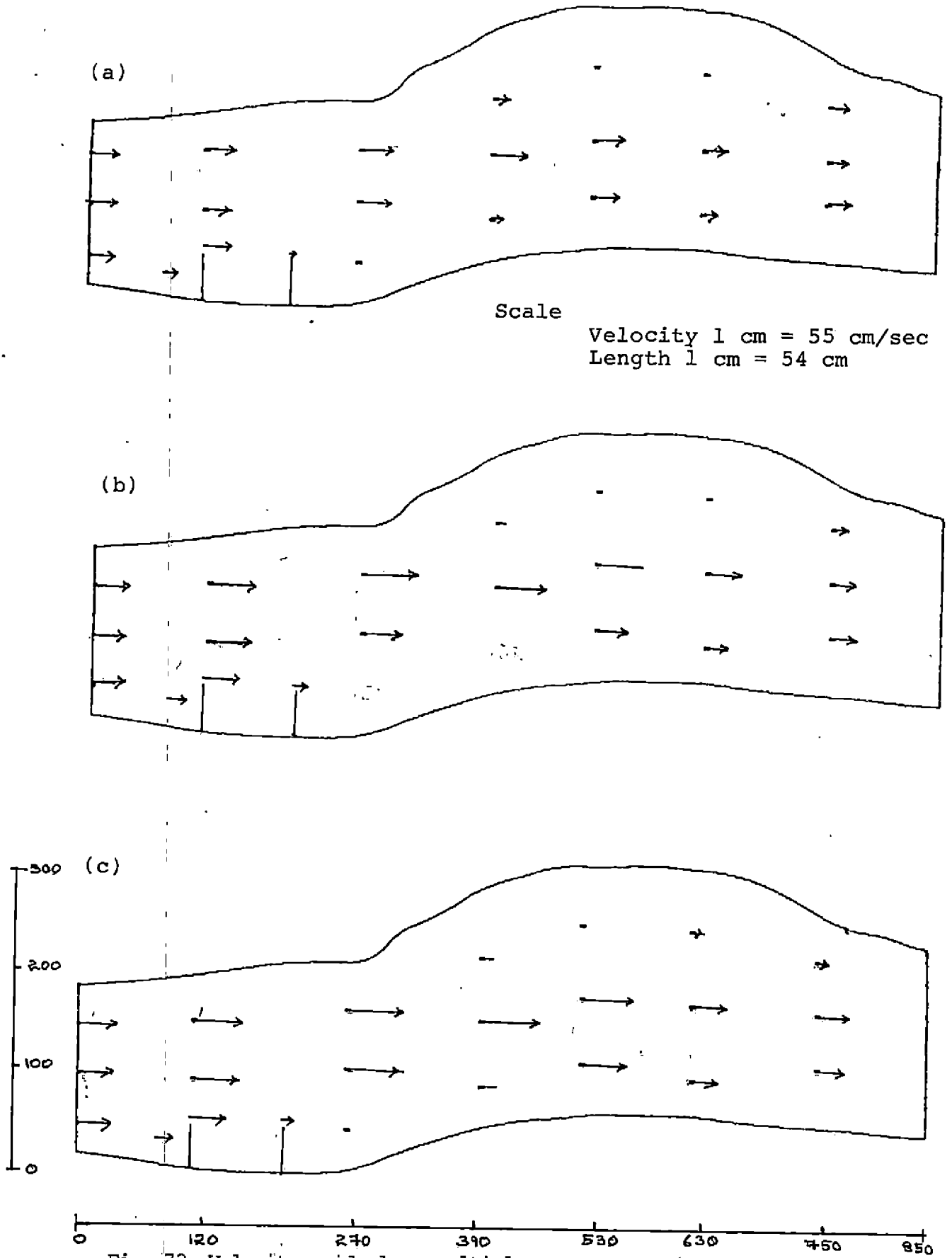


Fig. 72. Velocity grid along multiple spur scheme ( $L=45\text{cm}$ ,  $\text{spacing}=2L$ ) for discharge rates (a) 14.14 lps (b) 28.28 lps (c) 42.42 lps

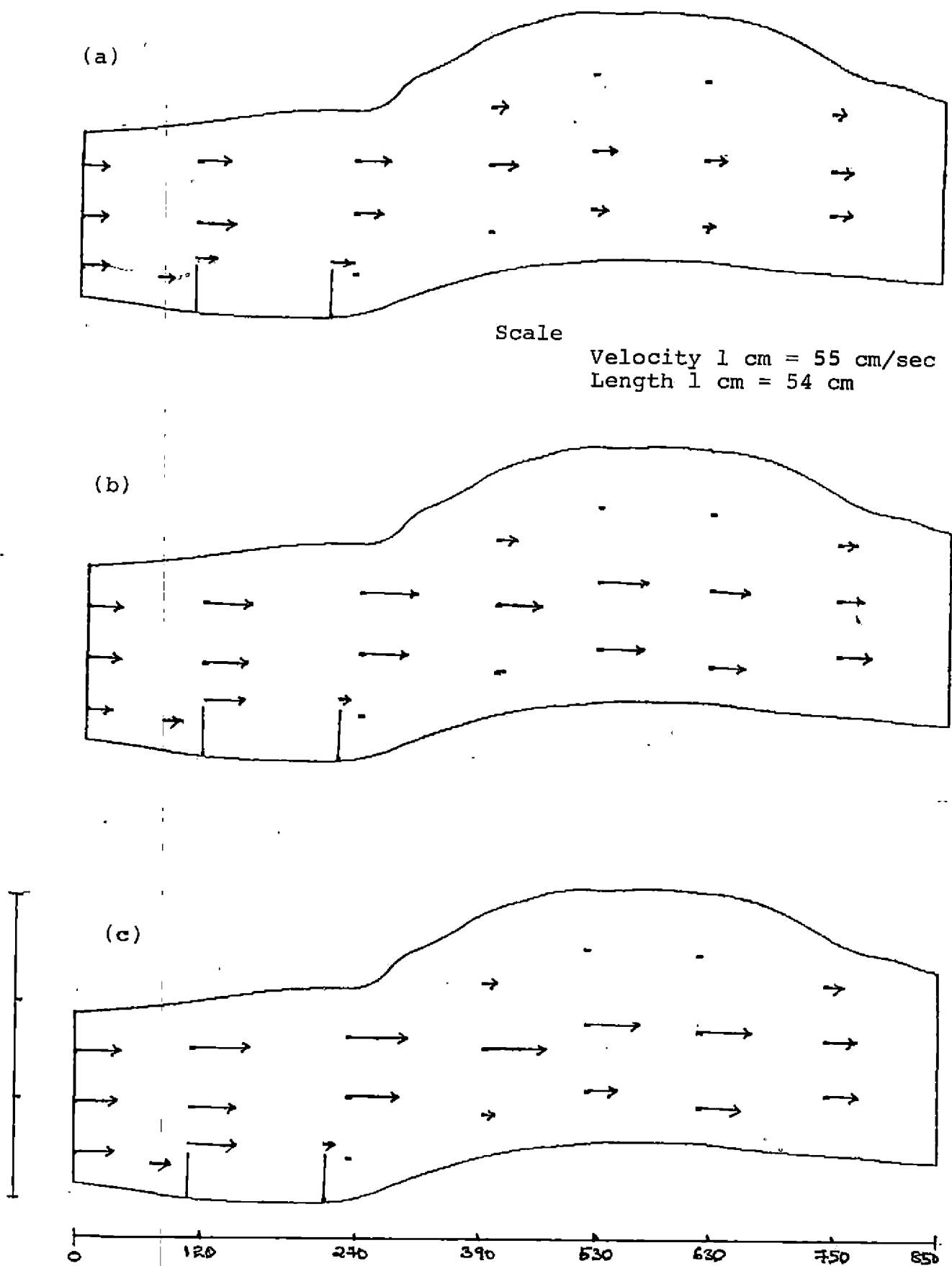


Fig. 73. Velocity grid along multiple spur scheme ( $L=45\text{cm}$ , spacing= $3L$ ) for discharge rates (a)14.14 lps (b)28.28 lps (c)42.42 lps

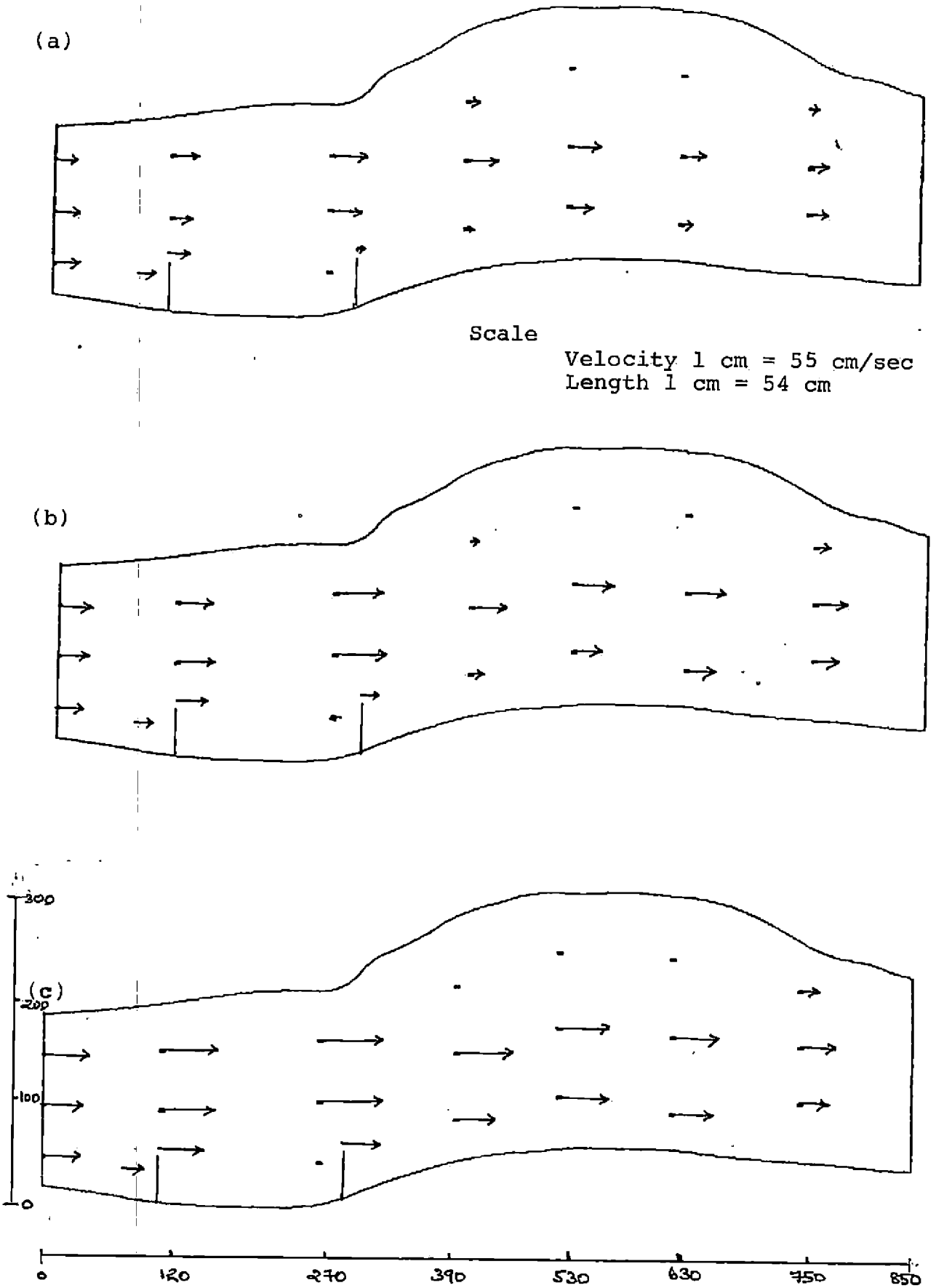


Fig. 74. Velocity grid along multiple spur scheme ( $L=45\text{cm}$ ,  $\text{spacing}=4L$ ) for discharge rates (a) 14.14 lps (b) 28.28 lps (c) 42.42 lps

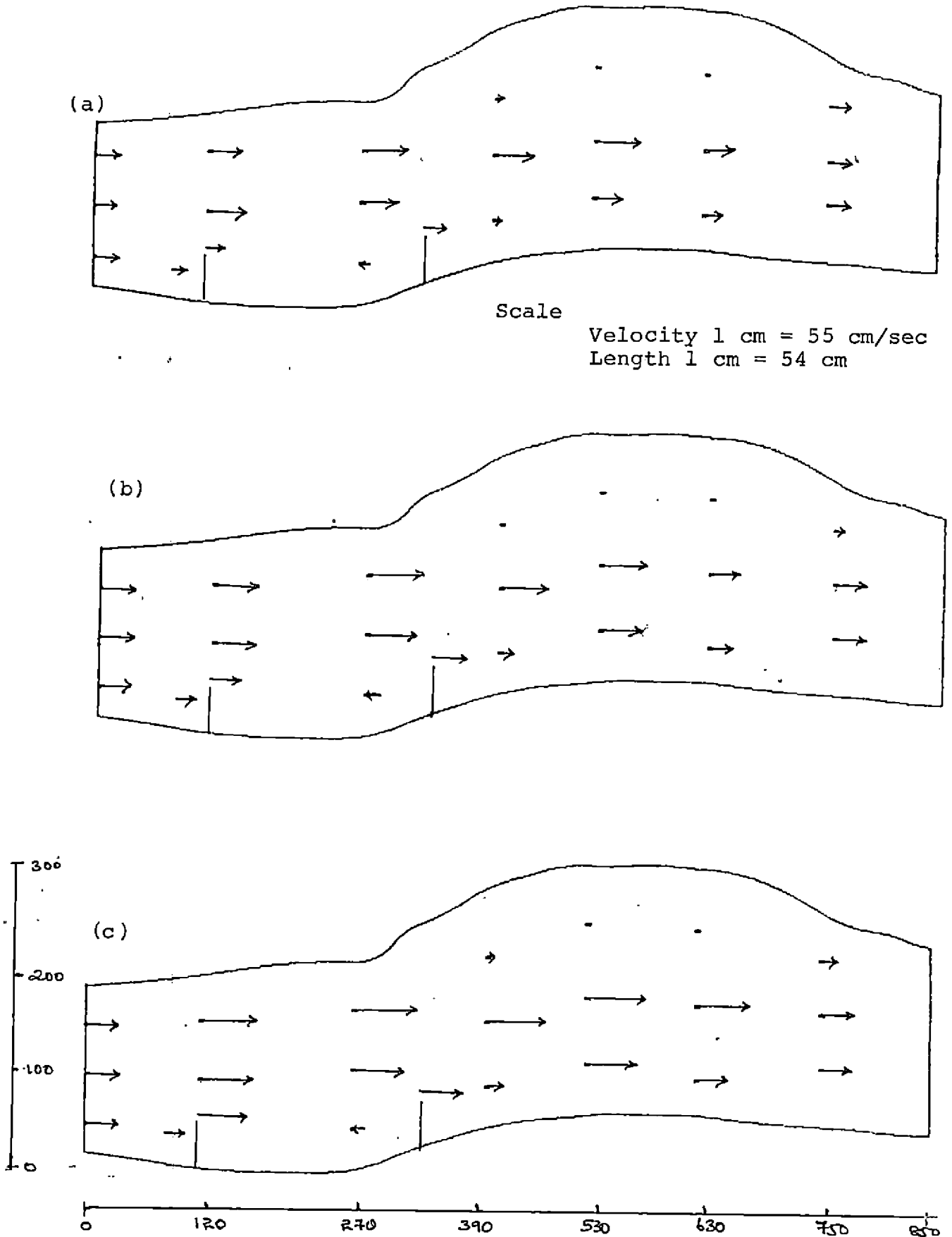
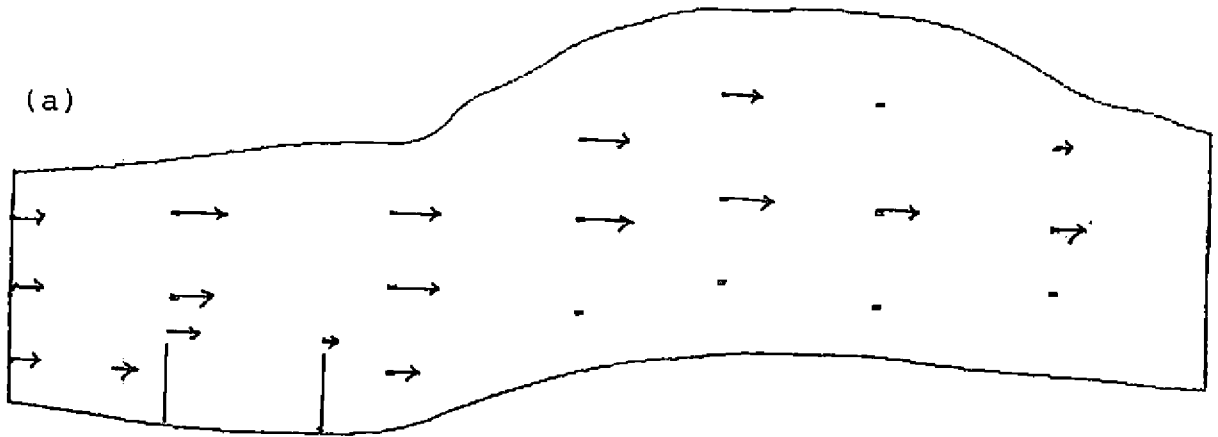


Fig. 75. Velocity grid along multiple spur scheme (L=45cm, spacing=5L) for discharge rates (a)14.14 lps (b)28.28 lps (c)42.42 lps



Scale  
 Velocity 1 cm = 55 cm/sec  
 Length 1 cm = 54 cm

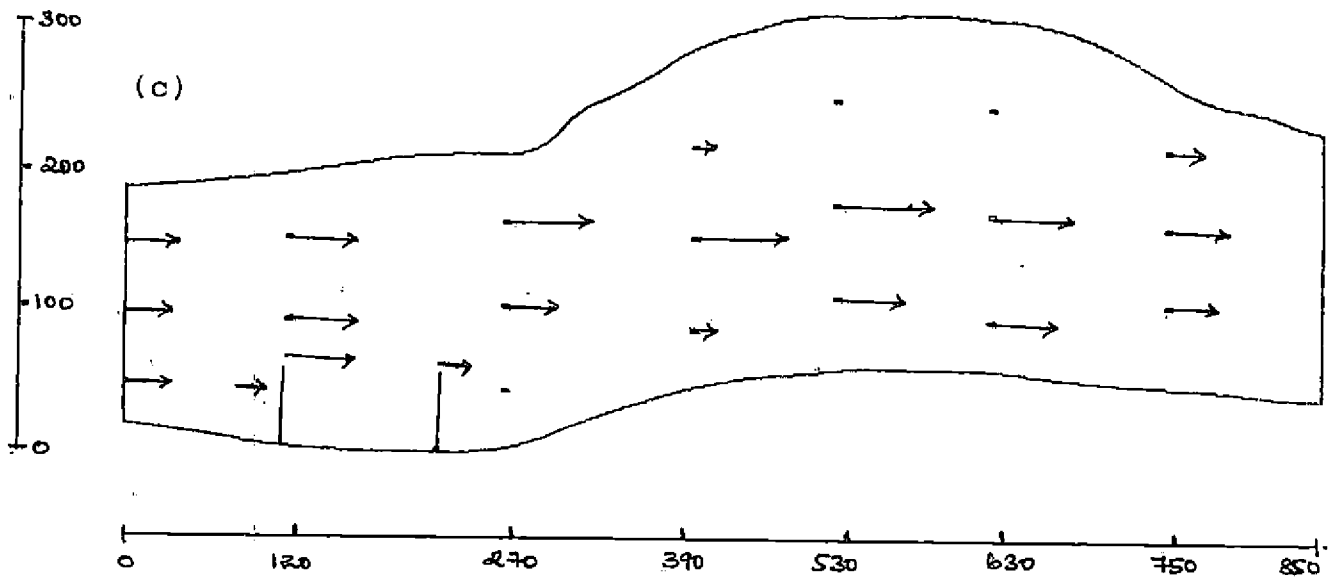
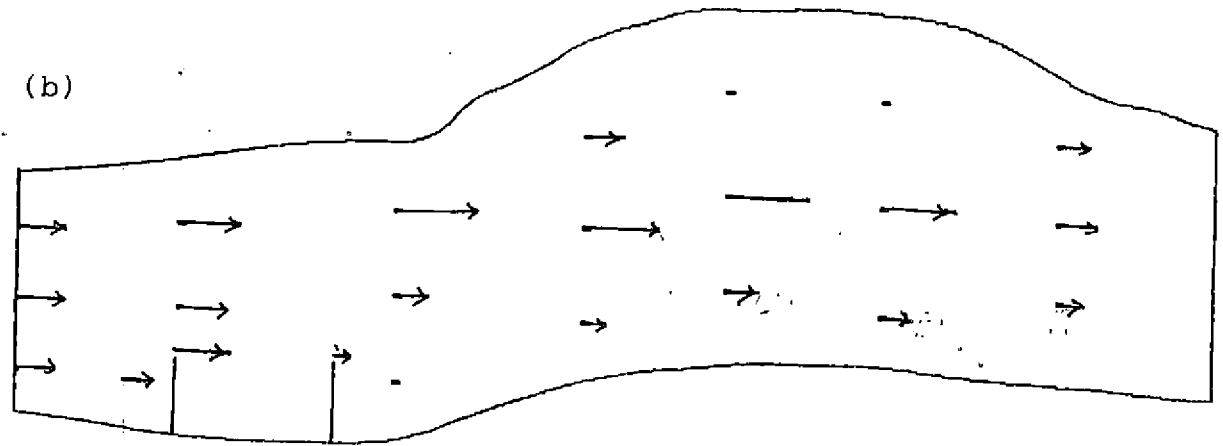


Fig. 76. Velocity grid along multiple spur scheme ( $L=55$  cm, spacing= $2L$ ) for discharge rates (a)14.14 lps (b)28.28 lps (c)42.42 lps

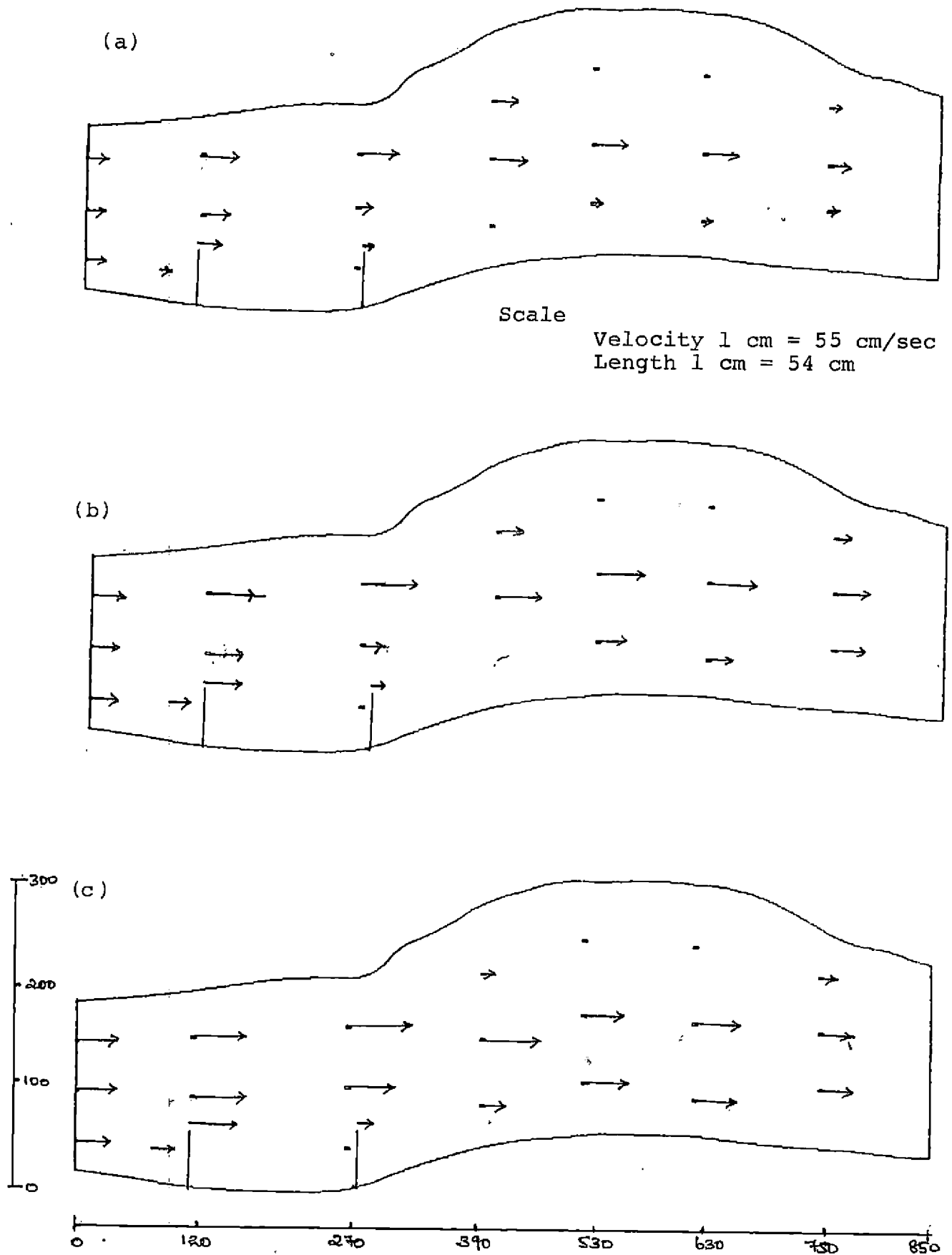
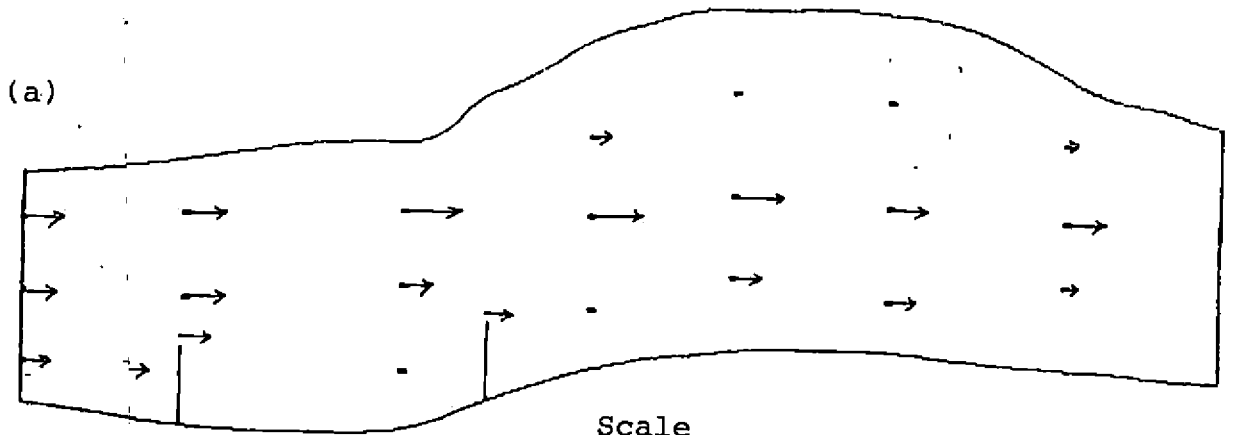


Fig. 77. Velocity grid along multiple spur scheme ( $L=55$  cm, spacing= $3L$ ) for discharge rates (a) 14.14 lps (b) 28.28 lps (c) 42.42 lps



Scale  
 Velocity 1 cm = 55 cm/sec  
 Length 1 cm = 54 cm

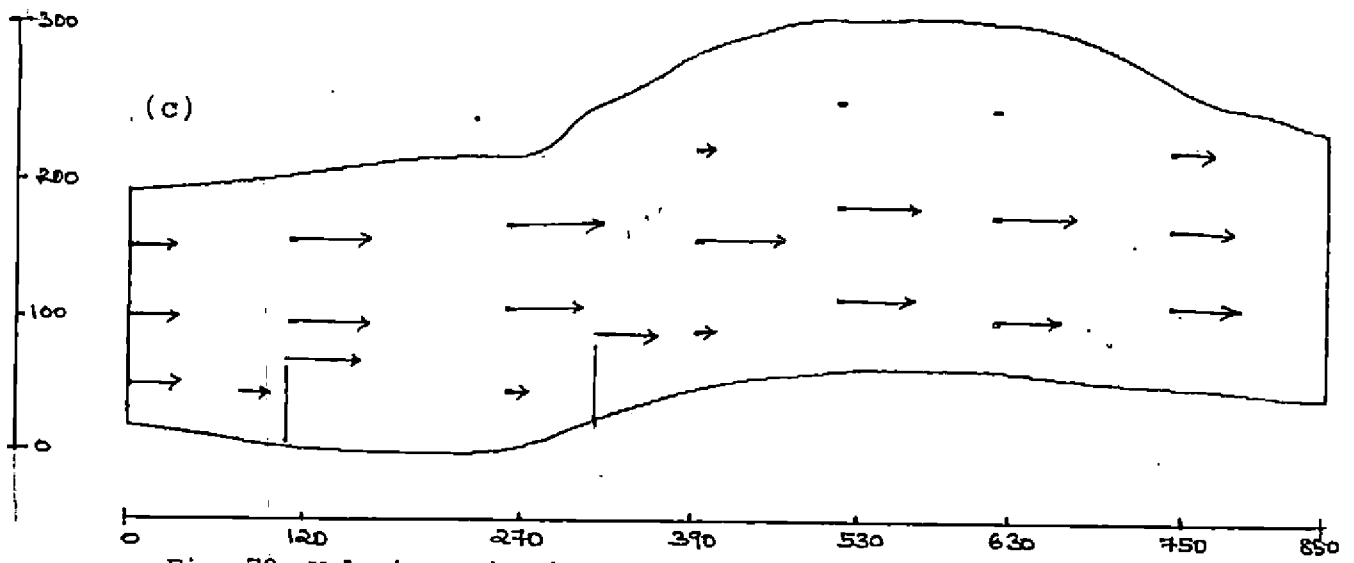
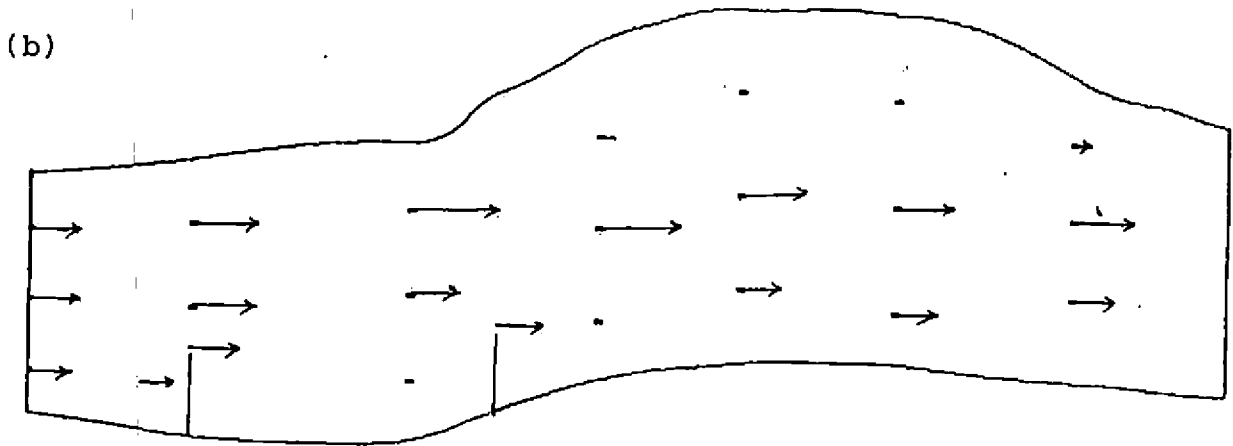


Fig. 78. Velocity grid along multiple spur scheme ( $L=55$  cm, spacing= $4L$ ) for discharge rates (a) 14.14 lps (b) 28.28 lps (c) 42.42 lps

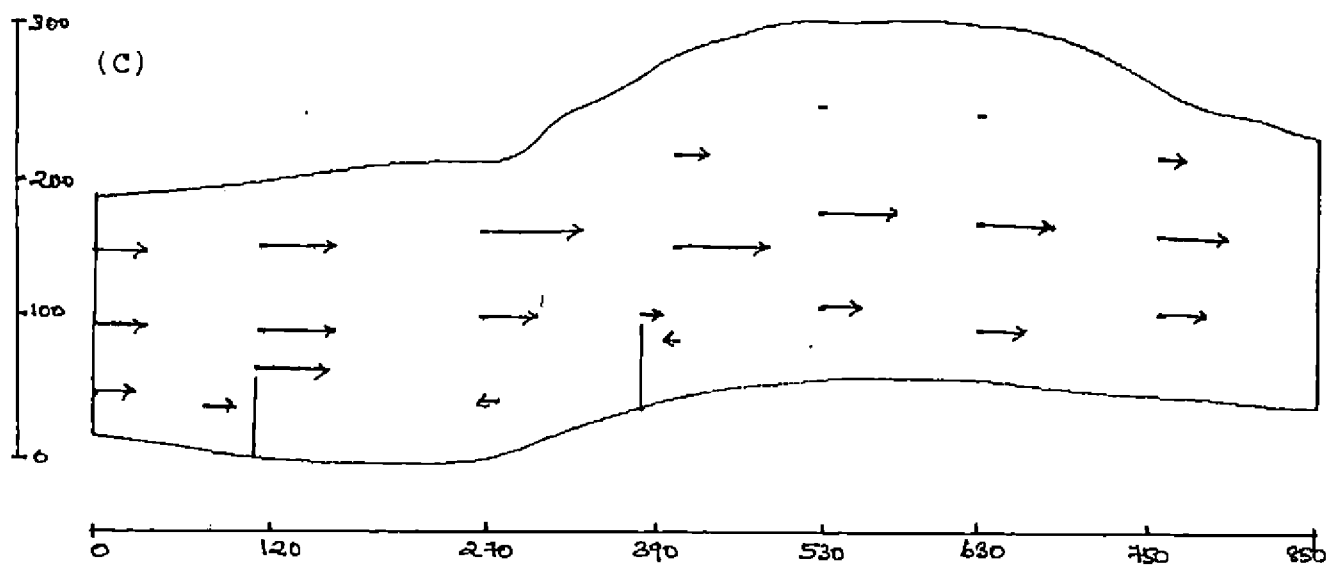
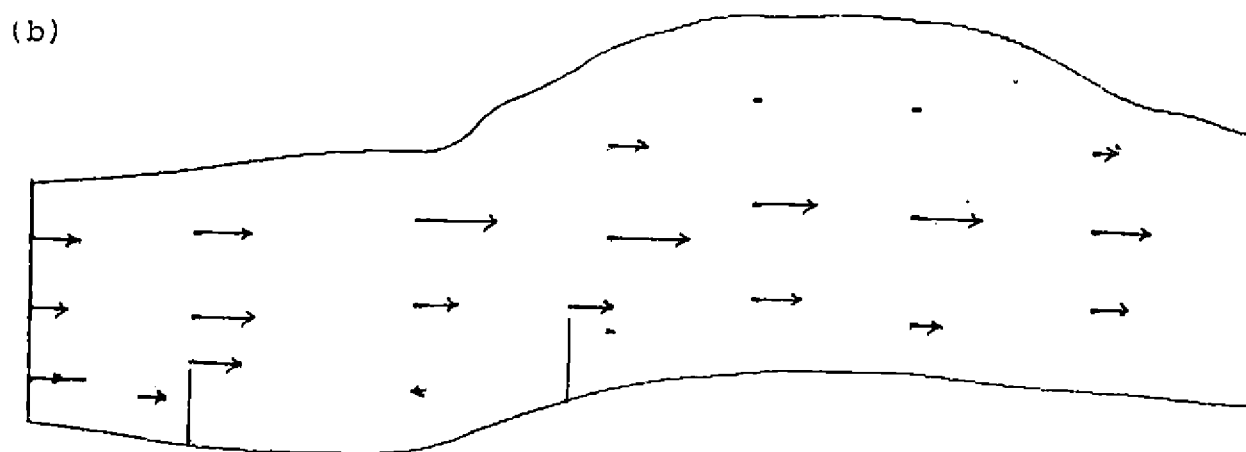
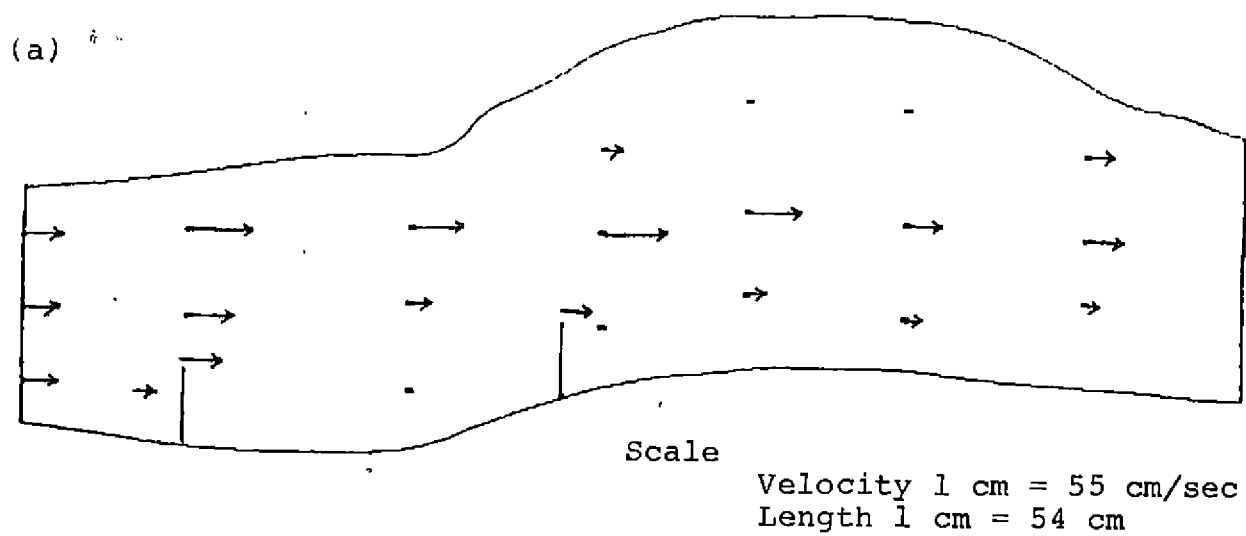


Fig. 79. Velocity grid along multiple spur scheme ( $L=55\text{cm}$ , spacing= $5L$ )  
for discharge rates (a)14.14 lps (b)28.28 lps (c)42.42 lps



multiple spurs with lengths 45 cm and 55 cm. As indicated earlier, it may also be due to the fact that the constriction of the channel is getting increased as the spur length as well as spur spacing increases. Thus it is evident from the analysis of flow pattern and velocity distribution in the test section that the spur spacing also has a significant effect on length of bank protected flow diversion, velocity distribution etc. The data on velocities at opposite bank for different L/B ratios with different spacings are presented in Appendix-2

## **4.2 Mobile bed experiments**

### **4.2.1 Single spur**

Experiments were conducted on mobile bed in chapter 3.14.1. Initially data on scour pattern and velocity distribution were collected without spur. After this, experiments were conducted with different spur configurations in the test section. Detailed analysis of the collected data and the results so obtained are presented under following sub headings.

#### **4.2.1.1 Size and specific gravity of sand**

A representative sample of soil from the river sand used for this study was collected, oven-dried and subjected to sieve analysis. The results of the sieve analysis of the

sand is as shown in Table.5. Mean diameter ( $D_{50}$ ) of the sand was determined from the grain size distribution curve plotted (Fig.80 ) with the sieve analysis results. It was found that the sand used was a well graded one with  $D_{50} = 0.57$  mm.

Representative samples of the sand were also collected and subjected to pycnometer test to determine specific gravity of the sand used. The results of the pycnometer test are as shown in Table 6. It can be seen from the results that specific gravity of the sand is 2.48.

#### 4.2.1.2 Scour pattern data

Data on scour pattern in the test section was collected from the model by measuring cross sectional bed profile data with the help of a point gauge. With the collected data, scour patterns at each experiment condition were plotted and are presented in Fig.81 to 97.

In order to obtain the optimum spur angle and spur length, it was not possible to make similar comparison of velocities as in the case of rigid bed due to scouring nature of the bed. Hence scour depths near the nose of the spur were compared for different spur lengths and spur angles.

Figures 98, 99 and 100 presents the relationship between spur angle and scour depth near the nose of the spur for

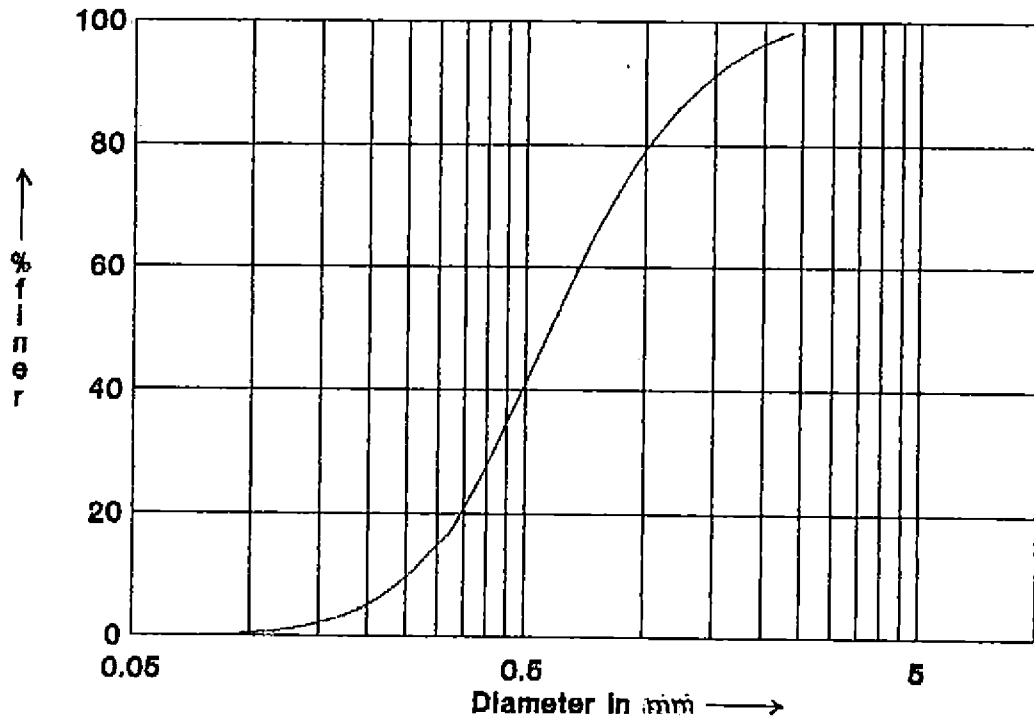


FIG. GRAIN SIZE DISTRIBUTION CURVE

Fig. 80. Grain size distribution curve of the sand used

31

**Table 5. Sieve analysis**

Total weight of the sample= 1812.7 g

Sieve designation (mm)	Weight retained (gm)	% Retained	Cumulative retained	% Finer
2.36	30.60	1.69	1.69	98.31
1.18	123.50	6.81	8.50	91.50
0.60	679.30	37.47	45.98	54.03
0.30	854.30	47.13	93.10	6.90
0.15	121.40	6.70	99.80	0.20
0.08	2.40	0.13	99.93	0.07
pan	1.20	0.07	100.00	0.00

**Table. 6 Specific gravity determination (Pycnometer method)**

(a) Sample 1

Weight of pycnometer + sample (A) = 1931 g

Weight of pycnometer + water (B) = 1481 g

Saturated surface dry weight (C) = 743.7 g

Oven dry weight (D) = 727.7g

$$\begin{aligned}
 (\text{Specific gravity})_1 &= (g_1) = D / \{C - (A - B)\} \\
 &= 727.7 / \{743.7 - (1931 - 1481)\} \\
 &= 2.477
 \end{aligned}$$

(b) Sample 2

Weight of pycnometer + sample (A) = 1956 g

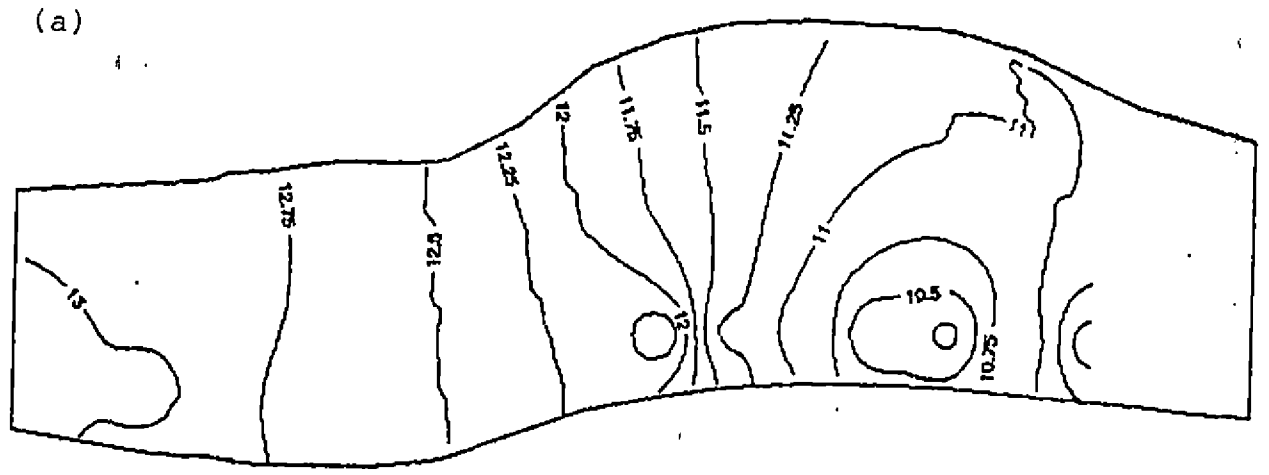
Weight of pycnometer + water (B) = 1481 g

Saturated surface dry weight (C) = 773.7 g

Oven dry weight (D) = 742.16g

$$\begin{aligned}
 (\text{Specific gravity})_2 &= (g_2) = D / \{C - (A - B)\} \\
 &= 742.16 / \{773.7 - (1956 - 1481)\} \\
 &= 2.484
 \end{aligned}$$

$$\begin{aligned}
 \text{Average specific gravity (g)} &= (g_1 + g_2) / 2 = \\
 &= (2.477 + 2.484) / 2 \\
 &= 2.48
 \end{aligned}$$



Average bed level = 12.8 cm  
All dimensions in cm  
Scale 1:54

Flow direction  
→

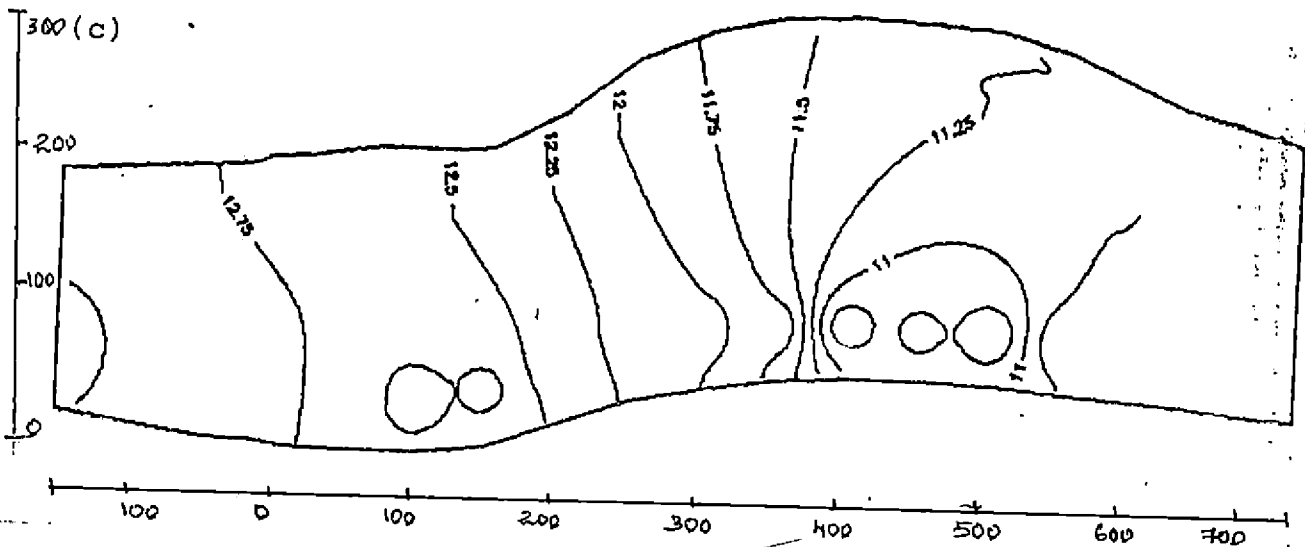
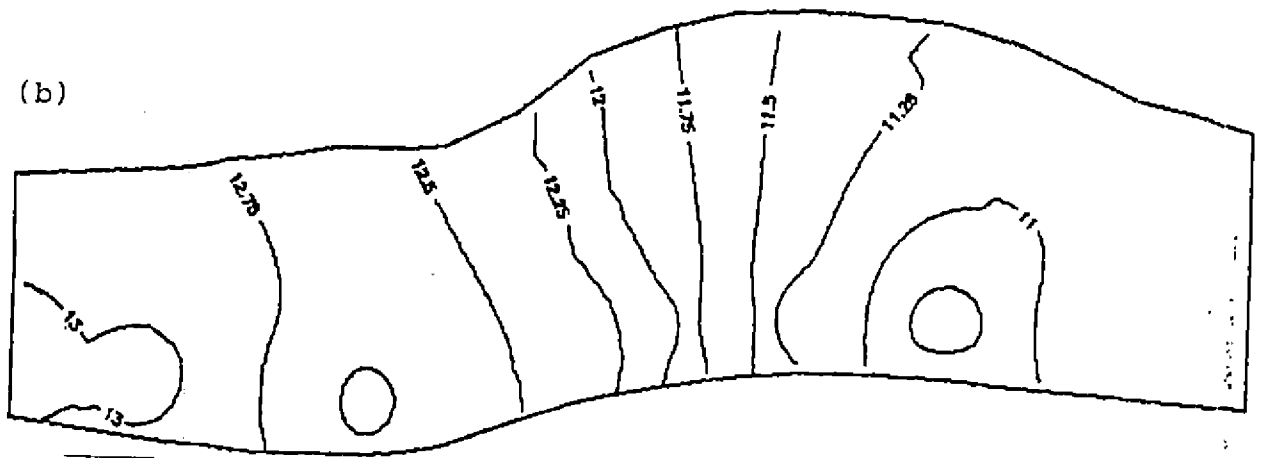


Fig. 81. Scour pattern without spur for discharge rates (a) 28.28 lps  
(b) 42.42 lps.

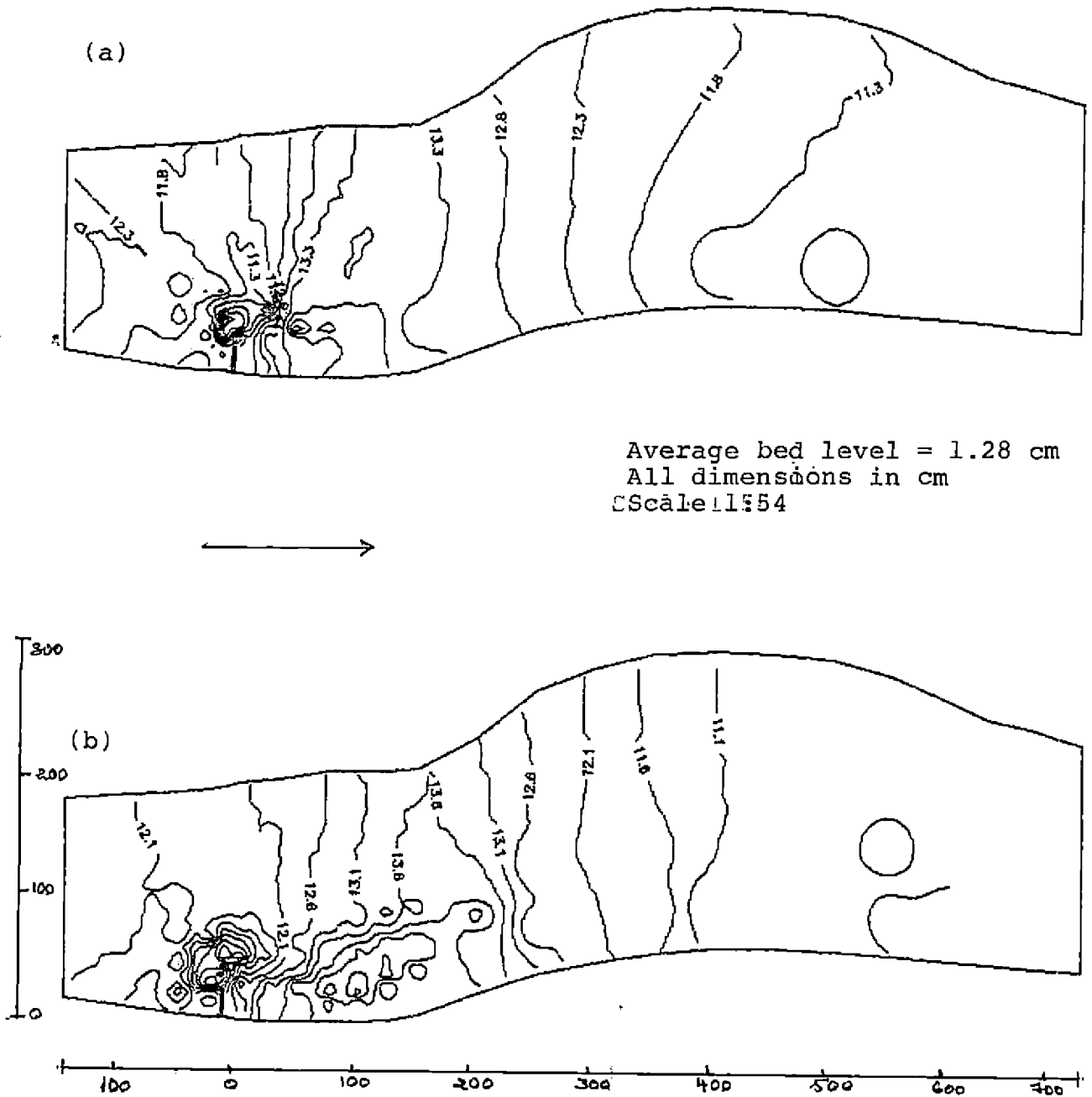
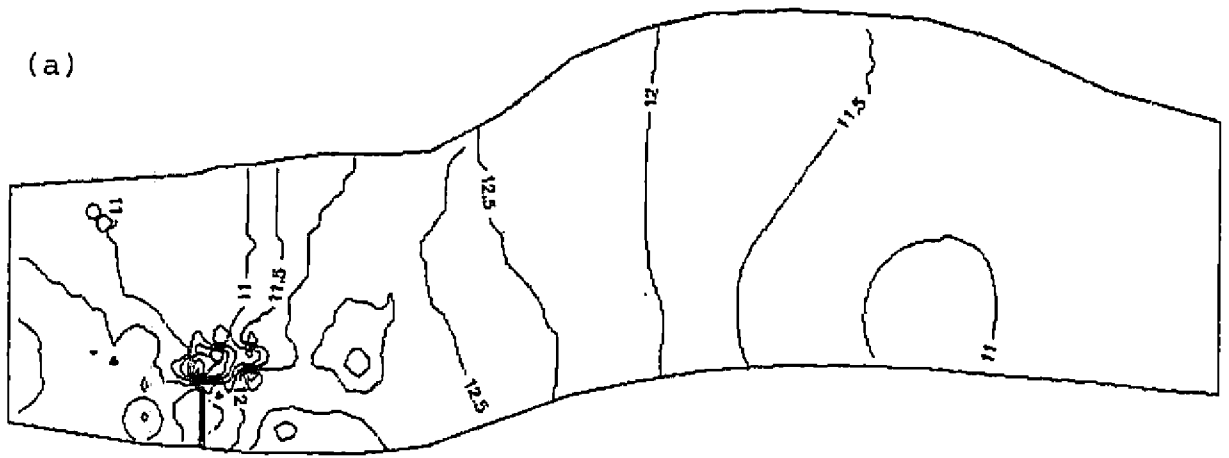


Fig. 8.2 Scour pattern for single spur ( $L=25\text{ cm}, \theta = 90^\circ$ ) for discharge rates (a) 28.28 lps (b) 42.42 lps



Average bed level = 1.28 cm  
 All dimensions in cm  
 Scale 1:54

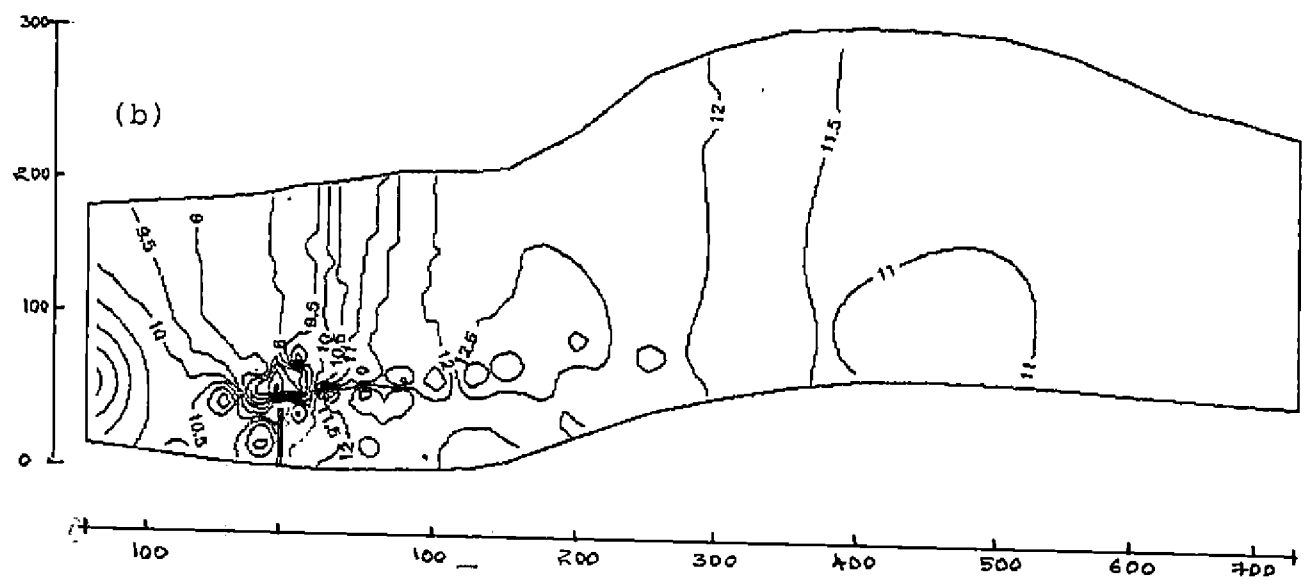
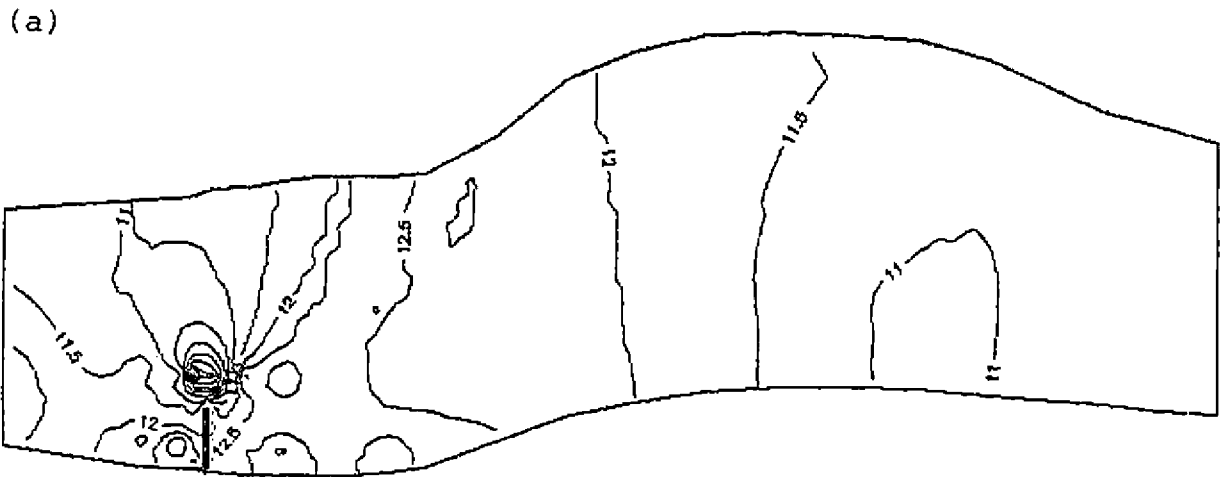


Fig. 83. Scour pattern for single spur ( $L=35$  cm,  $\theta=90^\circ$ ) for discharge rates (a) 28.28 lps (b) 42.42 lps



Average bed level = 1.28 cm  
 All dimensions in cm  
 Scale 1:54

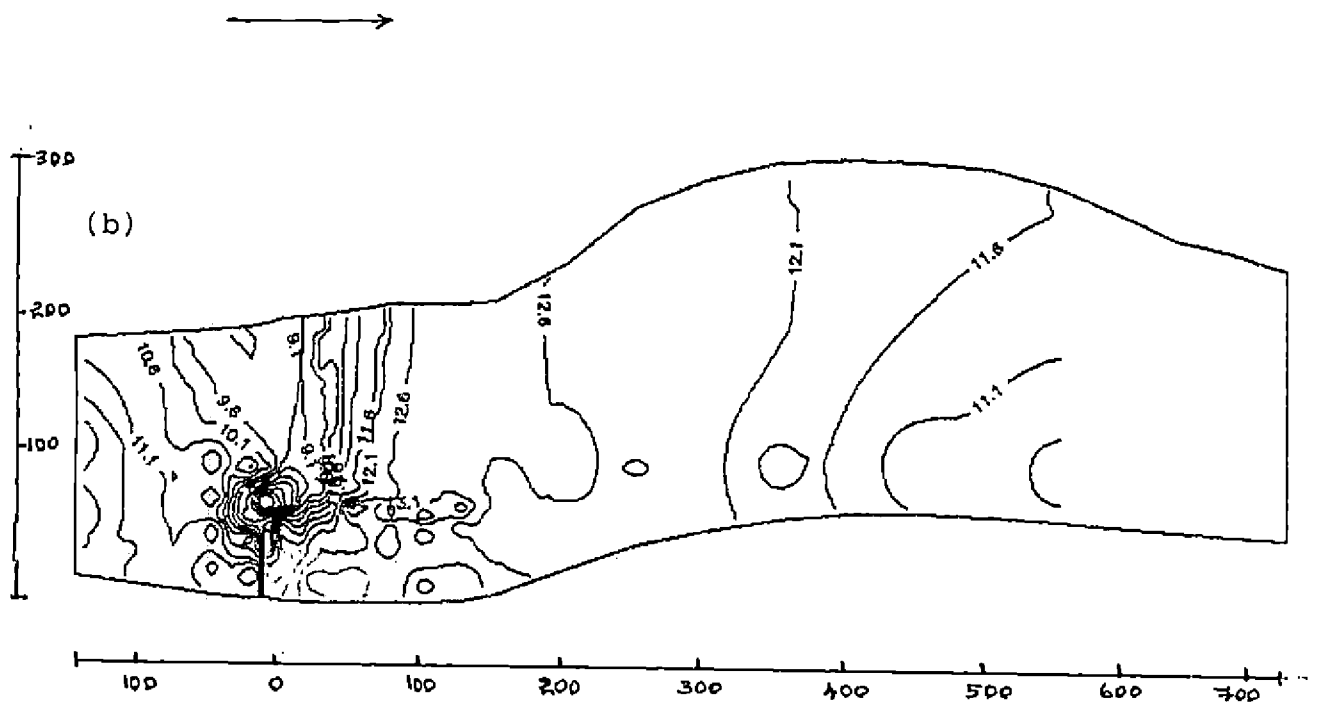


Fig. 84. Scour pattern for single spur ( $L=45$  cm,  $\theta=90^\circ$ ) for discharge rates (a) 28.28 lps (b) 42.42 lps



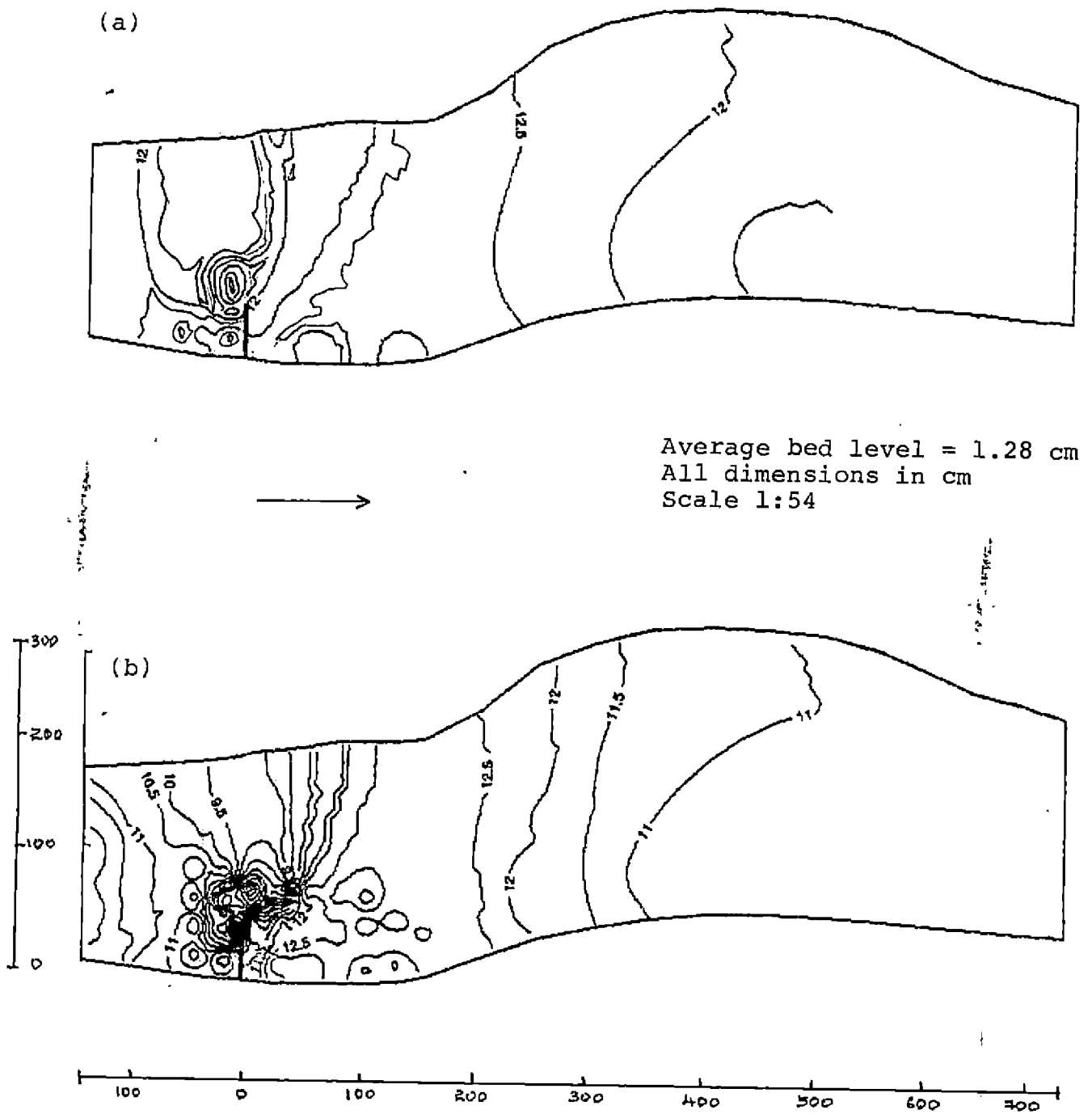
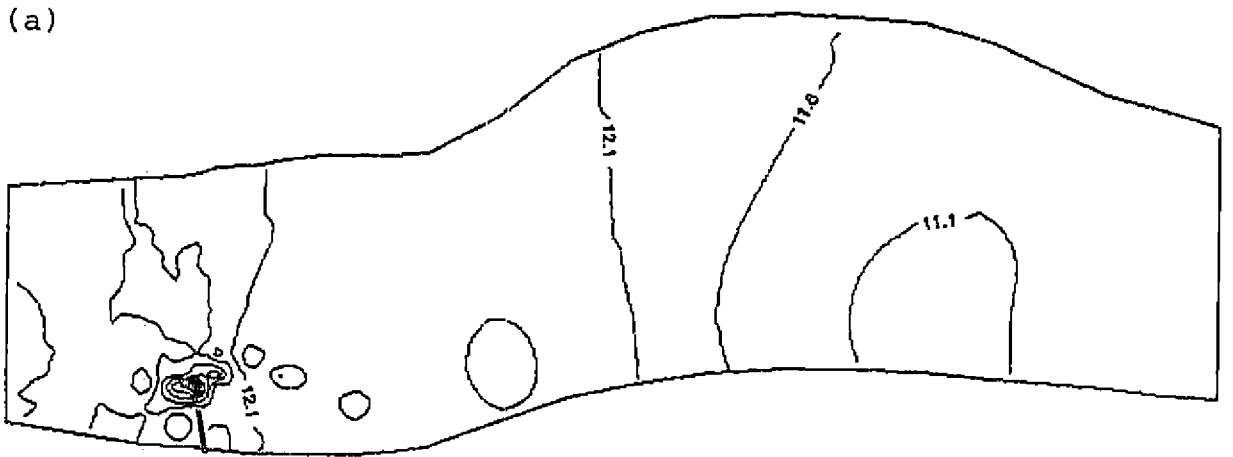


Fig. 85. Scour pattern for single spur ( $L=55$  cm,  $\theta = 90^\circ$ ) for discharge rates (a) 28.28 lps (b) 42.42 lps



Average bed level = 1.28 cm  
 All dimensions in cm  
 Scale 1:54

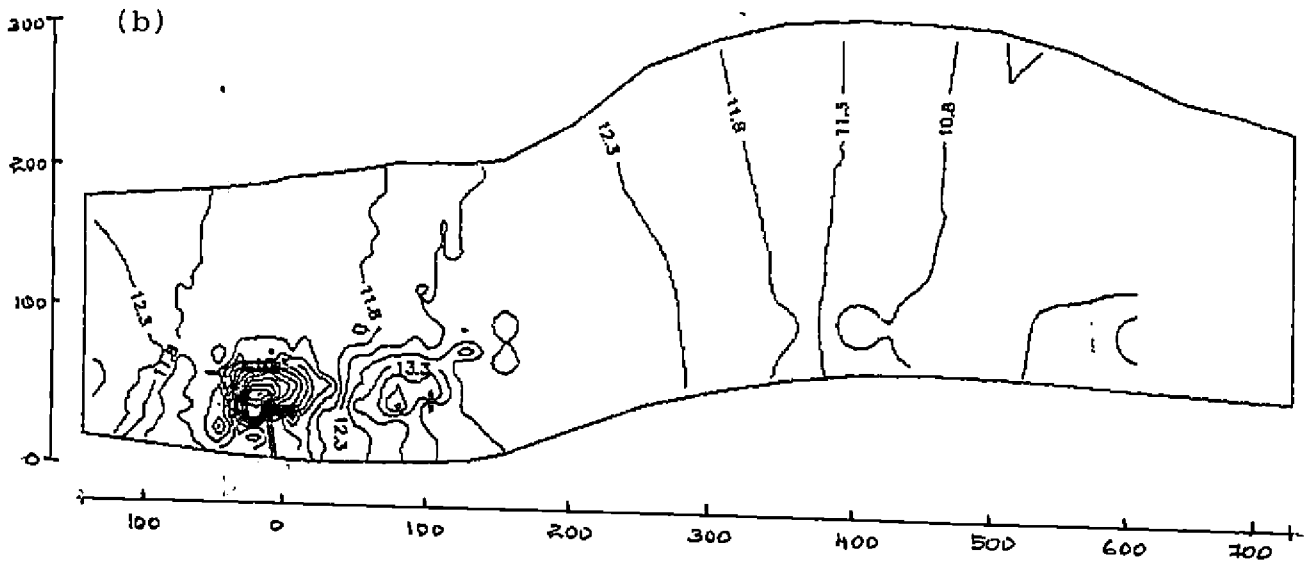
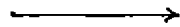
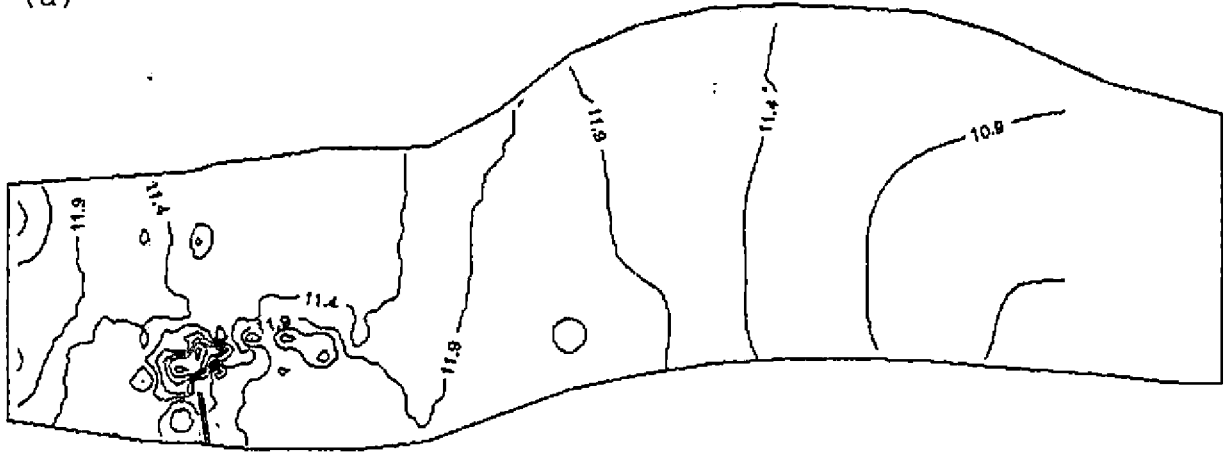


Fig. 86. Scour pattern for single spur ( $L=25$  cm,  $\theta=100^\circ$ ) for discharge rates (a) 28.28 lps (b) 42.42 lps

(a)



Average bed level = 1.28 cm  
 All dimensions in cm  
 Scale 1:54



(b)

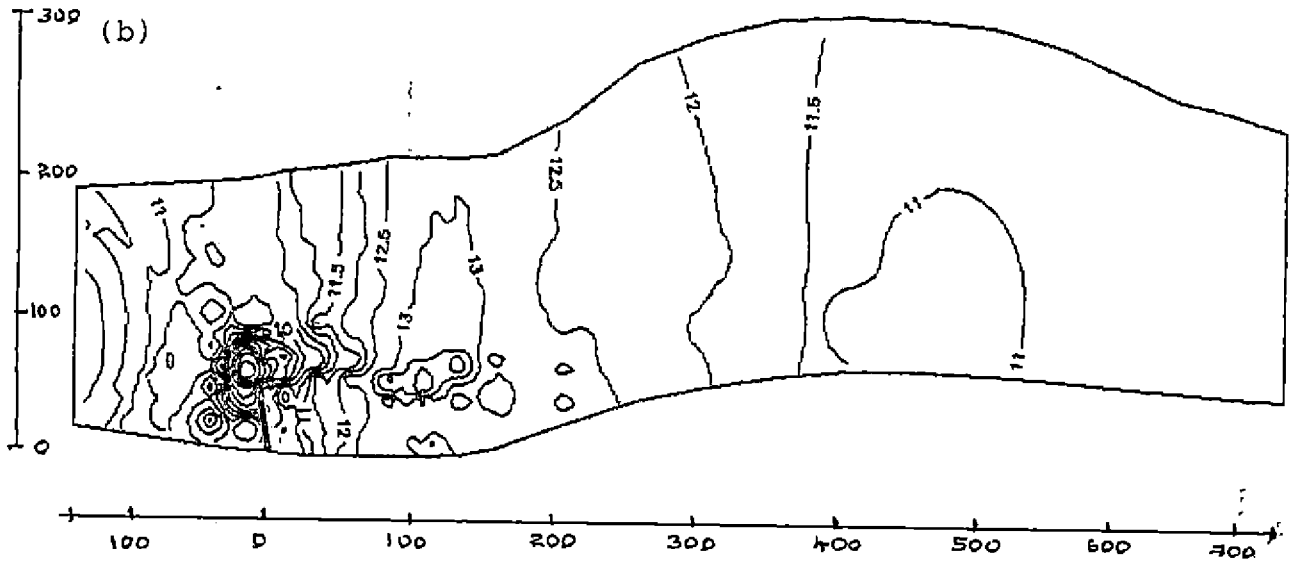
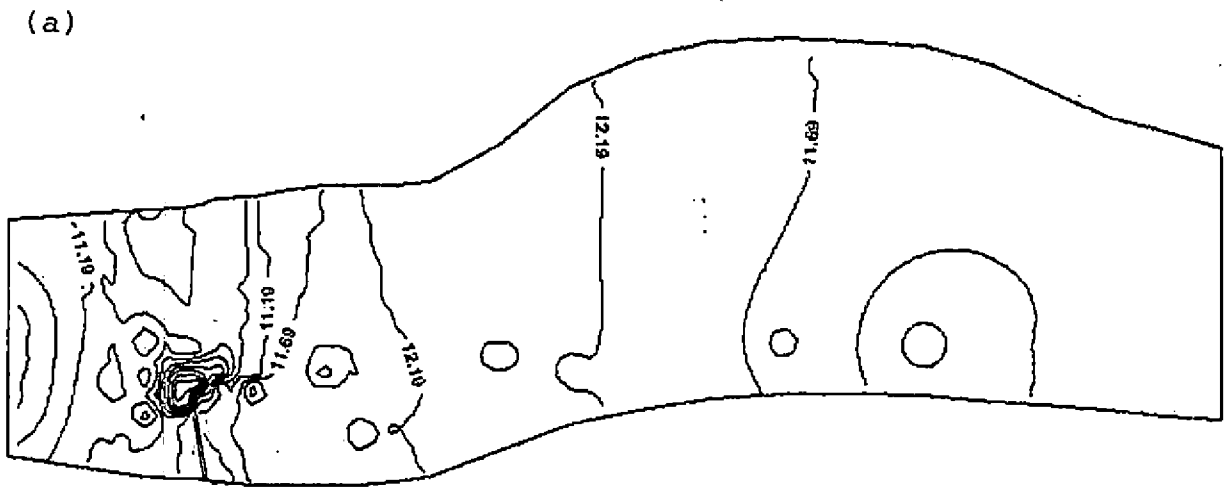


Fig. 87. Scour pattern for single spur ( $L=35$  cm,  $\theta=100^\circ$ ) for discharge rates (a) 28.28 lps (b) 42.42 lps



Average bed level = 1.28 cm  
 All dimensions in cm  
 Scale 1:54

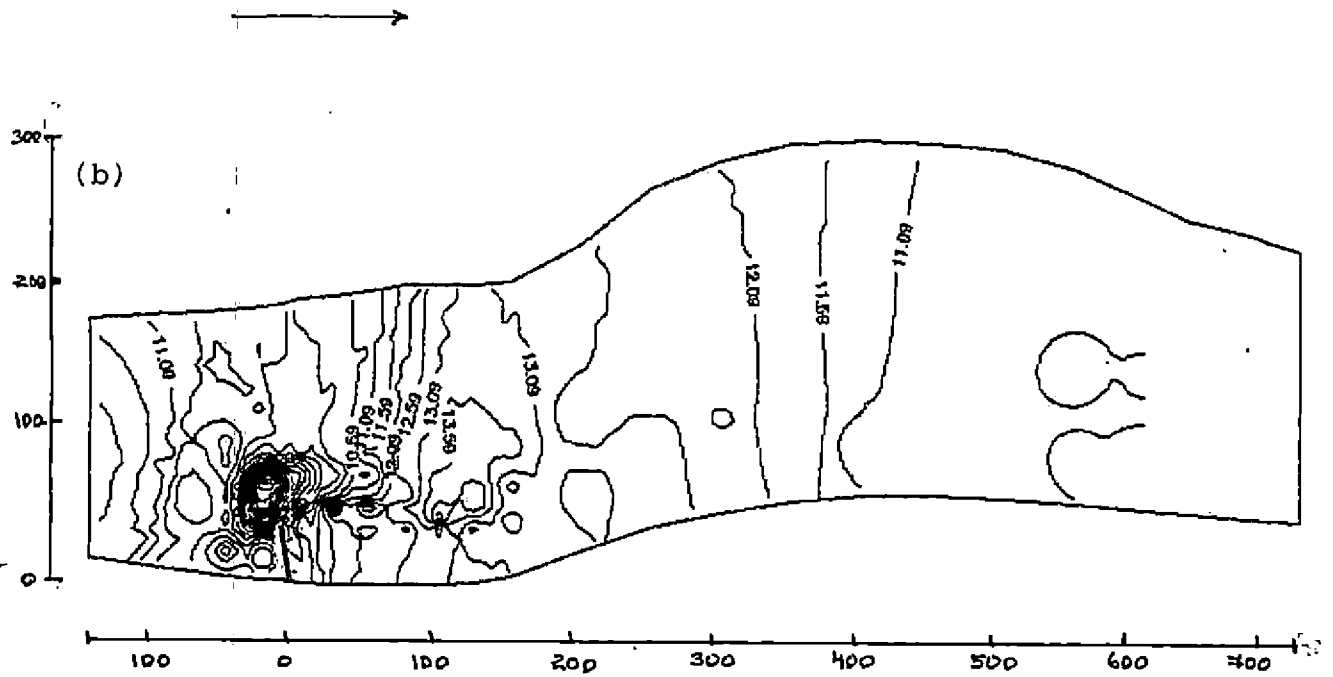
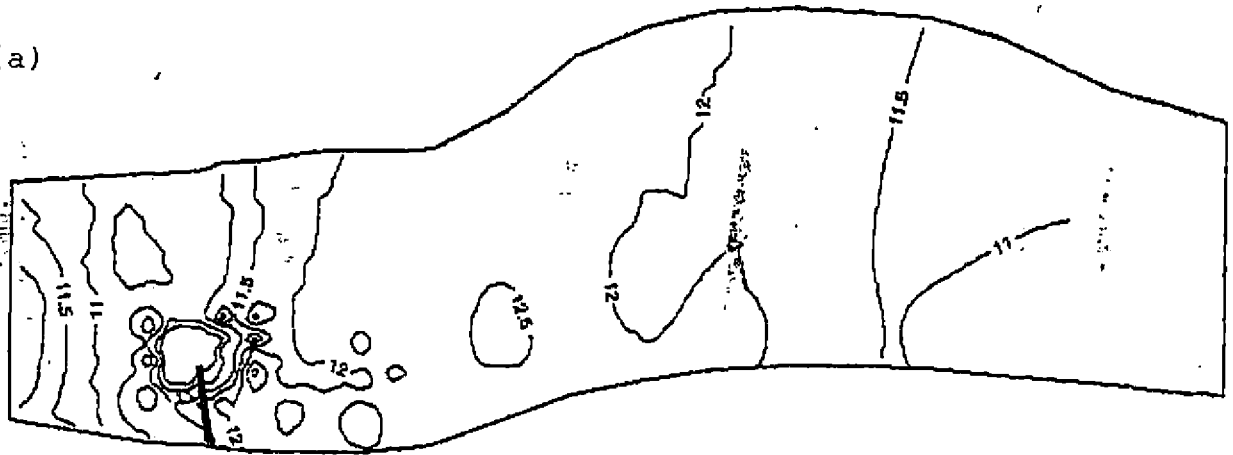


Fig. 88 Scour pattern for single spur ( $L=45$  cm,  $\theta = 100^\circ$ ) for discharge rates (a) 28.28 lps (b) 42.42 lps

(a)



Average bed level = 1.28 cm  
All dimensions in cm  
Scale 1:54

(b)

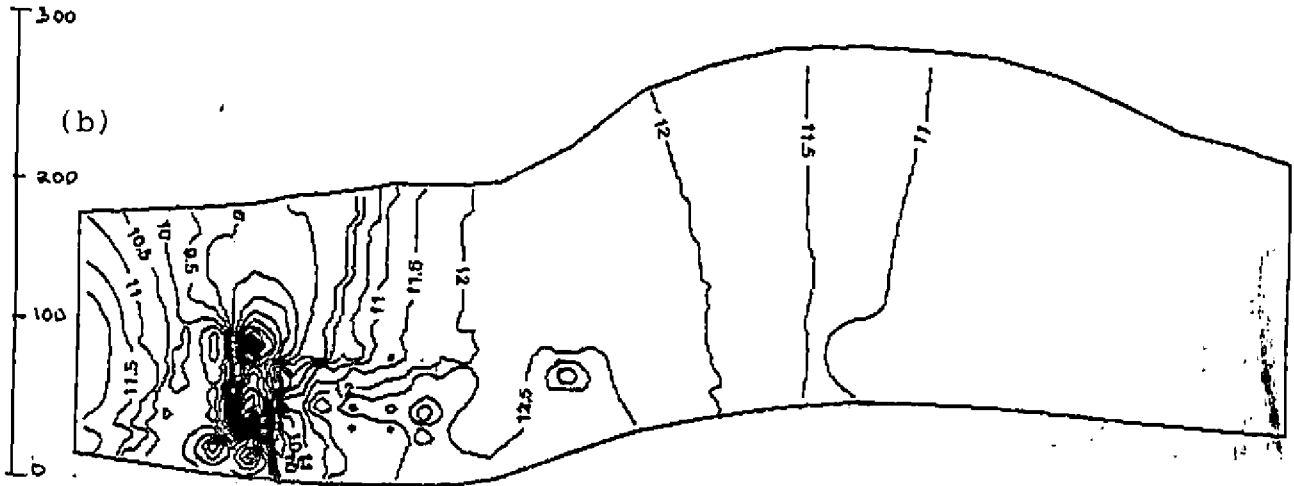
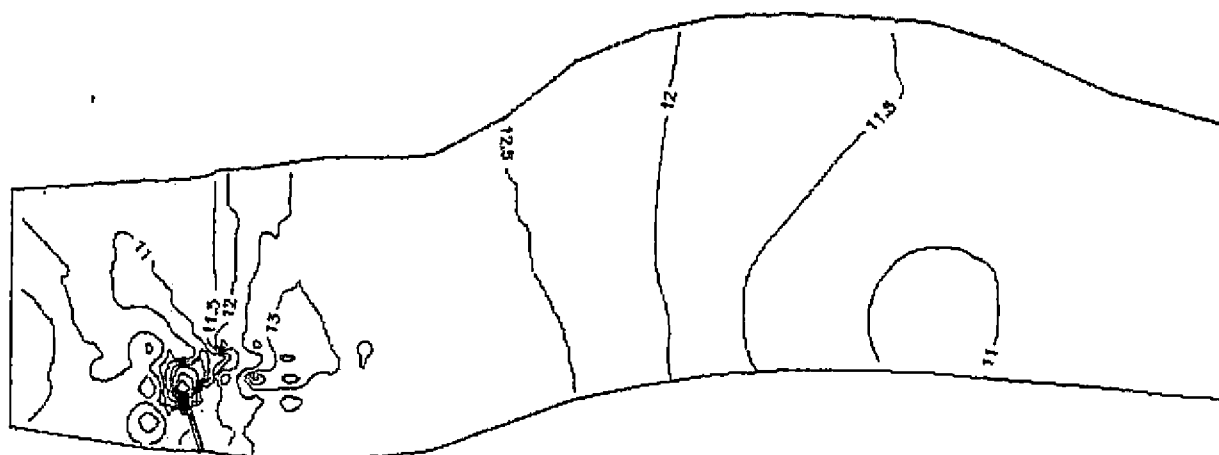


Fig. 89. Scour pattern for single spur ( $L=55$  cm,  $\theta=100^\circ$ ) for discharge rates (a) 28.28 lps (b) 42.42 lps

(a)



Average bed level = 1.28 cm  
 All dimensions in cm  
 Scale 1:54

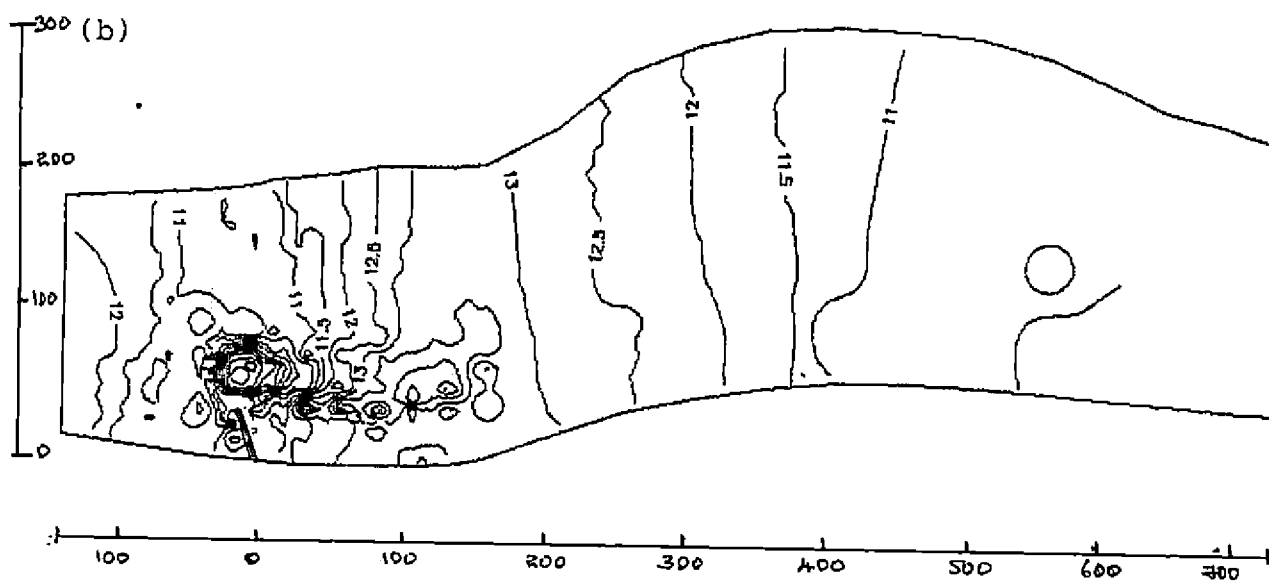
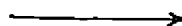
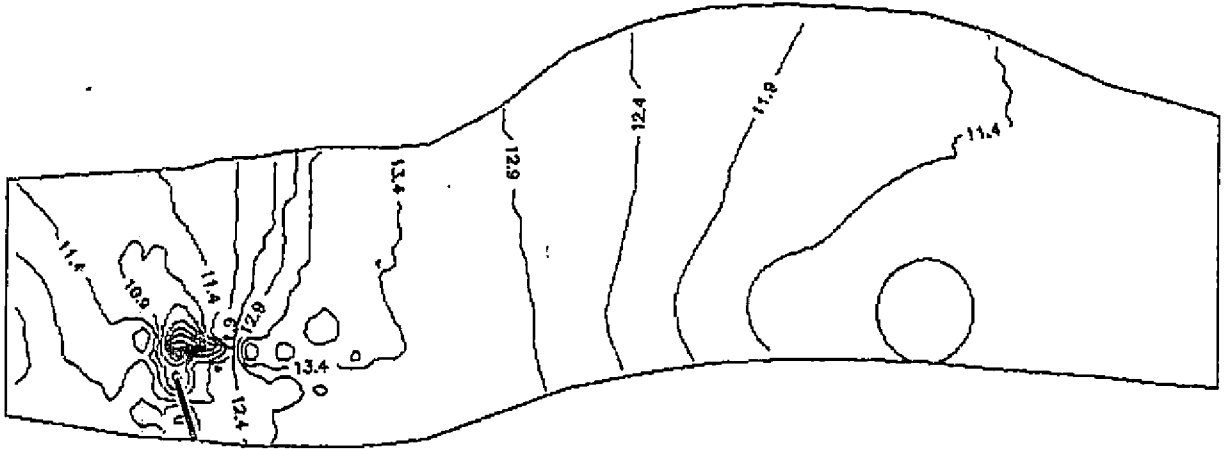


Fig. 91. Scour pattern for single spur ( $L=35$  cm,  $\theta=11\frac{1}{2}^\circ$ ) for discharge rates (a) 28.28 lps (b) 42.42 lps

(a)



Average bed level = 1.28 cm  
 All dimensions in cm  
 Scale 1;54

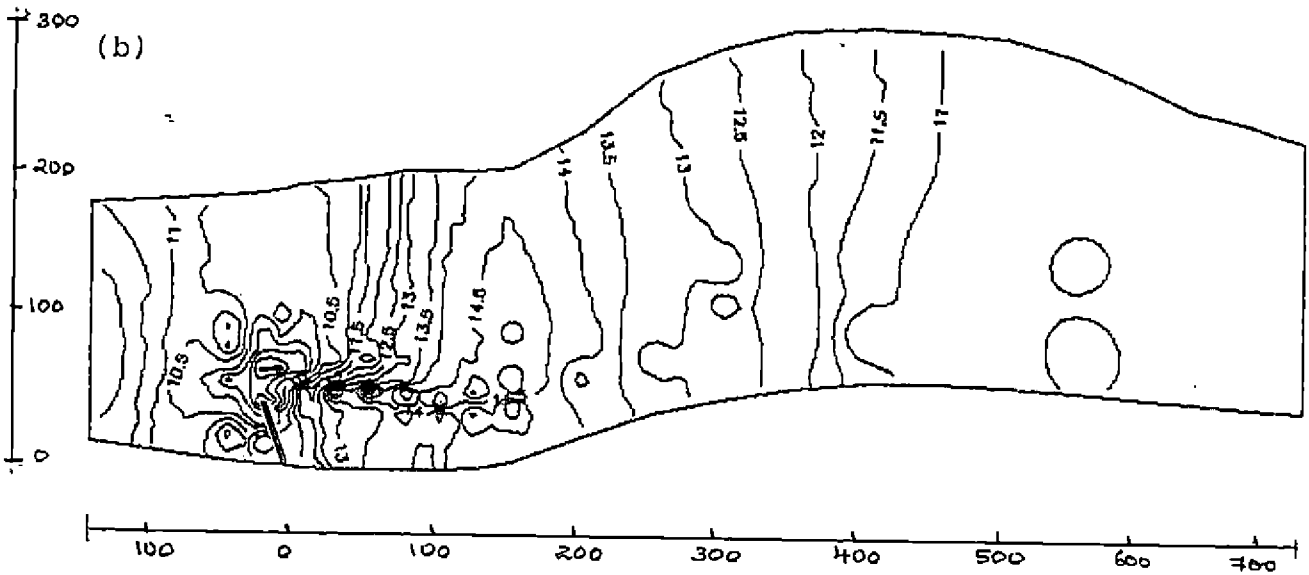
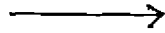
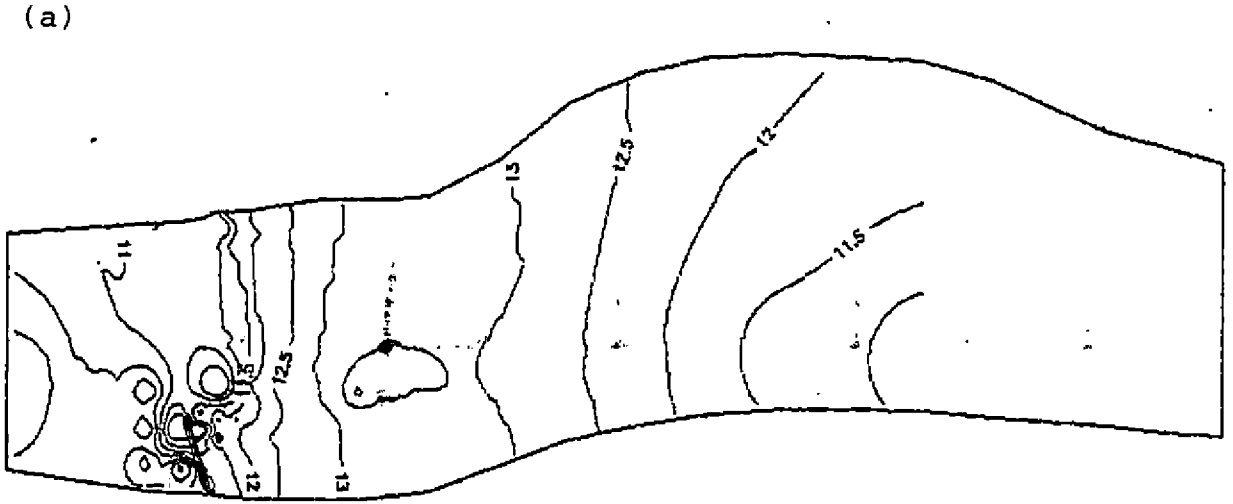


Fig. 92. Scour pattern for single spur ( $L=45$  cm,  $\theta=110^\circ$ ) for discharge rates (a) 28.28 lps (b) 42.42 lps



Average bed level = 1.28 cm  
All dimensions in cm  
Scale 1:54

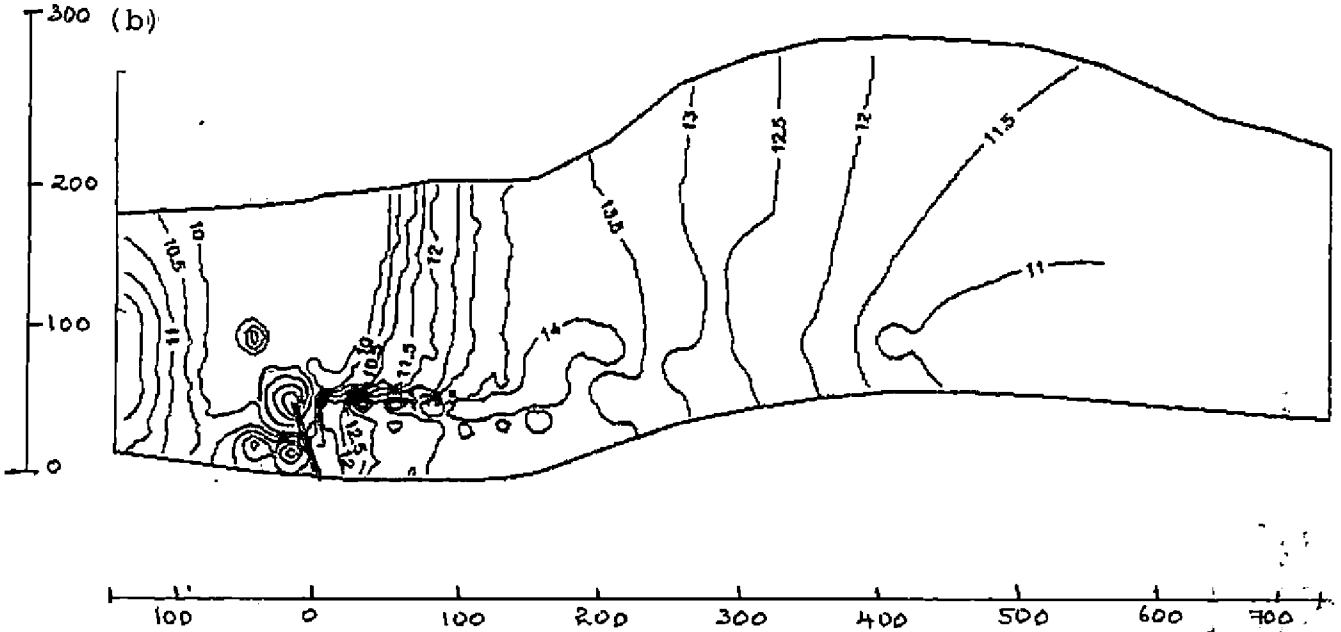
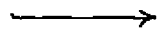


Fig. 93. Scour pattern for single spur ( $L=55$  cm,  $\theta = 110^\circ$ ) for discharge rates (a) 28.28 lps (b) 42.42 lps



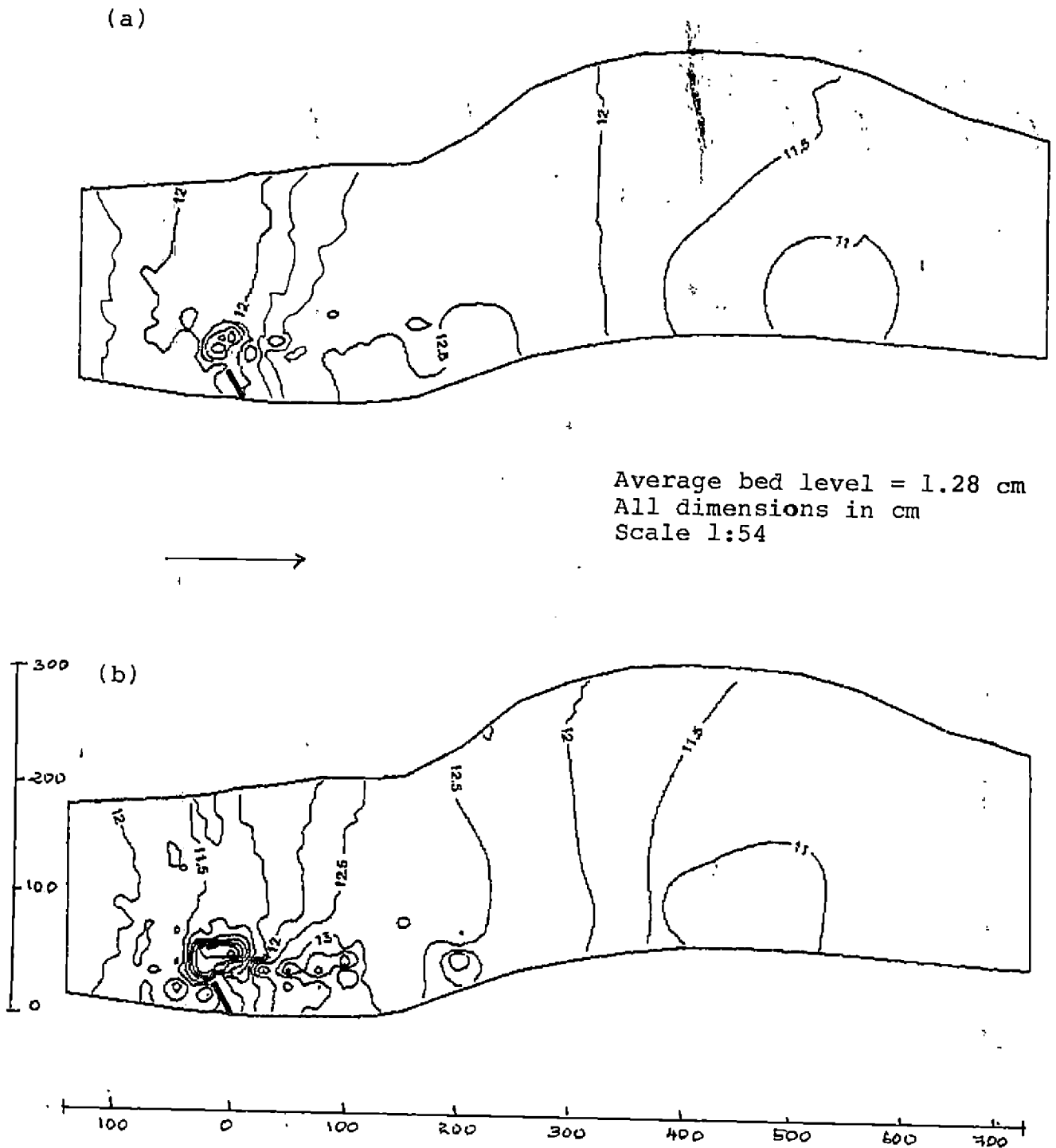
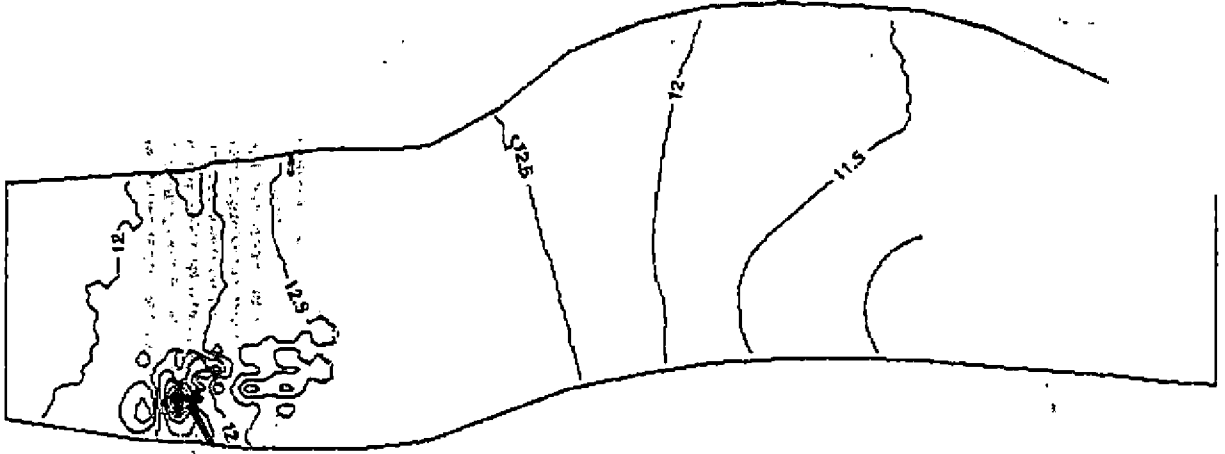


Fig. 94. Scour pattern for single spur ( $L=25$  cm,  $\theta = 120^\circ$ ) for discharge rates (a) 28.28 lps (b) 42.42 lps

(a)



Average bed level = 1.28 cm  
All dimensions in cm  
scale 1:54



(b)

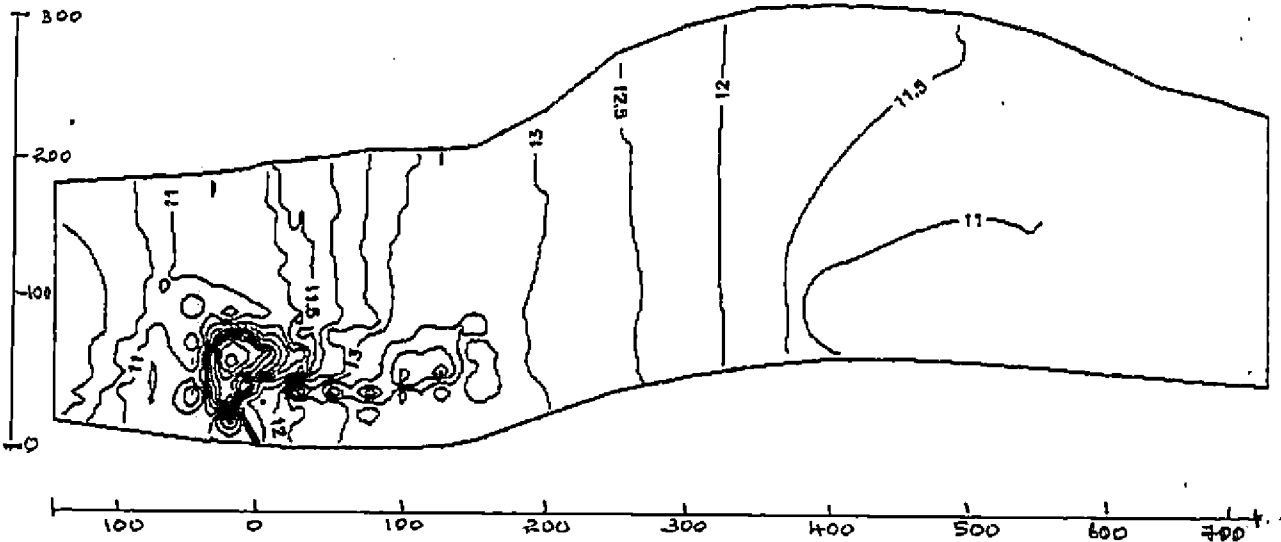
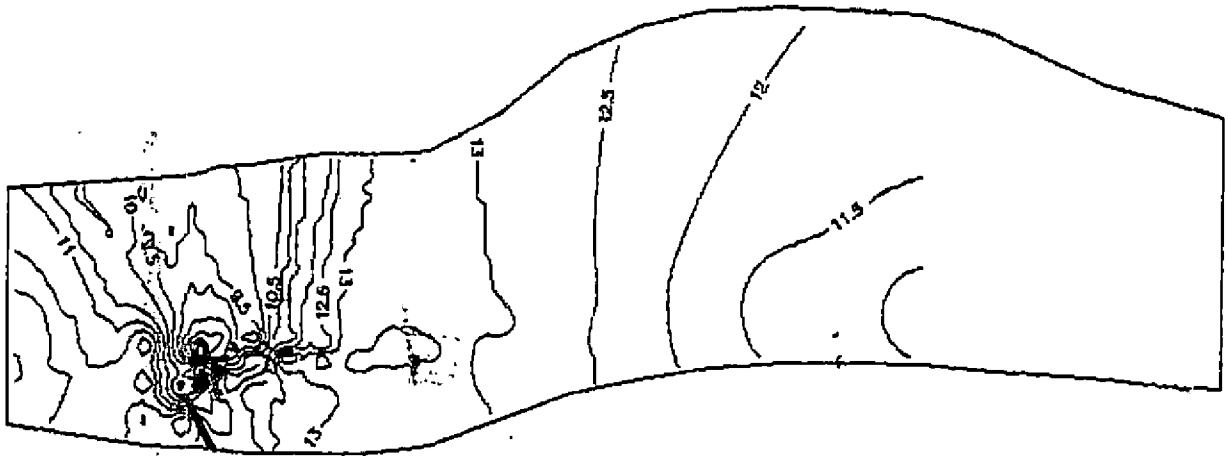


Fig. 95. Scour pattern for single spur ( $L=35$  cm,  $\phi=120^\circ$ ) for discharge rates (a) 28.28 lps (b) 42.42 lps

(a)



Average bed level = 1.28 cm  
 All dimensions in cm  
 Scale 1:54

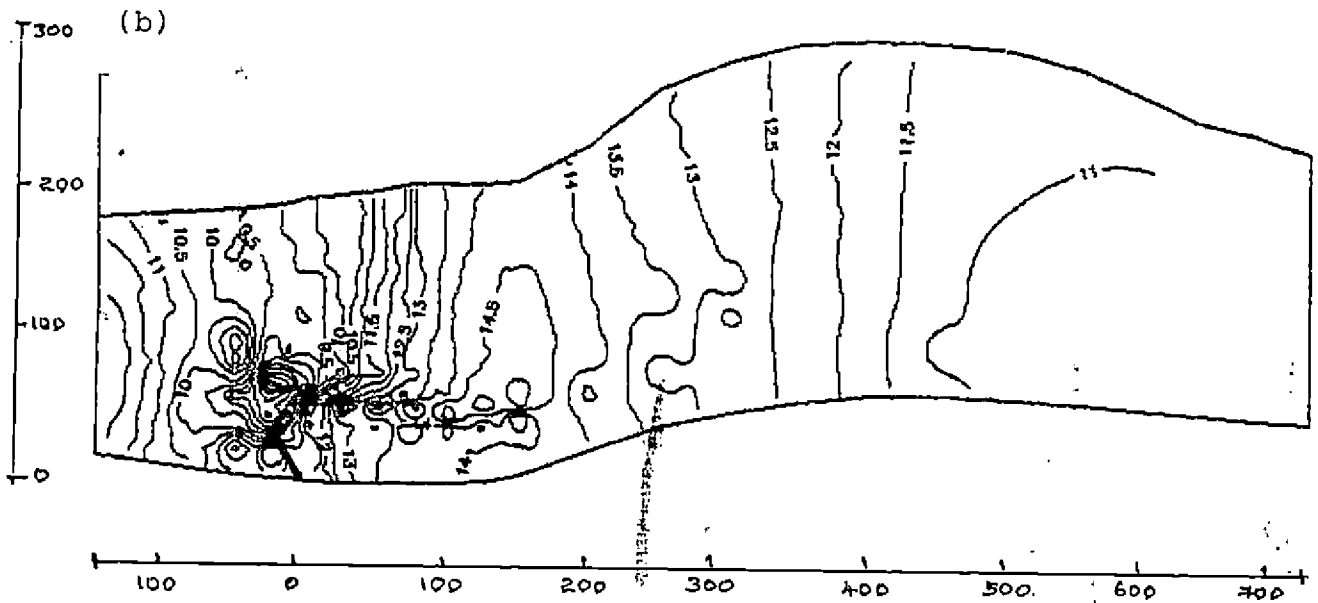
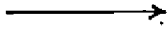
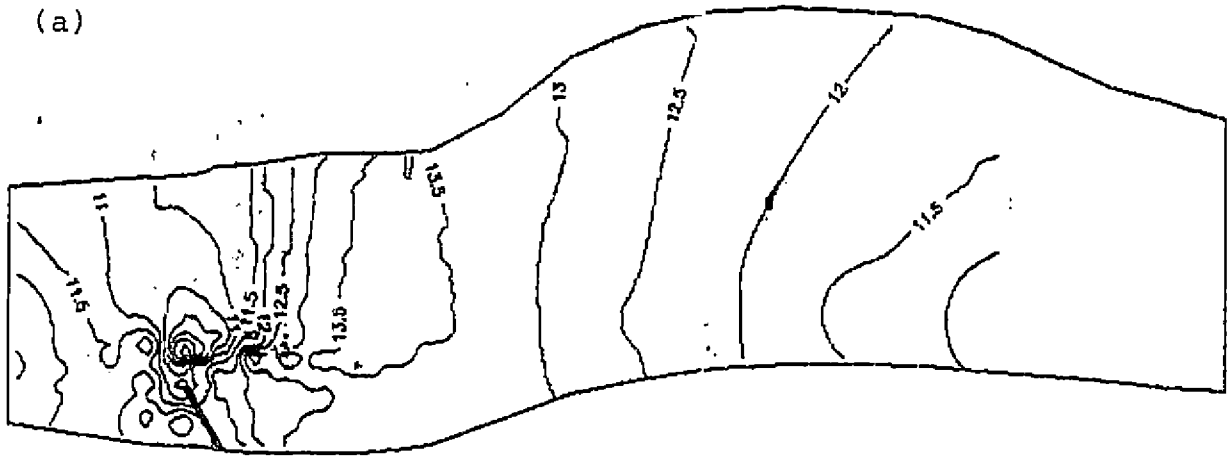


Fig. 96. Scour pattern for single spur ( $L=45$  cm,  $\theta=120^\circ$ ) for discharge rates (a) 28.28 lps (b) 42.42 lps



Average bed level = 1.28 cm  
 All dimensions in cm  
 Scale 1:54

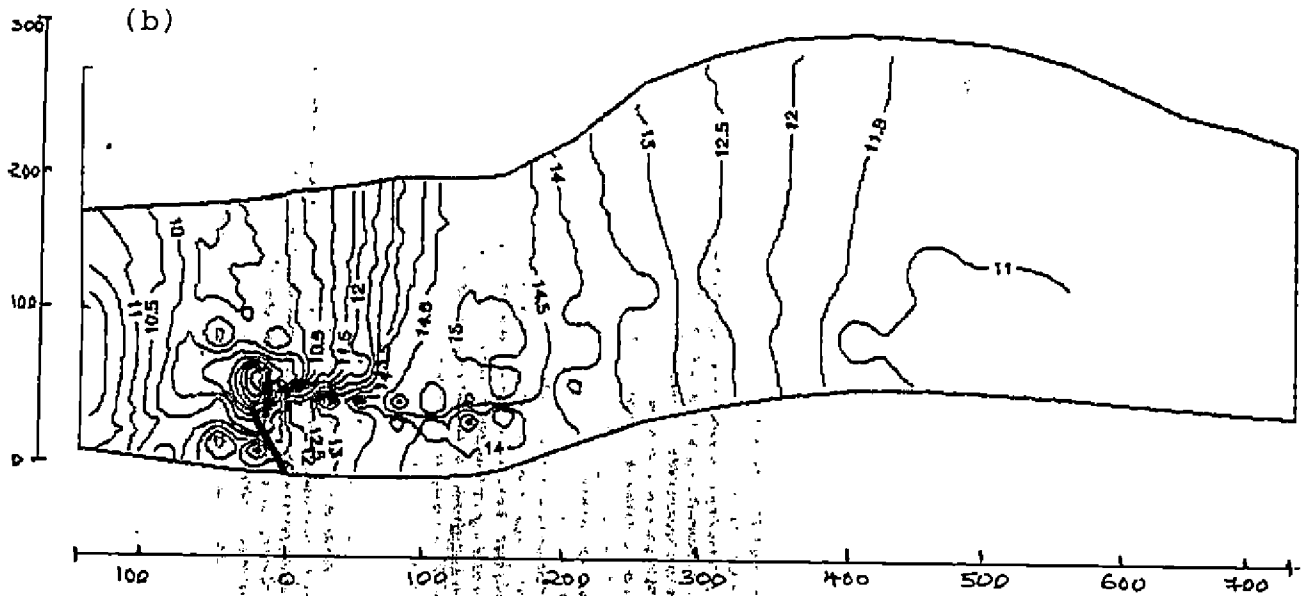


Fig. 97. Scour pattern for single spur ( $L=55$  cm,  $\theta=120^\circ$ ) for discharge rates (a) 28.28 lps (b) 42.42 lps

different discharge rates 14.14 lps ,28.28 lps and 42.42 lps respectively. The lines sketched on these figures represents the data trends for each of the spur configurations tested. The scattering of the data points about the trend lines is due to the movement of bed forms that had an impact on the measured bed elevation. However the data trends are still quite obvious. In all cases, the scour depth decreased with increasing spur angle. This implies that the greater the spur angle the smaller the magnitude of local scour produced at the spur tip. This conclusion holds regardless of spur length.

Another observation seen from these figures is the effect that channel constriction have on local scour at the tip of the spur. The experimental data indicated that the smaller the magnitude of flow constriction, the less severe the scour at the spur tip. The data of scour depths near the nose of the spur for various spur angles are presented in Appendix-3.

Figure 101 depicts a graph of  $ds/d$  versus  $L/B$  ratio in which  $d$  is the depth of flow for non scouring bed and  $ds$  is the maximum depth of scour at the spur tip. It can be seen from this figure that the slope of line  $ds/d$  rapidly increase after  $L/B = 0.20$ . Thus from above observation related to scour depths, it can be concluded that spur model with  $L/B = 0.19$  and angle  $\phi = 90^\circ$  is again found suitable for the test section. The data of scour depths at spur nose for different  $L/B$  ratios tested are presented in Appendix 3.

Grade et al. have carried out experiments in a long tilting flume and presented non dimensional plots in respect of  $(D+ds)/D$  versus  $F$  and  $F^2/\alpha^3$  in which  $D$  = average flow depth,  $ds$  = maximum scour depth,  $\alpha$  = opening ratio and  $F$  is the Froude's number. Similar analysis of data in the present studies have been carried out and the relationships obtained are shown in Fig. 102 and Fig.103 for single spur configuration. It can be seen from these plots that scour depth increased with froude number  $F$  as well as  $F^2/\alpha^3$ .

#### 4.2.1.4 Null point determination

Inorder to find the length of bank protected at each spur configuration, null point was determined by dropping potassium permanganate solution in the test section as explained in chapter 3.11. Fig.104 and Fig.105 presents graphs of  $LBP/L$  versus  $\theta$  in which  $LBP$  = length of bank protected downstream of the spur tip,  $L$  = spur projected length and  $\theta$  = spur angle. It can be seen form this figure that the length of bank protected by the spur configurations tested , does not vary significantly with spur angles except for very large spur angles. However  $LBP/L$  was found to vary directly with spur length and its value ranged from 5 to 8. The data of  $LBP$  for various spur configurations are presented in Appendix-4.

#### 4.2.2 Multiple spurs

Experiments were conducted with  $L/B$  ratios as 0.14, 0.19 & 0.25 and spacing between spurs as  $3L$ ,  $4L$  and  $5L$  under

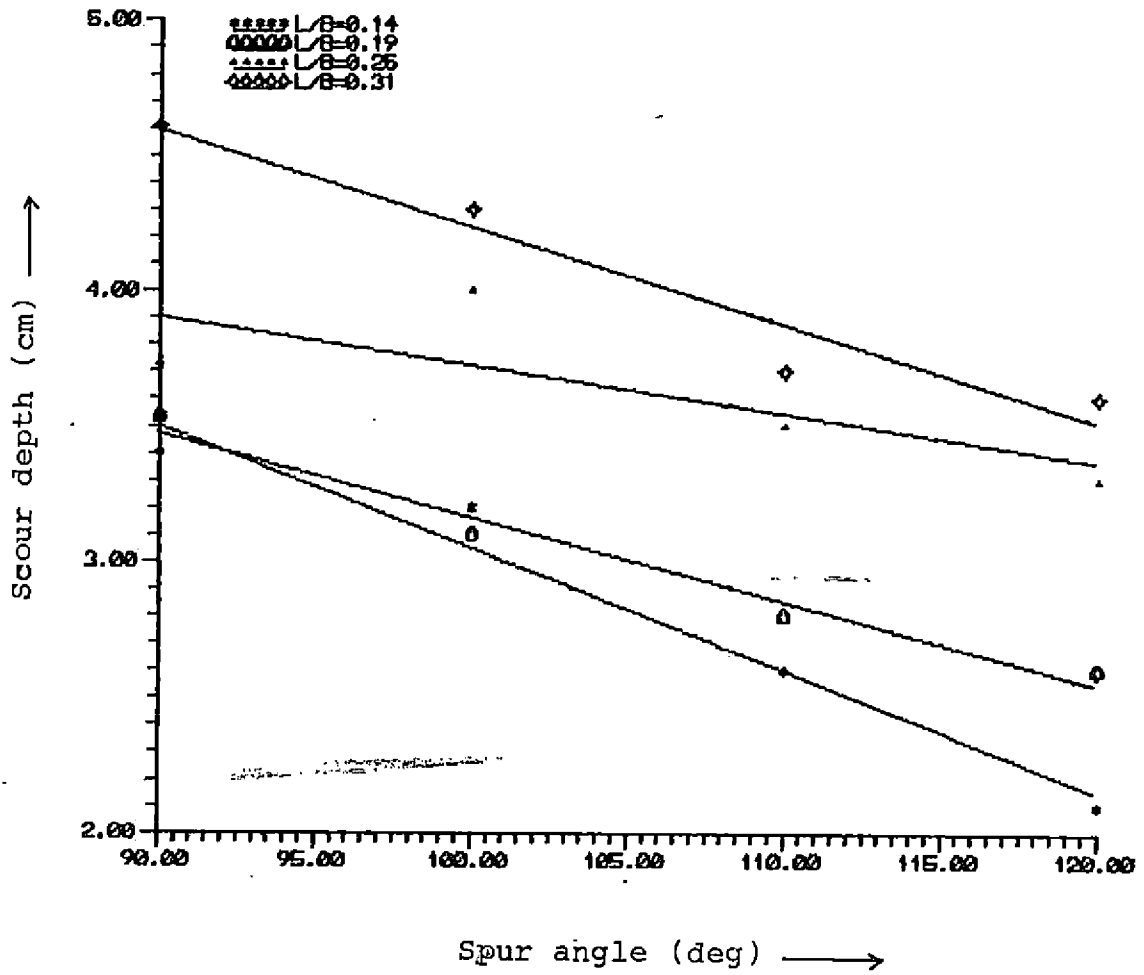


Fig. 98. Trend lines for scour versus spur angles for the constrictions tested (Discharge = 14.14 lps)

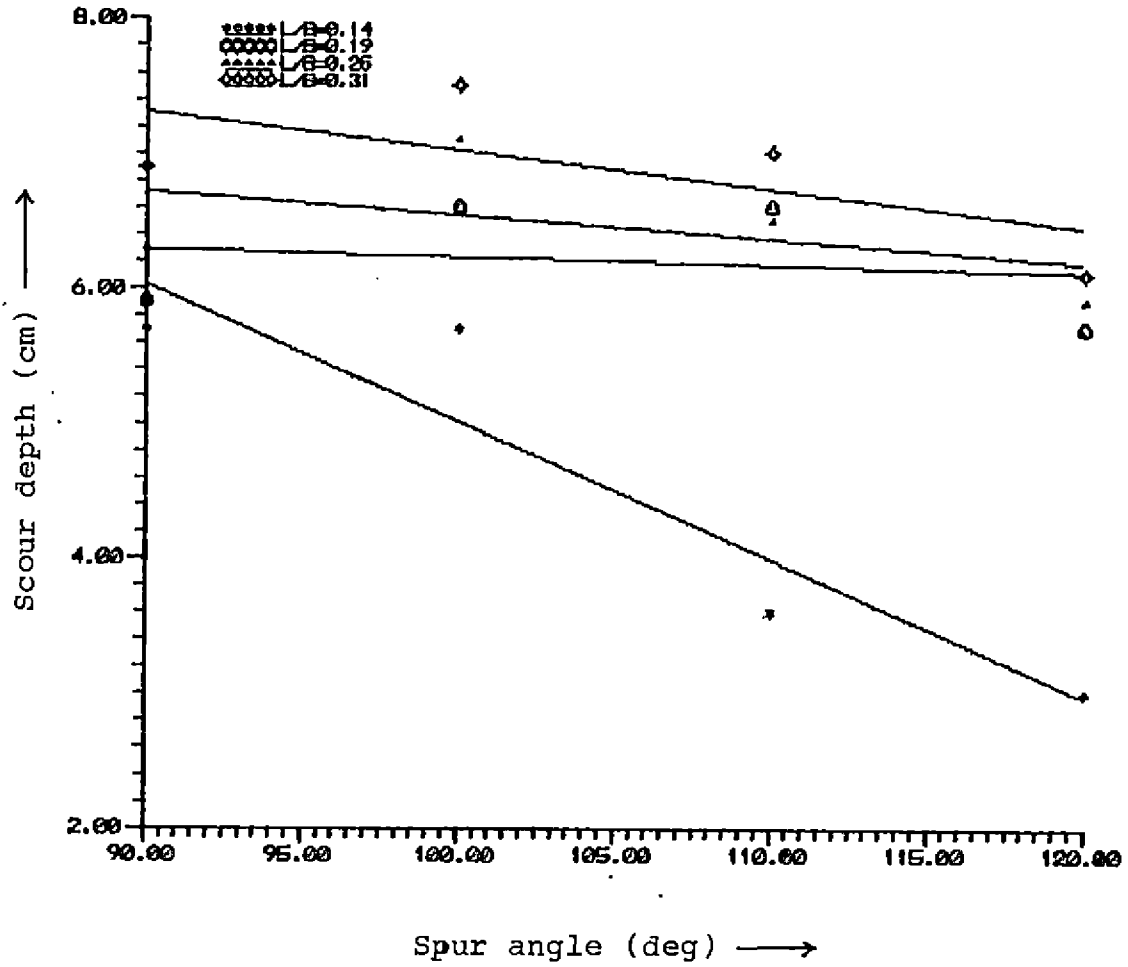


Fig. 99. Trend lines for scour versus spur angles for the constrictions tested (Discharge = 28.28 lps)



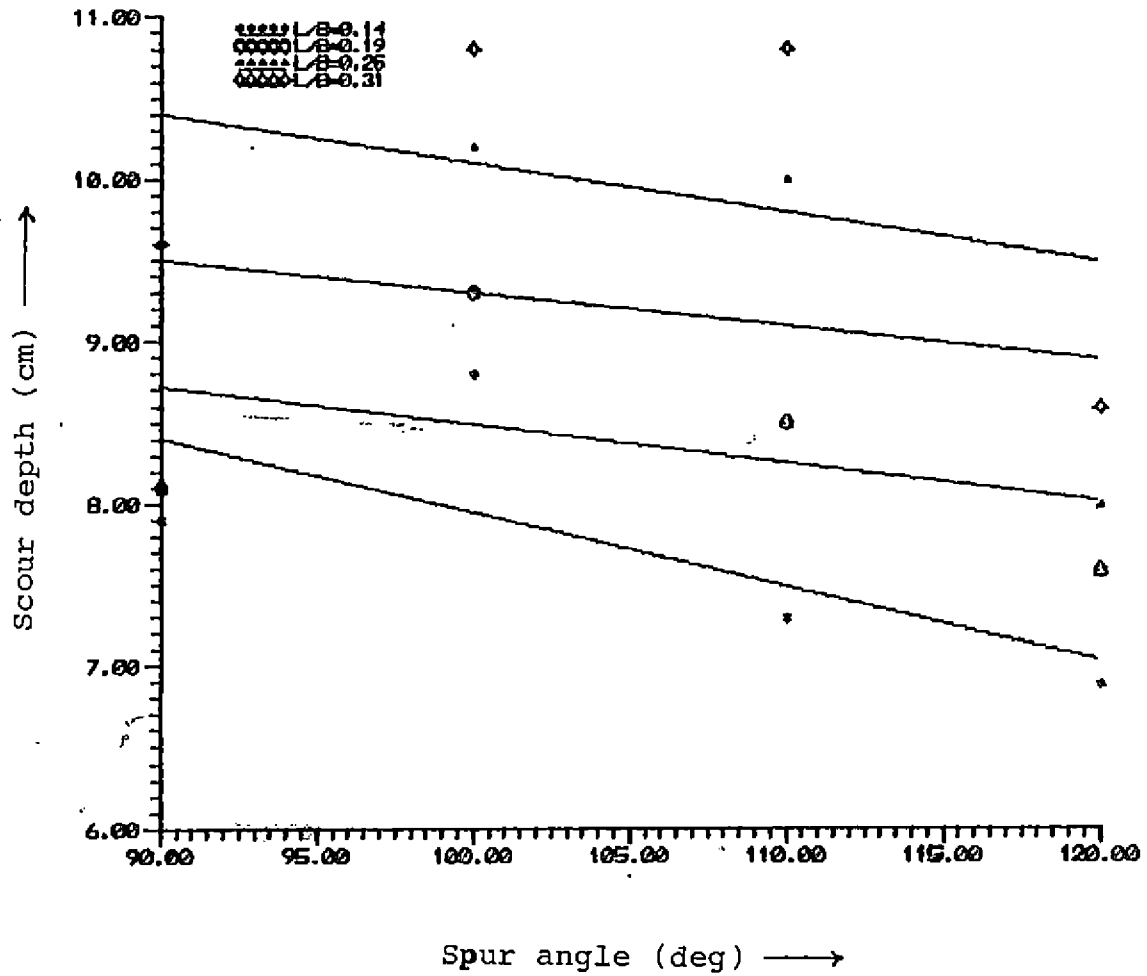


Fig. 100. Trend lines for scour versus spur angles for the constrictions tested (Discharge = 42.42 lps)

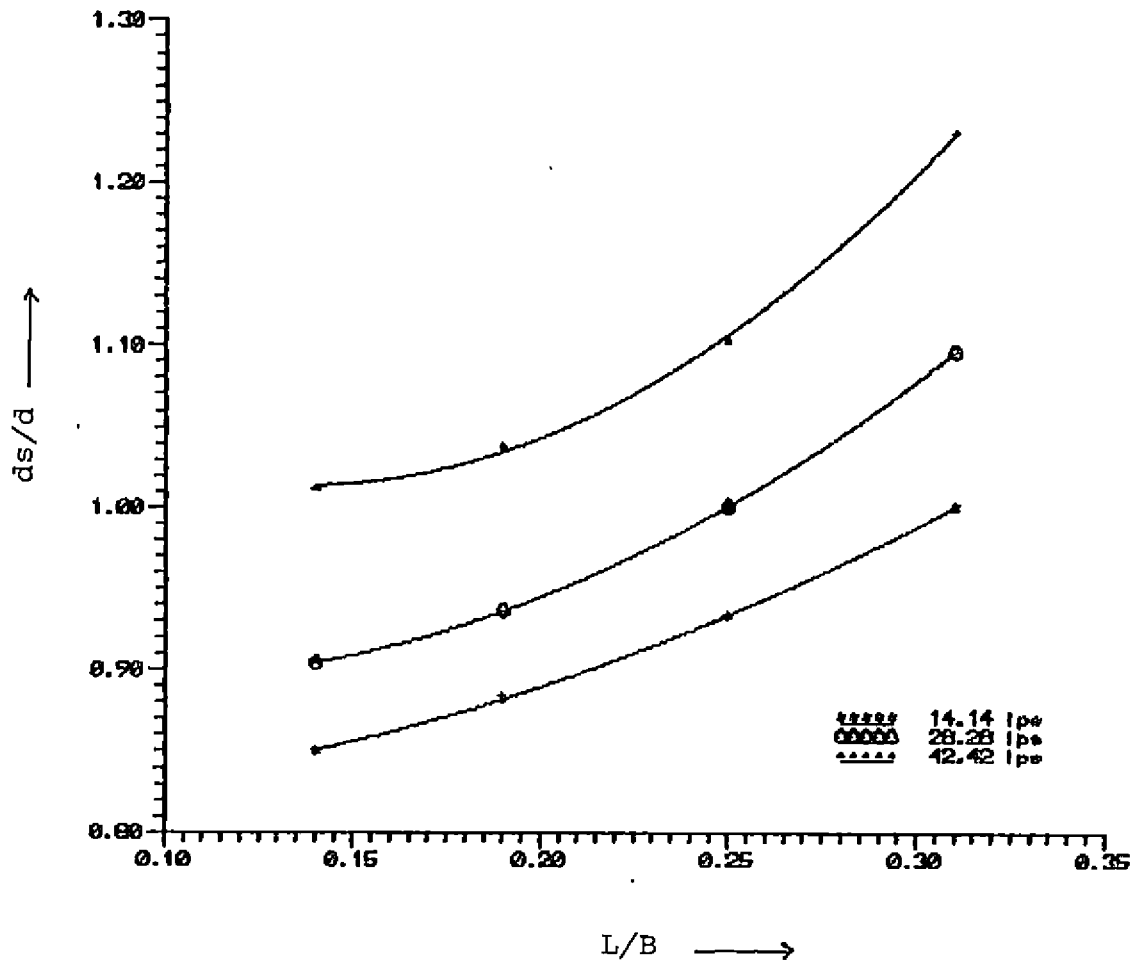


Fig. 101. Maximum depth of scour versus length of spur (spur angle=90°)

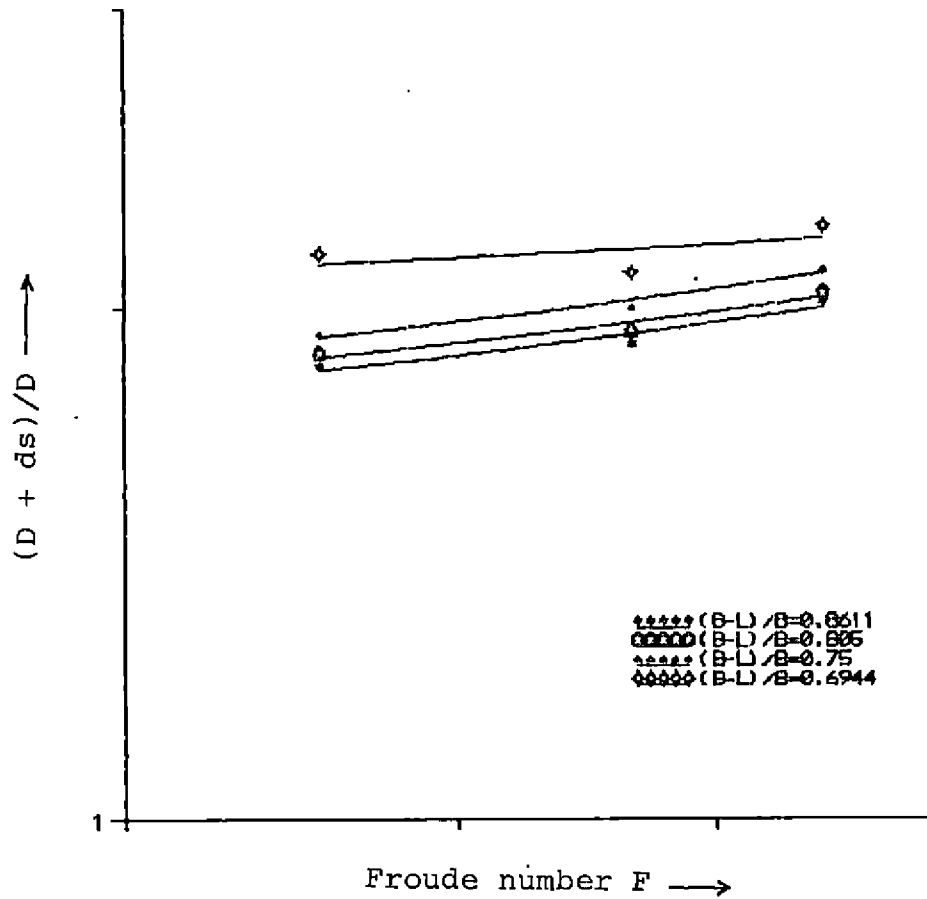


Fig. 102. Variation of  $(D + ds)/D$  with  $F$  and  $\alpha$  for single spur

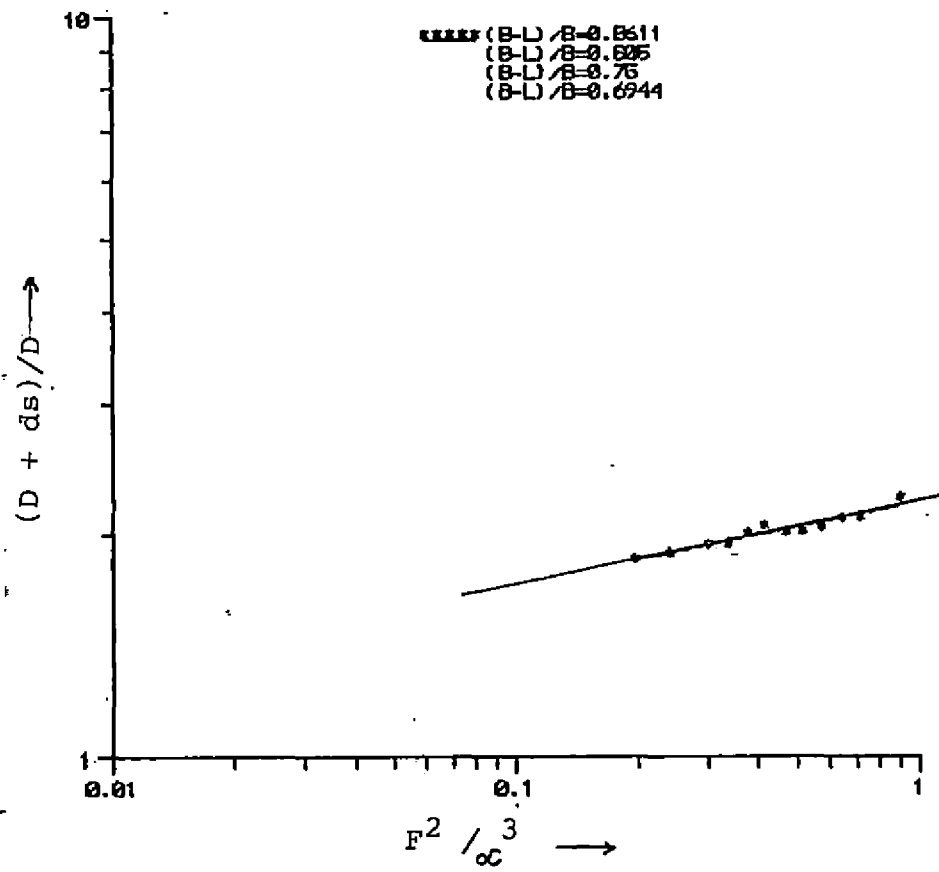


Fig. 103. Variation of  $(D + ds)/D$  with  $F^2/\omega^3$  for single spur

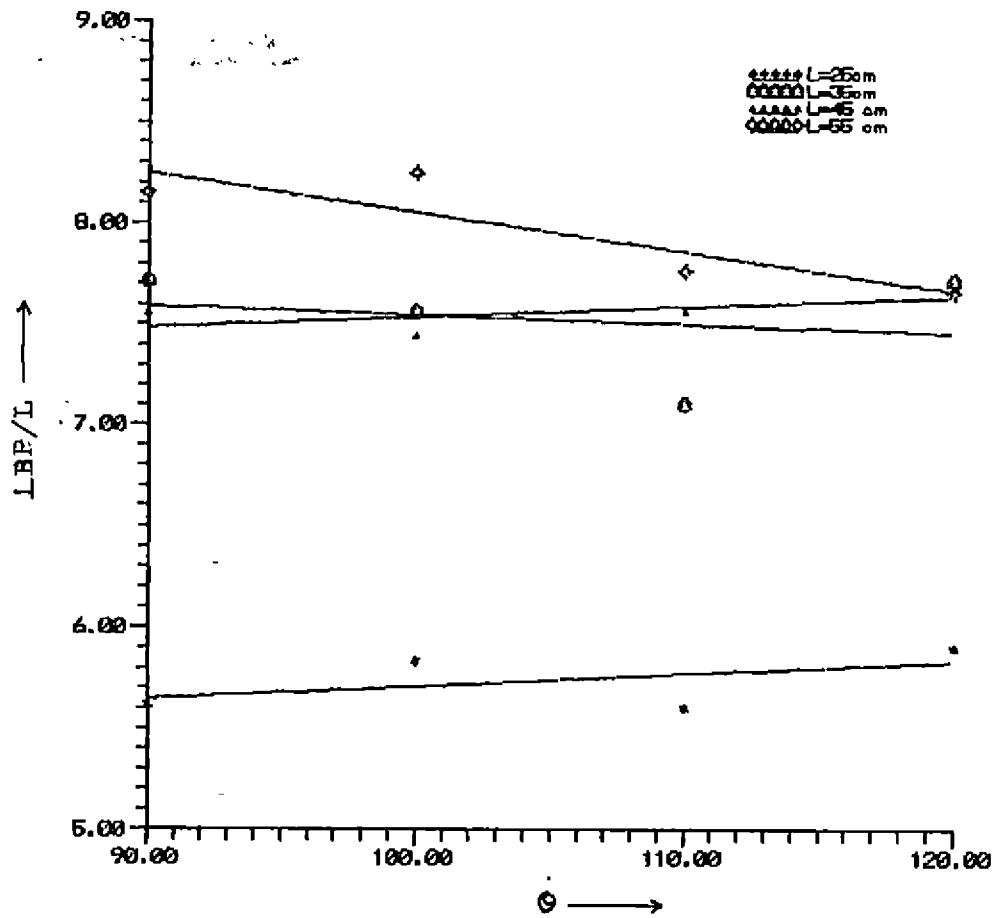


Fig. 104. Trend lines for LBP/L versus spur angles for the constrictions tested (Discharge = 28.28 lps)

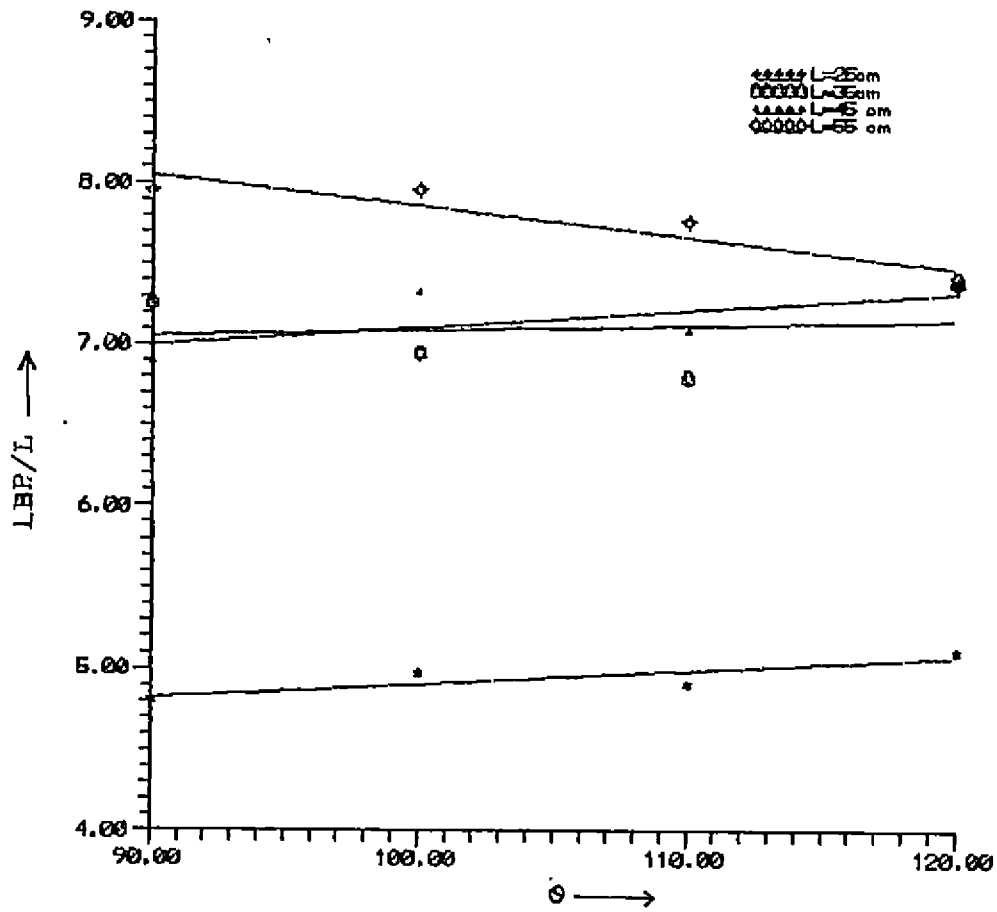


Fig. 105. Trend lines for LBP/L versus spur angles for the constrictions tested (Discharge = 42.42 lps)

these studies. Observations in respect of (1) scour pattern (2) maximum scour depth around spur dike and (3) relations such as maximum scour depth versus intensity of discharge were made which are given in subsequent sub headings.

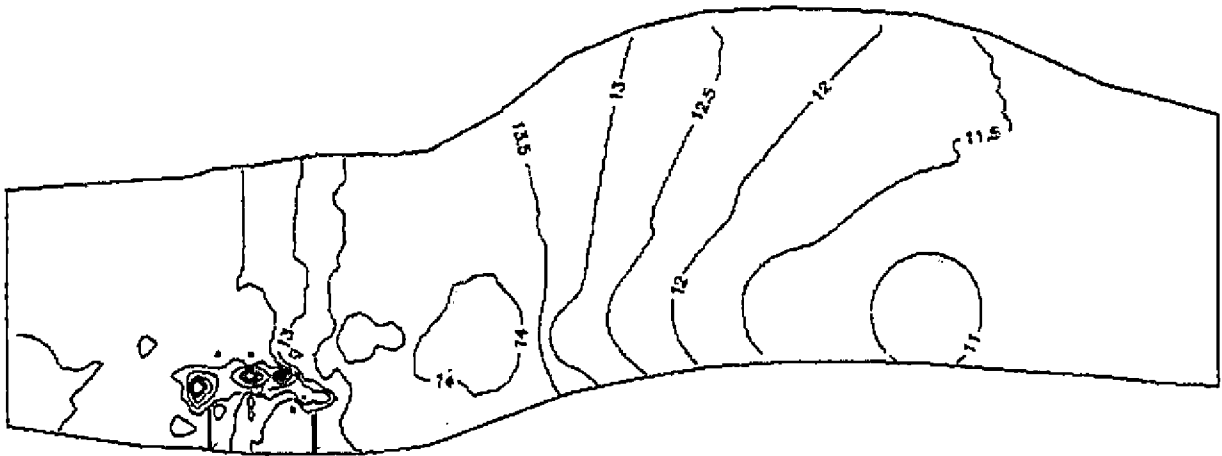
#### 4.2.2.1 Scour pattern

In this scheme of multiple spur, data at the first spur which generally affected more as compared to subsequent downstream spurs, have been considered. Thus data for parameters such as maximum scour depth, Froude number and opening ratio have been analysed. With the collected data, scour pattern at each multiple spur configuration were plotted in Fig. 106 to 114.

From these scour pattern plots, it was observed that spurs with 3L spacing behave like single unit and purpose of protecting larger reach of the bank is not fully served. On the other hand, if a larger spacing of 5L is maintained each spur acts independently as seen from extent of scour. Thus from the experimental analysis of scour pattern it can be concluded that spur scheme with  $L/B = 0.19$  and spacing as 5L is more effective for bank protection. The data for scour depths near to nose of the spur are presented in Appendix-5

The inter relationship plots of  $(D+d_s)/D$  versus  $F$  and  $F^2 / \omega^3$  were plotted similar to single spur study and are shown in Fig. 115 and Fig. 116. It can be seen from these

(a)



Average bed level = 1.28 cm  
 All dimensions in cm  
 Scale 1:54

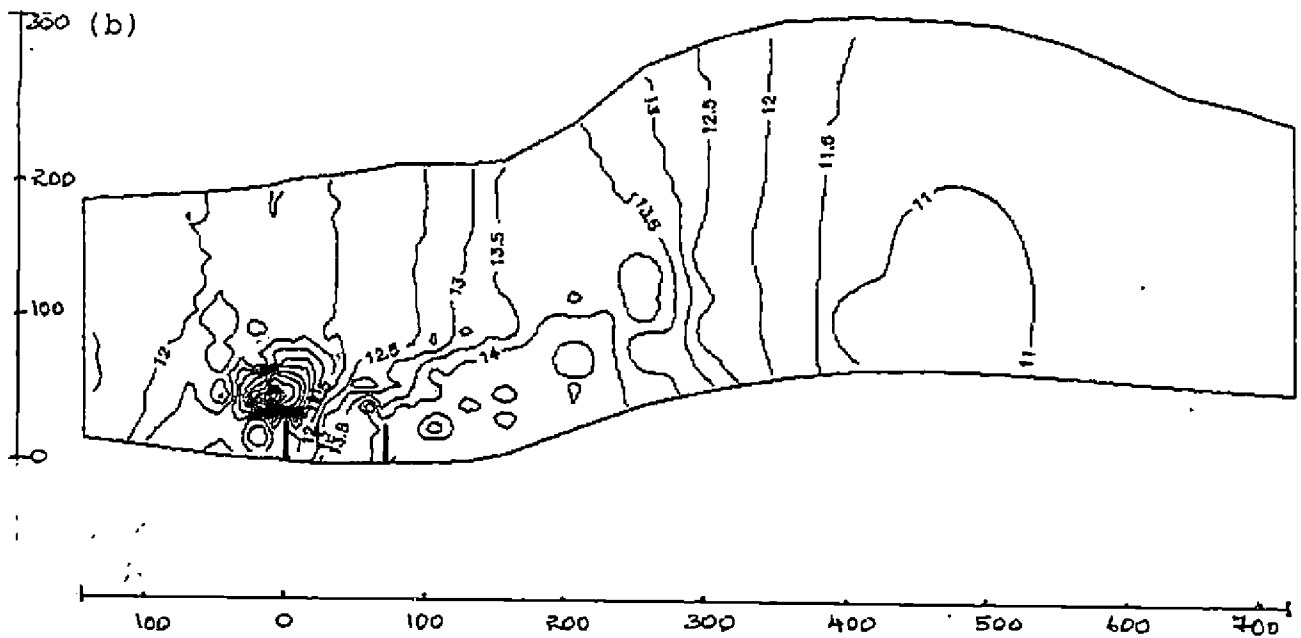
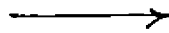
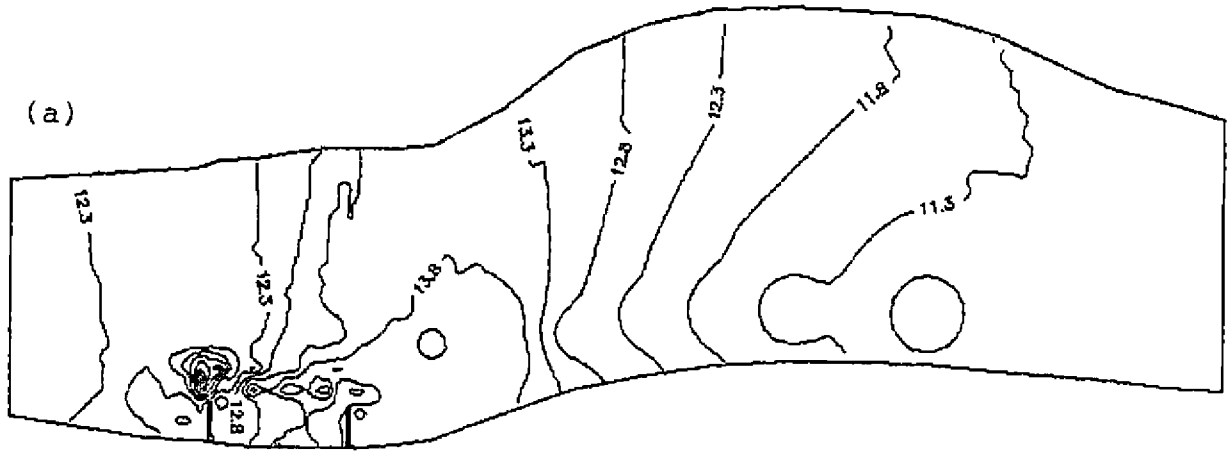


Fig. 106. Scour pattern for multiple spur scheme ( $L=25$  cm, spacing =  $3L$ ) for discharge rates (a) 28.28 lps (b) 42.42 lps





Average bed leve = 1.28 cm  
 All dimensions in cm  
 Scale 1:54

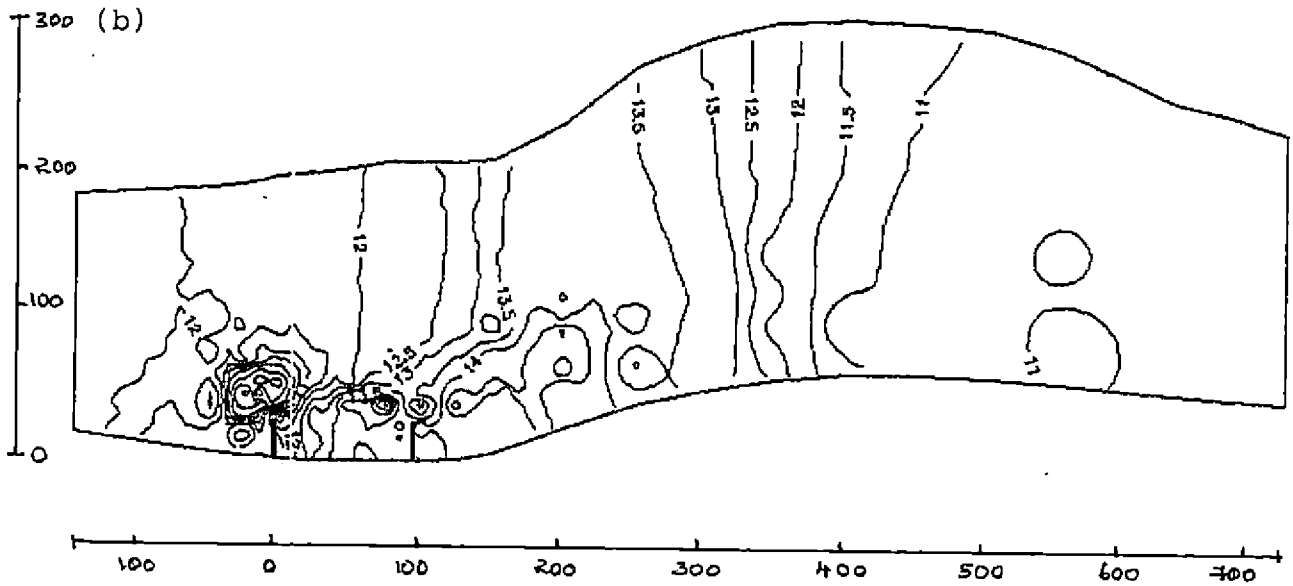
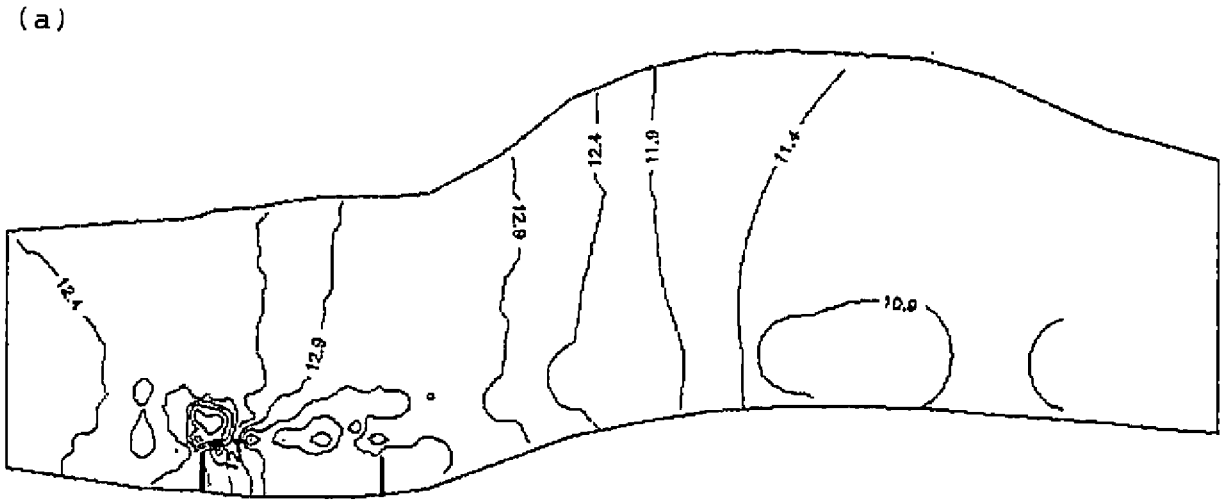


Fig. 107. Scour pattern for multiple spur scheme ( $L=25$  cm, spacing =  $4L$ ) for discharge rates (a) 28.28 lps (b) 42.42 lps



Average bed level = 1.28 cm  
 All dimensions in cm  
 Scale 1:54

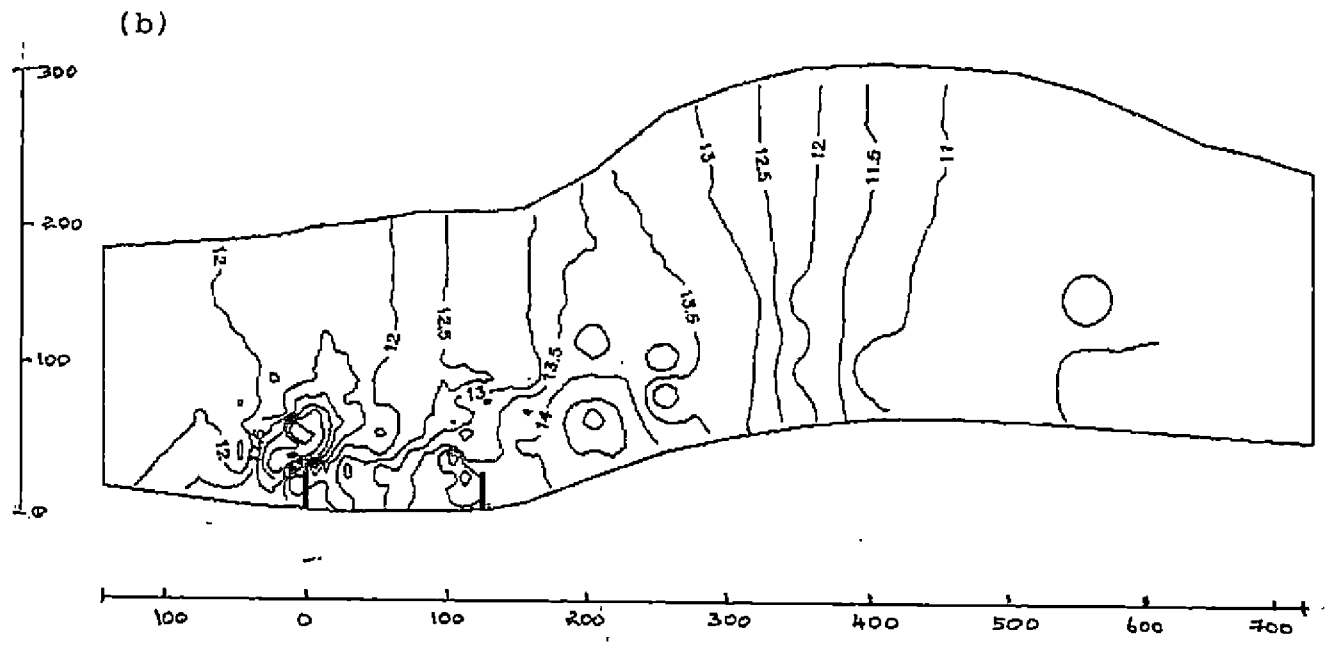
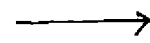
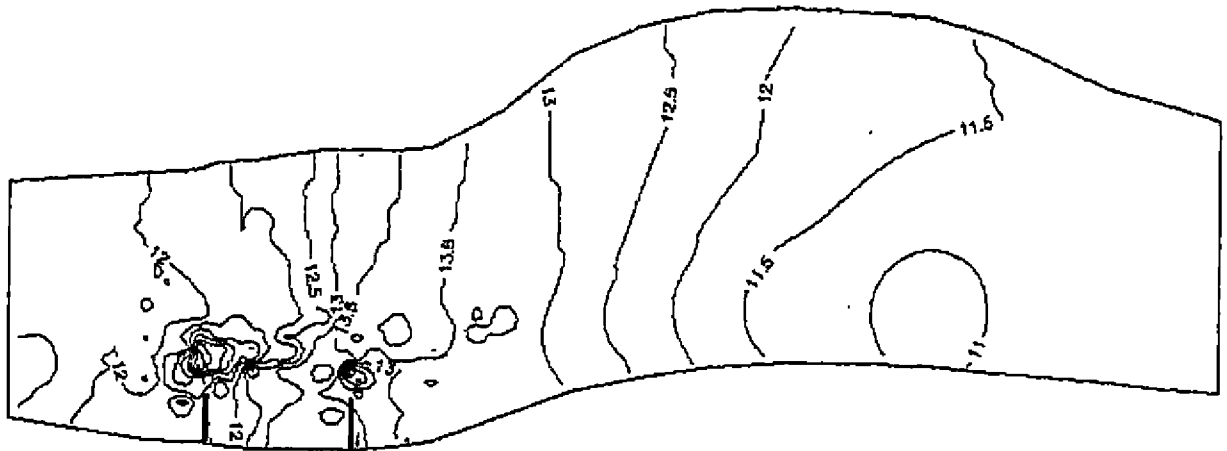


Fig. 108. Scour pattern for multiple spur scheme (L=25 cm, spacing = 5L ) for discharge rates (a) 28.28 lps (b) 42.42 lps

(a)



Average bed level = 1.28 cm  
 All dimensions in cm  
 Scale 1:54

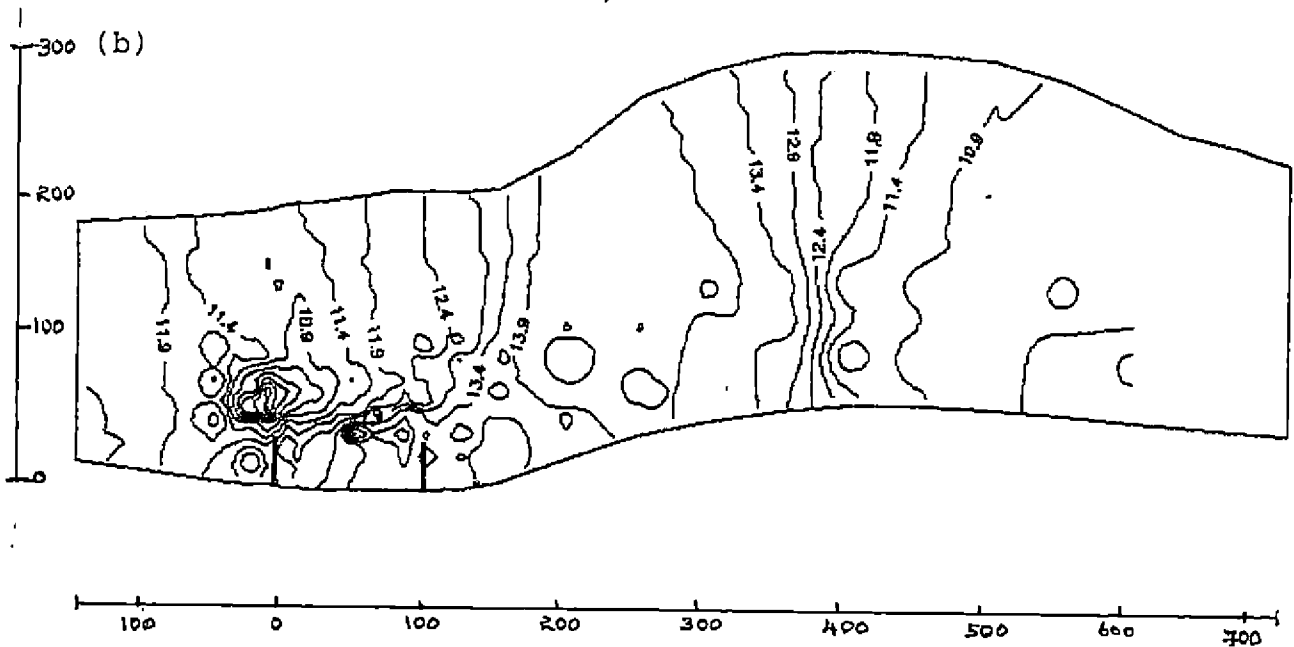
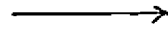


Fig. 109. Scour pattern for multiple spur scheme ( $L=35$  cm, spacing  $= 3L$ ) for discharge rates (a) 28.28 lps (b) 42.42 lps

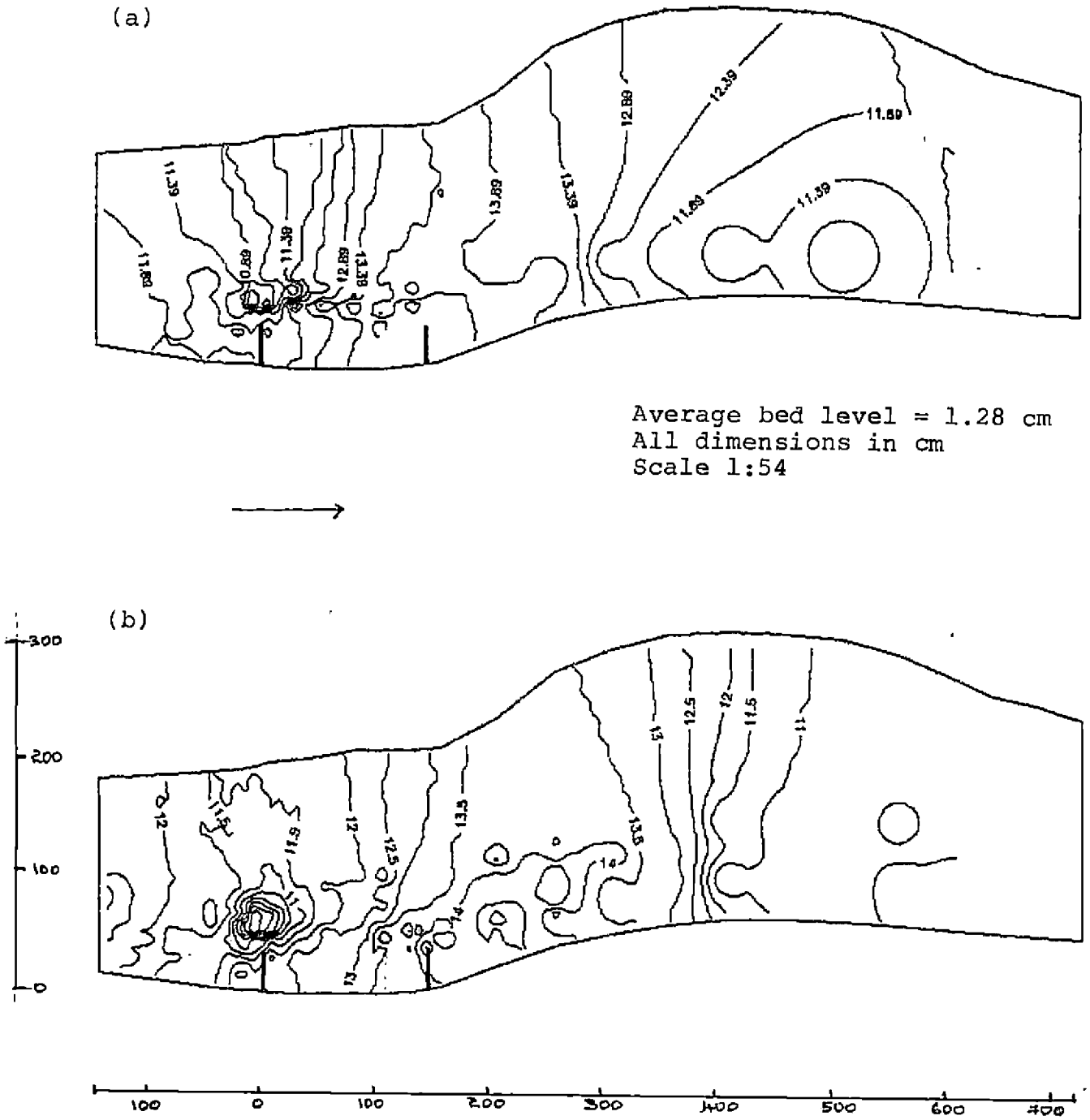
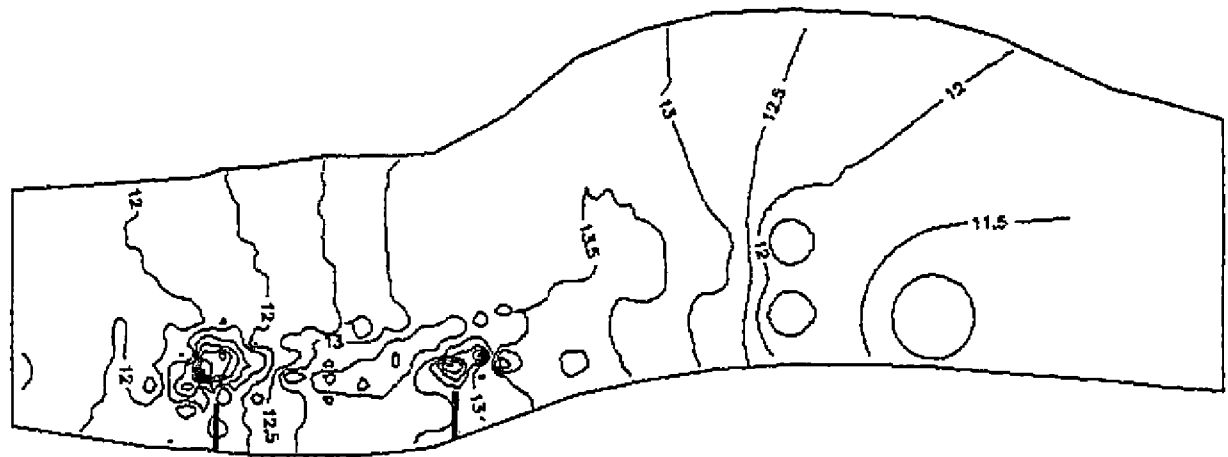


Fig. 110. Scour pattern for multiple spur scheme ( $L=35$  cm, spacing =  $4L^2$ ) for discharge rates (a) 28.28 lps (b) 42.42 lps

(a)



Average bed level = 1.28 cm  
All dimensions in cm  
Scale 1:54

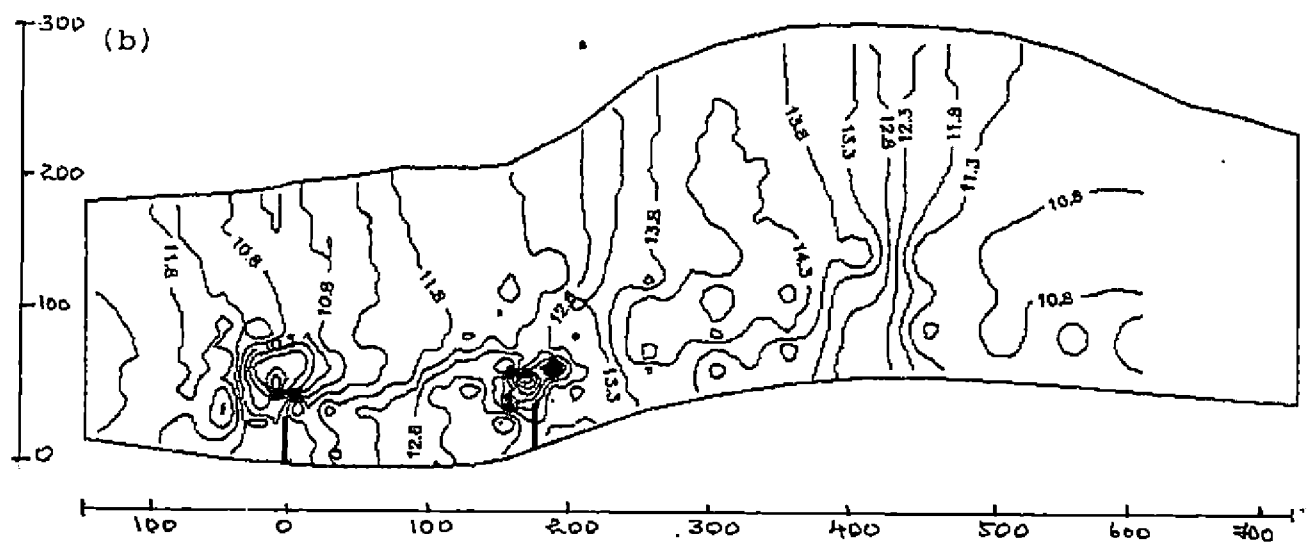
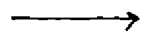
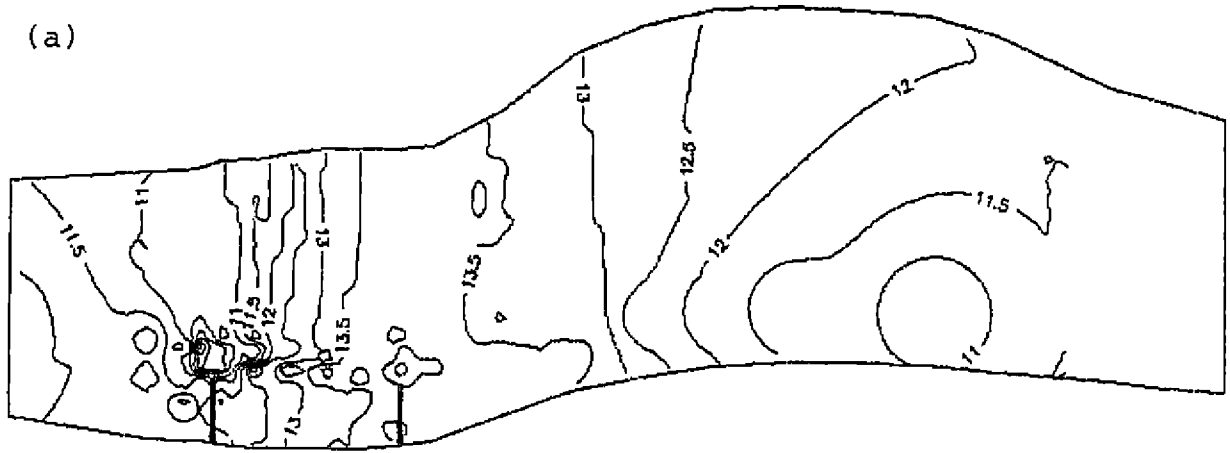


Fig. 111. Scour pattern for multiple spur scheme (L=35 cm, spacing = 5L') for discharge rates (a) 28.28 lps (b) 42.42 lps



Average bed level = 1.28 cm  
 All dimensions in cm  
 Scale 1:54

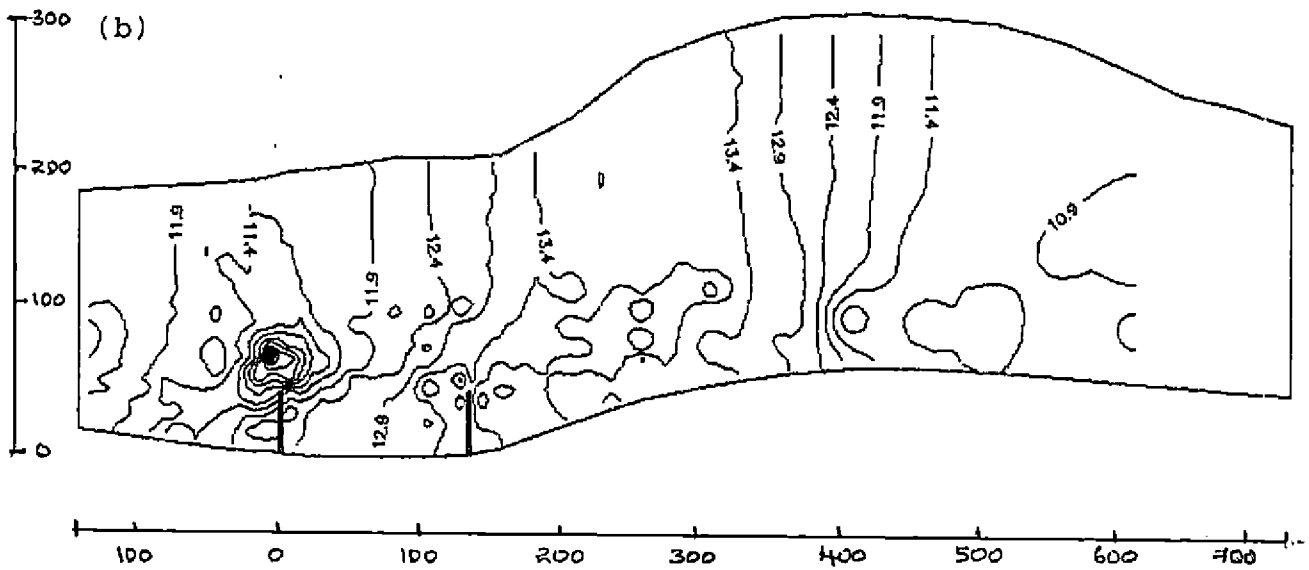
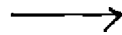
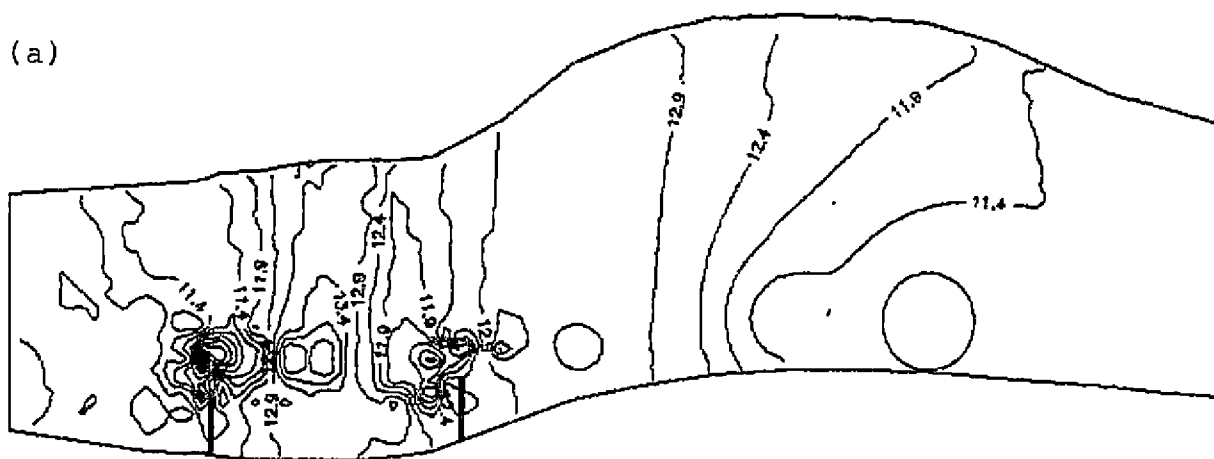


Fig. 112. Scour pattern for multiple spur scheme ( $L=45$  cm, spacing =  $3L$ .) for discharge rates (a) 28.28 lps (b) 42.42 lps



Average bed level = 1.28 cm  
 All dimensions in cm  
 Scale 1:54

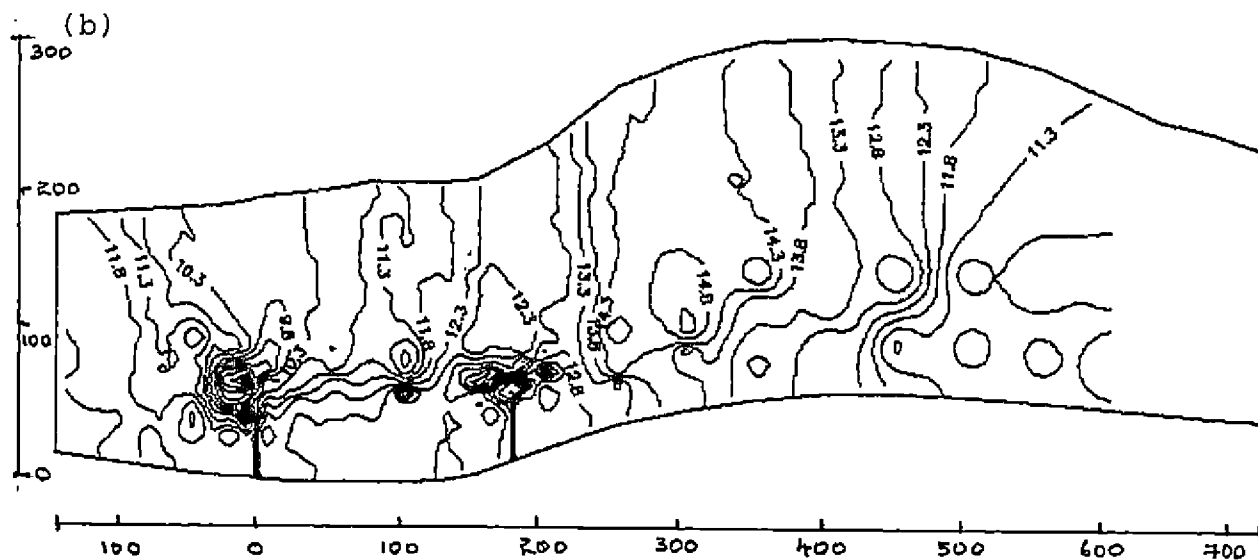
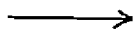
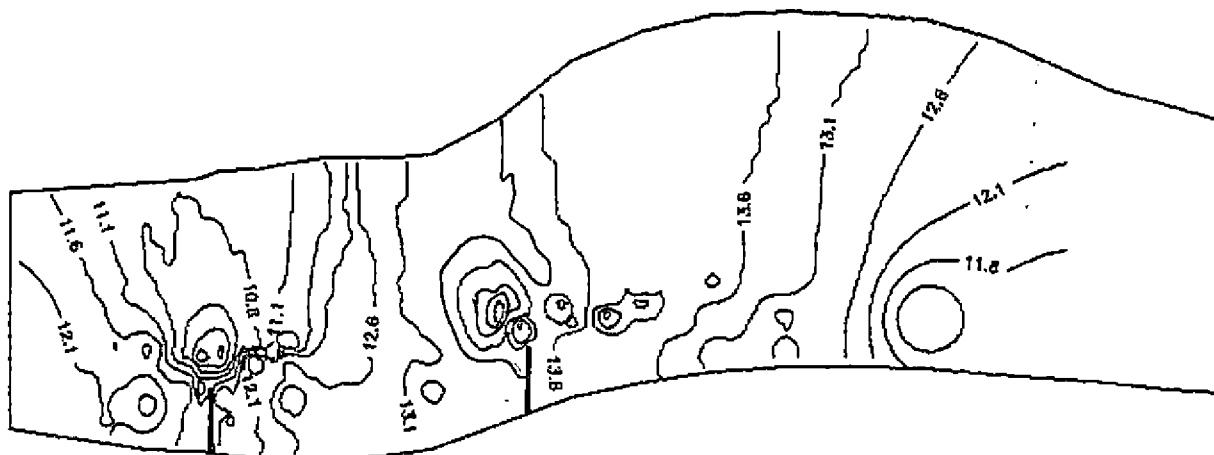


Fig. 113. Scour pattern for multiple spur scheme ( $L=45$  cm, spacing =  $4L$ ) for discharge rates (a) 28.28 lps (b) 42.42 lps

(a)



Average bed level = 1.28 cm  
 All dimensions in cm  
 Scale 1:54



(b)

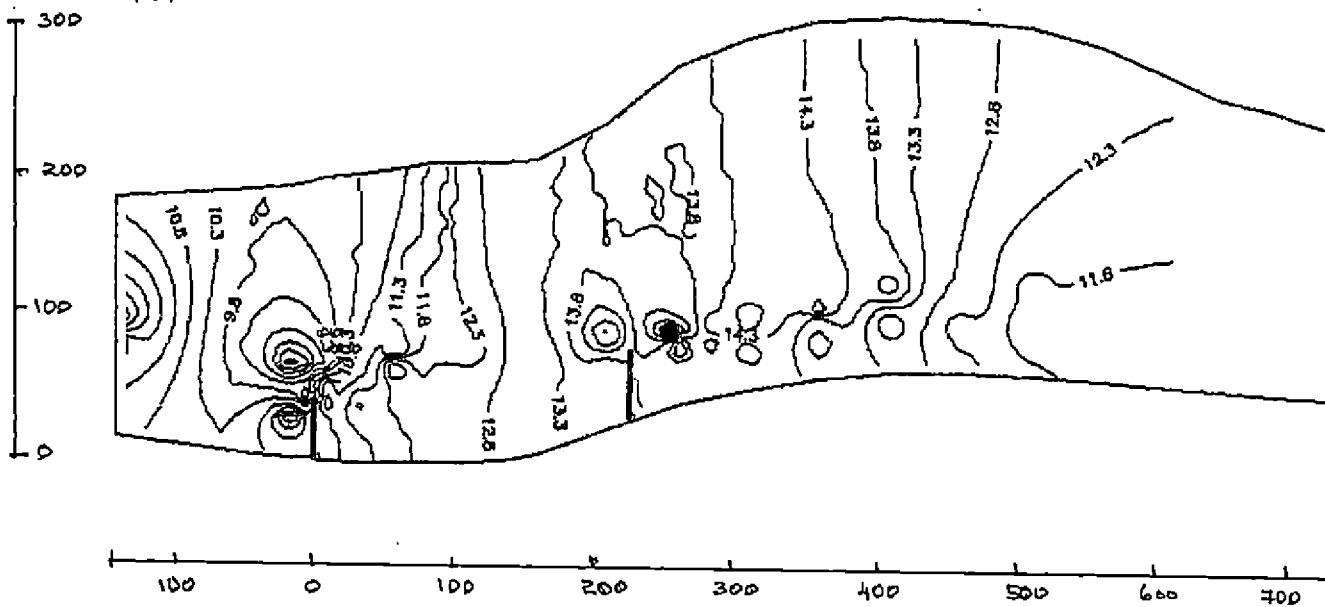


Fig. 114. Scour pattern for multiple spur scheme ( $L=45$  cm, spacing =  $5L$ ) for discharge rates (a) 28.28 lps (b) 42.42 lps



figures that the slope of the curve  $(D+ds)/D$  Vs  $F$  change as spacing increases. For all spacing scour depth increases with Froude number as well as  $F^2/\alpha^3$ .

Mushtaq Ahmed, Garde et al and Quader have conducted model experiments to study the effect of discharge, flow concentration and angle of attack of the flow on the scour depth at a spur nose. They proposed the formula for estimating maximum scour depth as  $D_1 = K q^{2/3}$  in which  $D_1$  = depth of maximum scour below maximum water level,  $q$  = discharge intensity at the spur constriction and  $K$  = a constant dependent upon flow concentration and inclination of spur and angle of attack.

Present data for multiple spur scheme have been plotted vide., Fig.11.7 for spacing 3L, 4L and 5L. First spur takes direct attack and at this location more scour is developed compared to downstream spurs, data at this spur was taken for plotting purposes. Thus Fig.11.7 shows that scour depth increases as intensity of discharge increases.

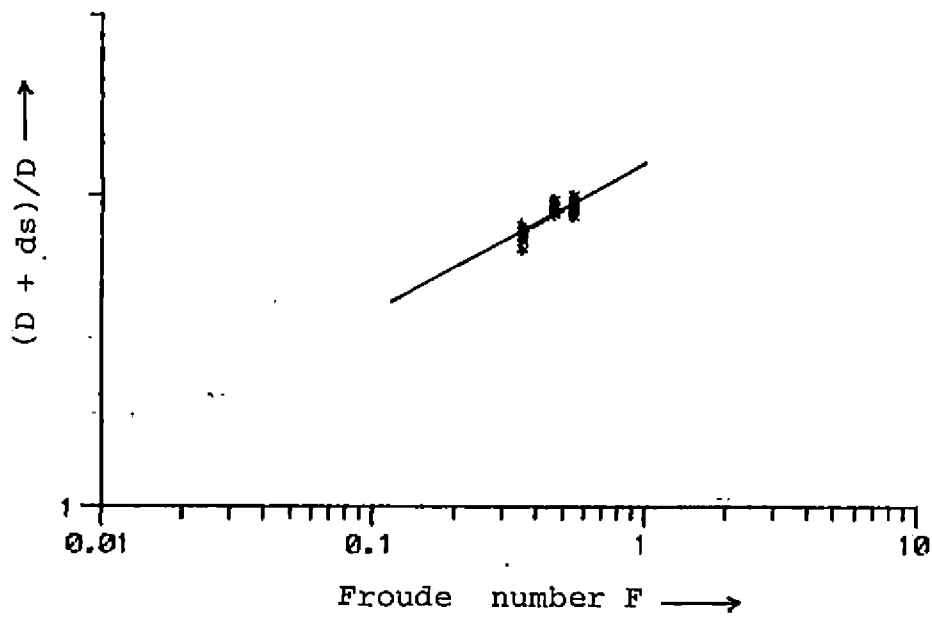


Fig. 115. Variation of  $(D + ds)/D$  with  $F$  and  $\alpha$  for multiple spur scheme

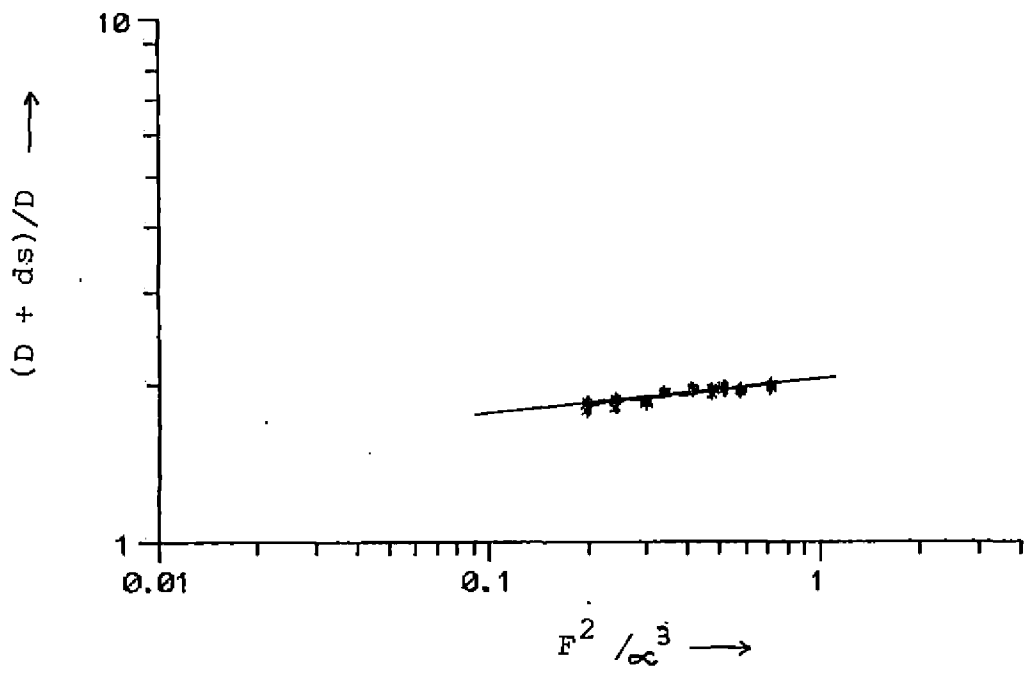


Fig. 116. Variation of  $(D + ds)/D$  with  $F^2/\omega^3$  for multiple spur scheme

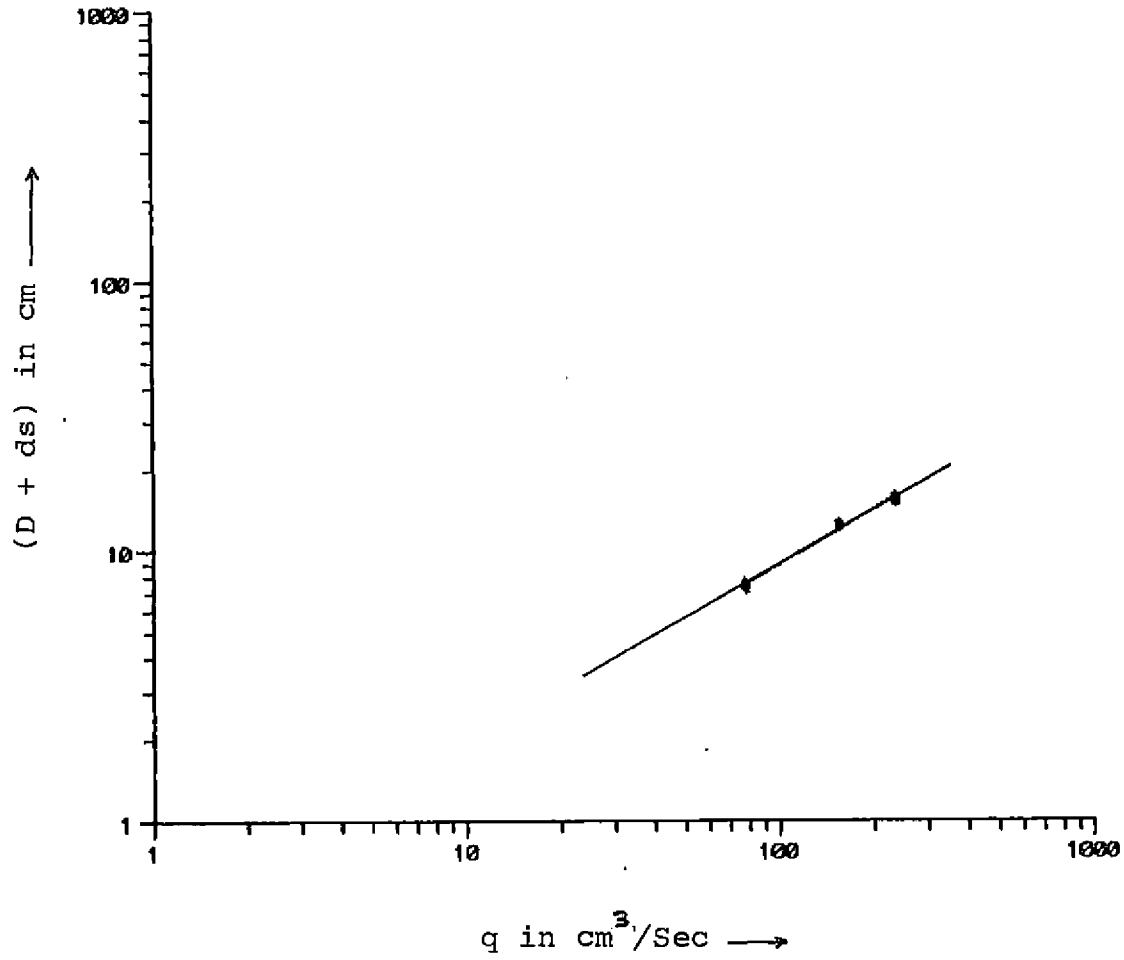


Fig. 117. Variation of  $(D + ds)/D$  with discharge intensity ( $q$ )

# Summary

---

## SUMMARY AND CONCLUSION

River training measures, which are meant to make rivers behave as we desire and prevent their ravages, have become essential for flood control and bank protection on a large scale. The most widely used training measure is probably the use of spurs, which are structures constructed transverse to the river flow and extend from the bank to the river. Spurs are regarded more successful than other training measures when it comes to protect a valuable land, town, village, highway etc., against erosion or for flow diversion or maintenance of depth of flow in a particular channel. No serious attempt has been made so far to evolve standard designs for spurs, indicating conditions under which they could be used. With an objective of studying characteristics such as flow pattern, velocity distribution and scour pattern for different parameters of spurs by simulation techniques, a study was conducted at KERI, Peechi during the months from March to September 1994.

A distorted type 3D river model with horizontal scale 1 in 100 and vertical scale 1 in 50, of Aranmula water stadium in Pamba river was selected for the study. River bed was formed as rigid as well as mobile bed condition according to the objectives of the study. The test section measures a length of 8.5m, depth of 0.4m and width varying

from 1.6m to 2.6m. The different design parameters of spurs such as length, angle, spacing etc. were analysed for different discharges to evolve suitable values for the parameters. The different lengths chosen were 25cm, 35cm, 45 cm and 55 cm. The spur angles chosen were 90°, 100°, 110° and 120° downstream with the bank. Spacing of spurs chosen were 2L, 3L, 4L and 5L where L is the length of the spur. A Cipolletti weir fitted at the end of inlet chamber was used to regulate the model discharge. Water was supplied from the dam reservoir near the experiment site through a controlled supply line and a flume.

Rigid bed study was used to analyse the flow pattern and velocity distribution whereas the mobile bed study was mainly aimed at analysing the scour pattern. In this study, rigid bed was formed with cement plaster where as the mobile bed was formed with a well graded sand of size  $D_{50} = 0.57$  mm. The flow patterns were observed by using pearls as floats and their paths were traced relating to one of the banks by visual observation. The velocity was measured at  $0.6D$  at various cross sections using a pigmy water current meter where  $D$  is the depth of flow at the measuring section. A point gauge mounted on a rectangular frame was used for measuring cross sectional bed profile data as well as depth of flow at various cross sections. These observations were used to evaluate scour patterns for the test section. For

single spur at mobile bed condition, null point was determined by dropping potassium permanganate solution at different points along the side wall.

The analysis of experimental results evolved the following conclusions:-

#### I. Rigid bed experiment - Single spur

(i) From the analysis of flow pattern obtained it was observed that (a) the flow concentration at the spur tip increased with the increasing spur length and it decreased with the the increasing spur angle, (b) the flow diversion to the opposite bank increased with increase in spur length and spur angle, (c) the length of bank protected increased with the increase of spur length regardless of spur angle and, (d) under these conditions, a spur length ranging between 25 cm and 55 cm and at an angle between  $90^\circ - 110^\circ$  was found desirable.

(ii) From the analysis of velocity data it was found that (a) percentage increase in velocity at opposite bank had a general increasing trend with increase in spur angle as well as spur length, (b) an L/B ratio of 0.19 (ie. spur length = 35 cm) combined with spur angle of  $90^\circ$  was found optimum for the test section under the present study and, (c) length of bank protected by the spur increased with increase in spur length regardless of spur angle.



## II. Rigid bed experiment - Multiple spur

(i) From the flow pattern and velocity distribution obtained, it was observed that (a) the length of bank protected downstream of the spur tip is found to increase with spacing between spurs, (b) spur length of 25 cm with 2L spacing was found to function as single spur and it could be discarded for subsequent studies.

(ii) from the analysis of velocity distribution in the test section it was observed that the velocity along the affected bank reduced with increase in spur length and spur spacing.

## III. Mobile bed experiment - Single spur

From the analysis of scour pattern obtained it was observed that (a) maximum scour depth at spur tip was decreased with increase in spur angle, but increased with increase in spur length, (b) an L/B ratio of 0.19 (ie., spur length = 35 cm) with spur angle 90° was found suitable and, (c) from the relationships obtained of Froude number  $F$  and  $F^2 / \alpha^3$  ( $\alpha$  = opening ratio) with  $(D+ds)/D$  it was observed that scour depth increases with Froude number  $F$  as well as  $F^2 / \alpha^3$ .

## IV. Mobile bed experiments - Multiple spur

(i) From the analysis of scour pattern it was observed that (a) with spacing of 5L both the spurs behaved

independently of each other, (b) as in the case of single spur scour depth increases with  $F$  as well as  $F^2 / \alpha^3$  and, (c) the scour depth increased with increase in intensity of discharge.

Thus it was concluded that the provision of spurs was effective in protecting the affected bank and the design of spurs is greatly dependent on its parameters. Experimental analysis for the present test section shows that (i) the constriction achieved by the spurs should not exceed 20% of the flow width, (ii) spur angle of  $90^\circ$  downstream with the bank gives best results. (iii) for multiple spurs a spacing of  $5L$  is more effective for bank protection.

The following recommendations are also suggested for further studies. (i) studies could be carried out for different sediment size of the bed material as it is known to have an effect on scour pattern. (ii) studies could be carried out for different types of spurs with different construction material and crest condition.

## References

---

## REFERENCES

- \*Ahmed, M. (1951). Spacing and protection of spurs for bank protection. Civil Engineering and Public works Review. 46 (437 & 538).
- \*Andru, P. (1956). Study of scour at obstruction in non cohesive bed. M.Sc.Thesis, University of Alberta, Canada.
- CBIP (1971). Manual on River Behaviour Control and Training. Central Board of Irrigation and Power Publication.(60).
- CWPRS (1987). Design of spurs (Groynes). Technical Report. Central Board of Irrigation and Power.(39).
- \*Dou Guoren (1978). An investigation on the whirl pool flow and its similarity laws. Journal of Nanjing Hydraulics Research Institute.No. 3.
- \*France J. R. D. (1968). Observation of flow patterns around some simple groyne structures in channels. Proceedings of Institutions of civil Engineering. 41 : 828-837.

- Garde, R. J. and Gopal Sharma (1969). Criteria for determination of length of a spur bank protection Symposium on simulation techniques and prototype behaviour in water resources. CBIP. II(3-6).
- Garde, R. J., Subramanya, K. and Namboothiripad, K.D. (1961). Study of scour around spur dikes. Journal of Hydraulic Division, ASCE. 87 (HY6):23-27.
- Garge, S. K. (1976). Irrigation Engineering and Hydraulic Structures., Khanna Publishers, Delhi. pp.436-442
- \*Govinda Rao, N. S. and Sharma, K. V. N. (1965). Scour around bridge piers. Annual report, Indian institute of science, Bangalore.
- Gupta, S. M., Sharma, J. P., Jindal, S. R. and Chandra, S. (1969). Alluvial river behaviour - A few aspects of its simulation in a model. Symposium on simulation techniques and prototype behaviour in water resources. CBIP. II:7-8
- Helmut Kobus. (1980). Hydraulic modelling. German association for water resource and land improvements, Bulletin 7. IAHR.

- \*Inglis. C. C. (1939). Behaviour and control of river and canals with the aid of models. Research publication No. 13. Part II CWINRS. Poona. India.
- ISI (1976). Indian standard criteria for river training works for barrages and weirs in alluvium. IS: 8408 - 1976. Indian Standard Institutions, New Delhi, India.
- KERI (1970). River training works-A technical note. Report No. 7/70, Hydraulic division no. 1., KERI, Peechi.
- \*Lacey, G. (1930). Stable channels in Alluvium. Proceedings of Institution of civil Engineers. 229: 259-321.
- \*Laursen E.M. (1953). A generalised model study of scour around bridge piers and abutments. Proceedings, IAHR. Minnesota.
- \*Lu Yongjun and Zhi Xuan Chang.(1992). Advances in flow near groyne like structures. Proceedings of eighth congress of the Asian and Pacific regional division of the international association for hydraulic research. CWPRS. Pune. Vol III. 209-218.
- Miller, A. C., Kerr, S. N. and Sarto, J. P. (1983). Physical modelling of spurs for bank protection. Proceedings of the symposium on river meandering. ASCE. pp. 996-1007.

- Moni, M. S. (1961) Control of river behaviour (A study on the effect of groynes on movable beds and banks.)  
M. E. thesis, Civil Engineering Department, College of Engineering, Trivandrum.
- \*Quader, A. (1982). The effect of sediment size on limiting scour depth. Irrigation and power. 39 (10).
- Rajaratnam, N. and Nwachukwu, B. A. (1983). Flow near groyne like structure. Journal of Hydraulic division, ASCE. 109(3) : 463-480.
- Rajaratnam , N. and Nwachukwu, B.A. (1983). Erosion near groyne likes structures Journal of Hydraulics research .21(4): 277-287.
- Varshney, R. S. and Mathur, B. E. (1972). An analysis of location and orientation of repelling spurs in rivers. Journal of Central Board of Irrigation and Power. CBIP.29(1): 59-76.
- Ven te chow. (1982). Open channel hydraulics. Mcgraw Hill international book company, Tokyo.
- \*Wan Desheng (1987). Experimental study on groynes. Tianjin Institute of water transport Engineering Research Report.

\* Originals are not seen

# Appendices

---



APPENDIX-I

Velocity observations with different single spur configurations

Discharge (Ips)	velocity at c/s 3 near left bank with out spur (m/s)	l/b	Velocity at c/s 3 near left bank with spur (m/s)				
			Spur angle	90°	100°	110°	120°
14.14	0.224	0.14		0.268	0.291	0.281	0.247
		0.19		0.272	0.336	0.347	0.325
		0.25		0.325	0.347	0.325	0.347
		0.31		0.336	0.393	0.393	0.370
28.28	0.381	0.14		0.436	0.451	0.449	0.415
		0.19		0.472	0.516	0.483	0.472
		0.25		0.538	0.545	0.550	0.566
		0.31		0.555	0.595	0.561	0.561
42.42	0.463	0.14		0.482	0.516	0.516	0.527
		0.19		0.494	0.572	0.561	0.572
		0.25		0.561	0.573	0.629	0.618
		0.31		0.606	0.673	0.663	0.651

APPENDIX-II

Velocity observations with different multiple spur schemes

Discharge (lps)	l/b	Spacing	Velocity at c/s near left bank with multiple spurs (m/s)			
			c/s No.	3	4	5
14.14	0.14	2L	0.268	0	0	0
		3L	0.28	0	0	0
		4L	0.26	0	0	0
		5L	0.29	0	0	0
28.28	0.14	2L	0.37	0	0	0
		3L	0.4	0	0	0
		4L	0.44	0.02	0	0
		5L	0.42	0.03	0	0
42.42	0.14	2L	0.47	0	0	0
		3L	0.48	0.04	0	0
		4L	0.48	0.055	0	0
		5L	0.49	0.04	0	0
14.14	0.19	2L	0.292	0	0	0
		3L	0.298	0	0	0
		4L	0.26	0	0	0
		5L	0.303	0	0	0
28.28	0.19	2L	0.426	0	0	0
		3L	0.471	0.157	0	0
		4L	0.449	0.044	0	0
		5L	0.45	0.04	0	0
42.42	0.19	2L	0.505	0	0	0
		3L	0.573	0.16	0	0
		4L	0.539	0.08	0	0
		5L	0.561	0.04	0	0
14.14	0.25	2L	0.348	0.123	0	0
		3L	0.325	0.157	0	0
		4L	0.325	0.03	0	0
		5L	0.382	0.022	0	0
28.28	0.25	2L	0.518	0.157	0	0
		3L	0.516	0.179	0.01	0
		4L	0.471	0.01	0.02	0
		5L	0.539	0	0	0
42.42	0.25	2L	0.565	0.078	0	0
		3L	0.595	0.078	0.04	0
		4L	0.618	0.01	0.05	0
		5L	0.6	0.02	0	0
14.14	0.31	2L	0.37	0.269	0	0
		3L	0.370	0.224	0.04	0
		4L	0.370	0.12	0.05	0
		5L	0.382	0.14	0	0
28.28	0.31	2L	0.555	0.28	0	0
		3L	0.584	0.22	0.06	0
		4L	0.595	0.2	0.08	0
		5L	0.56	0.314	0.02	0
42.42	0.31	2L	0.635	0.146	0	0
		3L	0.604	0.1	0	0
		4L	0.632	0.06	0	0
		5L	0.644	0.258	0	0

APPENDIX-IV

Null point observations with different single spur configurations

Discharge (lps)	l/b	Spur angle	Length of bank protected downstream of the spur (m)			
			90°	100°	110°	120°
28.28	0.14		1.40	1.46	1.35	1.62
	0.19		2.70	2.65	2.48	2.70
	0.25		3.40	3.35	3.40	3.46
	0.31		4.48	4.54	4.27	4.21
42.42	0.14		1.19	1.24	1.30	1.51
	0.19		2.54	2.43	2.38	2.59
	0.25		3.10	3.29	3.19	3.29
	0.31		4.37	4.10	4.27	4.05

APPENDIX- V

Scour depth observations with different multiple spur schemes

Discharge (lps)	l/b	Spur spacing	Maximum scour depth at spur tip (cm)		
			3L	4L	5L
14.14	0.14		3.1	3.3	3.4
	0.19		3.2	3.4	3.5
	0.25		3.3	3.4	3.3
28.28	0.14		5.9	5.8	5.8
	0.19		5.9	6	6.1
	0.25		5.9	6.1	6.2
42.42	0.14		7.5	7.4	7.1
	0.19		7.2	7.4	7.3
	0.25		7.5	7.7	7.8

APPENDIX-III

Scour depth observations with different single spur configurations

Discharge (lps)	l/b	Spur angle	Maximum scour depth at spur tip (cm)			
			90°	100°	110°	120°
14.14	0.14		3.4	3.2	2.6	2.1
	0.19		3.53	3.1	2.8	2.6
	0.25		3.73	4	3.5	3.3
	0.31		4	4.3	3.7	3.6
28.28	0.14		5.7	5.7	3.6	3
	0.19		5.9	6.6	6.6	5.7
	0.25		6.3	7.1	6.5	5.9
	0.31		6.9	7.5	7	6.1
42.42	0.14		7.9	8.8	7.3	6.9
	0.19		8.1	9.3	8.5	7.6
	0.25		8.6	10.2	10	8
	0.31		9.6	10.8	10.8	8.6

# **SIMULATION STUDIES ON DIFFERENT DESIGN PARAMETERS OF SPURS (GROYNES)**

By

**ROY MATHEW**

## **ABSTRACT OF A THESIS**

submitted in partial fulfilment of the  
requirement for the degree

*Master of Technology in Agricultural Engineering*

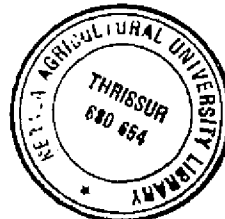
**Faculty of Agricultural Engineering & Technology  
Kerala Agricultural University**

*Department of  
Land and Water Resources & Conservation Engineering*  
Kelappaji College of Agricultural Engineering and Technology  
**TAVANUR 679 573  
MALAPPURAM**

**1995**

## ABSTRACT

The use of spurs as river training measure has proved to be an effective means of protecting river bank and their design requires indepth knowledge about its parameters related to the solution of a specific river training problem. To analyse various design parameters of spurs, a simulation study was conducted at KERI, Peechi. Characteristics such as flow pattern, velocity distribution and scour pattern were analysed for different spur lengths 25 cm, 35 cm, 45 cm and 55 cm, spur angles  $90^\circ$ ,  $100^\circ$ ,  $110^\circ$  and  $120^\circ$ , spur spacings 2L, 3L, 4L and 5L and for discharge rates 14.14 lps, 28.28 lps and 42.42 lps. Single spur and multiple spur scheme were tested on rigid as well as mobile bed condition. The analysis of the obtained flow pattern, velocity distribution and scour pattern reveals that the specified design parameters have a significant effect on flow diversion, length of bank protected, maximum scour depth at the spur nose, percentage increase in velocity at opposite bank etc. The analysis of the present study also led to the conclusion that L/B ratio of 0.19, spur angle of  $90^\circ$  was the best combination for single spur study and the same with a spacing of 5L was most effective for multiple spur scheme.



170621